

Technische Universität München

Fakultät Chemie

Lehrstuhl für Biotechnologie

The Small Heat Shock Proteins and the Heat Stress Response of
Baker's Yeast

Christopher Gordon Stratil

Vollständiger Abdruck der von der Fakultät für Chemie der Technischen Universität München zur Erlangung des akademischen Grades eines Doktors der Naturwissenschaften (Dr. rer. nat.) genehmigten Dissertation.

Vorsitzender: Univ.-Prof. Dr. Stephan A. Sieber

Prüfer der Dissertation:

1. Univ.-Prof. Dr. Johannes Buchner

2. Univ.-Prof. Dr. Sevil Weinkauff

Die Dissertation wurde am 29.12.2015 bei der Technischen Universität München eingereicht und durch die Fakultät für Chemie am 15.02.2016 angenommen.

Contents

1. Summary	1
2. Introduction	2
2.1 Investigations on the small heat shock proteins of baker's yeast	2
2.1.1 Protein folding.....	2
2.1.2 Protein folding within a cell.....	4
2.1.3 Protein folding in disease	5
2.1.4 Molecular chaperones and protein folding.....	5
2.1.5 Cooperation of the chaperone systems.....	6
2.1.6 Small heat shock proteins.....	8
2.1.7 Structure of small heat shock proteins	9
2.1.8 Approaches to study sHsp structure	11
2.1.9 The small heat shock protein system of <i>Saccharomyces cerevisiae</i>	12
2.2. Revisiting the heat stress response of baker's yeast	15
2.2.1 A short history on the heat shock response	15
2.2.2 Influences of heat on the cell.....	16
2.2.3 Transcriptional heat shock response.....	18
2.2.4 Crosstalk of stress responses	20
2.3. Objective	21
3. Materials and methods	22
3.1 General equipment and expendable items.....	22
3.2 Chemicals.....	24
3.3 Software, databases & web-based tools	25
3.4 Oligonucleotides and plasmids.....	26
3.5 Bacterial and yeast strains	28
3.6 Media and antibiotics	29
3.7 Buffers.....	31
3.8 Molecular biology methods.....	32
3.8.1 Cultivation of <i>E. coli</i> and <i>S. cerevisiae</i>	32

3.8.2 Yeast transformation protocols.....	33
3.8.3 Polymerase chain reaction (PCR).....	34
3.8.4 PCR-based gene deletion.....	35
3.8.5 Cloning of yeast shuttle vectors	36
3.9 Protein chemical methods	37
3.9.1 Determination of protein concentration.....	37
3.9.2 SDS-polyacrylamide gel electrophoresis (SDS-PAGE).....	38
3.9.3 Immunoblotting.....	38
3.10 Synthetic genetic array	39
3.11 Methods for transcriptional studies	41
3.12 Microscopy.....	44
3.12.1 Fluorescence and bright field microscopy.....	44
3.12.2 Soft X-ray tomography.....	44
3.13 Metabolic labeling of yeast cells	47
4. Results	50
4.1 Small heat shock proteins of baker's yeast.....	50
4.1.1 SGAs reveals sHsps involved in protein trafficking	50
4.1.2 The sHsps in models of protein aggregation	57
4.2 Heat stress and the inner cellular morphology	67
4.2.1 X-ray tomography of unstressed <i>S. cerevisiae</i>	67
4.2.2 X-ray tomography of heat stressed yeast.....	69
4.2.3 X-ray tomography of gene deletion mutants	71
4.2.4 Generation of 3D-models of baker's yeast.....	73
4.3 Transcriptional studies on wild type <i>S. cerevisiae</i> under heat shock	76
4.3.1 The transcriptional response to mild heat stress.....	77
4.3.2 The transcriptional response to sub-lethal heat stress	81
4.3.3 Origin of transcriptional waves	83
4.3.4 The heat shock response and the molecular chaperone system.....	86

4.3.5	Transcriptional regulation of selected pathways	93
4.3.6	Transcriptional regulators of the mild heat shock response	100
4.4	Transcriptional heat stress response in the genetic background of TF deletions	104
4.4.1	<i>Rpn4</i> deletion has broad effects on the transcriptome	105
4.4.2	<i>Sko1</i> deletion has minor effects on the transcriptome	110
4.4.3	<i>Msn2/4</i> deletion has vast influences on the transcriptome	114
4.5	Transcriptional heat stress response in <i>hsp12</i> and <i>sHsp</i> deletion yeast.....	117
4.5.1	<i>Hsp26/42</i> deletion results in vast transcriptional changes.....	118
4.5.2	<i>Hsp12</i> deletion affects ion homeostasis	124
4.6	Proteomic investigations on <i>S. cerevisiae</i> under heat shock	128
4.6.1	The cellular proteome after 10 min of heat stress	128
4.6.2	The cellular proteome after 30 min of stress.....	132
5.	Discussion	143
5.1	The small heat shock proteins of baker's yeast.....	143
5.2	The transcriptional heat shock response.....	148
5.3	Heat stress and the proteome.....	153
5.4	X-ray tomography	155
6.	Appendix	158
6.1	Microarray data on the heat shock response	158
6.2	Proteome data on the heat stress response.....	183
7.	Abbreviations	205
8.	References	207

1. Summary

Life depends on resistance to stress, such as elevated temperature. Evolution has put forth an ancient protective mechanism, which includes the transient expression of heat shock proteins. In this thesis, the heat stress response of *Saccharomyces cerevisiae* was revisited in a detailed global approach. The transcriptional reprogramming was investigated with high temporal resolution using microarrays. Heat-induced changes on the cellular proteome and phosphoproteome were analyzed by a combination of metabolic labeling and mass spectrometry, and morphological consequences by means of X-ray tomography. These studies were carried out for two different scenarios: a mild heat shock at 37°C and a sub-lethal stress at 42°C. Bi-directional transcriptional reprogramming starts within the first minutes of stress, however, different kinetics and fold-changes of gene regulation exist. The heat shock proteins and metabolic genes of carbohydrate metabolism are most prominent among rapidly up-regulated genes, while RNA-processing and ribosome biosynthesis and assembly are among down-regulated genes. Baker's yeast adapts to a new transcriptional steady-state level under 37°C stress, but is unable to do so at 42°C, illustrating the cells need for a sustained high transcriptional response at temperatures near the upper limit of viability. X-ray microscopy on heat-stressed *S. cerevisiae* revealed that the inner cellular architecture remains intact for temperatures up to 42°C, while 50°C has profound influences on the inner morphology. Mitochondria are fragmented, cytosolic and nuclear aggregates accumulate, and the vacuoles swell. Hence, a general overview of the influences of heat stress on cellular architecture was obtained.

Furthermore, the small heat shock proteins (sHsps) Hsp26 and Hsp42 of *S. cerevisiae* were investigated. Small Hsps are ubiquitous molecular chaperones that suppress the irreversible aggregation of unfolding proteins without the need of ATP-hydrolysis. Also, they have been implicated in protein sequestration processes. Here, using synthetic genetic arrays, novel genetic interaction partners were identified and they point to an involvement of Hsp26 and Hsp42 in protein trafficking from the Golgi apparatus to the vacuole, and of Hsp42 in the protein translocation into the peroxisome. This suggests a novel role for Hsp26 and Hsp42 in protein transport in the cell. An aggregation model using reporters of non-toxic, destabilized firefly luciferase-GFP mutants reveals that disruption of both sHsps leads to a higher level of proteome stress under permissive conditions, suggesting that the sHsps contribute to cellular proteostasis also in non-stress conditions. This was also found in microarrays of the sHsp-double mutant, where higher basal transcript levels of proteasomal degradation and autophagy-related genes exist.

2. Introduction

2.1 Investigations on the small heat shock proteins of baker's yeast

2.1.1 Protein folding

Proteins represent one of the major classes of bio-macromolecules and are found in every living organism. Their existence is pivotal, not only as structural building blocks of a cell but also for every cellular process imaginable: from signal perception and transduction, cellular metabolism, and DNA replication to transcription, just to name a few. Without proteins, life could not exist. In order to fulfill their respective function, proteins must first find their way from their polypeptide chain into their unique, correct, three-dimensional fold: a process termed protein folding. In Anfinsen's pioneering experiment in the 1960s, ribonuclease A was able to refold into its native structure *in vitro* and regained its catalytic activity. This experiment demonstrated that folding is a reversible process. Furthermore, it revealed that the three-dimensional structure of a protein is based on a primary blueprint in its intrinsic amino acid sequence, thus, linking the genetic code to protein function (Anfinsen et al., 1961).

From the long linear polypeptide chain, a protein can adopt a sheer unlimited number of conformations, these being: folding intermediates, non-productive intermediates, misfolded structures, and even aggregated protein. This phenomenon is best illustrated in the folding energy landscape of a protein (Dobson and Karplus, 1999; Dobson et al., 1998). Starting from the unfolded state and localized at the topmost edge of the folding landscape, many weak non-covalent interactions must form for the protein to reach its native structure that is present at the energy minimum of the folding funnel. During its folding pathway, a protein may adopt misfolded conformations or may become trapped in local, non-native conformation and be unable to overcome the energy barrier necessary for further folding steps. Proteins may even become trapped in aggregates possibly causing serious deleterious effects on the cell (Figure 1).

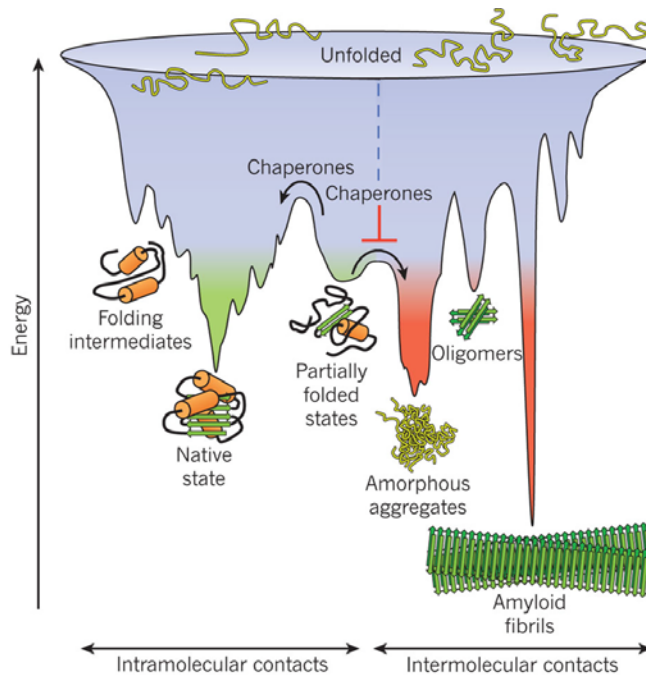


Figure 1 Scheme of the funnel-shaped, free-energy surface that proteins explore as they fold into the native state (green).

The free energy landscape is rugged, where folding proteins may become trapped in local energy minima unable to overcome the energy barrier to fold into the native structure. *In vivo*, molecular chaperones aid in guiding the folding process along the favorable downhill path. In diseases of the proteostasis system or under stress conditions, proteins may become trapped in folding intermediates, misfolded proteins or even in aggregates (red), trapping proteins in low energy state. Reprinted with the permission of the Nature Publishing Group: *Molecular chaperones in protein folding and proteostasis* © 2011 (Hartl et al., 2011).

The reversible, spontaneous folding of a protein *in vitro* may be true for a number of small proteins in low concentration and for proteins that usually fold into their functional, native structure without the help of assisting components (Jaenicke, 1987). But since more and more proteins of larger size and higher complexity have been expressed and purified, it has become clear that most polypeptide chains do not find their correct fold without the cooperation of folding assisting factors.

The Levinthal paradox illustrates the need of folding assistants (Levinthal, 1969): If a polypeptide chain of 100 aa length were allowed to randomly fold into its native structure (with two possible configurations per residue), there are 10^{30} possible conformations the polypeptide chain can obtain. Assuming a time of 10^{-11} seconds per transition from one configuration to another, it would require close to 10^{19} years to search all possible conformations. Since generation times are much shorter, e.g. bacteria 30 min and yeast 90 min to 120 min, it became obvious that folding catalysts within a cell must exist (Dobson and Karplus, 1999).

Cells in all kingdoms of life have evolved elaborate machinery that aid in the maintenance of proteostasis. This evolved machinery is not only a protective mechanism for coping with external or internal proteotoxic stressors but also an assistant in protein folding under physiological conditions. This is often referred to as the protein quality control system (Bukau et al., 2006; Kim et al., 2013; Papsdorf and Richter, 2014; Saibil, 2013). Key players of this protective machinery are the heat shock proteins, more commonly referred to as molecular chaperones. This term was introduced in the late 1970s for proteins that assist in the folding process of other proteins or prevent their irreversible aggregation under conditions of stress (Ellis 1987). A more detailed classification of stress inducible proteins, in general, and of the molecular chaperones is given later in this thesis.

Beside *de-novo* protein folding, these molecular chaperones are involved in numerous cellular processes that govern protein homeostasis, such as protein refolding, degradation, quality control, transport and trafficking, assembly and maturation, and sequestration (Hartl et al., 2011).

2.1.2 Protein folding within a cell

The intracellular surroundings differ drastically from the conditions inside an experimental test tube. In the cellular environment, where protein concentration can reach up to 200 mg/ml (Ellis, 2001) and high concentrations of other macromolecules (sugars, lipids) and ions exist, it is not surprising that this crowding effect leads to a favoring of intermolecular interactions between exposed hydrophobic stretches of proteins. This possibly results in the formation of protein aggregates (Ellis and Minton, 2006). The correct folding of a nascent polypeptide chain exiting from a ribosome into its functional native conformation is assisted by folding catalysts, such as peptidylprolyl isomerases (PPIases) and protein-disulfide isomerases (PDIs). Additionally, molecular chaperones bind to synthesized polypeptide chains, stabilizing hydrophobic, aggregation-prone intermediates, and thereby stalling off-pathway folding into unfavorable conformations (Richter et al., 2010). An alternative mode of action is that molecular chaperones provide cavities for the nascent polypeptide chains, in which unfavorable interactions are excluded and the folding process can continue or be completed (Rothman and Schekman, 2011). Examples are the bacterial chaperone trigger factor (TF), or Hsp70 associated complexes (e.g. ribosome associated complex RAC; nascent-chain-associated complex NAC) in eukaryotes. They participate in co-translational protein folding and chaperone the early folding steps. This eliminates the propensity of newly synthesized peptides to aggregate (Hoffmann et al., 2010). Chaperones

that do not associate with ribosomes, on the other hand, catalyze the later steps of protein folding.

2.1.3 Protein folding in disease

Not only freshly synthesized proteins are capable of un- and misfolding. Native proteins can also lose their correct structure under conditions of stress and are in need of ‘chaperoning’ by folding helpers. Mutations can also render a stable protein unstable and aggregation-prone, and many diseases involving the accumulation of misfolded or aggregated proteins have been identified and are often referred to as diseases of protein conformation (Morimoto, 2008). Neurodegenerative diseases, such as Huntington’s, Alzheimer’s, and Parkinson’s disease are classic examples. The accumulation of proteins with alternate unfolded and misfolded states that are highly aggregation-prone and cause toxicity is common among the diseases (Morimoto, 2008). Chaperones, therefore, are of interest as potential pharmaceutical targets and in the development of pharmaceutical strategies, because they may prevent the aggregation of mutant proteins and reduce pathological effects. Chaperones can also have an opposite effect in that a disaggregation or solubilization of aggregation-prone proteins may serve as ‘seeds’ for further protein aggregation (Chiti and Dobson, 2006). Next to neurodegenerative diseases, chaperones have also been implicated in various types of cancers. For instance, Hsp90 dictates final steps in the maturation of oncogenic kinases or transcription factors, and has moved more into the focus of pharmaceutical companies as a potential therapeutic target, with the spotlight on Hsp90 inhibitors (Neckers and Workman, 2012; Whitesell and Lindquist, 2005) .

2.1.4 Molecular chaperones and protein folding

Molecular chaperones represent the predominant class of stress-inducible proteins, and they can be further sub-classified into six different families according to their molecular weight - the Hsp100s, Hsp90s, Hsp70s, Hsp60s, Hsp40s and small heat shock proteins (sHsps) (Buchner, 1996; Richter et al., 2010). The function of molecular chaperones, as stated above, is to bind non-native polypeptides, assisting in their proper folding and transport within the cell. They accomplish this task by binding to their respective substrates transiently, never becoming part of the final structure (Lodish et al., 2000). For many of the molecular chaperones, organelle specific variants have evolved, for instance,

endoplasmatic reticulum or mitochondria specific Hsp70s. With the exception of the sHsps, all families actively contribute to protein folding in an ATP-dependent manner and hence are often referred to as ‘foldases’, in contrast to the ATP-independent sHsp-‘holdases’. Foldases, such as the Hsp70/40 system, the chaperonins (Hsp60), and the Hsp90 system, exploit the energy generated by repeated binding and hydrolysis of ATP and the release of ADP and phosphate (P). They thereby guide their individual substrates into a specific folding pathway. The hydrolysis of the nucleotide and the interaction with many other regulating co-chaperones drive the conformational changes of the multi-component foldases and switch them from high- to low-affinity states for client binding. Holdases function by binding to exposed hydrophobic regions of unfolding proteins, thus keeping those in a ‘refolding-competent state’, hindering their irreversible aggregation. This is explained in more detailed below (see chapter 2.1.6). Denaturation of proteins may occur under harmful stress conditions shifting protein homeostasis towards unfolding, and, therefore, holdases represent one of the first lines of defense under conditions that challenge proteostasis.

2.1.5 Cooperation of the chaperone systems

The different chaperone systems do not exclusively work on their own. Experiments have revealed a rather intricate interplay between them. Hsp70, the workhorse of eukaryotic chaperones, for instance, transfers substrates to the Hsp90 machinery with the help of an Hsp40 protein (Hop/Sti1). In this respect, Hsp70 catalyzes the initial folding steps of most proteins and then Hsp90 takes over for the final maturation steps of its specific ‘clients’ (Figure 2, top). Another well-researched example of chaperone cooperation lies in the interplay of Hsp104, Hsp70 and the sHsps in yeast (Figure 2, top right and bottom). Hsp104, an AAA⁺ ATPase (ATPase Associated with various cellular Activities) forms a barrel-like structure capable of disentangling misfolded protein from aggregates and is often referred to as ‘unfoldase’. In this context, Hsp70 then is the actual chaperone that returns disentangled proteins into their native conformations (Goloubinoff et al., 1999). This interplay is completed by the action of the sHsps that co-aggregate with proteins under stress conditions, capturing and maintaining them in metastable conformations necessary for the resolubilization (Haslbeck et al., 2005a).

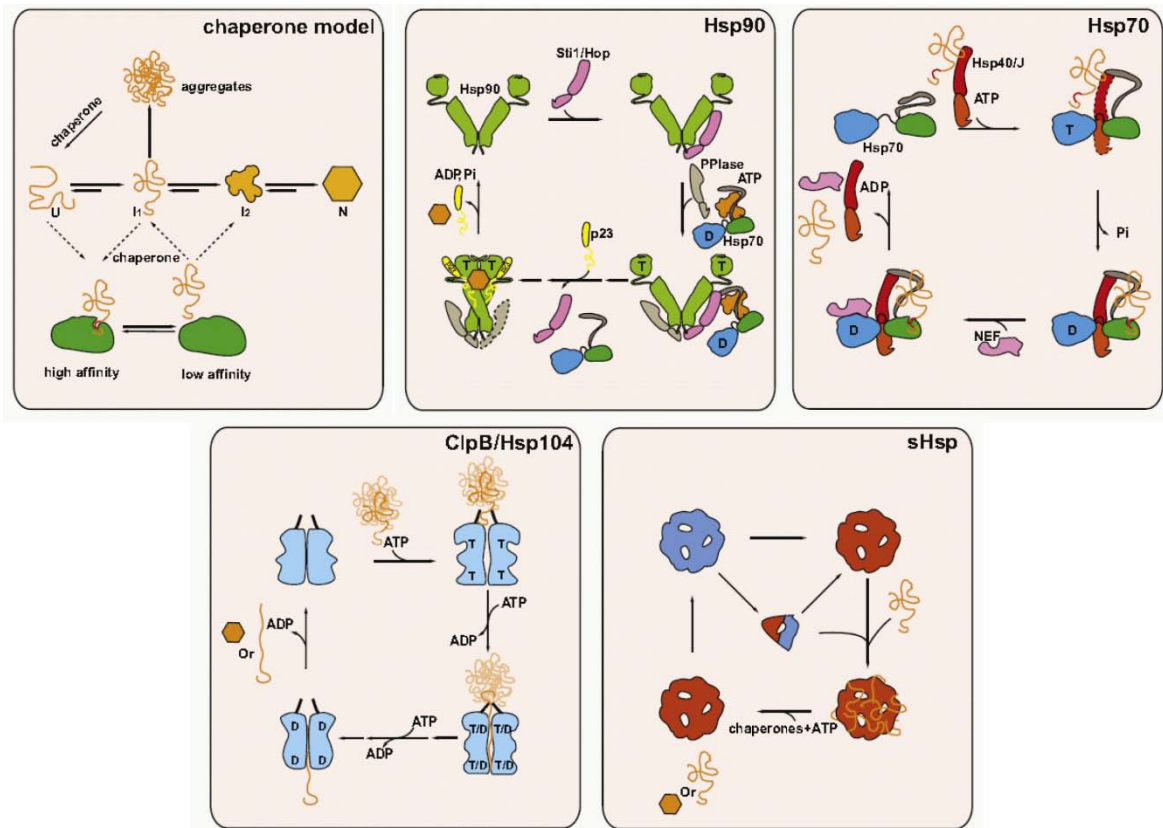


Figure 2 Effects of heat shock on the eukaryotic cell

Chaperone model: In general, proteins fold via increasingly structured intermediates (I1, I2) from the unfolded state (U) to the folded state (N). Under heat shock conditions, this process is assumed to be reversed. Molecular chaperones bind proteins in non-native conformations. The shift from the high-affinity binding state to the low-affinity release state is often triggered by ATP binding and hydrolysis.

Hsp90: In this chaperone system a large number of proteins work together. First, for a number of substrate proteins, Hsp70 delivers the substrates to Hsp90. It is not clear whether this is true for all substrate proteins and whether this also occurs under stress conditions. More than a dozen cochaperones of Hsp90 exist in eukaryotes, which seem to modulate the system. One of them, Stt1/Hop, binds both Hsp70 and Hsp90 and, at the same time, inhibits Hsp90s ATPase (in yeast). In this complex, which also contains an additional PPIase cochaperone, the substrate protein is transferred from Hsp70 to Hsp90. Stt1/Hop is released once Hsp90 binds nucleotide and a further cochaperone (p23). In contrast to other chaperones, the protein in complex with Hsp90 is assumed to be bound and released as a structured intermediate.

The Hsp70 system comprises two cochaperones, an activating protein (Hsp40/J-protein, and a nucleotide exchange factor (NEF). The activating protein can bind the non-native protein and deliver it to Hsp70. It forms a complex with Hsp70 and stimulates its ATPase. The dashed line in the Hsp70-ATP complex indicates a transient interaction. It may also modulate the conformation of Hsp70 to stabilize a substrate protein-accepting state. Hsp70 binds a stretch of seven amino acids in the substrate protein. The NEF will induce the exchange of nucleotide. This further accelerates the ATPase cycle. The substrate protein is released presumably in a non-native form.

ClpB/Hsp104: In bacteria and yeast, this chaperone is able to dissolve aggregates by actively pulling proteins through a central channel of the hexameric structure. Each protomer contains two ATPase sites, which have quite distinct characteristics concerning turnover and function. During passage through the chaperone complex, the substrate protein is unfolded. Refolding can occur upon release, and, to some extent, it can also occur in cooperation with other chaperones.

sHps are oligomeric complexes that are often activated, e.g., by heat or modifications. Many are believed to dissociate into smaller oligomers to become active. sHsps can bind many non-native proteins per complex. Release requires cooperation with other ATP-dependent chaperones, such as Hsp70.

Reprinted with the permission of Elsevier: Molecular Cell: The Heat Shock Response: Life on the Verge of Death © 2010 (Richter et al., 2010).

2.1.6 Small heat shock proteins

Small heat shock proteins are ubiquitous chaperones found in almost every living organism studied with very few exceptions identified. The pathogenic *Mycoplasma genitalium* and *Helicobacter pylori* that lack any sHsp representative are such exceptions. Their numbers range from one or two in most bacteria, archaea, and lower single-cell eukaryotes, to ten in humans and 16 in the nematode worm *Caenorhabditis elegans*. In plants this number increases. *Arabidopsis thaliana* has 19 and *Populus trichocarpa* possesses as many as 36 sHsps (Haslbeck et al., 2005b).

As molecular chaperones, their function lies in binding polypeptides or proteins in intermediate conformation and stabilizing them. They are often referred to as 'holdases' because they elicit their function without cycles of ATP-hydrolysis (Figure 2, bottom right). The chief purpose of sHsps, therefore, lies in the maintenance of the cellular protein homeostasis, and their pivotal role becomes apparent when considering that sHsps are among the most rapidly and strongly up-regulated proteins under conditions of proteotoxic stress (Stengel et al., 2010). The molecular chaperone family name already indicates that sHsps cannot be ascribed an exact molecular mass, but it lies in a weight range of 12 kDa to 42 kDa for the monomer. Yet, they can form highly dynamic, large homo- and, in some cases, hetero-oligomeric structures with up to 48 subunits (SU) reaching molecular weights close to 1 MDa. In a balanced equilibrium, sHsps are present in several different oligomeric states, and it is this highly dynamic ensemble of conformations that hinders a direct and easy approach to their structural and functional examination. Recent studies, therefore, have employed sophisticated 'hybrid-approaches', exploiting a variety of methods for the structural and functional analysis of sHsps (Braun et al., 2011).

2.1.7 Structure of small heat shock proteins

Primary Structure

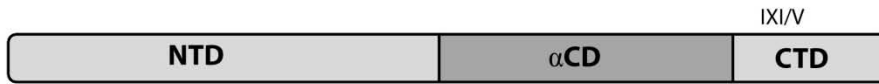
Although ubiquitous and numerous, the conservation within small heat shock proteins is not as pronounced as it is for molecular chaperones of the high molecular weight families. The common characteristic and most important benchmark for classifying a protein into the sHsp family is the central ‘ α -crystallin domain’ (α CD). The domain is derived from the well-studied mammalian sHsps: the α -crystallin family of the eye lens. A detailed, *in silico* comparison of over 8700 putative sHsps identified in a search of databases analyzed the average primary structure of sHsps (Kriehuber et al., 2010). sHsps have in common a tripartite organization: An α CD, with an average length of 96 aa, is flanked by poorly conserved N- and C-Terminal extensions with varying length and structure (Figure 3A). The N-Terminus (NTD, average 56 aa) usually is longer than the C-Terminus (CTD, average 10 aa). To show the diverse nature of the NTD, two extremes can be named: on one end, the 24 aa long NTD of *C. elegans*’ Hsp12 class proteins, and, on the other end of the spectrum, the 246 aa long NTD of Hsp42 of *S. cerevisiae* (de Jong et al., 1998). The NTD contributes most to the high variety between sHsps.

Even with their common structural arrangement - most secondary structural features are conserved -, sHsps share hardly any sequence homology. In a sequence alignment study of sHsps, few conserved residues were identified (Caspers et al., 1995; de Jong et al., 1998). One of them is the tripeptide Ile-Xxx-Ile (IXI-) motif located within the CTD, separating the CTD into ‘tail’ and ‘extension’, the latter being present mainly in higher eukaryotes.

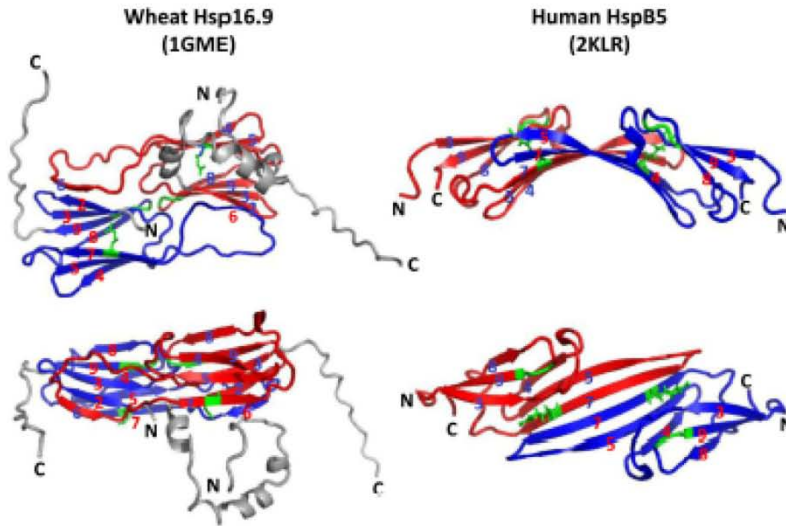
Figure 3 Structural features of small heat shock proteins.

A: Primary architecture with the variable N-Terminal Domain (NTD), the α -Crystallin Domain (α CD) and a short C-Terminal Domain (CTD) with the conserved IXI motif. B: Alpha-crystallin domain dimer structure of wheat and human. Individual monomers are colored red and blue. C: Quaternary structures of 4 exemplary sHsp oligomers, Hsp16.5, Hsp16.9, Hsp16.3 and Hsp26. The α CD-dimer localization is indicated. The blue diagrams indicate the molecular symmetry of the structure: a solid line represents the localization of a α CD-dimer. B and C reprinted with the permission of Elsevier: Small heat shock proteins and α -crystallins: dynamic proteins with flexible functions, © 2012 (E, Basha et al., 2012). (Figure on next page).

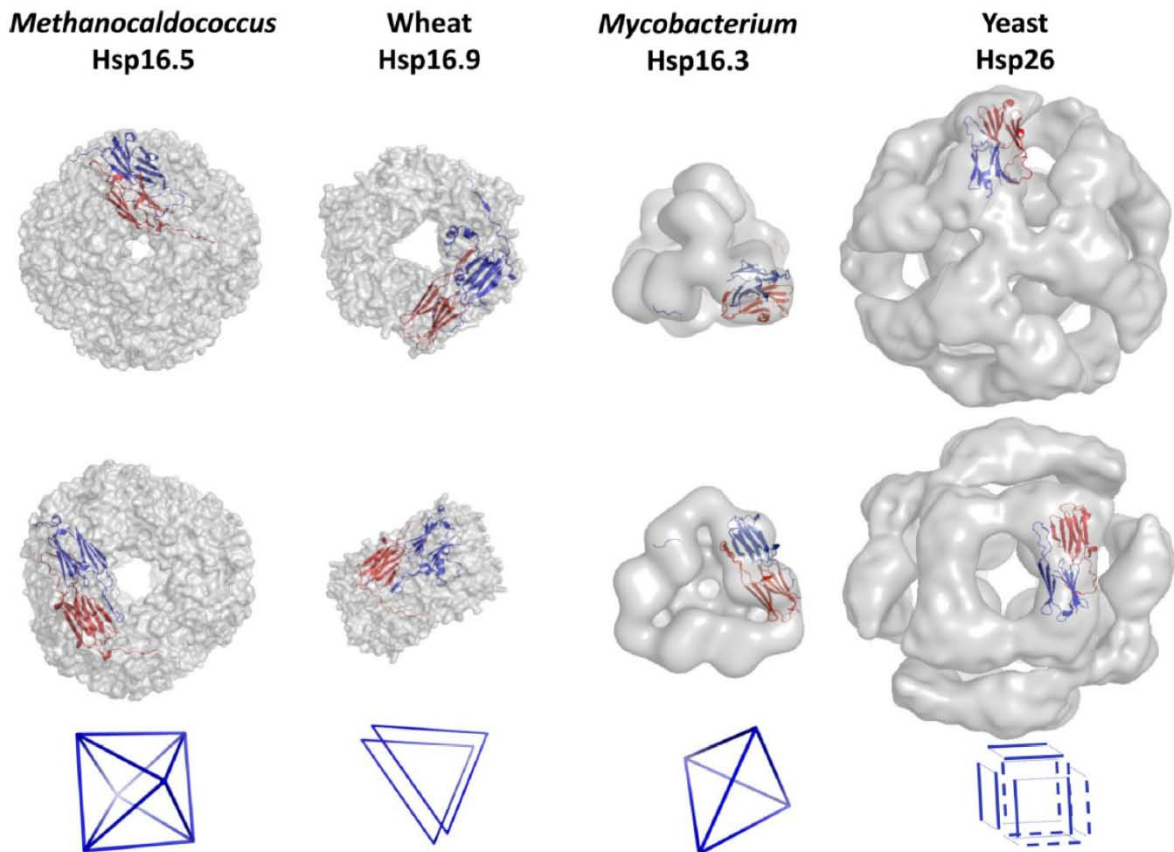
A



B



C



Dimerization and oligomerisation

Structural investigations on full-length sHsps have proven to be difficult due to the highly flexible NTDs that make their resolution by using electron microscopy (EM) a tedious affair. An additional challenge lies in the polydispersity. sHsps form a continuum of oligomeric structures with variable numbers of subunits, and they do not necessarily appear in a single defined state (Haley et al., 2000). For this reason, structural research has mainly focused on the investigation of truncated sHsps. In many cases, this research has been carried out on the isolated conserved α CD of different sHsps, since the α CD is the domain that possesses homology on the level of the primary structure, which is even augmented on the structural level.

The basic building block of sHsps is considered to be a dimer; and while there is a common immunoglobulin-like β -sheet sandwich of up to nine antiparallel β -strands, two different possible dimer interfaces have been reported. First, as is the case for bacterial, archaeal and plant sHsps, dimerisation occurs by reciprocal β 6-strand swapping into the β -sandwich of the adjacent monomer. Second, in metazoans, β 6 is fused to β 7 resulting in an elongated strand β 6+7 that, in antiparallel orientation to the β 6+7 strand of the other sHsp monomer, constitutes the dimer interface (Figure 3B).

Oligomerization is one of the key characteristics of the sHsps, but only a limited number of structures of sHsps oligomers have been resolved, two of which in high resolution by X-ray crystallography: Hsp16.9 from the wheat *Triticum aestivum* and Hsp16.5 (van Montfort et al., 2001) from the hyperthermophile archaeon *Methanocaldococcus jannaschii* (Kim, Kim, & Kim, 1998). Hsp16.5 is described as a spherical complex with 24 subunits with octahedral symmetry along with triangular and square openings into the hollow center. Hsp16.9, in contrast, is a barrel shaped dodecamer, comprised of two hexameric discs that in turn are built up of trimers of dimers (Figure 3C). These two sHsps have the following in common: Both are assembled from similar dimers and the C-Terminal extensions with their conserved IXI-motif are required for the stabilization. The difference in quaternary structure is thought to arise mainly from the highly variable NTDs and differences within the CTDs (Hilton et al., 2013).

2.1.8 Approaches to study sHsp structure

Since structural investigations on sHsp oligomers are difficult, several experimental approaches have been developed to address this issue. For instance, the dynamics of the sHsps can be measured by a Fluorescence Resonance Energy Transfer (FRET)-based

approach *in vitro* in which subunits of sHsps are labeled with donor and acceptor dyes allowing for a spectroscopic observation of subunit exchange (Peschek et al., 2013).

More recently, integrated approaches of structural biology methods have been established. Here, a combination of nuclear-magnetic resonance (NMR), solid-state NMR, structural modeling, cryo-electron microscopy (cryo-EM), small-angle-Xray scattering (SAXS), among others, are employed (Hilton et al., 2013). Information gained by one method on the structure of the monomer can then be transferred to data reporting on the oligomer, thereby selectively exploiting one method's advantages to supplement those of others. In particular, cryo-EM has been extremely helpful in analyzing polydisperse sHsps, since oligomers of different sizes can be separated and clustered during data processing.

For example, a study in the recent past used a "triple-hybrid approach" for the structural investigation of α B-crystallin (Braun et al., 2011). NMR, structural modeling, and cryo-EM were combined to obtain a pseudoatomic model of the 24mer of α B-crystallin with a 9.4 Angstrom (\AA) resolution. There, α B-crystallin forms a spherical hollow sphere.

2.1.9 The small heat shock protein system of *Saccharomyces cerevisiae*

Baker's yeast has been widely used as a eukaryotic system due to its advantages as a model organism: its short generation time (approx. 90 to 120 min under optimal conditions), easy cultivation, fully sequenced genome, easy genetic manipulability, its presence in haploid and diploid state, and the fact that it is a eukaryotic organism.

S. cerevisiae possesses a two-component small heat shock protein system, which is often the case for lower eukaryotes. Both sHsps, Hsp26 and Hsp42, are cytosolic proteins that suppress the aggregation of approx. 30% of all cytosolic proteins, and they have a 90% overlapping substrate spectrum (Haslbeck et al., 2004). They are non-essential proteins, and their gene deletion was reported not to have an influence on cell viability and temperature tolerance (Petko and Lindquist, 1986). In the following, both sHsps will be introduced briefly.

Structure and function of Hsp26 and Hsp42

Hsp26 is the smaller of the two baker's yeast sHsp and is barely expressed under physiological condition. Under conditions of stress its expression is strongly induced. Its basic primary sequence is common to the sHsps, however, the NTD of Hsp26 can be divided into an NTD and a 'middle domain (MD)' (Stromer et al., 2004). Early studies on Hsp26 revealed a temperature-induced activation process in which an Hsp26 24mer with

low chaperone activity dissociates into dimers. These dimers have the full chaperone activity *in vivo* and *in vitro* (Haslbeck et al., 1999). However, subsequent studies with a mutant Hsp26 unable to dissociate demonstrated that dissociation of the oligomer is not required for Hsp26 to obtain chaperone activity, since the oligomer retained full chaperone activity under heat stress (Franzmann et al., 2005). Therefore, structural rearrangements within the oligomers were thought to be responsible for the activation process. Indeed, a region within the MD has been found to induce conformational rearrangements in Hsp26 that change the substrate affinity from low to high. This region within the ‘middle domain’ of Hsp26 has been termed the ‘thermosensor’ and makes Hsp26 unique in its activation and regulation (Franzmann et al., 2008). The structure of Hsp26 has long been thought to be a 24mer in compact or extended conformation next to Hsp26 dimers (White et al., 2006). Recent investigations point to a more complex ensemble of different oligomeric states - similar to that observed for α B-crystallin (Braun et al., 2011). A mass spectrometry-based investigation of Hsp26 complexes, identified a main species of a 24mer next to a wide variety of other oligomeric species at room temperature. Heat stress changes the equilibrium toward monomers, dimers and even higher order oligomers with 40 SUs (Benesch et al., 2010).

Hsp42, the larger of the baker’s yeast small heat shock proteins, is less well-characterized. In contrast to Hsp26, it is constitutively expressed and active under physiological conditions, but is also up-regulated under stress. This heat-stress induced induction is even five to ten fold higher than Hsp26 on the protein level, making Hsp42 the general sHsps in the cytosol of baker’s yeast (Haslbeck et al., 2004). Structurally, Hsp42 has not yet been characterized in detail; however, negative stain electron microscopy, gel filtration and gel electrophoresis-based experiments point to a heterogeneous population of Hsp42, as is the case for other sHsps (Haslbeck et al., 2004).

Beside its role in suppression of protein aggregation under stress conditions, Hsp42 contributes to proteostasis by participating in the sequestration of proteins within the cell. Protein sequestration is sometimes looked upon as the ‘second tier’ of quality control, should refolding and degradation systems fail (Roth and Balch, 2013; Specht et al., 2011). Within the cytosol, protein aggregates can be directed to two quality control inclusions: first, the intra nuclear quality control compartment (INQ) - formerly thought be a juxtannuclear quality control compartment (JUNQ) -, where misfolded polypeptides in a detergent soluble state are collected; and secondly, the insoluble protein deposits (IPOD), located at the cell periphery for terminally aggregated proteins (Kaganovich et al., 2008;

Miller et al., 2015; Prasad et al., 2010). Hsp42 participates in the process of directing misfolded proteins towards the cell periphery but does not co-localize to the INQ. Hsp26 is not involved in this sequestration process; only as a chimeric protein with Hsp42's NTD was it able to restore the formation of peripheral aggregates in a $\Delta hsp42$ strain (Specht et al., 2011).

A recent study challenges the two-tiered quality control system of first protein refolding or degradation, followed by sequestration, where refolding or degradation fails. The study states that sequestration occurs simultaneously with protein refolding and degradation, a pathway described as the 'Q-body pathway' (Escusa-Toret et al., 2013). Therein, misfolded proteins sequester into Q-bodies that merge and coalesce into larger inclusion. Hsp42 and Hsp104 have been implicated in these steps, where the disaggregase resolubilizes proteins from present Q-bodies, and Hsp42 stimulates the addition to other Q-bodies, resulting in larger inclusions.

2.2. Revisiting the heat stress response of baker's yeast

2.2.1 A short history on the heat shock response

All organisms are constantly exposed to external stressors that are deleterious to their cells. Such stressors can be of diverse nature, including a shift in temperature, exposure to metals, toxic substances, changes in osmolarity, radiation, and many others. A common feature is that stress shifts the balance of cellular homeostasis towards protein unfolding and protein aggregation, which may have unfavorable consequences for the cell or perhaps even result in cell death. In order to cope with these different stresses, cells have obtained a remarkable molecular machinery to reduce these deleterious effects.

The heat stress response, describing the response of one cell to a shift to higher temperatures, was first identified by Ritossa in 1962 (Ritossa, 1996): An increase in temperature leads to the formation of new puffs in the giant chromosomes in the salivary glands of the fruit fly with a remarkable velocity. These puffs appeared the first minutes after exposure to heat. This chromosomal reorganization was not limited to heat, but was also induced by chemical shock (Arrigo et al., 1980; Ritossa, 1996; Tissières et al., 1974). These findings sparked further research on the heat shock response over the next decades.

The focus then soon shifted to the molecular analysis, and in 1973, it was shown that heat stress not only resulted in chromosomal structural rearrangements but coincided with an increased transcription rate (Ashburner and Bonner, 1979; Tissières et al., 1974). This linked the external stressor heat to a transcriptional response within the cell.

The effect of the thermal stress is not only limited to the level of transcription. Shortly after this finding, it was furthermore revealed that the biosynthesis of a small number of new proteins occurs with the proteins being detectable already minutes after exposure to heat (Ashburner and Bonner, 1979; Tissières et al., 1974). Here, for the first time, the term “heat shock polypeptides” or “heat shock proteins” was introduced into the field. Initially, they were named according to their apparent weight on SDS-acrylamide gels by comparison with molecular weight markers (Ashburner and Bonner, 1979). The functions of the heat shock proteins in the context of heat stress response still remained elusive. While a small number of proteins were synthesized under heat stress, it was also found that constitutively expressed proteins were actually diminished after heat stress, indicating a reduced global level of protein biosynthesis under stress conditions (Tissières et al., 1974). In the following years, studies showed the presence of these heat shock proteins in nearly every organism analyzed, i.e. *E. coli*, yeasts, chicken, plants and mammals (Lindquist,

1986), making the heat stress response an evolutionary conserved, general, protective mechanism in every living organism known. Over the decades, structural, biochemical and biophysical characterization on the heat shock proteins has gathered vast information on the heat shock response, as described in Part A of this thesis.

2.2.2 Influences of heat on the cell

Shifting an organism from their physiological temperatures to higher temperatures (a rather small increase of 5°C to 7°C being sufficient) activates the organism's heat stress response (Feder and Hofmann, 1999). Remarkably, not only mesophilic organisms, such as yeast, are exposed to thermal stress but also hyperthermophiles, such as *P. occultum*, an archaeobacteria found near deep-sea hydrothermal vents and existing in temperatures from about 80°C to 105°C (Parsell and Lindquist, 1993; Phipps et al, 1991).

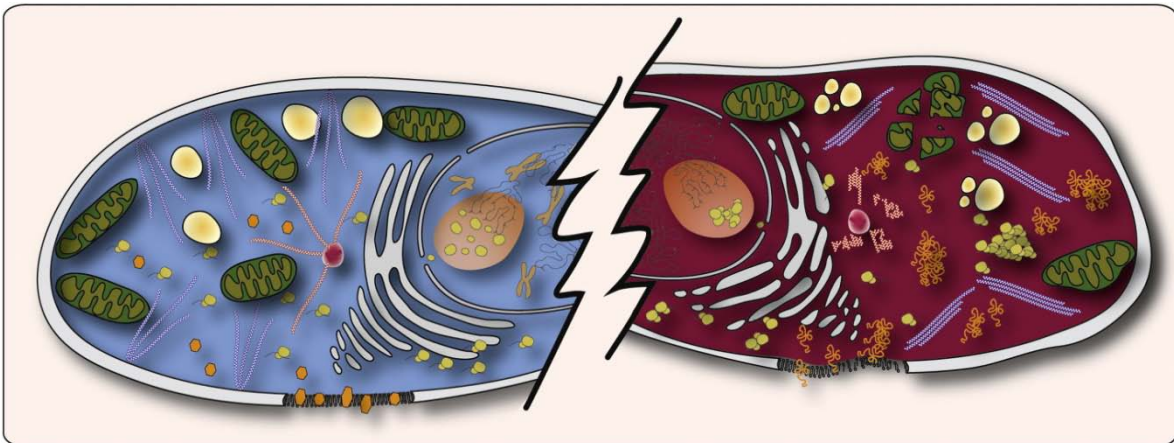


Figure 4 Effects of heat shock on the organization of the eukaryotic cell.

*An unstressed eukaryotic cell (left) is compared to a cell under heat stress (right). Heat stress leads to damage to the cytoskeleton, including the reorganization of actin filaments (blue) into stress fibers and the aggregation of other filaments (microtubuli, red). Organelles like the Golgi and the endoplasmic reticulum (white) become fragmented and disassemble. The number and integrity of mitochondria (green) and lysosomes (yellow-white gradient) decrease. The nucleoli, sites of ribosome (yellow) assembly, swell, and large granular depositions consisting of ribosomal proteins become visible. Large depositions, the stress granula (yellow), resulting from assemblies of proteins and RNA, are found in the cytosol in addition to protein aggregates (hexagonal versus spaghetti style, orange). Finally, there are changes in the membrane morphology, aggregation of membrane proteins, and an increase in membrane fluidity. Together, all these effects stop growth and lead to cell-cycle arrest as indicated by the noncondensed chromosomes in the nucleus. Reprinted with the permission of Elsevier: *Molecular Cell: The Heat Shock Response: Life on the Verge of Death* © 2010 (Richter et al., 2010).*

Heat shock does not only result in protein misfolding and potential aggregation, but it has numerous deleterious effects on cellular organization (Figure 4). A drastic effect of heat, especially in eukaryotic cells, is a fragmentation of the cytoskeleton with mild heat stress resulting in the reorganization of actin filaments into stress-fibers. Severe thermal stress can lead to a complete collapse of the cytoskeleton due to aggregation of filament-forming proteins. Also, cellular organelles are affected: the endoplasmic reticulum (ER) and Golgi system can fragment, which results in an improper posttranslational modification and transport of proteins. Furthermore, mitochondria fragment and their number decreases, as do the numbers of lysosomes (Richter et al., 2010). The influence of heat on the integrity and number of mitochondria has severe effects on the ATP-levels of the cell, which have been found to drop rapidly upon heat stress (Patriarca and Maresca, 1990).

Nuclear structures and components also suffer detrimental effects of heat stress. For instance, RNA-splicing events are affected, and nucleoli - sites of ribosome assembly – swell. Nuclear granular deposits appear, aggregates composed of incorrectly processed ribosomal RNAs and ribosomal proteins (Lindquist, 1980; Yost & Lindquist, 1986). Additionally, in the cytosol, stress granules are formed consisting of (non-translating) mRNAs, proteins of the translation initiation machinery and others (Grousl et al., 2009; Richter et al., 2010). As a consequence, this hijacks translational components, resulting in a global reduction in translation, one of the early hallmarks of the heat shock response (Ashburner and Bonner, 1979). Upon recovery, the mRNAs sequestered into stress granules, can be redistributed in the cytosol and associate with ribosomes for translation (Grousl et al., 2009).

Cellular membranes may be affected, with alterations in their lipid composition, as well as the lipid-to-protein ratio, resulting in a changed fluidity and permeability. This, in turn, allows small molecules and ions to pass uncontrolled, with severe impact on the cytosolic pH and ion homeostasis (Piper, 1995; Verghese and Morano, 2012).

All these factors taken together make it clear, that upon (heat) stress, the ordinary growth and proliferation are severely affected, and cells may arrest their cell cycle until the stress has subsided or cells have adapted (Verghese et al., 2012). In the worst-case scenario, cellular defense mechanisms are incapable of repairing or buffering the stress-induced effects, and cell death may be the consequence. In summary, (heat) stress has a multitude of effects on the cell that go beyond simple protein unfolding and initiation of a transcriptional response.

2.2.3 Transcriptional heat shock response

The heat shock response, in general, describes the initiation of transcription for a set of target genes (in the range of roughly 50 to 200) depending on the organism studied. The stress inducible proteins encoded by these genes were recently grouped into seven distinct protein classes, depending on their individual function. The groups are: (I) Molecular chaperones as the main representatives (see 2.1.4); (II) proteins involved in metabolism; (III) DNA/RNA repair; (IV) protein degradation; (V) transport; (VI) cell organization and (VII) gene regulation. These groups have been the subject of a review in the recent past (Richter et al., 2010). All these proteins serve to protect cells from above-mentioned, stress-induced, deleterious effects and contribute to processes, such as protein (re-)folding, DNA repair, the proteolytic machinery, reorganization of cellular metabolism, guaranteeing cellular integrity, proteostasis and sub-cellular organization (Richter et al., 2010).

Regulation of the heat stress response

After the discovery of the heat shock response, it became clear rather quickly that a transcription factor must be responsible for governing the rapid expression of heat shock genes, occurring within minutes after onset of stress. In bacteria, sigma factor σ_{32} , an alternative regulatory subunit of the RNA-polymerase complex, was identified as mediating the transcriptional heat stress response (Gross and Craig, 1987). For eukaryotes, Hsf1 was identified as the primary transcriptional regulator of the heat stress response (Wu, 1985). Vertebrates have four homologs of Hsf1 with three of them proposed to have regulatory and modulatory functions for Hsf1. Invertebrates, such as baker's yeast, possess only one essential copy of Hsf1 (Anckar and Sistonen, 2011; Wu, 1995).

Hsf1 binds to specific DNA sequences (termed the heat shock elements, HSEs) with a repeat of the pentanucleotide -nGAAn- in the promoter of target genes. This consensus sequence was first described as a triple-inverted repeat of the pentamer (coined 'canonical HSE') to which a trimer of Hsf1 binds (Sorger and Pelham, 1988). Later it was shown that Hsf1 is also capable of activating the transcription of genes that do not contain the canonical HSE in their promoter. In those cases, a 'non-canonical' variant of the binding site, consisting of two -nGAAn- repeats, a pentameric spacer followed by another -nGAAn- repeat, was identified as a Hsf1 binding site (Tamait et al., 1994). Since then, more variants of HSEs have been reported in yeast, and the three most common ones are listed below (Table 1). The existence of different consensus sequences adds complexity to

the level of transcriptional regulation, since they were shown to be targeted differently for Hsf1 binding (Morano et al., 2012).

Table 1 HSE consensus sequences

Type	Consensus sequence	Examples
Perfect-type	nnGAAAnnTTCnnGAAAnn	HSP26, HSP104, SSA1
Gap-type	nnGAAAnnTTCnnnnnnnnGAAAnn	HSP82, CPR6, CUP1
Step-type	nnGAAAnnnnnnnnnGAAAnnnnnnnnnGAAAnn	HSP12, YDJ1, SSA3

Hsf1-regulation by chaperones

The question of how Hsf1 regulation occurs has long been puzzling. Some studies indicate structural rearrangements within the protein, induced by temperature shift. Others favored additional factors interacting with Hsf1 responsible for its regulation. Commonly, under non-stressful conditions, Hsf1 has been found as an inactive monomer in the cytosol and nucleus unable to bind DNA and activate transcription. Under conditions of proteostatic stress, Hsf1 is enriched in the nucleus, trimerizes, is post-translationally modified, and obtains its' activity as a transcription factor (Akerfelt et al., 2010; Anckar and Sistonen, 2011). In a common model of chaperone-mediated regulation of Hsf1 activity, the cellular proteostasis system is linked to the transcriptional heat shock response. Under permissive conditions, Hsf1 is bound by several proteins, such as Hsp70, Hsp90 and other cochaperones, keeping Hsf1 in an inactive, monomeric complexed state in the cytosol. Upon thermal stress, the equilibrium of proteostasis is shifted towards protein misfolding, and Hsf1-complexed chaperones are titrated towards binding stress-induced unfolded proteins. As a consequence, inactive monomeric Hsf1 is released, trimerizes and enters the nucleus where it binds to HSE repeats and activates the transcription of heat shock genes (Anckar and Sistonen, 2011; Morimoto, 1998; Richter et al., 2010). After stress subsides or cells have adapted to the stress, the amount of unfolded proteins diminishes, and Hsp90 and Hsp70 are free again to bind Hsf1. This yields a stop to the transcriptional response.

The heat-inducible trimerization with the subsequent transport into the nucleus and the coinciding DNA-binding capacity is not present in *S. cerevisiae*. Here, even under normal growth conditions, Hsf1 is DNA-bound in the trimeric state, but without transcriptional activity (Morano et al., 2012). The question arises: How do chaperones serve as Hsf1-repressors within this context? Hsp70 and Hsp90 have both been shown to be able to localize to the nucleus, where they can bind to DNA-bound Hsf1 trimers and block the transactivation domain, rather than the regions necessary for trimerization. This would suggest, that accumulating misfolded proteins in the cytosol, leads to a depletion of the

nuclear pools of Hsf1-inhibiting Hsp70 and Hsp90, which in turn frees the Hsf1-trimers' activity as a transcription factor (Morano et al., 2011; Trott and Morano, 2003).

Hsf1-regulation via posttranslational modifications (PTMs)

The trimeric state and interaction with chaperones are not the sole mediators of Hsf1 activity. A variety of posttranslational modifications have also been identified to modulate Hsf1 activity. Hsf1 is highly phosphorylated even under non-stress conditions; and, by the action of phosphatases and kinases that catalyze the addition or hydrolysis of phosphate residues on multiple P-sites, Hsf1 activity can be fine-tuned. Further, PTMs include sumoylation, ubiquitinylation, and acetylation, that are thought to contribute to activating or repressing the functional activity of Hsf1 (Akerfelt et al., 2010; Morano et al., 2011; Richter et al., 2010).

2.2.4 Crosstalk of stress responses

Not only heat shock elicits a transcriptional response, but also other challenging conditions result in changes on the transcriptome. Studies display a stereotypical regulation of roughly 14% of the baker's yeast genome to a diverse set of stress conditions, including H₂O₂, menadione, diamide, starvation, hyperosmotic shock, DTT, and heat shock (Causton et al., 2001; Gasch, 2002; Gasch et al., 2000; Roy et al., 2013). This shows that stress can be of various kinds, to elicit a specific stress response, but it also yields a transcriptional regulation of a common protective mechanism. Hence, a high degree of cross-talk among the diverse stress response mechanisms exists as well as a functional overlap of the protective apparatus of the cell. In this context, the transcription factor Msn2/4, composed of Msn2 and Msn4, must be mentioned, a regulator coined the mediator of the 'general stress response' (Estruch, 2000; Morano et al., 2012). This TF has been shown to regulate transcription not only to heat shock, but also to nutrient starvation, osmotic shock, oxidative stress, low pH, and others (Martinez-Pastor et al., 1996). Comparable to the HSEs for Hsf1, a DNA binding sequence for Msn2/4 is known: a pentamer of 5'-CCCCT-3', commonly referred to as the stress response element (STRE) (Martinez-Pastor et al., 1996). In many cases, genes possess consensus sequences in their promoters for more than one transcriptional regulator. This explains their transcriptional regulation under different stress response programs. Hence, the heat shock response is not only an Hsf1-mediated response, but also the contribution of other genetic regulators must be considered.

2.3. Objective

The cellular response to heat shock had been discovered nearly 50 years ago and, subsequently, a basic description of the genes involved was presented. However, the focus then shifted to the characterization of the key players involved, the heat shock proteins. An exact and comprehensive analysis of the heat stress response is still lacking. Here, the heat shock response of *Saccharomyces cerevisiae* was re-addressed in a detailed global approach. The transcriptional reprogramming of the cells to two different heat shock scenarios - mild stress at 37°C and sub-lethal stress at 42°C - was to be investigated with high temporal resolution using state-of-the-art microarrays. In the next step, using a combination of metabolic-labeling and mass-spectrometry, the influence of heat stress on the cellular proteome and phosphoproteome was to be addressed. The changes on mRNA level were to be correlated to changes on the proteome. Furthermore, the consequences of heat shock on the cellular morphology were to be investigated by X-ray microscopy. In the next step, above-mentioned studies were expanded to selected knock-out yeast strains and the consequences of gene deletions on the heat stress response were to be assessed.

A second objective of this thesis was to gain more insight on the function of the small heat shock proteins (sHsps) of *S. cerevisiae*, Hsp26 and Hsp42. sHsps are ubiquitous molecular chaperones that act without ATP-hydrolysis. Their main function lies in the suppression of irreversible protein aggregation but they have also been shown to participate in protein sequestration. With synthetic genetic arrays, novel genetic interaction partners of Hsp26 and Hsp42 were to be identified, with the goal of detecting cellular pathways or processes with an unknown function of the sHsps. In addition, their role in protein quality control and cellular proteostasis was to be addressed in models of protein aggregation. In a non-toxic model of firefly luciferase aggregation, the level of cellular proteome stress was to be estimated and in the toxic poly-glutamine aggregation model, the role of the small heat shock proteins in the aggregation process was to be investigated. Furthermore, the heat stress response in the sHsp-double deletion strain was to be monitored kinetically.

3. Materials and methods

3.1 General equipment and expendable items

All expendable items, such as falcon tubes, reagent tubes, pipette tips, petri dishes etc. were purchased from Roth, Sigma, Merck or Eppendorf unless otherwise stated.

Table 2 List of general equipment

Apparatus	Manufacturer
Gel Documentation	
ImageQuant LAS4000	General Electric
ImageQuant 300	General Electric
Image Scanner III	General Electric
BioDocII	Biometra
Scanner Powerlook1120	Umax
Centrifuges	
Benchtop centrifuge 5415R, 5418	Eppendorf
Benchtop centrifuge 5418R (Rotor FA-45-18-11)	Eppendorf
Avanti J25 and J26 XP (Rotors JA-10, JA25.50)	Beckman
Rotina 420R	Hettich
Max E Ultracentrifuge (swing out rotor MLS50)	Optima
PCR Equipment	
Thermal Cycler MJ Mini	Biorad
Thermal Cycler T100	Biorad
Thermal Cycler Primus, Primus25	Peqlab
Power Supply EPS 601	General Electric
Agarose Gel Running Chamber HU10	AlphaMetrix Biotech
Chromatography Systems	
ÄKTA FPLC	General Electric
AKTA Prime	General Electric
Frac900/950 fraction collectors	
HPLC System (PU-1580, UV-1575, FP-1520, AS-950, LG-980-02S)	Jasco
HPLC System Prominence (LC-20AT, SPD-20A, RF-10AXL-FRC-10A, DGU-20AS, SIL20AC)	Shimadzu
Superloops (various sizes)	GE Healthcare
Sterilization Equipment	
Autoclav Varioclav EP-Z	H+P
Autoclav La-MCS-203	Sanoclav
Sterilization Incubator BM 500	Memmert
UV Spectrometers	
Ultrospec 1100pro, - 3100pro	Amershan Biosciences
Varian Cary50 / Cary 100	Agilent
NanoDrop2000	Thermo Scientific
Scales	
Scale BL1500S	Sartorius

Apparatus	Manufacturer
Precision scale SI-234	Denver Instruments
Microscopes & Equipment	
Glass slides	Marienfeld
Superfrost microscope slides	Thermo Scientific
Cover glass	Thermo Scientific
Axiovert 200 inverted microscope	Carl Zeiss
C4742-95 camera	Hamatsu
Immersion oil	Various sources
Synthetic Genetic Array	
Biomek FX 384 pin robot	Beckman
Microplate carousel	Thermo Scientific
Petri dishes	Sigma
Omnitray dishes	Nunc
Diverse Equipment	
Ice machine	Zieger
Western Blotting Apparatus Fasblot B34	Biometra
SDS-PAGE Running Chamber (Mighty Small II Deluxe)	Serva
Pipettes 'Research' (2.5, 10, 20, 200, 1000, 5000 μ l)	Eppendorf
Incubator WB120	Mytron
Temp.-Gradient Unit TGGE MAXI System	Biometra
Waterbath SW22	Julabo
Thermomixer compact,- comfort	Eppendorf
Vortexer REOX control	Heidolph
Magnetic Stirrer MR3001	Heidolph
Cell disruption apparatus BasicZ	Constant Systems
Bead Mill MM-400	Retsch
Orbitrap Fusion Mass Spectrometer	Thermo Scientific
Soft X-ray Tomography Equipment	
Dewars various sizes	Isotherm KGW
Dry shipper BS2002	Cryoson
X-ray microscope U41-TXM	BessyII Helmholtz Zentrum Berlin
Inverted tweezers style N5	DuMont
PAP pen liquid blocker	Sigma
Plunge freezer	Self-made by chair of EM; TUM
Grids HZB-2A-Copper	Gilder Grids
Plasma cleaner	Blazers
Holey carbon film R2/4	Quantifoil
Cryo transfer holder 626	Gatan

3.2 Chemicals

Table 3 List of chemicals

Chemical	Distributor
2-Mercaptoethanol (β -ME)	Sigma
4',6-Diamidin-2-phenylindole (DAPI)	Sigma
5,5'-Dithiobis(2-nitrobenzoic acid) (DTNB)	Sigma
Acetic acid	Roth
Acrylamid/Bis solution 38:2 (40% w:v)	Serva
Adenosin-5'-triphosphate (ATP) disodium salt	Roche
Agar Agar	Serva
Agarose	Serva
Amino acids	Sigma
Ammonium persulfate (APS)	Roth
Ampicillin sodium salt	Roth
Azetidin-2-carbonic acid (ACS)	Bachem
Bacto-pepton	BD Biosciences
Bacto-trypton	BD Biosciences
Canavanine	Bachem
Coomassie Brilliant Blue R-250	Serva
Deoxynucleoside triphosphates (dNTPs)	Roche
Difco Nutrient Broth	BD Bioscience
Dimethyl sulfoxide (DMSO)	Sigma
Dithiothreitol (DTT)	Roth
Ethidium bromide	Sigma
Ethylenediaminetetraacetic acid (EDTA)	Merck
Galactose	Merck
Geneticin G418	Roth
Glucose	Merck
Glutathione, oxidized (GSSG)	Sigma
Glutathione, reduced (GSH)	Sigma
Glycerol	Roth
Imidazole	Sigma
Isopropyl β -d-1-thiogalactopyranoside (IPTG)	Serva
Kanamycin sulfate	Roth
L-Arginine:HCl (13C6, 99%)	Cambridge Isotope Laboratories, Inc
L-Arginine:HCl (U-13C6, 99%; U-15N4, 99%)	Cambridge Isotope Laboratories, Inc
L-Lysine:2HCl (4,4,5,5,-D4, 96-98%)	Cambridge Isotope Laboratories, Inc
L-Lysine:2HCl(U-13C6, 99%; U-15N2, 99%)	Cambridge Isotope Laboratories, Inc
LB ₀ medium	Serva
Milk powder	Roth
Monosodium glutamate (MSG)	Roth
N-(2-Hydroxyethyl) -piperazine-N'-2 ethane-sulfonic acid (HEPES)	Roth
N,N,N',N'-Tetramethylethylenediamine (TEMED)	Roth
Noble Agar	BD Bioscience
Nourseothricin	Jena Bioscience
Oxaloacetic acid	Sigma

Chemical	Distributor
Phenylmethanesulfonyl fluoride (PMSF)	Sigma
Phosphatase Inhibitor Cocktail 2	Sigma
Phosphatase Inhibitor Cocktail 3	Sigma
Phosphoenolpyruvate (PEP)	Sigma
Polyethylene glycol 4000 (PEG-4000)	Sigma
Potassium chloride	Roth
Protease inhibitor Mix FY, G, HP, M	Serva
Radicicol	Roth
S-2-aminoethyl-L-cysteine (AEC)	Bachem
Single Stranded DNA (Salmon testis)	Sigma
Sodium chloride	Roth
Sodium dodecylsulfate (SDS)	Serva
Sodium fluoride (NaF)	Sigma
Sodium orthovanadate (Na ₃ VO ₄)	Sigma
Stain G	Sigma
Tetracycline	Roth
Tris(2-carboxyethyl)-phosphine (TCEP)	Pierce
Tris-(hydroxylethyl)-aminomethane (TRIS)	Roth
Tween-20	Merck
Yeast Nitrogen Base (YNB) w/o aa	BD Bioscience
YNB w/o aa & ammonium sulfate	BD Bioscience
2-Mercaptoethanol (β -ME)	Sigma
4',6-Diamidin-2-phenylindole (DAPI)	Sigma
5,5'-Dithiobis(2-nitrobenzoic acid) (DTNB)	Sigma

3.3 Software, databases & web-based tools

Table 4 Software, databases and web-based tools

Program	Source
DAVID Bioinformatics Resources	http://david.abcc.ncifcrf.gov/
Blast	https://blast.ncbi.nlm.nih.gov/Blast.cgi
Saccharomyces genome database	http://www.yeastgenome.org/
Saccharomyces regulator database	http://www.yeastgenome.org/
GO Term Finder	http://www.yeastgenome.org/
GO Slim Mapper	http://www.yeastgenome.org/
SPELL database	http://spell.yeastgenome.org/
Expasy	http://www.expasy.org
Expasy ProtParam	http://web.expasy.org/protparam/
Yeasttract database	http://www.yeasttract.com/
Mendeley citation program	Version 1.3.1. Mendeley Ltd. © 2008
HPLC Software	
ChromNav	Version 2.0, Jasco © 2014
LabSolutions	Version 5.6, Shimadzu, © 2015
Word; Excel	Microsoft Office Package 2007
BioEdit	© 1997-2013 Tom Hall

Program	Source
Image Processing Software	
Illustrator CS4	Adobe 14.0.0. © 2008
ImageJ	1.43m Wayne Rasband NIH, USA
X-ray Tomography Software	
Cygwin Bash Shell	Red Hat, Inc © 2013
IMOD/ etomo	Version 4.5.7; © 2010 Boulder Laboratory for 3-Dimensional Electron Microscopy of Cells & the Regents of the University of Colorado
Cytoscape	Version 3.2.1. © 2001-2015 Cytoscape Consortium
Origin	Version 8.1, © OriginLab Corporation
String10 database	http://string10-db.org/

3.4 Oligonucleotides and plasmids

Oligonucleotides

Table 5 Oligonucleotides. All oligos were synthesized by MWG Eurofins.

Name	Sequence (5'-3')
NatMX-fw	CCATGGGTACCCTCTTGACG
NatMX-rev	GATTAGGGGCAGGGCATGC
Msn2-NatMX-fw	TCTTTCTTTTTCACCTTTTATTGCTCATAGAAGAACTAGATCT AAAATGCGTACGCTGCAGGTCGAC
Msn2-NatMX-rev	AATTATCTTATGAAGAAAGATCTATCGAATTAATAAAAAATGGGGT CTATTAATCGATGAATTCGAGCTCG
Msn4-NatMX-fw	TTATCAGTTCGGCTTTTTTTCTTTTCTTCTTATTAATAACAAT ATAATGCGTACGCTGCAGGTCGAC
Msn4-NatMX-rev	CATACCGTAGCTTGTCTTGCTTTTATTTGCTTTTGACCTTATTT TTTTCAATCGATGAATTCGAGCTCG
Hsp26-NatMX-fw	TAAAACAGGTATCCAAAAAGCAAACAAACAACTAAACAAATT AACATGCGTACGCTGCAGGTCGAC
Hsp26-NatMX-rev	CAACAATGGTCCCTCGGAGAGGGACAACACTATAGAGCCAGGTC ACTTTAATCGATGAATTCGAGCTCG
Hsp42-NatMX-fw	CAATTGTCCATATCCACACAAATTAAGATCATACCAAGCCGAA GCAATGCGTACGCTGCAGGTCGAC
Hsp42-NatMX-rev	TATTATAAATATAAATGTATGTATGTGTGTATAAACAGATACGA TATTCATCGATGAATTCGAGCTCG
NatMX-ctr-rev	ACGAGACGACCACGAAGCC
Msn2-ctr-fw	GCGTAAACCGTGTTCCC
Msn4-ctr-fw	GCGCATTGCTATTCTCCGG
26NatDelctr_fw	CCCCTAAAGAACCTTGCCCTG
42NatDelctr_fw	GCTTTCCCTATCAGCCGCTC
Hsp26-His3-fw	GATATATCAGATCTCTATTAAAACAGGTATCCAAAAAGCAAAC AAACAACTAAACAAATTAACATGTCAATTTTAGCCTAGAATGTA CGTGAGCGTATTTT
Hsp26-His3-rev	GTTTCAAGCCATATGCAAGCAACAATGGTCCCTCGGAGAGGGAC AACACTATAGAGCCAGGTCACTTTAGTTACCGTTATTTCTGGCA

Name	Sequence (5'-3')
	CTTCTTGTTTT
Hsp42-Ura3-fw	CATAGGGACACGTTTCAGGCAATTGTCCATATCCCACACAAATTA AGATCATACCAAGCCGAAGCAATGAGTTTTTTAGCGGTAATCTCC GAGCAGAAGG
Hsp42-Ura3-rev	GAAATTTTAACGCTTATTATAAATATAAATGTATGTATGTGTGT ATAAACAGATACGATATTTCAATTTTCCATTACGACCGAGATTCC CG
SpeI-EGFP_fw	CTAGTACTAGTATGGTGAGCAAGGGCGAG
Fluc_fw_SpeI	CTAGTACTAGTATGGAAGACGCCAAAAACATAAAGAAAGGC
GFP_rev_HindIII	TCCATAAGCTTTTACTTGTACAGCTCGTCCATGCCG
Fluc_rev_HindIII	TCCATAAGCTTTTACACGGCGATCTTTCCGCC

Plasmids

Table 6 List of plasmids

Plasmid	Comment	Origin
pAG25 (pNATMX)		(Goldstein and McCusker, 1999)
p425GPDLeu		ATCC
p426GPDUra		ATCC
p423GPDHis		ATCC
p415GPDLeu		ATCC
pCneoFluc	wt, single mutant (SM) and double mutant (DM) sequence of firefly luciferase)	(Gupta et al., 2011)
pCneoFluc-EGFP	wt, single mutant and double mutant sequence of firefly luciferase	(Gupta et al., 2011)
p425GPDLeu-FlucWT p425GPDLeu-FlucWT-EGFP	p425GPDLeu with FlucWT or FlucWT-EGFP inserted using restriction sites <i>SpeI</i> and <i>HindIII</i>	This work
p425GPDLeu-FlucSM p425GPDLeu-FlucSM-EGFP	p425GPDLeu with FlucSM or FlucSM-EGFP inserted using restriction sites <i>SpeI</i> and <i>HindIII</i>	This work
p425GPDLeu-FlucDM p425GPDLeu-FlucDM-EGFP	p425GPDLeu with FlucDM or FlucDM-EGFP inserted using restriction sites <i>SpeI</i> and <i>HindIII</i>	This work
p425GPDLeu-YFPQ0		(Kaiser et al., 2013)
p425 GPDLeu-YFPQ56		(Kaiser et al., 2013)
p425 GPDLeu-mCherryQ0		(Kaiser et al., 2013)
p425GPDLeu-mCherryQ56		(Kaiser et al., 2013)

3.5 Bacterial and yeast strains

Bacterial strains

Table 7 Bacterial strains

Strain	Genotype	Origin
BL21 (DE3) codon plus	F ⁻ ompT hsdS(rB ⁻ mB ⁻) dcm ⁺ Tetr gal endA Hte [argU proL Camr]	Stratagene
DH5α	F ⁺ ϕ 80dlacZΔM15 Δ(lacZYA-argF) U169 recA1 endA1 hsdR17(r _k ⁻ m _k ⁺) phoA supE44 λ ⁻ thi-1 gyrA96	Invitrogen
Mach1 T1R	F ⁻ Φ80lacZΔM15 ΔlacX74 hsdR(rK ⁻ , mK ⁺) ΔrecA1398 endA1 tonA	Invitrogen
XL1-Blue	recA1 endA1 gyrA96 thi-1 hsdR17 supE44 relA1 lac	Stratagene

Yeast strains

Table 8 *Saccharomyces cerevisiae* strains

Strain	Genotype	Origin
BY4741	MATa, <i>his3Δ1</i> , <i>leu2Δ0</i> , <i>met15Δ0</i> , <i>ura3Δ0</i>	Euroscarf
BY4741 <i>hsp26Δ</i> (I)	BY4741; YBR072Δ:: <i>his3</i>	This work
BY4741 <i>hsp26Δ</i> (II)	BY4741; YBR072wΔ:: <i>natMX4</i>	This work
BY4741 <i>hsp42Δ</i> (I)	BY4741; YDR171wΔ:: <i>ura3</i>	This work
BY4741 <i>hsp42Δ</i> (II)	BY4741; YDR171wΔ:: <i>natMX4</i>	This work
BY4741 <i>hsp42-GFP</i>	BY4741; YDR171w-GFP, <i>his3MX</i>	(Huh et al., 2003)
BY4741 <i>hsp26-GFP</i>	BY4741; YBR072w-GFP, <i>his3MX</i>	(Huh et al., 2003)
Y2454	MATa, <i>mfa1Δ::MFA1pr-HIS3</i> , <i>can1Δ</i> , <i>ura3Δ0</i> , <i>leu2Δ0</i> , <i>his3Δ1</i> , <i>lys2Δ0</i>	(Tong et al., 2001)
Y2454 <i>hsp26Δ</i>	Y2454, YBR072wΔ:: <i>natMX4</i>	This work
Y2454 <i>hsp42Δ</i>	Y2454, YDR171wΔ:: <i>ura3</i>	This work
Y2454 <i>hsp26Δ hsp42Δ</i> (I)	Y2454; YBR072w:: <i>his3</i> , YDR171wΔ:: <i>ura3</i>	This work
Y2454 <i>hsp26Δ hsp42Δ</i> (II)	Y2454, <i>hsp26Δ::natMX4</i> YDR171wΔ:: <i>kanMX4</i>	This work
BY4741 <i>sko1Δ</i>	BY4741, Mata, <i>his3Δ1</i> , <i>leu2Δ0</i> , <i>met15Δ0</i> , <i>ura3Δ0</i> , YNL167c:: <i>kanMX4</i>	Euroscarf
BY4741 <i>rpn4Δ</i>	BY4741, Mata, <i>his3Δ1</i> , <i>leu2Δ0</i> , <i>met15Δ0</i> , <i>ura3Δ0</i> , YDL020c:: <i>kanMX4</i>	Euroscarf
BY4741 <i>hsp12Δ</i>	BY4741, Mata, <i>his3Δ1</i> , <i>leu2Δ0</i> , <i>met15Δ0</i> , <i>ura3Δ0</i> , YFL014w:: <i>kanMX4</i>	Euroscarf
BY4741 <i>msn2Δ</i>	BY4741, Mata, <i>his3Δ1</i> , <i>leu2Δ0</i> , <i>met15Δ0</i> , <i>ura3Δ0</i> , YMR037c:: <i>kanMX4</i>	Euroscarf
BY4741 <i>msn2Δ msn4Δ</i>	BY4741, <i>msn2Δ::kanMX4</i> YKL062w:: <i>natMX4</i>	This work
YAL6B	BY4741, MATa, <i>his3Δ1</i> , <i>leu2Δ0</i> , <i>met15Δ</i> , <i>ura3Δ0</i> , <i>lys1::kanMX6</i> , <i>arg4Δ::kanMX4</i>	(Gruhler et al., 2005)

3.6 Media and antibiotics

All media was sterilized by autoclaving for 30 min at 121°C. All amino acid and antibiotic stock solutions were passed through a 0.22 µm sterile filter, distributed to 2 ml aliquots and stored at -20°C. Multiple freeze-thaw cycles were avoided.

Table 9 Media and compositions

Medium name	Composition	Concentration
Standard <i>E.coli</i> Cultivation Medium		
LB medium	LB	20 g l ⁻¹
for plates	Agar	20 g l ⁻¹
LB _{amp} , LB _{kana}	LB medium/plates	
	Ampicillin	100 µM
	Kanamycin	35 or 50 µM
Standard Yeast Cultivation Medium		
YPD Medium	YPD	50 g l ⁻¹
for plates	Agar	20 g l ⁻¹
Complete Supplement	Glucose	20 g l ⁻¹
Mixture	YNB	6.7 g l ⁻¹
(CSM)	aa drop out mix	1.5 g l ⁻¹
	NaOH (1 M)	2 ml l ⁻¹
for plates	Agar	20g l ⁻¹
Amino Acid Drop Out Mix	Adenine	0.5 g
(aa drop out mix, omit	L-Arginine	2.0 g
respective amino acid for	L- Aspartic Acid	2.0 g
selection process)	L-Histidine	2.0 g
	L-Leucine	10.0 g
Use mortar to homogenize	L-Lysine	2.0 g
and mix well by inverting for	L-Methionine	2.0 g
2 h	L-Phenylalanine	2.0 g
	L-Threonine	2.0 g
	L-Tryptophan	2.0 g
	L-Tyrosine	2.0 g
	Uracil	2.0 g
Medium for Synthetic Genetic Array		
Library cultivation medium	YPD	50 g l ⁻¹
	G418	100 µg ml ⁻¹
	Tetracycline	20 µg ml ⁻¹
Bait cultivation medium		
For $\Delta hsp26$, $\Delta hsp26\Delta hsp42$	YPD	50 g l ⁻¹
	clonNAT	100 µg ml ⁻¹
	Tetracycline	20 mg ml ⁻¹
For $\Delta hsp42$	CSM-Ura w/o Agar	
Mating Medium	YPD	50 g l ⁻¹
	Tetracycline	20 mg ml ⁻¹

Medium name	Composition	Concentration
Diploid selection medium		
For $\Delta hsp26$, $\Delta hsp26\Delta hsp42$	Difco nutrient broth	60 g l ⁻¹
	Glucose	20 g l ⁻¹
	Yeast extract	20 g l ⁻¹
	Tetracyclin	5 µg ml ⁻¹
	clonNAT	100 µg ml ⁻¹
	G418	100 µg ml ⁻¹
	Agar	20 g l ⁻¹
For $\Delta hsp42$	YNB w/o aa & w/o ammonium sulfate	1,7 g l ⁻¹
	Monosodium Glutamate	1 g l ⁻¹
	aa drop out mix - ura	2 g l ⁻¹
	Glucose	20 g l ⁻¹
	Tetracycline	20 µg ml ⁻¹
	G418	100 µg ml ⁻¹
	NaOH	pH adjusted to 6.5
Sporulation medium	Yeast extract	2 g l ⁻¹
	Glucose	0.5 g l ⁻¹
	Agar Noble	25 g l ⁻¹
	KAc	10 g l ⁻¹
	Histidin	30 mg l ⁻¹
	Uracil	30 mg l ⁻¹
	Leucin	60 mg l ⁻¹
	Tetracycline	20 µg ml ⁻¹
Haploid selection 1 medium (Mat a selection)	YNB w/o aa & a/o ammonium sulfate	1.7 g l ⁻¹
	Ammoniumsulfate	5 g l ⁻¹
	Glucose	20 g l ⁻¹
	aa-drop out mix -arg-lys-his	2 g l ⁻¹
	Tetracycline	20 µg ml ⁻¹
	Canavanine	100 µg ml ⁻¹
	NaOH	pH adjusted to 6.7
Haploid selection 2 medium (Mat a & G418 KO library marker selection)	YNB w/o aa & a/o ammonium sulfate	1.7 g l ⁻¹
	Monosodiumglutamat	1 g l ⁻¹
	Glucose	20 g l ⁻¹
	aa drop out mix -arg-his	2 g l ⁻¹
	Canavanine	50 µg ml ⁻¹
	G418	350 µg ml ⁻¹
	Tetracycline	20 µg ml ⁻¹
	NaOH	pH adjusted to 6.5
Final selection medium		
For $\Delta hsp26$	YPD	20 g l ⁻¹
	G418	200 µg ml ⁻¹
	clonNAT	100 µg ml ⁻¹
	Agar	20 g l ⁻¹
For $\Delta hsp42$	YNB w/o aa & w/o ammoniumsulfate	1.7 g l ⁻¹
	Monosodiumglutamat	1 g l ⁻¹

Medium name	Composition	Concentration
	Glucose	20 g l ⁻¹
	aa drop out mix –ura	2 g l ⁻¹
	G418	200 µg ml ⁻¹
	Agar	20 g l ⁻¹
For <i>Δhsp26Δhsp42</i>	Same as for <i>Δhsp42</i> clonNAT	100 µg ml ⁻¹
Medium for SILAC-Experiment		
SILAC-Medium	YNB w/o aa	6.7 g l ⁻¹
	Glucose	20 g l ⁻¹
	aa dropout mix (-Lys/Arg)	1.5 g l ⁻¹
	NaOH (1 M)	2 ml l ⁻¹
add respective SILAC-aa	Lys ⁰ (558 mM stock)	657 µM
	Lys ⁴ (558 mM stock)	657 µM
	Lys ⁸ (558 mM stock)	657 µM
	Arg ⁰ (285 mM stock)	453 µM
	Arg ⁶ (285 mM stock)	453 µM
	Arg ¹⁰ (285 mM stock)	453 µM
Antibiotics		
(1000x stocks)	Ampicillin	200 mg ml ⁻¹ (in H ₂ O _{dd})
	Chloramphenicol	35 mg ml ⁻¹ (in EtOH)
	Kanamycin	35 mg ml ⁻¹ (in H ₂ O _{dd})
	Kanamycin	50 mg ml ⁻¹ (in H ₂ O _{dd})
	Tetracycline	5 mg ml ⁻¹ (in EtOH)
	Nourseothricin	100 mg ml ⁻¹ (in H ₂ O _{dd})
	Geneticin G418	100 mg ml ⁻¹ (in H ₂ O _{dd})

3.7 Buffers

All buffers were prepared in H₂O_{dd}. Buffers used for washing steps in handling of *E. coli* or *S. cerevisiae* were sterile filtered through 0.22µm filters.

Table 10 Buffers and compositions

Buffer	Components	Concentration
SDS running buffer (10x)	TRIS	250 mM
	Glycine	2 M
	SDS	1% (w/v)
Laemmli buffer (5x)	SDS	10% (w/v)
	Glycerol	50% (v/v)
	TRIS/HCl	300 mM
	Bromophenol blue	0.1% (w/v)
	β-ME	5% (v/v)
TAE buffer (50x)	TRIS/Acetic acid	2 M, pH 8.0
	EDTA	50 mM
Separation gel buffer (4x)	TRIS/HCl	250 mM, pH 8.8

Buffer	Components	Concentration
Stacking gel buffer (2x)	SDS	0.8% (w/v)
	TRIS/HCl	250 mM, pH 6.8
Western Blot transfer buffer	SDS	0.4 % (w/v)
	Tris	25 mM, pH 8.3
	Glycine	190 mM
	Methanol	20% (v/v)
SILAC wash buffer	SDS	0.3% (w/v)
	Hepes	40 mM, pH 7.5
SILAC lysis buffer	KCl	150 mM
	HEPES	40 mM, pH 7.5
	KCl	150 mM
	EDTA	2 mM
	NaF	20 mM
	Na ₃ VO ₄	5 mM
	Protease Inhibitor Mix G	200 µl per 10 ml
	Phosphatase Inhibitor Cocktail 2	200 µl per 10 ml
Phosphatase Inhibitor Cocktail 3	200 µl per 10 ml	
		pH 7.5 verified after addition of all components
Yeast transformation buffer 2	PEG 4000	35% (w/v)
	LiAc	100 mM
	Tris-HCl	10 mM , pH 7.4
	EDTA	2 mM

3.8 Molecular biology methods

For all methods listed below, standard protocols were used as described elsewhere (Green and Sambrook, 2012). All solutions and chemicals were sterile and methods were carried out at RT, unless specifically stated otherwise. The most common methods and procedures for molecular biology are briefly described.

3.8.1 Cultivation of *E. coli* and *S. cerevisiae*

Cultivation of E. coli

E. coli was incubated at 37°C on LB plates or with shaking in liquid LB. Medium was inoculated either with a single colony from plate or by 1:100 dilution of a fresh overnight culture. Growth was monitored photometrically at 600 nm. Selection pressure was upheld by addition of appropriate antibiotics to the media. Short-term storage of plates was possible at 4°C. For long-term storage, 2 ml of a freshly inoculated culture were centrifuged (2 min 5,000 rpm), and the cell pellet was resuspended in 600 µL medium. 600 µL 50% glycerol were added to the bacterial suspension resulting in a 25% glycerol culture stock. The culture was frozen in liquid nitrogen and stored at -80°C.

Cultivation of yeast

S. cerevisiae was grown at 25°C or 30°C on YPD plates or in liquid medium. Medium was inoculated with a single colony directly or from a fresh over night culture (1:100 dilution). Liquid yeast cultures were incubated with vigorous shaking at 140 rpm. For selective pressure, appropriate antibiotics (Kan, clonNAT) were added to the medium or strains were grown on drop-out medium, exploiting amino acid prototrophy introduced by means of plasmid transformation or genomic integration.

3.8.2 Yeast transformation protocols

High efficiency transformation

For integrating constructs into the yeast genome (e.g. for gene disruption), high efficiency yeast transformation was carried out, as described by (Gietz and Schiestl, 2008).

For this, the respective yeast strain was grown overnight in 5 ml YPD at 30°C in a rolling incubator. This overnight culture was used to inoculate 50 ml of fresh YPD to an $OD_{595}=0.15$ (approximate dilution of overnight culture 1:50). After incubation at 30°C until $OD_{595}=0.6$ (approx. 4.5 h), cells were harvested by centrifugation (5 min, 3,000 g) and the supernatant was discarded. The yeast pellet was washed in 25 ml of sterile water (re-suspension and centrifugation) and subsequently re-suspended in 1 ml 0.1 M LiAc and transferred to a 1.5 ml reaction tube. Cells again were harvested by centrifugation (15 s, 5,000 rpm) and the supernatant was aspirated. The resulting pellet was again re-suspended in 500 μ l 0.1M LiAc. For each transformation, 50 μ l of cells were transferred to a new sterile reaction tube and spun down for 15 s at 5,000 rpm. In the order listed, the following substances were pipette to the pellet: 240 μ l PEG4000 (50% w/v), 36 μ l 1.0 M LiAc, ten μ l single stranded carrier DNA (Salmon testis 10 mg ml⁻¹, Sigma-Aldrich), 0.1 μ g to 10 μ g of DNA and sterile H₂O to obtain a final volume of 100 μ l. After vigorous vortexing, cells were incubated for 30 min at 30°C and then heat stressed at 42°C for 30 min. After harvesting (15 sec, 8,000 rpm), the supernatant was removed and cells were re-suspended in 100 μ l sterile water or appropriate medium and plated on selective medium plates. In the case of deletion by means of NatMX or KanMX cassette, cells were rescued by incubation in YPD at 30°C for two to three hours before plating on YPD containing kanamycin or nourseothricin (100 μ g ml⁻¹). For plating, re-suspended cells were distributed over the entire plate using as few strokes as possible. After two to four days colonies of transformants became visible and big colonies were cultivated for verification of positive transformants.

Quick chemical yeast transformation

For transformation of a plasmid, 1 ml exponentially growing yeast culture was harvested by centrifugation (1 min, 10,000 rpm). The medium was discarded and the cell pellet supplemented with 50 ng of plasmid (approx. 1 μ l) and re-suspended. Next, 5 μ l of single stranded DNA (salmon testis) was added and the cells were vortexed shortly. 1 ml of yeast transformation buffer 2 was added along with 5 μ l of 1 M sterile filtered DTT. After vortexing, cells incubated at RT overnight. After heat shock for 1 h at 42°C cells were chilled on ice and harvested (1 min, 14,000 rpm). The viscous supernatant was pipetted off and the pellet was re-suspended in 50 μ l to 100 μ l of sterile medium or water. In the case of selection for amino acid protrophy, cells were immediately plated on appropriate media. For selection for an antibiotic resistance (KanMX6, NatMX) cells were rescued by 2 h incubation in YPD at 30°C with gentle shaking. Cells were harvested and spread. After two to four days of incubation at 25°C or 30°C, small round colonies of transformants appeared.

3.8.3 Polymerase chain reaction (PCR)

PCR amplification is an *in vitro* method to amplify specific DNA stretches by exploiting the enzymatic function of polymerases. In general, a pair of short, single-stranded DNA oligomers, called primers, is designed to anneal upstream (sense-strand, forward primer) and downstream of the target-sequence (antisense strand, reverse primer). A thermal cycler with a defined number of cycles of DNA-melting (95°C), primer-annealing (55°C to 70°C) and elongation (65°C to 72°C) was used. Hence, the DNA-Polymerase specifically amplifies the sequence located between the two primers.

Primers were designed with the BioEdit software and ordered at MWG Eurofins. For downstream cloning steps, primers were designed with 5' overhangs. These carry the recognition motif of the respective restriction enzyme.

A typical PCR reaction was set up in 20 μ l (analytical PCR) or 100 μ l (preparative PCR) volumes, shown exemplary for Taq-Polymerase (Promega).

Table 11 General setup of a PCR

Component	20 μl	100 μl
Template (100 ng μ l ⁻¹)	1 μ l	1 μ l
Buffer (10x)	2 μ l	20 μ l
Primer forward	0.1 μ l	1 μ l
Primer reverse	0.1 μ l	1 μ l
dNTP-Mix (10 mM)	0.2 μ l	2 μ l
Polymerase	0.1 μ l	0.5 μ l
H ₂ O nuclease free	20 μ l	74,5 μ l

The general cycling scheme for most templates is as follows and needed to be adjusted for the individual polymerase used.

Table 12 General cycling scheme of a PCR

Step	Settings
Melting	95°C; 45 sec (2 min before 1 st cycle)
Annealing	55°C to 68°C (depending on primers); 45 sec
Elongation	70°C; 1 min per kb, 5 min after last cycle
Cycles	35

3.8.4 PCR-based gene deletion

Single, double and triple mutants of a given baker's yeast strain were obtained by using one-step PCR-based gene deletion technique described in (Janke et al., 2004; Longtine et al., 1998).

Exemplary, for the deletion of *hsp26* in BY4741 wild-type yeast strain, the NatMX4 gene was amplified from pAG25 plasmid with primers carrying 55 bp overhangs homologous to the *hsp26* promoter and terminator region. After amplification, the obtained deletion cassette was integrated into the yeast genome by means of homologous recombination. This replaced *hsp26* with the selectable marker NatMX4. Transformation of the cassette was carried out using the high efficiency yeast transformation protocol.

PCR-based verification of gene-disruption used a forward primer annealing approximately 500 bp upstream of the gene-to-be-deleted and a reverse primer that annealed in the middle of the NatMX4 sequence. Isolated genomic DNA of a potential positive transformant or 1 µl of lysed cells from a single colony (incubation in 10 µl 20 mM sterile NaOH) was used as template. Only in case of a site-specific, successful, homologous recombination event, can a PCR-product at the length of 1.4 kb be seen after separation on a 1% agarose gel.

PCR sample cleanup

PCR samples can be directly processed for downstream applications (such as ligation or gene disruption) or be processed after excision from the respective bands from an agarose gel. In general, the instructions in the manual of the used Kitsystem 'Wizard[®] SV Gel and PCR Clean-Up System' (Promega) were followed. The basic steps were:

1. Addition of binding buffer to PCR sample (directly or piece of gel)
2. Binding of DNA to silica-column
3. Washing steps to remove protein contaminations

4. Elution of DNA with 50 mM TE-buffer pH 7.5 or H₂O.

Purified DNA was checked by Nanodrop for purity and concentration. DNA was stored at -20°C until further use.

3.8.5 Cloning of yeast shuttle vectors

The sequence to be cloned was PCR amplified (3.8.3) using a suitable template with primers carrying 5'-overhangs with restriction enzyme sites.

Plasmids or PCR samples can be treated with REs for downstream processing (e.g. ligation). REs cut double-stranded DNA on specific short palindromic sequences resulting in "sticky ends" on the DNA that can be ligated in the following step by means of treatment with ligase. This enables the addition of a PCR-amplified RE digested insert DNA into a linearized vector treated with the identical REs as the insert. Restriction sites can be introduced into PCR products by using oligonucleotides with 5'-overhangs containing the respective restriction enzyme sequences.

In general, REs were obtained from NEB and - if possible - a 'High Fidelity' (HF) version of the enzyme was used. Incubation, inactivation, and sample cleanup were carried out according to the manufacturer's instructions. For most steps in cloning, 1 µg of DNA was digested with 1 unit (U) of HF-enzyme for 5 min at 37°C.

RE digested insert DNA and plasmid backbone are joined by action of T4-Ligase (Promega), as stated in the instructions given by the manufacturer. Usually ligation occurred at RT for 3 h or at 4°C overnight. For quick-ligation (12 min at RT) a dedicated 'Quik-Ligase' (NEB) was utilized and reactions were used for transformation of competent *E. coli* cells immediately.

Transformation of E. coli

Transformation describes the process of introducing naked DNA into competent cells, in this case Mach1 or XL1 *E. coli* cells. Competent cells were thawed on ice, 50 ng to 100 ng of plasmid was added and cells were left to incubate on ice for 30 min. After heat shock for 45 sec, cells were cooled on ice (1 min), 1 ml of LB-medium was added and cells are incubated at 37°C for 45 min. Next, harvest by centrifugation (2 min, 7,000 rpm), the draw off of the supernatant, and resuspension in 100 µl sterile medium or water followed. Then, cells were spread on LB dishes containing the appropriate antibiotic selection marker.

Plasmid preparation

For plasmid preparation, *E. coli* Mach1 or XL1, for protein purification an expression strain (e.g. *E. coli* BL21, HB101) were used. Plasmids were isolated according to the manufacturer's instructions given in the handbook of the 'Wizard[®] Plus Minipreps DNA Purification System' (Promega). Final elution of DNA was carried out with H₂O_{nuclease free} and isolated DNA was stored at -20°C.

Agarose gel electrophoresis

The backbone of DNA carries a negative overall charge due to its phosphate residues, therefore, fragments of different length can be separated on an agarose gel in an electric field. The larger DNA fragments move slower through the matrix of the gel towards the cathode, while shorter fragments do so faster. By means of digestion with suitable restriction enzymes, a plasmid can be linearized, or separated into fragments of known basepair (bp) length and then be run on an agarose gel. Ethidiumbromid (EtBr) or DNA StainG (Serva) was used to visualize DNA under UV-light, since it intercalates with double-stranded (ds) DNA. A comparison with a DNA standard that contains multiple DNA fragments of defined length served as control and allowed a determination if a plasmid carries the insert.

A 1% (w/v) agarose gel was cast and 5 µl to 10 µl DNA sample, for analytical purposes, or up to 100 µl for preparative samples, were mixed with DNA-loading buffer and pipetted into the gel pockets next to a DNA-ladder (100 bp or 1 kB ladder, PeqGold). An electric voltage of 120V was set for 30 min. Under UV light of an ImageQuant (GE Healthcare, USA) DNA was visualized and gels were documented.

3.9 Protein chemical methods

3.9.1 Determination of protein concentration

In the process of absorption, electrons are excited and lifted from the electronic ground state to an excited state. Chromophores are the molecular elements that are responsible for absorption. Various functional groups in proteins, including aromatic amino acids, peptide bonds, and disulfide bonds, absorb light in the UV range (100 nm to 400 nm). UV spectroscopy was used to determine protein concentrations according to the Beer-Lambert law (Equation 1).

$$A = \varepsilon \cdot c \cdot d \leftrightarrow c = \frac{A}{\varepsilon \cdot d}$$

Equation 1 Beer-Lambert law.

A= Absorbance, ε = molar extinction coefficient ($M^{-1} \text{ cm}^{-1}$), c = molar protein concentration (M), path length (cm)

Theoretical molar extinction coefficients were determined with the ProtParam tool (Gasteiger et al., 2015). All UV spectra were recorded with a Cary 50 UV/Vis spectrophotometer (Varian) at 20°C and baseline corrected for buffer absorbance.

3.9.2 SDS-polyacrylamide gel electrophoresis (SDS-PAGE)

The protocol of Laemmli (1970) served as a blueprint for the procedure of SDS-PAGE. A separation gel was cast to a final concentration of 12.5% (w/v) acrylamide/bisacrylamide 19:1 (40% w/v). A thinner stacking gel of 5% (w/v) acrylamide/bisacrylamide 19:1 (40% w/v) was cast on top the separation gel. Polymerisation of the respective stacking or separation gel was induced by the addition of ammonium persulfate (APS, 10% w/v) and tetramethylethylenediamin (TEMED). All samples were boiled at 95°C in 5x Laemmli for 5 min prior to loading into the gel pockets by means of a Hamilton syringe. Separation according to molecular weight was carried out at a constant voltage of 175V for 60 min. Gels were stained according to a modified protocol of Fairbanks et al. (1971) using Coomassie.

3.9.3 Immunoblotting

Immunoblotting (also Western blotting) enables a specific detection of a desired protein using suitable antibodies. In general, proteins are transferred from an SDS-gel to a more stable membrane and incubated with a primary antibody directed against the protein of interest. A secondary enzyme-coupled antibody targets the primary antibody and catalyzes a chemoluminescent reaction that can be used to visualize the proteins on a film or with a camera.

SDS-PAGE separated proteins were transferred on polyvinylidene fluoride or nitrocellulose membranes by means of a semidry blotting system. The basic setup consisted of three Whatmann 3MM filter papers, the PVDF or NC membrane, the SDS-gel and again three Whatmann 3MM filter papers stacked from bottom to top; between the cathode and the anode of the blotting apparatus. All components were soaked in WB-transfer buffer for 5

min prior to the blotting procedure. For the standard transfer procedure, 1 h of 75 mA per gel was set. Successful blotting was verified by transient staining with Ponceau Red. In an optional step, NC-membranes were incubated in Western-Blot Signal Enhancer (Thermo Scientific) that amplifies the signal of the following chemoluminescent reaction by three- to ten-fold. For immunodetection, the membrane was washed in PBS-T (1x PBS with 0.1% Tween) and, subsequently, unspecific binding to the background was blocked by incubation in PBS-T with 1% (w/v) milk powder for 1 h at RT. After a wash in PBS-T for 3x 10 min at RT with gentle shaking, incubation with the primary antibody solution occurred. To this end, the antibody was diluted 1:3,000 to 1:5,000 in PBS-T with 1% milk powder for two to four hours at RT or overnight at 4°C with gentle agitation. Three washing steps followed (3x 15 min, PBS-T) before addition of the secondary antibody solution. This peroxidase-conjugated secondary antibody was diluted 1:5,000 in PBS-T with 1% milk-powder (w/v) and incubated at RT for 1 h. Three to five washing steps followed and the blot was analyzed by chemo luminescent detection using the ECL-Western Blotting Detection Reagents (GE Healthcare) as described in the manufacturer's instructions. When using X-Omat X-Ray films (Kodak), they were illuminated in a dark chamber and developed or, alternatively, the ImageQuant LAS4000 system (GE) was used for visualization and digitalization of the western blot membranes.

3.10 Synthetic genetic array

A synthetic genetic array (SGA) is a useful tool to investigate genetic interactions of a known gene. In general, a SGA compatible haploid yeast strain (here: Y2454), carrying a query gene deletion (e.g. $\Delta hsp26$) was systematically crossed with a library of all viable haploid single gene deletion strains of the opposite mating type (Deletion Mutant Array, DMA). 4786 viable single deletion mutants of *S. cerevisiae* were contained in the DMA. After selection for the haploid double deletion strain, phenotypes were scored for differences compared to the individual single deletion of the library. For instance, a weaker growth was considered as ‘synthetic sick’ interaction, while unviable double KO strain described ‘synthetic lethal’ genetic interaction. For this study the following yeast strains were used as query deletions strains:

1. Y2454 $hsp26\Delta::natMX4$
2. Y2454 $hsp42\Delta::ura3$
3. Y2454 $hsp26\Delta::natMX4 hsp42\Delta::ura3$

The general procedure of the SGA is described below; a more detailed description can be found in (Tong et al, 2001).

A BiomekFX 384 pin robot with a microplate carousel was used for the SGA. The deletion mutant array (DMA) was propagated on rich medium (YPD) supplemented with G418 (200 $\mu\text{g ml}^{-1}$). Query deletion strains were grown in 5 ml YPD medium overnight and transferred to empty omnitrays. Query strain cultures were pinned on YPD-agar omnitrays in a 384 spot fashion and incubated for two days at 30°C. This produces a fresh query strain source for the following mating step. In the second step - the mating reaction - the respective query strain was pinned onto a new YPD-plate using flathead pins, and the deletion mutant library was pinned on top of the query strains. These plates were incubated at room temperature for one day. This yields zygotes of MATa/a (mating type), which were pinned onto medium for diploid selection. For instance, in the case of the Y2454 *hsp26 Δ ::natMX4* strain, diploids were selected on rich medium containing G418 (200 $\mu\text{g ml}^{-1}$) and clonNAT (100 $\mu\text{g ml}^{-1}$). In the case of the Y2454 *hsp42 Δ ::ura3* strain, selection occurred on a synthetic dextrose (SD) medium lacking uracil but containing G418 (200 $\mu\text{g ml}^{-1}$). Third, diploid cells were sporulated by pinning on the pre-sporulation medium and subsequently on the sporulation medium, followed by incubation for ten days at 22°C. Plates were checked in three-day intervals for growth of microbial contaminants. The fourth step encompassed the first haploid selection. To this end, MATa spore progeny were selected by pinning spores on SD-medium lacking histidine and arginine (SD-His/Arg) but containing canavanine (50 $\mu\text{g ml}^{-1}$). Incubation at 30°C for two days followed. This haploid selection step was repeated in a fifth step, with incubation at 30°C for 24 h. Sixth, selection for meiotic progeny that possess the deletion of the DMA parental strain was accomplished. To this end, MATa haploids were pinned on mono-sodium-glutamate (MSG)-medium containing G418 (200 $\mu\text{g ml}^{-1}$). Incubation for one day at 30°C followed. MSG medium was used as nitrogen source because ammonium sulfate impedes the action of G418 and clonNAT. This allowed a more stringent progeny selection. In the seventh step, final haploid selection for progeny containing query and DMA mutations occurred on SD - His + clonNAT (100 $\mu\text{g ml}^{-1}$) + G418 (200 $\mu\text{g ml}^{-1}$) for the *hsp26 Δ ::natMX4* strain, SD-His-Ura + clonNAT (100 $\mu\text{g ml}^{-1}$) + G418 (200 $\mu\text{g ml}^{-1}$) for the *hsp26 Δ ::natMX4 hsp42 Δ ::ura3* strain, and on SD - His - Ura + G418 (200 $\mu\text{g ml}^{-1}$) for the *hsp42 Δ ::ura3* query strain. After incubation for two days at 30°C, double or triple deletion haploid yeast cells were pinned on YPD plates with fine tip pin. This is also done for the DMA. Plates were incubated at 30°C and digitalized in one day increments to monitor growth. In the

final step, colony size was scored by comparing growth of double or triple mutants to the growth of the respective DMA strain. A list of genetic interactors was compiled for strains that possessed a phenotype in both of the SGA replicas. These hits were re-screened in a manual repetition of the SGA and only those hits that appeared in three out of four replicas altogether were used for further analysis.

The screens were carried out at the MPI of Biochemistry in Martinsried, Germany, at the Institute of Molecular Cell Biology of Prof S. Jentsch, with the technical assistance of Jochen Rech.

3.11 Methods for transcriptional studies

Microarrays

Yeast cultures were grown in YPD at 25°C and kept in the logarithmic growth phase for two days by passaging to new medium. This logarithmic culture was used to inoculate fresh sterile YPD medium to a starting $OD_{595}=0.2$ and grown into mid logarithmic growth phase (approx. 6 h) at $OD_{595}=0.8$ before submitting the cells to thermal stress in a water bath. A schematic experimental workflow is depicted (Figure 5).

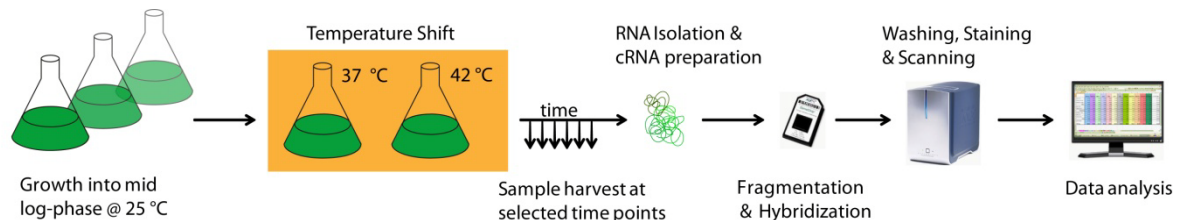


Figure 5 Scheme of the experimental workflow for microarray analysis.

Yeast cultures were cultivated in biological triplicates at 25°C into the mid-logarithmic growth phase. At $OD_{595}=0.8$ cultures were shifted to either 37°C or 42°C. Samples were taken at different time points. RNA isolation, cRNA preparation, fragmentation and hybridization to gene chips, as well as signal detection were carried out at the KFB Regensburg. Data analysis was carried out in house.

For transcriptional studies, gene chip analysis was employed. In general, 5 ml to 50 ml of the respective yeast culture was treated as required for the experimental setup (e.g. growth phase, time of stress, temperature of stress) and subsequently chilled on watered ice for two minutes. Cells were harvested by centrifugation (1 min, 4,500 rpm, 4°C) and washed once in half volume with cold H_2O_{dd} . Again, cells were harvested as before, the supernatant was discarded completely, the remaining pellet shock frozen in liquid nitrogen and stored

at -80°C until further use. The entire process from sample cooling on ice until freezing in liquid N₂ was carried out within 5 min.

Yeast Genome 2.0 arrays (Affymetrix, Santa Clara, USA) were made as a paid service by the ‘KompetenzZentrum für Fluoreszente Bioanalytik’ (KFB) Regensburg, Germany. These chips enable the analysis of the transcriptional levels of 5,717 genes of *S. cerevisiae*. Biological triplicates or duplicates were analyzed for all strains and conditions tested. Either complete yeast cell pellets or purified isolated RNA was provided as starting sample material to the KFB.

The basic procedure carried out by the KFB Regensburg is given below. For a more detailed description see the Affymetrix gene chips guide (2014)

1. Purification of total RNA including DNase digestion
2. Quality control and quantification of starting total RNA
3. Synthesis and cleanup of double-stranded cDNA
4. Synthesis and cleanup of labeled aRNA, with quality control and quantification
5. Fragmentation of normalized amounts of aRNA
6. Hybridization to Affymetrix Yeast Genome 2.0 gene chips
7. Washing, staining and scanning
8. Analysis of data

Data of different batches were normalized by means of quantile normalization using the open access software Solo 2.0. This normalization strategy averages the distribution of the signals over all datasets (Speed et al., 2003). The ratios of stressed versus unstressed or KO versus WT signal were calculated. Ratios were log₂ transformed to lift the skew of the data and display positive and negative gene regulation of identical magnitude with the same numeric value, except for the positive or negative prefix. In general, lists of differentially regulated genes were obtained by setting a threshold of two-fold up- and down-regulation, meaning at a log₂ value of |1|.

Classification of transcriptional regulation

For kinetic studies on the transcriptional response in wt baker’s yeast, genes were classified according to their relative transcriptional regulation over time in early-, late-, up- and down-regulated genes. In the case of the time course of mild heat shock at 37°C, for early up-regulation, a log₂-fold change of at least 1 at 5 min was assumed, along with an increase of 0.3 between 1 min, 3 min and 5 min. For early down-regulation, the same parameters apply with negative values. Late up-regulation was defined as a log₂ fold-

change below 0.5 for the initial duration of 10 min and a \log_2 fold-change above 1 at either of the times 10 min and 15 min. In the case of late down regulation, negative values with the same criteria as for late up regulation were set. By these means, roughly 300 genes were grouped into each category.

For the analysis of the response to shift to 42°C, early up genes were selected with a \log_2 fold change >0 at 3 min and >1 at 5 min. For early down-regulation criteria were: $fc < 0$ at 3 min and < -1 at 5 min. For late up-regulation, $\log_2 fc < 0.5$ at 3 min and >1 at 10 min or 40 min was set. For late down-regulation, the same values with a negative sign were used.

Comparison of absolute RNA values

Since fold-changes can be skewed (compare a change from 20 to 40 and from 2,000 to 4,000), the absolute RNA levels of molecular chaperones were looked upon. They were grouped into seven categories with respect to their basal non-stress levels and their levels after 10 min of 37°C heat shock. 1: very low basal signal ($x < 400$) and strong up-regulation (RNA-signal $x > 2,000$). 2: very high basal signal ($x > 4,500$) and up-regulation ($x > 6,000$). 3: high basal RNA signal ($1,000 < x < 4,000$), strong up-regulation ($x > 4,500$). 4: Low basal expression ($x < 1,000$), weak up-regulation ($1,000 < x < 2,500$). 5: Very high basal expression ($4,000 < x < 8,000$), no change. 6: high basal expression ($1,800 < x < 4,000$), weak down-regulation ($500 < x < 3,200$). 7: very low basal signal ($x < 800$), no change.

Analysis of large dataset lists

Lists of hits, as obtained by microarray analysis or SGA, were analyzed using the DAVID Gene Functional Classification Tool and DAVID Functional Annotation Tool, as described previously (Huang et al., 2009). In principle, a gene list was uploaded and compared to a reference list (e.g. genetic background of *S. cerevisiae*) and genes are clustered and grouped into biological processes, related genes, or other criteria of choice (e.g. cellular component, molecular function or biological process). Furthermore, DAVID assigns enrichment scores and p-values to enriched clusters within the input data lists, which enabled a quick identification of significantly enriched GO terms of potential interest.

For the $\Delta hsp26\Delta hsp42$ deletion strain a regulation network was generated, as described elsewhere (Papsdorf et al, 2015).

Search for regulators

Regulators of differentially regulated genes were searched for and ranked according to the yeasttract database (www.yeasttract.com). The p-value denotes the over representation of regulations of the given TF targets in the input-list relative to all known targets of the TF in the genome annotated in the yeasttract database. The p-value also denotes the probability that the TF regulates at least the number of genes found to be regulated in the list of interest if one were to sample a set of genes of the same size as the list of interest from all the genes in the yeasttract database. This probability is modeled by a hypergeometric distribution and the p-value is finally subject to a Bonferroni correction for multiple testing (Teixeira et al., 2014).

3.12 Microscopy

3.12.1 Fluorescence and bright field microscopy

A Zeiss Axiovert 200 inverted microscope equipped with a Hamamatsu camera C4742-95 was used to visualize yeast cells in bright field and under fluorescence illumination. On a microscope slide, a thin 2% agarose pad was prepared and yeasts were mounted in order to immobilize them. A cover-slide was placed on top of the pad and images were acquired at 100x magnification. For comparison of fluorescence intensities in different samples, the identical duration of image acquisition was used.

3.12.2 Soft X-ray tomography

Soft X-ray tomography is ideally suited to analyze the inner cellular morphology of whole cells in a near-native state with a spatial resolution of approximately 40 nm. At the employed energy range of 540 eV, organic material absorbs just about one order of magnitude more strongly than water, and, therefore, it is referred to as the 'water-window'. Consequently, carbon-rich structures produce high contrast while water-rich structures yield a low signal, enabling structural data acquisition without the necessity of adding substances generating contrast.

Prior to the sample preparation, special copper grids (HZB-2A) suitable for use at the beamline (U41-TXM; BessyII, Helmholtz Zentrum Berlin) were carbon-coated by means of flotation. Holey-carbon film or a self-prepared carbon-mesh was used. Carbon-coated grids were transiently hydrophilized by glow discharging for 30 sec under high vacuum conditions in a plasma cleaner. These grids were used within two hours for further sample preparation: First, using the tip of a toothpick, a thin fine line of pre-dried pap-pen is drawn

on the carbon-free side just below the copper-mesh sampling site and let set for a few minutes. Second, grids are picked up using inverted N5-tweezers and pap-pen is applied on the carbon-coated side. This 'pap-pen border' limits the area of the sample and concentrates it at the site of the copper-grid mesh. In a third step, 2 μ l of colloidal gold (100 nm or 250 nm diameter, BBI Solutions) is pipetted on the carbon-coated side of the mesh and blotted away from behind. The gold particles later serve as fiducials for the fine alignment process in tomogram generation.

Yeast cultures were kept in logarithmic growth phase for two days prior to X-ray sample preparation. Cultures were inoculated in fresh YPD to a starting OD₅₉₅ of 0.3 and grown at 25°C in the rolling incubator until OD₅₉₅ reaches 0.8. At this point, cultures were heat stressed at varying temperatures (37°C, 42°C and 50°C) in a water bath for different durations (e.g. 5, 10, 20, 30, 40, 60 and 120 min). Cells were spun down in 1.5 ml reaction tubes in a table-top centrifuge (5,000 g, 1min) and washed in cold 1x PBS. Then, PBS-resuspended cells were supplemented with colloidal gold fiducial markers, to reach an equal number of cells and gold particles. 1.5 μ l of this mix were pipetted on the carbon-coated mesh of the prepared copper grids, blotted from behind with filter paper (Whatman 5), and rapidly frozen in liquid ethane using a plunge freezer. This occurred immediately before the entire sample was drawn off. This process termed 'vitrification' freezes the sample in a near-native state. Samples were transferred into grid containers under liquid nitrogen atmosphere and stored therein until data acquisition. This was obtained by storage in a properly prepared dry shipper (Cryoson).

Dry shipper preparation is achieved by repeatedly filling the container along with the sample holder with liquid N₂, thereby, cooling the matrix inside. This is repeated until the level of liquid N₂ no longer drops (duration approx. 6h). After inverting the dry shipper three times to remove any free liquid N₂, the temperature is kept constantly below -170°C for up to six days.

X-ray tomogram data acquisition

For data acquisition, samples were brought to the beamline U41-TXM of the electron storage ring BessyII of the Helmholtz Zentrum (Berlin, Adlershof). Grids were mounted in the cryo holder and transferred into the U41-TXM beamline. Grids were scanned for yeast cells and images recorded in a tilt series from ideally -70° to + 70° in 1° increments. Ten flatfield-images were collected outside the copper-mesh that allows flat-field correction in

data-analysis. 0° images were recorded before and after tilt series in order to visualize potential radiation damage and sample drift.

The utilized general parameters for tilt series acquisition are listed (Table 13) and were adjusted to the quality and features of the individual object to be recorded.

Table 13 General parameters for data acquisition at beamline U41-TXM

Parameter	Value
Energy	540 eV
Temperature	-180°C
Starting angle	-70 °
Final angle	+70 °
Angle increment	1 °
Exit slit	10-20 μm
Exposure time	2 s
Double exposure time at high tilt angles	y/n at angles $> 65^\circ $
Beam current	300 mA

Tomograms were reconstructed using etomo of the IMOD software package (Boulder, Colorado). Whenever possible, the automated scripts were employed. In general, image stacks were generated from the projection images of the tilt series, and grey values were adjusted. Flatfield correction was applied using the flatfield images. Extreme X-rays were erased, and images of the stack were coarse-aligned by means of cross correlation. Wherever possible, 20 gold particles were utilized as fiducials to generate a fiducial model. Particles were tracked through the image stack and images were fine-aligned manually, if necessary. Final tomogram boundaries were set and the tomogram was calculated.

Segmentation and generation of 3D model

Segmentation of cellular organelles and boundaries was done semi-manually using the drawing tools of etomo. This resulted in the final three-dimensional (3D) model of the yeast cell. For this purpose, contours were drawn around organelles or cellular structures and traced through the Z-plane of the tomogram. For objects with spherical structure, the interpolator-tool of etomo was used to speed up the process of segmentation. For non-symmetric shapes, manual segmentation throughout the tomogram was warranted. Missing information at high and low tilt angles may be interpolated according to the experimenter's judgments. Segmented objects were colored according to their ascribed organelle or structure, and displayed using the meshing function of etomo.

3.13 Metabolic labeling of yeast cells

Labeling of yeast cultures was carried out by Stable Isotope Labeling with Amino Acids in Cell Culture (SILAC). This *in vivo* labeling approach introduces a specific mass shift for proteins due to the incorporation of amino acids with substituted stable isotopic nuclei. After a few cell divisions, the label is incorporated to 100 % and the introduced mass shift can be identified and quantified by mass spectrometry.

Here, a fresh overnight culture of the SILAC compatible yeast strain YAL6B was grown in CSM-Arg/-Lys medium, supplemented with 100 $\mu\text{g/ml}$ of Lys⁰ or Arg⁰. This culture was used to inoculate 50 ml of CSM-Arg/-Lys medium, supplemented with the respective combination of heavy-atom labeled L-Lysine-4,4,5,5-D₄ (Lys⁴), L-Lysine-U-¹³C₆-U-¹⁵N₂ (Lys⁸), L-Arginine-¹³C₆ (Arg⁶) and L-Arginine-U-¹³C₆-U-¹⁵N₄ (Arg¹⁰). The following incubation occurred overnight (14 h) at 25°C and 130 rpm for full metabolic incorporation of the label into the proteome. This fresh overnight-culture was used to inoculate two 50 ml flasks of fresh, labeled SILAC-medium to an OD₅₉₅=0.25. Cultures were incubated until OD₅₉₅=2.0 (mid-logarithmic growth phase). At this point, control cultures were left to incubate at 25°C, while heat-shock cultures were shifted to 37°C or 42°C in a water bath. Incubation occurred for either 10 or 30 min at 130 rpm. Next, cells were chilled on watered ice for two minutes, harvested by centrifugation at 4°C and 4,500 rpm for two minutes, and washed once in SILAC-lysis buffer. After resuspension in 9 ml of lysis buffer, yeast cells were distributed into ten 1.5 ml reaction tubes for each labeling condition. Cells were disrupted using glass beads ($r = 0.5$ mm) in the bead mill with three intervals of two minutes, at a frequency of 30 s⁻¹. Between lysis steps, short cooling on ice occurred. After centrifugation (16,000g, 2 min, 4°C), the supernatant of the lysate was drawn off and joined in one 15 ml falcon tube for each condition. Protein concentration was determined threefold using a Bradford-Assay (Pierce), concentrations adjusted using lysis buffer and the lysate was distributed in aliquots of 500 μl . Aliquots were flash-frozen in liquid nitrogen and stored at -80°C. Each control and stress condition is analyzed in biological triplicates, achieved by altering the combination of Lys⁰, Lys⁴, Lys⁸, Arg⁰, Arg⁶ and Arg¹⁰ in the experimental setup (Figure 6).

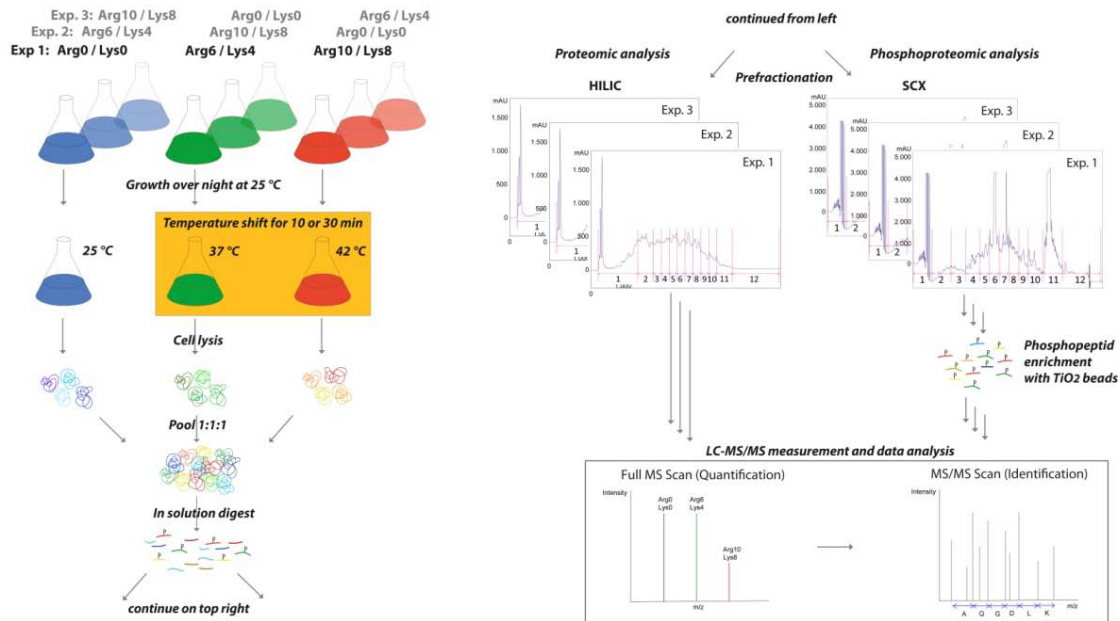


Figure 6 Scheme for metabolic labeling of yeast.

Log-phase yeast cultures were grown in stable isotope amino acids labeled medium and then shifted to higher temperatures. Cell lysates were prepared and mixed in a 1:1:1 protein ratio. After tryptic digestion proteins were separated by hydrophilic interaction liquid chromatography (HILIC) for total proteome analysis or strong cation exchange (SCX) into 12 fractions for each experiment. Phosphorylated peptides were further enriched by two washes with TiO₂ beads. Mass-spectrometry analysis was carried out on an Orbitrap Fusion mass spectrometer (Thermo Scientific). Scheme derived from Dr. Nina Bach.

Mass Spectrometry (MS) analysis

All MS experiments were carried out in collaboration with Elena Kunold of the Chair of Organic Chemistry II of the Chemistry Department of the TUM headed by Prof. S. Sieber. In general, samples of the respective yeast lysates (1 to 9) were mixed in a 1:1:1 protein ratio to obtain mixed lysates Exp.1, Exp.2 and Exp.3 (Figure 6). Proteins from mixed lysates were precipitated and either fractionated by hydrophilic interaction liquid chromatography (HILIC) for total proteome analysis, or strong cation exchange (SCX) for phospho-proteome analysis. Phospho-peptides were additionally enriched by two washes with TiO₂ beads. Liquid chromatography (LC-) mass spectrometry (MS) analysis was carried out on an Orbitrap Fusion (Thermo Scientific) instrument.

Protein network generation

The normalized SILAC-MS data was used to obtain lists of proteins that show elevated or decreased levels after heat shock compared to the untreated control conditions. Only proteins that showed the same directional changes in all three label-swap replicates and

with an average change by a factor equal or bigger than two ($\log_2=1$) in all three replicates were selected. The same criteria were used for class-1 P-site selection. Protein networks were built using the String-v10 database (<http://string10-db.org/>) with interactions inferred from experimental evidence only, and with high stringency (>0.700) criteria. For visualization, networks were exported to cytoscape and color coded according to the direction of protein level change. Red represents enrichment, blue represents diminishment. Proteins were represented as nodes, interactions between proteins by edges between the nodes. Proteins with no known interaction in the network were not displayed. For networks on the proteins with differential P-sites after heat shock, proteins were selected according to above-described criteria. When a protein showed more than one P-site with differential phosphorylation, the one with the highest change was used for coloring of the nodes. If a protein possessed P-sites with an increase in the phosphorylated state, as well as sites with an increase in the de-phosphorylated state, the respective node was colored in green.

4. Results

4.1 Small heat shock proteins of baker's yeast

The small heat shock proteins are a ubiquitous class of molecular chaperones found through all kingdoms of life. Their main function - in the context of cellular proteostasis - lies in the suppression of protein aggregation. sHsps act without cycles of ATP hydrolysis and - in a concerted action with ATP-dependent chaperones of the Hsp70 family, or with Hsp104 in yeast - the sHsp-holdases contribute to the protein disaggregation and refolding processes.

Saccharomyces cerevisiae has a two-component sHsp system consisting of Hsp26 and Hsp42. Studies have mainly focused on the characterization of their activity as molecular chaperones and on the structural investigation of Hsp26 (Chen et al., 2010; Haslbeck, 1999; Haslbeck et al., 2004; White et al., 2006). Only in the recent past has Hsp42 been linked to protein trafficking processes in the cell (Escusa-Toret et al., 2013; Roth and Balch, 2013; Specht et al., 2011). Studies on deletion strains of baker's yeast small heat shock proteins were unable to elicit a phenotype (Escusa-Toret et al., 2013; Petko and Lindquist, 1986; Stratil, 2010). For these reasons further investigations of the small heat shock protein system of *S. cerevisiae* were carried out.

4.1.1 SGAs reveals sHsps involved in protein trafficking

Synthetic genetic arrays (SGAs) were carried out in order to identify potential genetic interaction partners of the small heat shock proteins, Hsp26 and Hsp42. The single and double deletion strains were investigated to scrutinize potential genetic interactors of the sHsps. For this purpose, the *hsp26* locus was eliminated in the SGA-compatible Y2454 yeast strain, introducing the selectable marker gene for nourseothricin resistance, NatMX4. *Hsp42* was disrupted in Y2454 using the *ura3*-marker, enabling the selection on medium lacking uracil. The double deletion strain was generated by deletion of *hsp26* with the NatMX4 cassette in the *hsp42Δ::ura3* Y2454 yeast. In principal, each of these three yeast strains of mating type α was systematically mated to a library of 4,786 nonessential yeast single gene deletion strains (carrying the G418 resistance marker) of the opposite mating type. In a final step, the haploid double mutants (one *shsp*-deletion and the library strain deletion) or triple mutants ($\Delta hsp26\Delta hsp42$ with $\Delta geneXX$) were selected for, exploiting the marker genes of both yeast strains. Colonies with weak growth or no growth at all reveal potential parallel or compensatory pathways affected by the sHsps.

The screens were carried out at the Institute of Molecular Cell Biology headed by Prof. S. Jentsch at the MPI of Biochemistry in Martinsried, Germany. A list was compiled with all obtained genetic interaction partners from the SGA screens (Table 14). Genes involved in arginine-, histidine- or uracil biosynthesis were filtered from the genetic interaction partners, because the selection steps carried out during the SGA involved a medium lacking these amino acids. Therefore, the appearance of these genes cannot be attributed to synthetic genetic interaction with the sHsp gene disruptions. Nevertheless, they provide good controls, in that genes involved in uracil biosynthesis only appear in the $\Delta hsp42$ or $\Delta hsp26\Delta hsp42$ strain. Therefore, only genetic interactors were compiled that appeared in both replicas of the genetic array and in at least one replica of a manual re-screen of the hits.

Table 14 Genetic interaction partners of the small heat shock proteins.

Genes were identified in a SGA, as described in chapter 3.10. The hits of all three screens are listed. Genetic interaction partners belonging to the processes of arginine-, lysine-, uracil- or histidine biosynthesis were omitted, because they appear due to medium selection markers. An entry in the column $\Delta hspXX$ shows the respective gene was identified as an interaction partner of the sHsp. 0=no growth, synthetic lethal interaction; w= weak growth; synthetic growth weakness. The screen was carried out in technical duplicates, and hits were re-screened manually. Only hits that appeared in at least three replicas were compiled.

Systematic name	Gene name	Short name description	$\Delta hsp26$	$\Delta hsp42$	$\Delta hsp26/42$
YJL206C-A	NCE101	Non Classiscal Export		w w	
YJL204C	RCY1	ReCYcling		w w	
YBR097W	VPS15	Vacuolar Protein Sorting		0 0	0 0
YPL045W	VPS16	Vacuolar Protein Sorting		0 0	0 0
YJR102C	VPS25	Vacuolar Protein Sorting		0 0	0 0
YDR069C	DOA4	Degradation Of Alpha	w w	0 w	0 0
YPL065W	VPS28	Vacuolar Protein Sorting		w w	0 0
YLR417W	VPS36	Vacuolar Protein Sorting	w w	w w	0 0
YLR396C	VPS33	Vacuolar Protein Sorting			0 0
YCL007C	YCL007C	Dubious ORF, overlaps with VMA9		w w	w w
YPL234C	VMA11	Vacuolar Membrane Atpase			w w
YHR060W	VPH6	Vacuolar pH			w w
YKL119C	VPH2	Vacuolar pH			w w
YKL118W	YKL118W	Dubious ORF, overlaps with VPH2			0 0
YML097C	VPS9	Vacuolar Protein Sorting	w w		w w
YKL041W	VPS24	Vacuolar Protein Sorting	w w	w w	
YPR173C	VPS4	Vacuolar Protein Sorting	w w	w w	w w
YLR322W	VPS65	Vacuolar Protein Sorting	w w		
YGL153W	PEX14	PEroXisome related		w w	w w
YGR133W	PEX4	PEroXin		w w	w w
YMR026C	PEX12	PEroXin		w w	w w

4. Results

Systematic name	Gene name	Short name description	$\Delta hsp26$	$\Delta hsp42$	$\Delta hsp26/42$
YGR077C	PEX8	PEroXin		w w	w w
YDR265W	PEX10	PEroXin		w w	w w
YJL210W	PEX2	PEroXin		w w	w w
YGL152C	YGL152C	Dubious ORF, overlaps with PEX14		w w	w w
YJL211C	YJL211C	Dubious ORF, overlaps with PEX2		w w	
YOR036W	PEP12	carboxyPEPTidase Y-deficient	w w	w w	w w
YDR323C	PEP7	carboxyPEPTidase Y-deficient		w w	w w
YBL017C	PEP1	carboxyPEPTidase Y-deficient	w w		
YDR320C	SWA2	Synthetic lethal With Arf1	w w	w w	
YHL025W	SNF6	Sucrose NonFermenting		w w	0 0
YLR025W	SNF7	Sucrose NonFermenting	w w	w w	0 0
YPL002C	SNF8	Sucrose NonFermenting	w w	0 0	0 0
YOR290C	SNF2	Sucrose NonFermenting		0 0	
YEL009C	GCN4	General Control Nonderepressible	w w	w w	0 0
YGR252W	GCN5	General Control Nonderepressible		w 0	
YPR159W	KRE6	Killer toxin REsistant	w w	w w	0 0
YKR035W-A	DID2	Doa4-Independent Degradation		w w	
YDR455C	YDR455C	Dubious ORF, overlaps with NHX1		w w	0 0
YDR456W	NHX1	Na ⁺ /H ⁺ eXchanger		w w	0 0
YDL116W	NUP84	NUclear Pore		w w	0 0
YDR507C	GIN4	Growth Inhibitory			0 0
YBR133C	HSL7	Histone Synthetic Lethal	0 0		0 0
YPR139C	LOA1	Lysophosphatidic acid: Oleoyl-CoA Acyltransferase			0 0
YDR140W	MTQ2	Methyltransferase			0 0
YDL047W	SIT4	Suppressor of Initiation of Transcription			0 0
YNL064C	YDJ1	Yeast dnaJ	w w	w w	w w
YOL029C	YOL029C	Uncharacterized ORF, potential Hsp82/Hsc82 interactor	w w	w w	0 0
YOR289W	YOR289W	Uncharacterized ORF			0 0
YEL045C	YEL045C	Dubious ORF	w 0	w w	w w
YPR163C	TIF3	Translation Initiation Factor	w w	w 0	w w
YPL069C	BTS1	Bet Two Suppressor	w w	w w	w w
YAL021C	CCR4	Carbon Catabolite Repression	w w	w w	w w
YMR035W	IMP2	Inner Membrane Protease		w w	w w
YDR176W	NGG1	Histone acetyltransferase NGG1		w w	w w
YLR014C	PPR1	Pyrimidine Pathway Regulation		w w	w w
YDR178W	SDH4	Succinate DeHydrogenase		w w	w w
YCL008C	STP22	STerile Pseudoreversion		w w	w w
YER145C	FTR1	Fe TRansporter		w w	
YJL129C	TRK1	TRansport of potassium (K)	w w	w w	w w
YJL056C	ZAP1	Zinc-responsive Activator Protein		w w	w w
YLR056W	ERG3	ERGosterol biosynthesis			w w
YDR174W	HMO1	High MObility group (HMG) family			w w

4. Results

Systematic name	Gene name	Short name description	$\Delta hsp26$	$\Delta hsp42$	$\Delta hsp26/42$
YLR338W	OPI9	OverProducer of Inositol			w w
YEL060C	PRB1	PRoteinase B			w w
YMR063W	RIM9	Regulator of IME2			w w
YPL079W	RPL21B	Ribosomal Protein of the Large subunit			w w
YJL189W	RPL39	Ribosomal Protein of the Large subunit	w w		w w
YLR048W	RPS0B	Ribosomal Protein of the Small subunit	w w	w w	w w
YDR417C	YDR417C	Dubious ORF, overlaps with RPL12B	w w	w w	
YDR462W	MRPL28	Mitochondrial Ribosomal Protein, Large subunit	w w		0 0
YDL133C-A	RPL41B	Ribosomal Protein of the Large subunit		w w	
YPL198W	RPL7B	Ribosomal Protein of the Large subunit		w w	
YDR470C	UGO1	UGO (Japanese for fusion)			w w
YNL197C	WHI3	WHIskey			w w
YBR075W	YBR075W	Former ORF, now merged with PFF1			w w
YEL061C	CIN8	Chromosome INstability		w w	w w
YDR532C	KRE28				w w
YBR021W	FUR4	5-FIUoRouridine sensitivity	w w	w w	
YPL084W	BRO1	BCK1-like Resistance to Osmotic shock	w w	w w	
YJL101C	GSH1	glutathione (GSH)		w w	
YNL250W	RAD50	RADiation sensitive	w w	w w	
YKR091W	SRL3	Suppressor of rad53 Lethality		w w	
YKR092C	SRP40	Serine Rich Protein		w w	
YGR086C	PIL1	Phosphorylation Inhibited by Long chain bases	w w	w w	
YNL107W	YAF9	Yeast homolog of the human leukemogenic protein AF9		w w	
YJL188C	BUD19	BUD site selection	w w		
YPL086C	ELP3	ELongator Protein	w w		
YLR445W	GMC2	Grand Meiotic recombination Cluster	w w		
YPR134W	MSS18	Mitochondrial Splicing System	w w		
YPR131C	NAT3	N-terminal AcetylTransferase	w w		
YLR018C	POM34	POre Membrane	0 0		
YLR019W	PSR2	Plasma membrane Sodium Response	0 0		
YBL033C	RIB1	RIBoflavin biosynthesis	w w		
YLR079W	SIC1	Substrate/Subunit Inhibitor of Cyclin- dependent protein kinase	w w		
YCR084C	TUP1	dTMP-UPTake	0 0		
YLR193C	UPS1	UnProceSsed	w w		
YJL175W	YJL175W	Dubious ORF, overlaps with SWI3	w w		
YNL269W	BSC4	Bypass of Stop Codon		0 0	0 0
YDR364C	CDC40	Cell Division Cycle		0 0	0 0
YPL050C	MNN9	MaNNosyltransferase		0 0	0 0

The SGA enabled the identification of 39 potential interaction partners for the $\Delta hsp26$ strain, four yielding a synthetic lethal combination, 35 resulting in a growth weakness. Sixty-three genetic interactors were found for $hsp42$. Deletion of 55 of these interactors lead to a synthetic growth defect in the combination with $hsp42$ deletion and eight resulted in no growth at all. In the case of the sHsp double KO strain, 66 combinations of gene deletion showed a synthetic genetic interaction: 27 with a lethal interaction and 39 showing a growth weakness. Hence, most of the identified genetic interaction partners show a synthetic growth defect. The double mutant, on the other hand, possesses more genetic interactors resulting in lethality.

Overlaps between the SGA hits of the three screens exist: 19 of the 39 genetic interactors of $hsp26$ were also found in the double KO. For the $hsp42$ interactors, the overlap with the double KO was 42 out of the 63 genes. Fifteen genes were identified in all three SGAs. Interestingly, there were also 29 genes that appeared as an interactor only in combination with a single gene deletion but not in combination with the disruption of both sHsp loci. Twenty genes yielded synthetic genetic interaction only in the $\Delta hsp26\Delta hsp42$ strain. The hits were analyzed by means of functional annotation with the goal of identifying common biological processes or molecular functions of the genes (Table 15).

Table 15 Functional annotation of genetic interactors identified in the SGA screens of the sHsps deletion strains.

The functional annotation tool of the DAVID database (<https://david.ncifcrf.gov>) was used for classification. Only processes with an enrichment score >2 and with a significant p-value (<0.01) are listed.

GO ID	GO term	Enrichment Score	# of genes identified	p-value
SGA $\Delta hsp26$				
GO:0006511	Ubiquitin-dependent protein catabolic process	2.73	6	<0.000001
GO:0045184	Establishment of protein localization	2.73	13	0.000085
GO:0007034	Vacuolar transport	2.73	8	0.00001
SGA $\Delta hsp42$				
GO:0045184	Establishment of protein localization	6.38	26	<0.000001
GO:0006623	Protein targeting to vacuole	6.38	9	<0.000001
GO:0006625	Protein targeting to peroxisome	3.57	6	0.000003
SGA $\Delta hsp26\Delta hsp42$				
GO:0008104	Establishment of protein localization	7.52	25	<0.000001
GO:0007034	Vacuolar transport	5.00	13	<0.000001
GO:0006625	Protein targeting to peroxisome	3.52	6	0.000003
GO:0006511	Ubiquitin-dependent protein catabolic process	2.03	8	0.004413

The enrichment analysis revealed processes involving the targeting of proteins within the cell: ‘establishment of protein localisation’, ‘vacuolar transport’ and ‘protein targeting to peroxisome’ are enriched GO terms. The identification of processes involved in protein targeting applies for all three sHsp-gene deletion strains. Especially genes involved in targeting proteins to the vacuoles and also in their acidification were found in high number (*vps4*, *vps9*, *vps15*, *vps16*, *vps24*, *vps25*, *vps28*, *vps33*, *vps36*, *vps65*, *vma11*, *vph2*, *vph6*, *pep1*, *pep7*, *pep12*, *bts1*, *doa4*). Furthermore, genes contributing to peroxisome organisation were identified (*pex2*, *pex4*, *pex8*, *pex10*, *pex12*, *pex14*). These genes appear to be genetic interactors of *hsp42* only, since they did not show up in the SGA with Δ *hsp26* yeast. In summary, a significant enrichment exists for proteins of the endosomal transport system. This trafficking pathway describes the process of protein cargo transport from the late Golgi compartment into early endosomes, into the late endosome (also termed multi vesicular body, MVB), or directly into the vacuole (Bowers and Stevens, 2005). Hence, the SGAs suggest the yeast sHsps Hsp26 and Hsp42 are linked to protein trafficking processes in the cell.

It must be noted that many of the single KO strains of the genetic interactors themselves have a slow growth phenotype and, for this reason, could have been detected as genetic interactors of the sHsps. However, roughly 15% of all single KO yeast strains were reported to have a slow growth phenotype on rich medium (Giaver et al., 2002). The enrichment for those involved in vacuolar and peroxisomal protein transport being due to chance seems unlikely.

Transcription of genetic interactors is unaltered in sHsp-deletion strains

In order to investigate whether sHsp gene deletion has any effect on the gene regulation of the genes involved in endosomal transport, their RNA levels were analyzed using microarrays. The RNA levels of three biological replicates were averaged and plotted (Figure 7). The analysis was carried out for wild type, Δ *hsp26*, Δ *hsp42* and Δ *hsp26* Δ *hsp42* yeast under a physiological temperature of 30°C, for yeast exposed to severe heat shock for 20 min at 50 °C, and for yeast in the stationary phase. The later also represents a state of stress for baker’s yeast (Werner-Washburne et al., 1993).

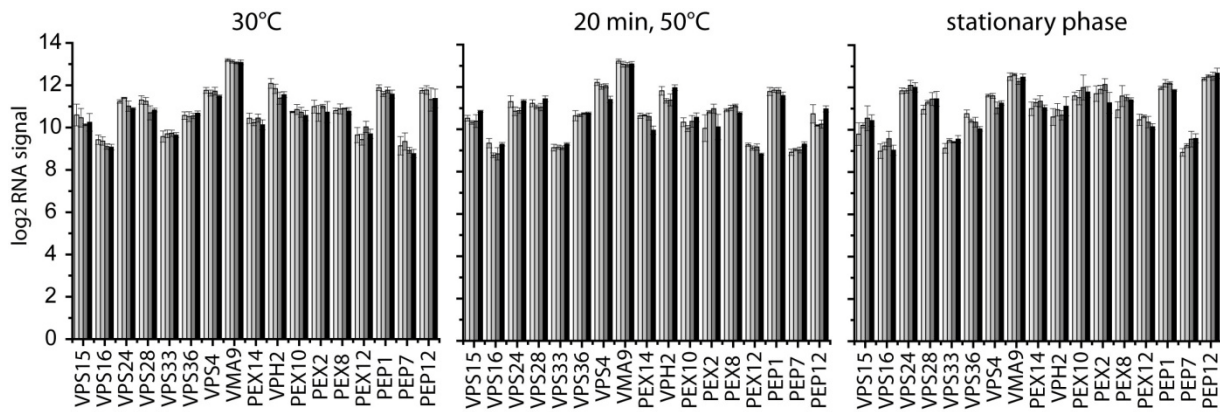


Figure 7 RNA levels of selected genetic interactors of the small heat shock proteins.

Genetic interactors involved in protein targeting to the vacuoles and membranes were analyzed with respect to their RNA levels in wt and sHsp deletion strains. Analysis was carried out for biological triplicates of yeast in exponential growth phase at 30 °C, after 20 min of 50°C heat shock and with yeast in stationary phase. The mean \log_2 RNA signal of three replicates is plotted with the standard deviations as error bars. Wt yeast is in light grey, $\Delta hsp26$ in grey, $\Delta hsp42$ in dark grey and $\Delta hsp26\Delta hsp42$ in black.

None of the genetic interactors involved in peroxisomal or vacuolar protein targeting displayed any differences in their RNA levels compared to wt yeast levels. Neither at 30°C in exponential growth phase, nor after severe heat shock can significant differences in the average \log_2 -mRNA signal be seen. All four bars of each gene lie close to the same height in the plot. In the stationary growth phase, the RNA levels of the peroxisomal targeting genes (*pex10*, *pex2*, *pex8*, *pex12*) show elevated RNA levels, however, no discrepancies between the yeast strains exist. Hence, the genetic interactors do not show altered transcriptional regulation in the genetic background of sHsp gene deletion. When expanding the analysis to the other genetic interactors and also to other yeast genes involved in protein targeting to vacuoles and peroxisomes, no differences between the yeast strains can be made out. In a kinetic analysis of the transcriptional response of $\Delta hsp26\Delta hsp42$ yeast exposed to 37°C (see chapter 4.3), the genetic interactors found in the SGA did not show up among the differentially regulated genes. Hsp42, indeed, has been implicated in protein sequestration within the cell (Escusa-Toret et al., 2013; Specht et al., 2011). Therefore, further investigations on the exact role of the sHsps in the transport process from Golgi to the vacuole are of interest.

4.1.2 The sHsps in models of protein aggregation

Firefly luciferase as a non-toxic model of protein aggregation

Protein homeostasis (proteostasis) is a complex process that involves, among other factors, a network of molecular chaperones. In order to elucidate whether disruption of the small heat shock protein system in *S. cerevisiae* affects cellular proteostasis, sensor proteins derived from firefly luciferase were used. These sensors, comprised of wt luciferase and two mutants with increasing structural instability, are fused to eGFP and have been shown to monitor the level of proteome stress in cells (Gupta et al., 2011). Furthermore, they represent an aggregation model of the non-toxic type, where the aggregating protein does not result in obvious proteotoxicity to yeast, such as diminished cell growth. The sensor proteins were cloned into yeast shuttle vectors under the control of the constitutive GPD promotor and transformed into wt and sHsp deletion yeast. The aggregation state of firefly luciferase was monitored microscopically in yeast under permissive conditions and under heat stress. The imaging focused on the destabilized single mutant (FlucSM) and double mutant (FlucDM), because wild-type luciferase remained soluble and active for temperatures up to 35°C and was even stable at 37°C for up to 30 min.

LuciferaseSM-GFP 30 °C

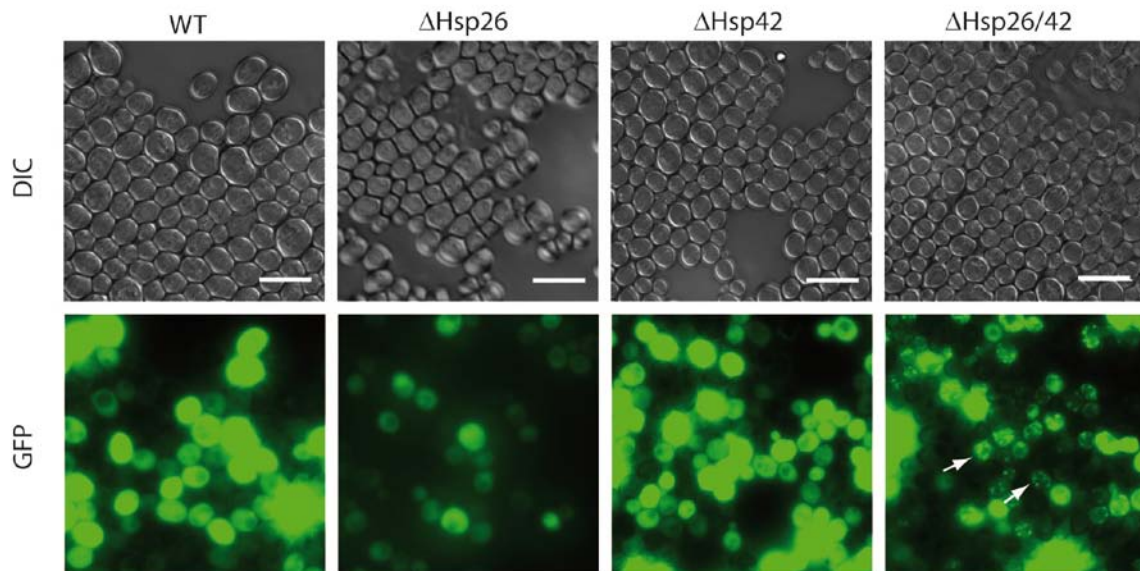


Figure 8 Firefly luciferase single mutant (SM)-GFP reporting on the level of proteome stress of baker's yeast.

Wt, Δhsp26, Δhsp42 and Δhsp26Δhsp42 yeast were transformed with the FlucSM-eGFP reporter under the control of the constitutively active GPD promotor. Cells were grown at 30°C, DIC and fluorescence images acquired at 100x magnification. Arrows point to GFP foci. Scale bar represents 10 μm.

Wt yeast at physiological temperature of 30°C expresses the FlucSM-GFP reporter at a high level in the soluble form, visible by high fluorescence intensity and a homogenous distribution of GFP emission (Figure 8, left column). For the single deletion strains $\Delta hsp26$ and $\Delta hsp42$, the same observations can be made. Under non-stressful conditions, the FlucSM reporter is expressed in the soluble form with no visible formation of GFP foci (Figure 8, middle columns). A different picture emerges with regard to the $\Delta hsp26\Delta hsp42$ double mutant. Here, beside the soluble expression of the FlucSM reporter, the formation of GFP foci can be observed, pointed out by the arrows in the image (Figure 8, right column). This suggests that already at 30°C the deletion of both small heat shock proteins in baker's yeast may lead to an elevated level of proteome stress. This is not yet the case in the genetic background of a single deletion of either sHsp gene.

LuciferaseSM-GFP 37 °C

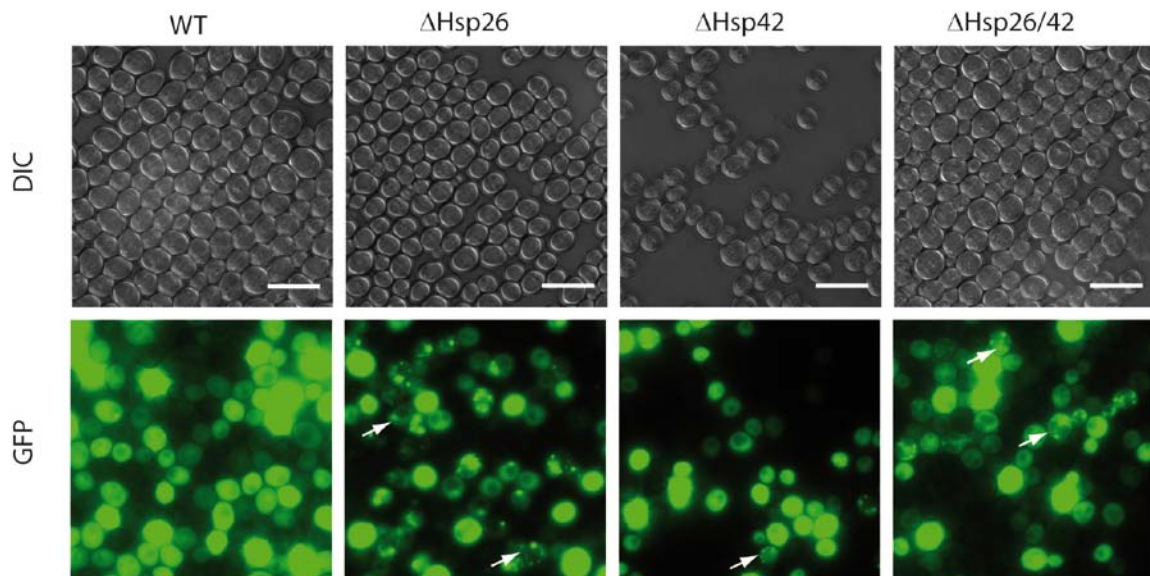


Figure 9 Firefly luciferase single mutant (SM)-GFP reporting on the level of proteome stress of 37°C heat-stressed baker's yeast.

Wt, $\Delta hsp26$, $\Delta hsp42$ and $\Delta hsp26\Delta hsp42$ yeast were transformed with the FlucSM-eGFP reporter under the control of the constitutively active GPD promotor. Cells were grown at 30°C and shifted to 37°C for 30min. DIC and fluorescence images were acquired at 100x magnification. Arrows point to GFP foci. Scale bar represents 10 μ m.

The FlucSM reporter was also used to assess the level of proteome stress in the context of heat shock. For this purpose, cells expressing FlucSM-GFP were grown at 30°C and shifted to 37°C for 30 min. Again by means of fluorescence microscopy, the expression and localization of the reporter protein was investigated (Figure 9). For wt yeast, shifting cells grown at 30°C to the higher temperature of 37°C did not have an influence on the expression level or cellular localization of the reporter. FlucSM-GFP was still present

predominantly in soluble form and did not yield any GFP foci (Figure 9, left column). Exposing the $\Delta hsp26$ or $\Delta hsp42$ yeast to 37°C stress for 30 min resulted in a reduced soluble amount of the reporter and the formation of GFP foci, indicating aggregation of the FlucSM reporter (Figure 9, middle columns). The double knockout strain also offered this observation. Here too, the FlucSM reporter was expressed in soluble form, and GFP foci were formed (Figure 9, right column). Compared to unstressed double KO yeast expressing the FlucSM reporter, no true enhancement of the level of proteome stress can be concluded in this case. However, the temperature induced foci-formation in the sHsp deletion strains but not in the wt, indicates an imbalance in proteostasis resulting in increased aggregation.

The firefly luciferase with two mutations (FlucDM) was also used to monitor the level of proteome stress in cells lacking the small heat shock proteins. For this purpose, cells transformed with the FlucDM-eGFP reporter were grown at 25°C and then shifted to 37°C before fluorescence microscopy was carried out. 25°C was chosen as the initial incubation temperature because FlucDM is already instable at 30°C (Gupta et al., 2011). At 25°C, FlucDM-GFP displayed diffuse cytosolic expression in all four yeast strains, however, a few cells (approx. 5%) with GFP foci were detected in the genetic background of sHsp-gene deletion (Figure 10, top). This may also indicate a marginally higher level of proteotoxicity in the sHsp-KO yeast strains. After a temperature shift to 37°C for 30 min, FlucDM showed a pronounced tendency of GFP foci formation, indicating aggregation of the luciferase-GFP reporter (Figure 10, bottom). Less protein is present in soluble form, as evident from a reduced level of diffuse GFP signal in the cells. This was the case for yeast strains of wt, single-gene KO, and sHsp-system deletion. However, one interesting observation can be made: wt and $\Delta hsp26$ yeast form GFP foci of large aggregates in low number per cell, while yeast with a deletion of *hsp42* show more granular like aggregations distributed throughout the cells. This may point to a contribution of Hsp42 in the sequestration or aggregation process of FlucDM-GFP.

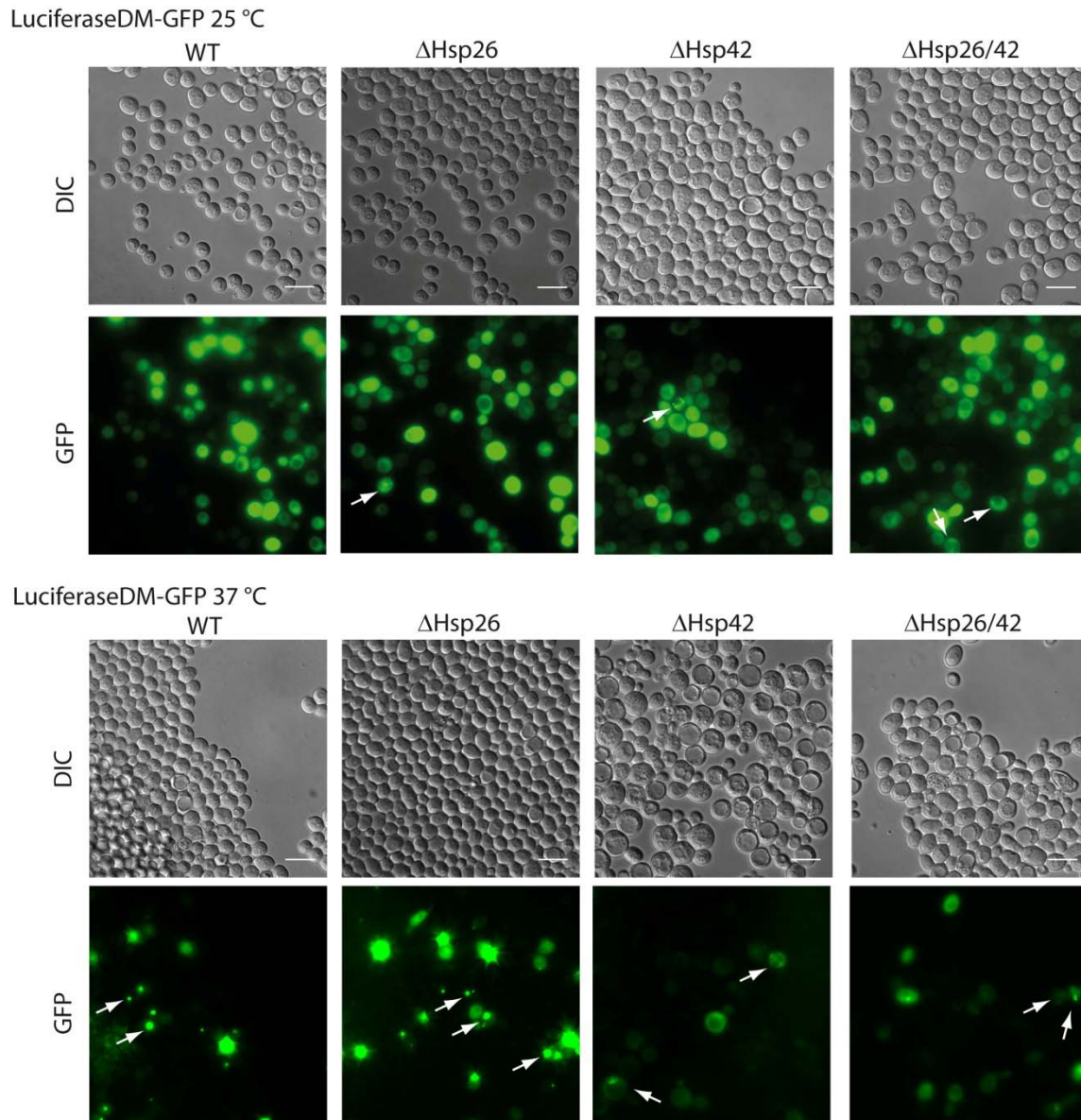


Figure 10 Firefly luciferase double mutant (DM) as sensor of proteome stress in baker's yeast. Wt, Δ hsp26, Δ hsp42 and Δ hsp26 Δ hsp42 yeast were transformed with the FlucDM-eGFP reporter under the control of the constitutively active GPD promotor. Cells were grown at 25°C and shifted to 37°C for 30 min. DIC and fluorescence images were acquired at 100x magnification. Arrows point to GFP foci. Scale bar represents 10 μ m.

The small granular-like aggregates of FlucDM-GFP in the Δ hsp42 and Δ hsp26 Δ hsp42 strains are difficult to display in images; therefore, a quantification of aggregate type was carried out by counting 500 heat stressed FlucDM-GFP expressing cells for each yeast strain (Figure 11).

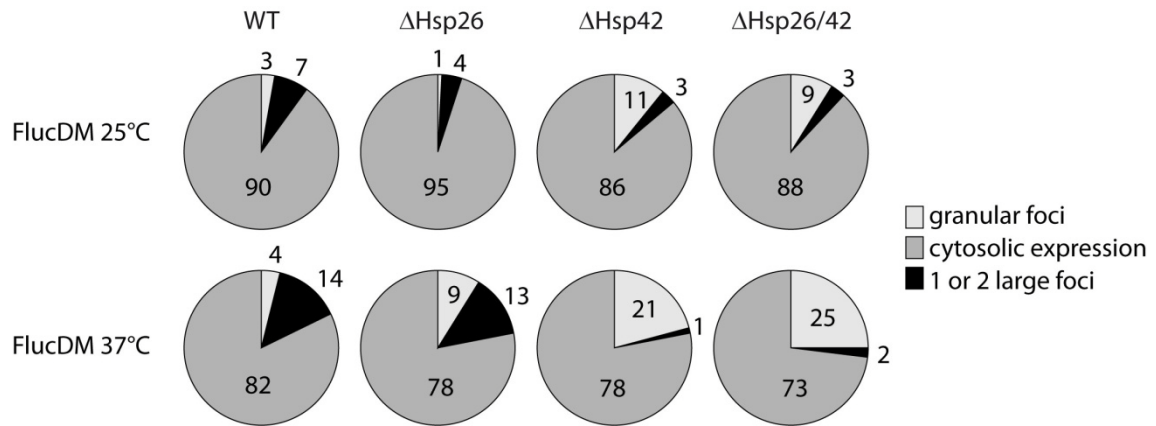


Figure 11 Quantification of FlucDM-GFP foci in wt, $\Delta hsp26$, $\Delta hsp42$, $\Delta hsp26/42$ yeast. Cells expressing the FlucDM-GFP reporter under the control of the constitutively active GPD promoter were cultivated at 25°C and then shifted to 37°C for 30 min. The numbers of FlucDM-GFP foci were counted for 500 cells of each yeast strain and condition, and pie charts generated. Cytosolic expression is in dark grey, mainly granular foci in light grey and one or two large foci in black. The values in or near the pie slices represent the percentage of cells attributed to the group.

At the physiological temperature of 25°C, 86% to 95% of the cells exhibited a diffuse GFP signal in the cytosol, signifying a soluble reporter protein. For wt yeast, a percentage of 3% of the counted cells possessed granular foci, and 7% had accumulated the GFP-signal to one or two large GFP foci in the cell. This tendency was also counted in $\Delta hsp26$ yeast, with 1% of the cells displaying granular GFP foci and 4% with one or two large aggregates. This is the opposite case with regard to $\Delta hsp42$ and $\Delta hsp26\Delta hsp42$ yeast, which have roughly 10% of the cells with a high number of small aggregates and only 3% that have an accumulation of FlucDM-GFP in one or two foci.

After 30 min of heat shock, this observation is augmented. In strains that contain Hsp42, the fraction of cells with only one or two large foci increases to around 13%. There is also an increase in the cells with more granular-like GFP signal distribution in the cells. Cells with an overall cytosolic expression of the reporter decrease by approximately 10%. For the yeast strains lacking Hsp42, 30 min of 37°C heat shock results in a two-fold increase in cells with a granular distribution of the GFP signal. Roughly 20% to 25% percent of the cells possess this phenotype. The percentage of cells with one or two large foci is similar to unstressed conditions at a low level of 1% to 2%. Hence, *hsp42* deletion results in the accumulation of small granular structures in high numbers, while cells with Hsp42 deposit the reporter protein in one or two larger aggregates.

sHsps in the toxic poly-glutamine aggregation model

In a next set of experiments, the influence of poly-glutamine (poly-Q) intoxication on proteostasis in wt and $\Delta hsp26$, $\Delta hsp42$ and $\Delta hsp26/42$ was focused on. The poly-Q disease-model of protein aggregation describes the aggregation of proteins with extensions of CAG-repeats in their genetic code that result in long poly-Q stretches, rendering the protein aggregation-prone. Poly-Q diseases have been identified and are in the focus of scientific investigations, for instance, in the neurodegenerative disorder of Huntington's disease. It has also been in the focus of previous research in the yeast model. In those studies it was shown that glutamine repeats longer than a critical threshold of 40 residues resulted in intoxicated yeast cells (Kaiser et al., 2013). The poly-Q model was to be investigated in the genetic background of sHsp gene deletion, because the sHsps possess chaperone activity, which suppresses the irreversible aggregation of proteins and contributes to Hsp104-mediated resolubilization of protein aggregates in the cell (Haslbeck et al., 2005a).

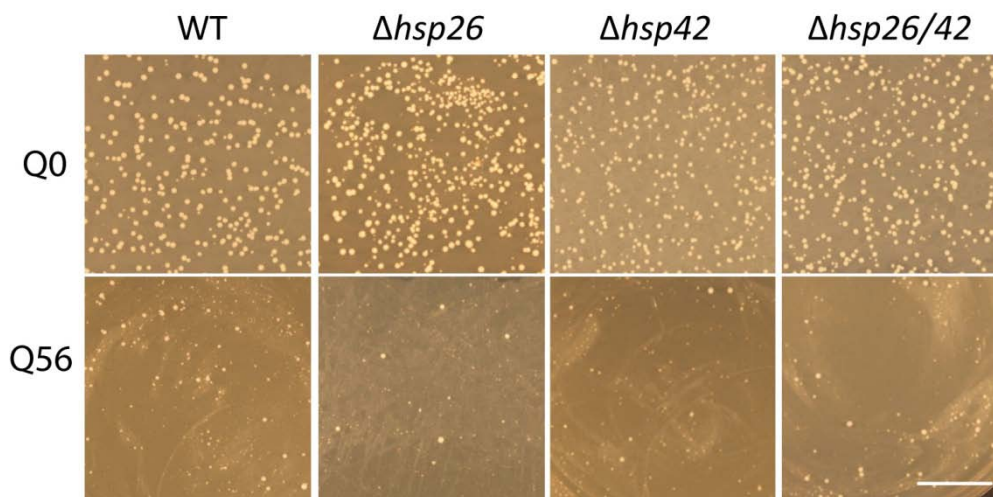


Figure 12 Poly-Q stretches of 56 amino acids are toxic to yeast.

Wt and sHsp deletion strains were transformed with YFP-Q0 and YFP-Q56 and incubated at 25°C for two days. Q0-transformed cells are viable and show normal colony formation after two days of incubation at 30°C. Q56-transformed cells show an intoxicated phenotype of small colony formation after four days of incubation at 30°C. Scale bar is 10 mm.

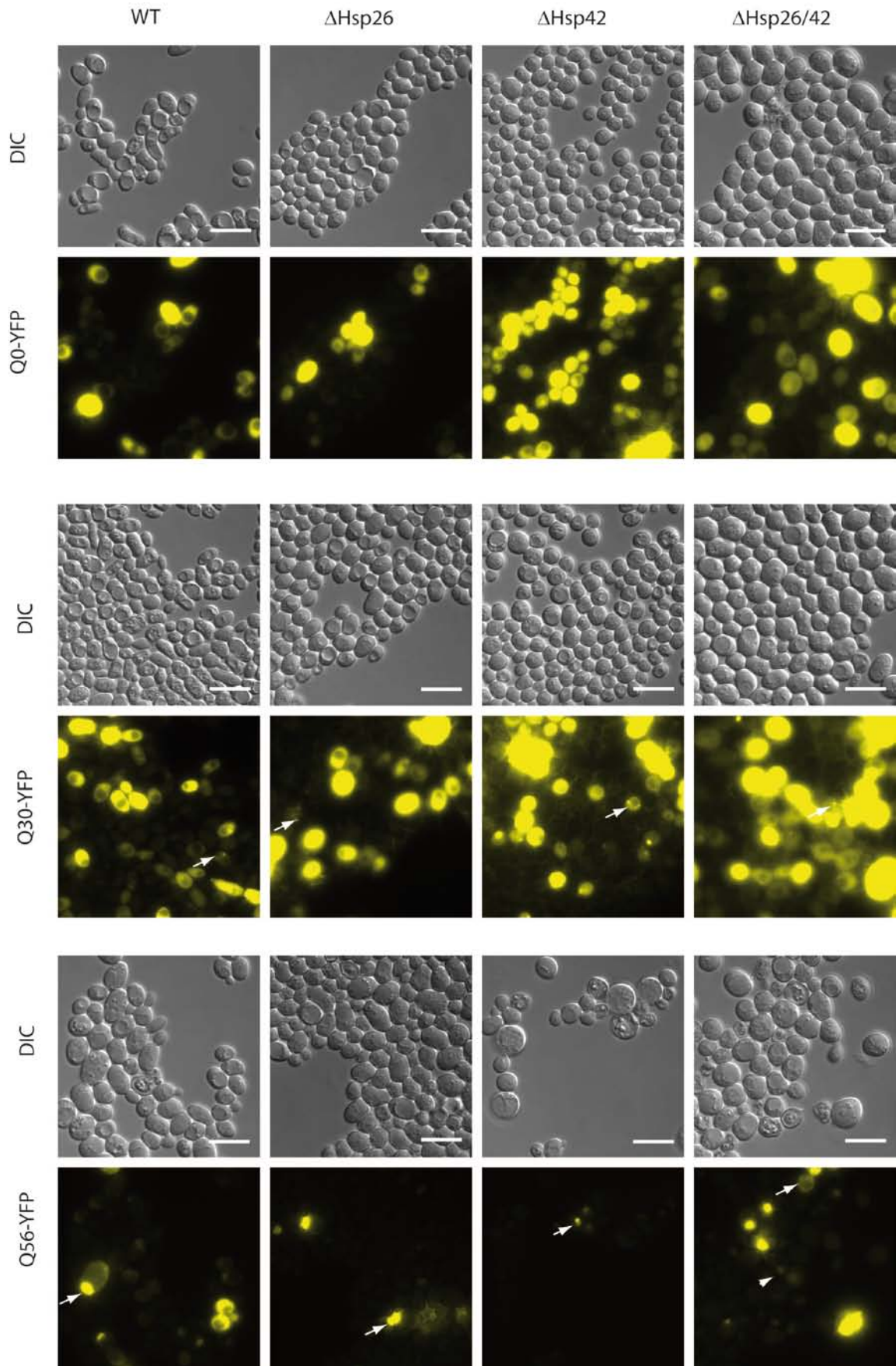
Transformation of yeast with the non-toxic Q0-YFP results in a normal colony formation of the cells in all four examined yeast strains. Transformation with YFP fused to a stretch of 56 glutamine residues resulted in the characteristic polyQ-induced cellular arrest (*pica*-) phenotype (Figure 12). The wt as well as the sHsp mutants displayed an identical growth

phenotype with small colonies of cell-cycle arrested cells and a low number of normalized colonies that escape toxicity by achieving a hyperploid state (Kaiser et al., 2013). By means of fluorescence microscopy detecting YFP emission, it was possible to gain insight into the cellular localization of the poly-Q constructs in the presence of the small heat shock proteins in wt yeast and in the genetic background of their gene deletions (Figure 13). All four yeast strains expressing Q0-YFP possess cytosolic soluble expression of the reporter, evident from a homogenous distribution of the YFP signal in the cytosol. This was expected for the non-toxic Q0-YFP (Figure 13, top). Next, Q30-YFP expression was investigated. This construct, which is still non-toxic and does not elicit a *pica*-phenotype in yeast, showed mostly soluble expression of the protein, however, the formation of foci was detectable to a low degree. For all four yeast strains, cells could be imaged that showed foci-formation, indicating aggregation of the reporter protein. No differences between the wt and sHsp-deletion strains were present. Therefore, Q30-YFP shows a minor tendency of aggregating, but not to a degree that would result in toxicity to the yeast cells (Figure 13, middle). Intoxicated cells of wt and sHsp-gene deletion strains expressing Q56-YFP display a morphological phenotype with enlarged cell sizes, as depicted in the DIC images. The emission of the YFP fluorophore is no longer detectable as homogenous cytosolic expression, but rather the formation of aggregates of Q56-YFP is visible and the overall signal intensity appears lower. No differences in YFP-foci formation between wt, $\Delta hsp26$, $\Delta hsp42$ and $\Delta hsp26\Delta hsp42$ yeast exists (Figure 13, bottom). Hence, deletion of the small heat shock proteins of baker's yeast does not visibly affect the aggregation process of polyQ constructs under the experimental conditions tested here.

Figure 13 Fluorescence microscopy analyzing the expression pattern of polyQ constructs of various length.

BY4741wt, $\Delta hsp26$, $\Delta hsp42$ and $\Delta hsp26\Delta hsp42$ cells expressing polyQ0, Q30 or Q56-YFP fusions under the control of a constitutively active GPD promotor were monitored. DIC images and YFP-emission images were taken. Q0-YFP expressing cells of all strains show soluble cytosolic distribution (top 2 rows). Q30-YFP expression is also mainly soluble, with a few fluorescent foci appearing, indicating a low level of aggregation of the reporter (2 middle rows). Q56-YFP intoxicated cells exhibit swelling and show reduced soluble expression of the reporter and formation of large foci of protein aggregates (bottom 2 rows). Scale bar is 10 μ m. Arrows point to foci. Images were taken with 100x magnification. (Figure on next page).

Polyglutamines-YFP



In yeast strains harboring endogenous GFP fusions with the two small heat shock protein loci, the localization of the sHsps was to be investigated in presence of polyQ0-mCherry and polyQ56-mCherry (Huh et al., 2003). The strains with chromosomal GFP fusions own the additional benefit of carrying the sHsp-GFP fusion under the control of the endogenous promotor, therefore, reflecting the actual expression level of the protein. The respective *hsp26*-GFP and *hsp42*-GFP strains were transformed with plasmids carrying Q0- or Q56 mCherry and incubated for two days (Q0) or four days (Q56) at 30°C, at which point, fluorescence microscopy images were acquired (Figure 14).

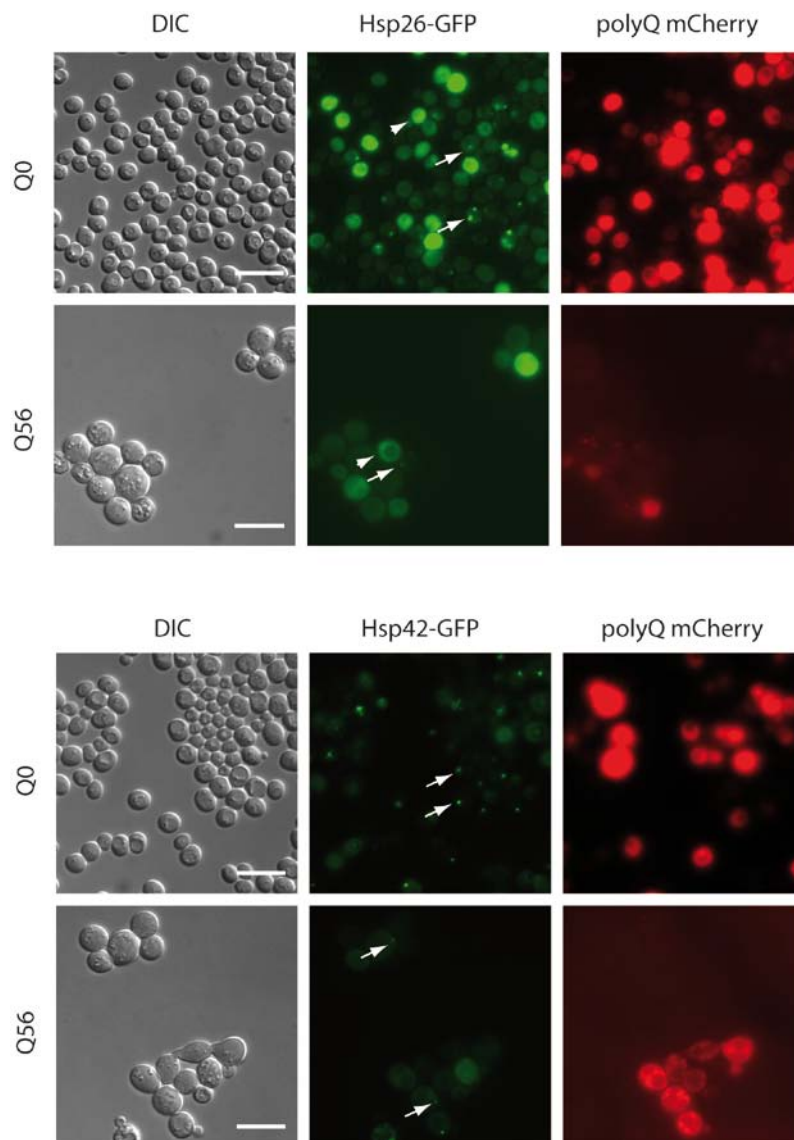


Figure 14 Poly-Q intoxication in sHsp-GFP fusion strains.

Yeast strains harboring chromosomal fusions to the GFP-reporter gene were transformed with plasmids if non-toxic Q0-mCherry or toxic poly-Q56-mCherry under control of the constitutively active GPD promotor. DIC images, GFP- and mCherry-fluorescence images were acquired at 100x magnification. Top: Cellular localization of Hsp26-GFP and of Q0- or polyQ56-mCherry. Bottom: Cellular localization of Hsp42-GFP and Q0- or polyQ56-mCherry.

Q0-mCherry, as well as Q0-YFP, displayed mostly homogenous soluble expression in the yeast cytosol. On the other hand, Q56-mCherry, as was the case for Q56-YFP, is expressed at a lower level and shows the formation of fluorescent foci, representing aggregation of the reporter protein (Figure 14, right). The Hsp26-GFP fusion protein displays mostly soluble cytosolic expression, however, with the formation of GFP foci indicating aggregation, or specific localization in the cell. It has been reported that Hsp26-GFP mainly is in diffuse cytosolic expression but also forms GFP foci in some cases (Thayer et al., 2014). This is also the case for Q56-intoxicated cells, where soluble expression, as well as foci-formation, is present (Figure 14, top, middle). In the Hsp42-GFP expressing strain, a high resemblance to the results obtained in the Hsp26-GFP strain is present. Hsp42-GFP is expressed soluble as seen by an even cytosolic fluorescence; also GFP foci appear in cells transformed with the non-toxic Q0 construct. In Q56-expressing yeast, the results are the same: soluble expression and the formation of GFP foci persist (Figure 14, bottom middle). To sum this experiment up, the small heat shock protein-GFP fusions do not show any differences in cellular localization between non-toxic Q0 or toxic Q56-protein expression. It must be noted that GFP is a large protein with a molecular weight of 28 kDa. Hence, a simple fusion to the C-termini of the small heat shock proteins most probably has large effects on the structure of the monomer, as well as on the oligomerization of the proteins. Furthermore, these effects on structure will probably also impact the functional activity of the sHsp proteins.

4.2 Heat stress and the inner cellular morphology

4.2.1 X-ray tomography of unstressed *S. cerevisiae*

Studies analyzing the influence of heat stress on inner cellular morphology have shown a number of deleterious effects on the cell including defects on the cytoskeleton, fragmentation of the Golgi or ER, or a decrease in number of mitochondria or lysosomes (Richter et al., 2010). Using soft-X-ray tomography the inner cellular morphology of the BY4741 wt baker's yeast strain was investigated under a variety of different thermal stresses, including mild, sub-lethal and lethal heat stress. Due to the fact that no staining procedures are necessary during sample preparation for soft-X-ray microscopy and because cells are vitrified in liquid ethane, cells and their inner morphology can be monitored in the near-native state with the best possible preservation of ultra structure (Hagen et al., 2012). Cellular components with a high carbon-content, e.g. in lipid-rich structures, scatter X-rays much stronger than water-rich structures, and they, therefore, generate regions of high contrast in the images. By means of segmentation, i.e. the tracing of the boundaries of structural components such as organelles through the Z-plane of the acquired image stacks, 3D-models of baker's yeast were obtained.

Soft-X-ray tomography of a wild-type baker's yeast cell cultivated at a physiological temperature of 25°C into early exponential growth phase ($OD_{595} = 0.8$) was carried out as an initial experiment. The projection images of the tilt series were reconstructed using the etomo package from IMOD as described in Materials and Methods (see chapter 3.12.2). Orthoslices of the reconstructed tomogram, averaged over 20 of the 640 sections of the tomogram, display the inner cellular morphology of unstressed yeast (Figure 15).

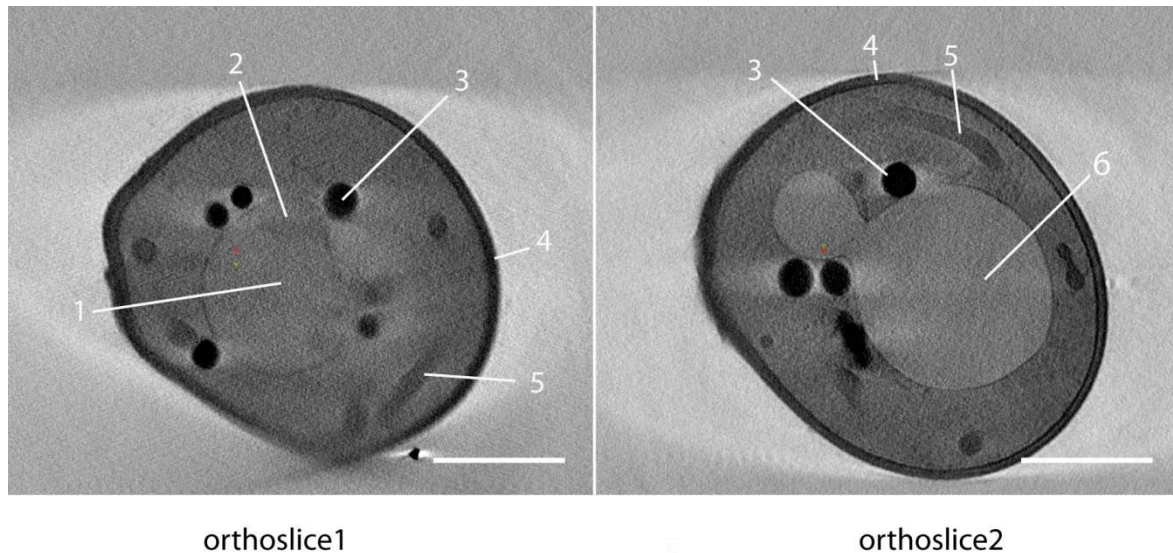


Figure 15 Cross-sections of a representative reconstructed tomogram of BY4741wt yeast at 25°C. Two different cross-sections, gathered over 20 sections of the reconstructed tomogram, are depicted. Resolvable structures are numbered: 1: nucleus; 2: nucleolus; 3: lipid bodies; 4: cellular membrane; 5: mitochondria and 6: vacuole. The scale bar on the bottom right is 1 μm . The tilt series was collected at the U41-TXM beamline at the electron storage ring BessyII (Helmholtz Zentrum Berlin, Germany).

The reconstruction of the tilt series for unstressed wild type yeast displays an intact cellular morphology. The cellular membrane and the comparably thick cell wall, the barrier to the extracellular environment, are visible as a darker structure surrounding the yeast cytosol, which appears less bright (Figure 15; 4). Lipid bodies show dense structures with a high contrast in the tomogram. They are numerous, mostly of spherical shape, and of different sizes with 0.1 μm to 0.4 μm in diameter. The lipid bodies are distributed throughout the yeast cytosol (Figure 15; 3). Other organelles visible in the reconstruction are less dense and appear more transmissive. The assignment of a cellular structure to a specific organelle type was inspired by known characteristics of organelle shape and size. These sub-cellular structures include the nucleus and therein lying nucleolus (Figure 15; 1 & 2). The nucleus is surrounded by a lipid-rich nuclear membrane separating it from the cytosol. The nucleolus, a sub-nuclear structure within the nucleus, is also visible. As the site of ribosome synthesis and assembly, it is of higher density and appears as a slightly darker substructure within the nucleus. Mitochondria can be distinguished clearly from other cellular structures because they are long and tubular-like, run through the yeast cytosol, and appear as darker structures in the tomograms (Figure 15; 5). Vacuoles are clearly distinguishable (Figure 15; 6) as they are of various sizes and shapes, and they appear as a

transmissive organelle, due to the high aqueous content. This makes them clearly distinguishable from the other structures. In summary, X-ray microscopy enables the investigation of the inner cellular morphology. The nucleus, nucleolus, vacuoles, lipid bodies and mitochondria are the cellular structures that can be visualized. The resolution of these cellular components is in agreement with existing studies using X-ray microscopy, which have analyzed the cell division processes of *S. cerevisiae* (Larabell and Nugent, 2010; Uchida et al., 2011). Smaller organelles and cellular structures, such as the endoplasmic reticulum (ER), Golgi-apparatus or cytoskeletal components lie below the spatial resolution limit of approximately 40 nm of the utilized X-ray microscope (Gu et al., 2007; Uchida et al., 2011).

4.2.2 X-ray tomography of heat stressed yeast

X-ray microscopy was utilized to investigate the influence of heat shock on the inner morphology of *S. cerevisiae*. First, cells were cultivated into the early exponential growth phase and then exposed to heat shock conditions. These included mild heat shock for 10 min at 37°C, short sub-lethal heat shock for 10 min at 42°C, and a severe heat shock for 10 min at 50°C. Cells were used immediately for vitrification and X-ray tomograms were obtained as described (see chapter 3.12.2).

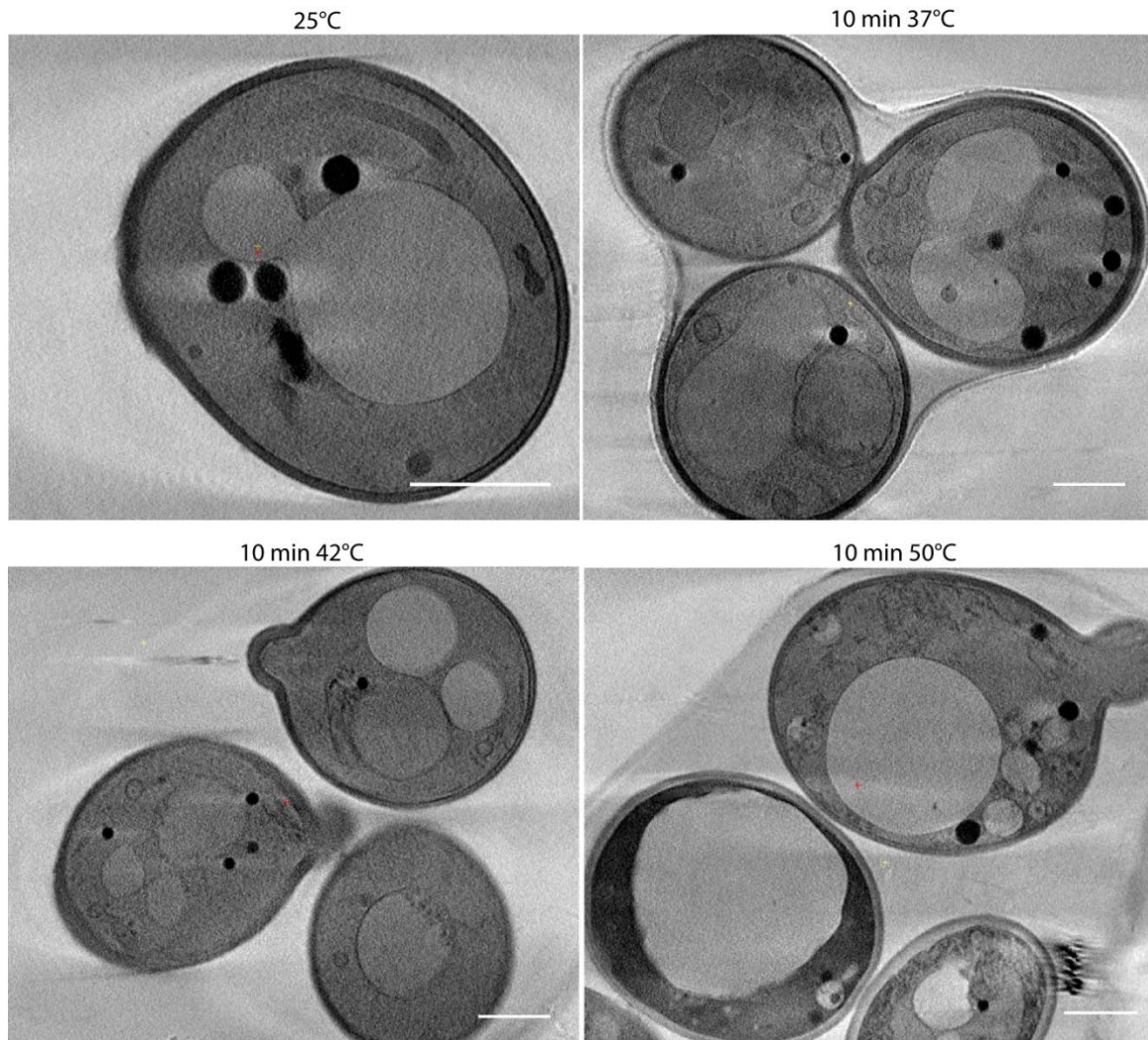


Figure 16 Inner cellular morphology of baker's yeast under heat shock conditions. BY4741wt yeast was cultivated at 25°C ($OD_{595}=1.0$) and then exposed to 10 min of either 37°C, 42°C or 50°C. Cells were immediately vitrified. Projection image series were obtained at the U41-TXM beamline (BessyII, Berlin, Germany). Tomograms were reconstructed. One cross-section (averaged from 20 sections of the 670) for each condition of heat stressed yeast is depicted. Scale bar is 1 μ m.

The reconstructed tomogram of unstressed BY4741 wild type yeast exhibits an intact inner cellular morphology. The tubular network of mitochondria is intact and runs through all planes of the yeast tomogram. The cytosol is homogenous, free of any visible aggregates and lipid bodies exist. Nucleus and nucleolus are undamaged (Figure 15 & Figure 16 top left). A 10 min shift to mild heat shock temperatures of 37°C, as well as a shift to sub-lethal temperatures of 42°C, has no influence on the inner cellular architecture of the cell, as far as it can be resolved by X-ray tomography. Organelles are still intact and the cytosol is without any visible aggregates (Figure 16, top right, bottom left). In conclusion, a 10 min shift to 37°C or 42°C does not result in alterations of detectable macromolecular

structures of baker's yeast. Yeast, therefore, is a robust system and is able to maintain its main cellular and sub-cellular integrity under thermal stress.

A harmful stimulus of 10 min at 50 °C, which lies well beyond the upper temperature limit of yeast viability at 42°C (Jones and Hough, 1970), was also investigated. Here, clear effects of thermal stress exist (Figure 16, bottom right). Very pronounced is the fragmentation of the mitochondrial network. Hardly any of the tubular structures of this organelle remain intact. Furthermore, granular-like structures with higher contrast accumulate in the cytosol as a consequence of protein aggregation or fragmentation of organelles. The formation of stress-granules, i.e. stress-induced agglomerates of RNA and proteins, under heat shock conditions is known (Wallace et al., 2015). The morphology of the vacuoles also suffers under 50°C heat shock and appears enlarged. Hence, a harmful stimulus of 50°C profoundly influences the inner cellular architecture of wt yeast.

4.2.3 X-ray tomography of gene deletion mutants

In a deletion mutant lacking the molecular chaperone Hsp12, heat stress has been shown to lead to an altered phenotype of the cell with a crumpled raisin-like morphology of the outer cell wall (Welker et al., 2010). Hsp12 is an intrinsically disordered protein that adopts α -helical structure upon binding to lipids. It is thought that heat stress directs Hsp12 towards the cellular periphery, where it contributes to maintaining cellular integrity and stabilizes the lipid bilayer of the membrane (Welker et al., 2010). The $\Delta hsp26$, $\Delta hsp42$ and $\Delta hsp26\Delta hsp42$ yeast strains were also analyzed by means of X-ray microscopy. A deletion of *hsp26* and *hsp42* was shown to yield a crumpled surface morphology with a raisin-like phenotype, similar to that observed for $\Delta hsp12$ yeast (Haslbeck et al., 2004). Here, it was to be examined if this phenotype can be recapitulated by means of X-ray microscopy. The influence of heat stress on the inner cellular morphology in the genetic background of above-listed gene deletions was to be investigated. An identical sample preparation as for the wild-type yeast strain was carried out, projection image series were acquired at the BessyII (Berlin, Germany) and tomograms were reconstructed (Figure 17).

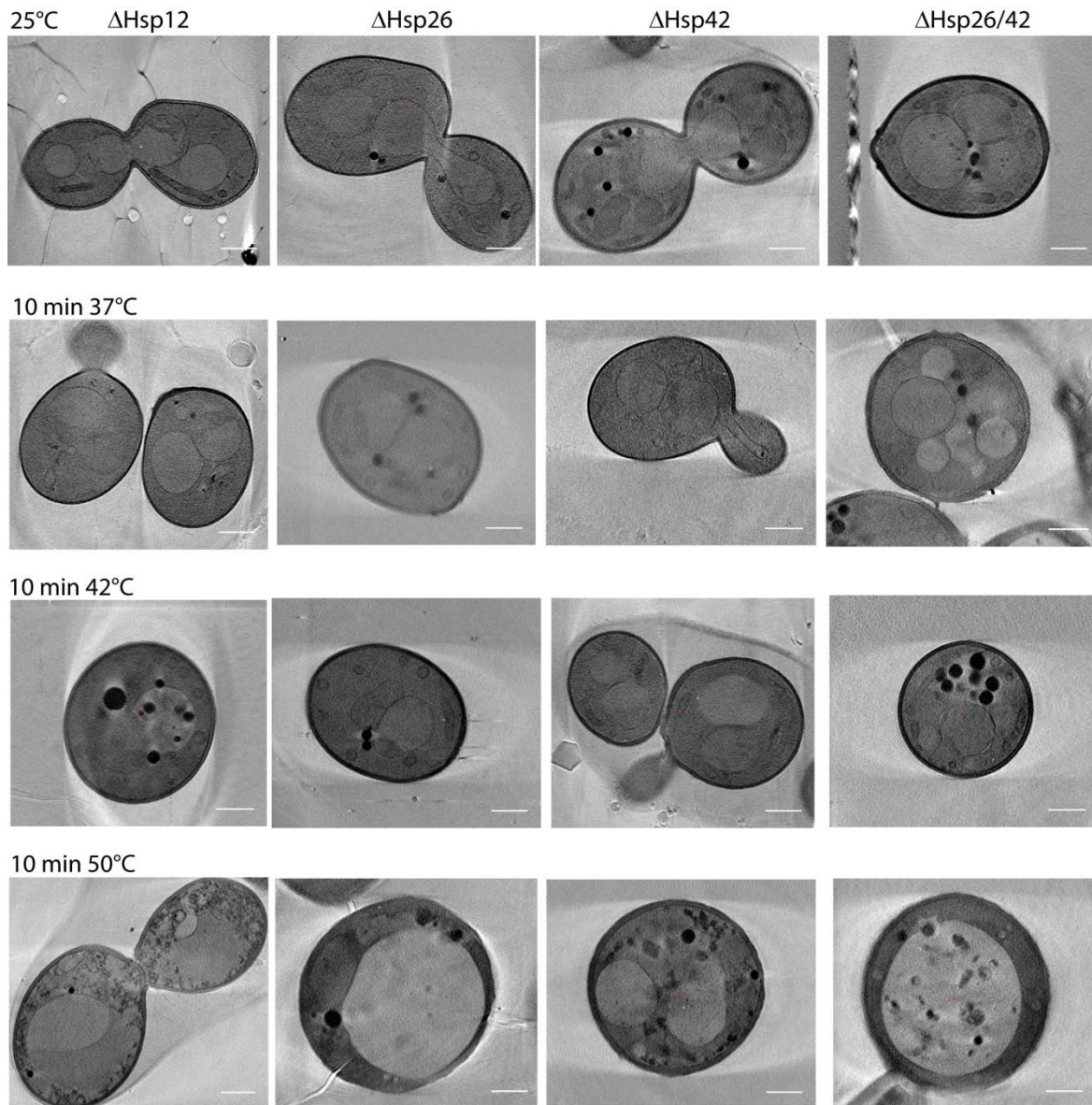


Figure 17 Cross-sections of reconstructed X-ray tomograms of BY4741 deletion strains. $\Delta hsp12$, $\Delta hsp26$, $\Delta hsp42$ and $\Delta hsp26\Delta hsp42$ yeast were grown at 25°C into the exponential growth phase ($OD_{595}=1.0$). Controls were directly flash-frozen in liquid ethane. Samples of heat stress conditions were treated for 10 min with 37°C, 42°C or 50°C before vitrification. Projection image series were gathered in 1° increments from -70 to +70° at the U41-TXM microscope of the BessyII (Berlin, Germany). Depicted are cross-sections (averaged over 20 sections) of reconstructed tomograms.

Deletion mutants of *hsp12*, *hsp26*, *hsp42* and *hsp26/hsp42* grown at the physiological temperature of 25°C possess an identical inner cellular morphology to wild type BY4741. The same mitochondrial network, nucleus, nucleolus, lipid droplets and vacuoles can be seen (Figure 17, top row). A shift to mild heat shock conditions at 37°C for 10 min has no effect on the inner morphology in any of the yeast strains. Here, reconstructed tomograms are indistinguishable from unstressed conditions (Figure 17, 2nd row from top). This is also

the case after sub-lethal heat shock at 42°C. A stress of 10 min did not have any effect on the inner cellular architecture in any of the four yeast KO strains examined. As was the case for the wild type, short sub-lethal heat shock did not impact inner morphology, at least with regard to the mitochondria, vacuole, nucleus and nucleolus, lipid droplets and cellular membrane (Figure 17, 3rd row from top). The phenotype of crumpled cellular surface morphology, reported to appear at 43°C in the sHsp deletion strains, was not recaptured here. Ten minutes of harmful heat shock again resulted in vast changes in the morphology. Mitochondria cannot be traced anymore, the vacuoles appear swollen, cytosolic granular aggregates are visible (Figure 17, bottom row). All in all, the cellular morphology resembles that of wild type baker's yeast exposed to the same heat shock conditions. The crumpled cell surface of the $\Delta hsp12$ strain was not detectable here. The cellular membrane still appears intact and cellular integrity is maintained. In conclusion, disruption of the small heat shock protein genes or *hsp12* does not evoke a phenotype of the inner cellular morphology, as far as can be determined by X-ray tomography.

It would be of interest to elucidate the temperature at which the inner cellular morphology of the yeast cell actually starts to be affected. No morphological changes are observed at 42°C, whereas 10 min incubation at 50°C causes a profoundly altered inner morphology. Due to the limited amount of beam time available for this project and the long duration for tomogram acquisition, more temperature ranges and durations of heat stress could not be investigated. Furthermore, replicate number is a major limitation of the utilized X-ray microscope. Only a handful of tilt series were acquired for a given yeast strain and condition, making a truly representative analysis of investigations on KO-effects not possible.

4.2.4 Generation of 3D-models of baker's yeast

Selected tomograms of high quality were used for segmentation of the organelles. By tracing the boundaries of cellular structures throughout all sections of the reconstructed tomograms, three-dimensional models of the inner cellular morphology of baker's yeast were built. Spherical structures, such as the plasma membrane, vacuole and nucleus can be interpolated, while the tubule-like network of the mitochondria and the many lipid droplets require elaborate manual tracing steps. Nevertheless, the utilized etomo package enabled a segmentation of above-mentioned organelles and the generation of three-dimensional models of baker's yeast.

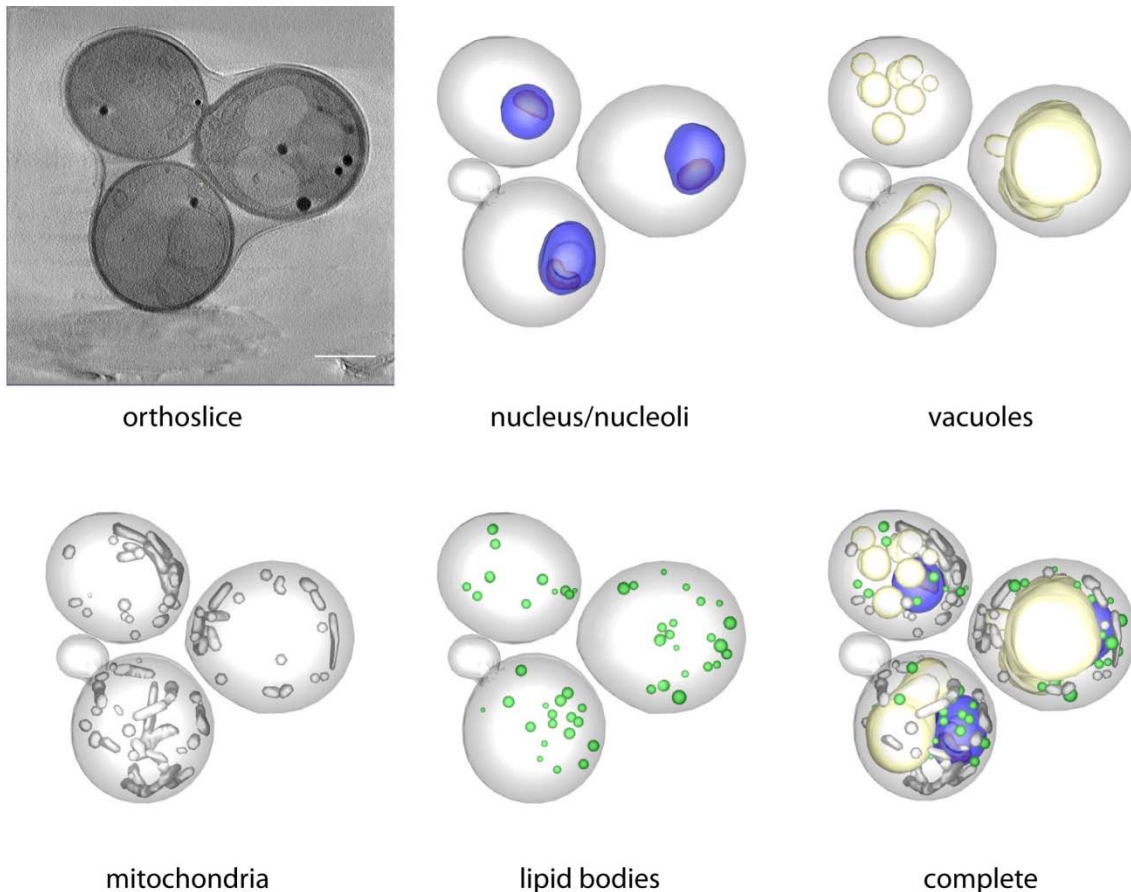


Figure 18 Segmentation of rapidly frozen BY4741wt baker's yeast.

A reconstructed tomogram of high quality of yeast treated for 10 min at 37°C was used for segmentation. Organelles and cellular boundaries were tracked through all 1,324 sections of the tomogram. For segmentation, the 3dmod package of etomo was used (IMOD, Boulder Colorado). The interpolator tool was used wherever possible (membranes, nucleus, vacuole), for non symmetrical structures (mitochondria, nucleolus) manual tracing was carried out. Nucleus is in blue, nucleolus in orange, vacuoles in yellow-white, mitochondria in grey, and lipid bodies in green. Scale bar is 1 μm .

A reconstructed tomogram of high quality was used to generate a three dimensional model of the inner morphology of *S. cerevisiae* exposed to 10 min of 37°C stress (Figure 18). The cellular membrane was traced by hand for selected sections of the tomogram and the remaining sections were interpolated and manually verified for correct positioning of the boundaries. Transparency was set high to enable a view into the three-dimensional model. The nuclei (blue), also spherical-like in shape, were interpolated and manually adjusted where necessary. Located inside the nucleus are the nucleoli (orange) of more irregular shape, and their contours were traced manually. Segmentation of the vacuoles displays their diversity (yellow-white): small round vacuoles and large vacuoles of irregular shape are contained in the 3D model. Lipid bodies (green), although they are mostly round in

shape, need cautious tracing of their contours. Due to their high carbon content, they result in objects of high contrast, which can result in incorrectly traced contours at the top and bottom of their appearance in the Z-plane. Mitochondria were segmented exclusively by hand due to their tubular like network that runs through the entire cell (grey). In the complete 3D-model of the 37°C heat stressed baker's yeast cell, the localization of all segmented structures is visible. This model nicely illustrates the crowded environment: the nuclei bordering on the vacuoles, the mitochondria running a pipe-like system around other organelles, and lipid bodies squeezed in between. Other cellular structures below the spatial resolution of approx. 40 nm, were not resolved by X-ray microscopy, and therefore, were unable to be segmented into the model.

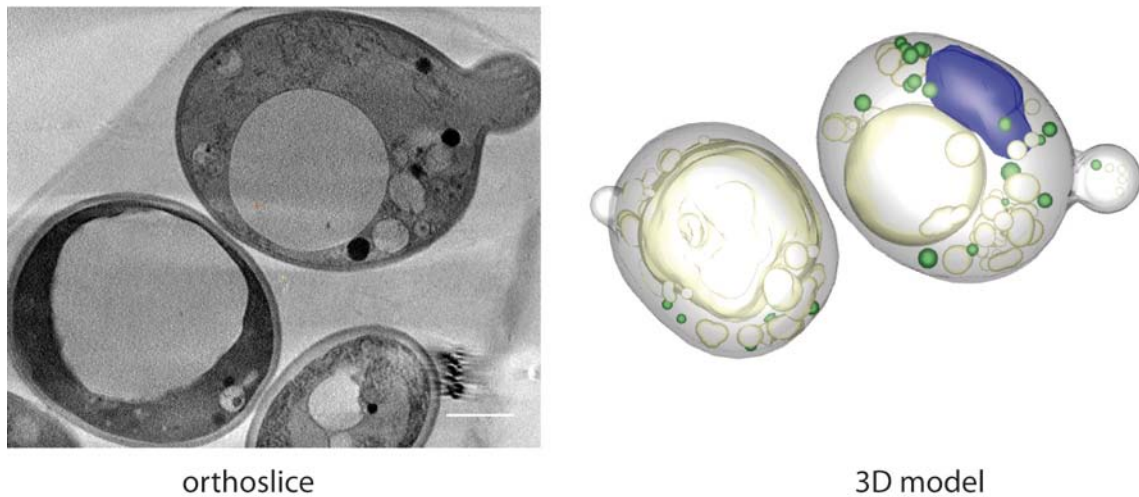


Figure 19 Segmentation of rapidly frozen BY4741wt baker's yeast under 50°C stress.

A reconstructed tomogram of BY4741wt yeast exposed to 10 min of 50°C stress was used for segmentation. Organelles and cellular boundaries were traced through all 1,324 sections of the tomogram. For segmentation, the 3dmod package of etomo was used (IMOD, Boulder Colorado). The interpolator tool was used wherever possible, otherwise manual segmentation was carried out. The nucleus is in blue, vacuoles in yellow-white, lipid-bodies in green. The transparency of the cellular membrane was reduced and displays the overall higher contrast in the cytosol. Scale bar is 1 μm .

A representative 3D model of BY4741wt yeast exposed to 50°C for 10 min was also generated (Figure 19). The morphological consequences of the harmful stimulus are difficult to incorporate in the model. The overall higher contrast in the cytosol, probably due to protein aggregation or organelle fragmentation, is displayed with a reduced transparency of the cellular membrane. Differences to the model of yeast with intact morphology are the lack of mitochondria, the swollen large vacuole of irregular shape, and a nucleus severely impaired in its structure. The small granular-like deposits of protein aggregates were unable to be integrated into the 3D model.

4.3 Transcriptional studies on wild type *S. cerevisiae* under heat shock

Microarrays are ideally suited for studying the transcriptional response of *Saccharomyces cerevisiae* exposed to potentially harmful environmental conditions, such as heat shock. Commercially available gene chips, carrying 5,717 *S. cerevisiae* open reading frames, allow a detailed and exact analysis of the kinetics of gene regulation under conditions of high temperature stress.

Here, the transcriptional response to two different heat stresses was investigated. In both cases, BY4741 wt yeast was maintained in the logarithmic growth phase at 25°C in full medium for two days prior to the shift to a higher temperature. In a first experiment, cells were exposed to mild heat shock conditions shifting the cells to 37°C, which lies above the optimal growth temperature of baker's yeast at 25°C to-30°C (Walsh and Martin, 1977); yet it was still well below the maximum temperature of *S. cerevisiae* viability at around 42°C (Arthur and Watson, 1976). The second study covered the kinetic response of cells shifted to 42°C, representing a more severe, nevertheless still, sub-lethal heat shock (Figure 20).

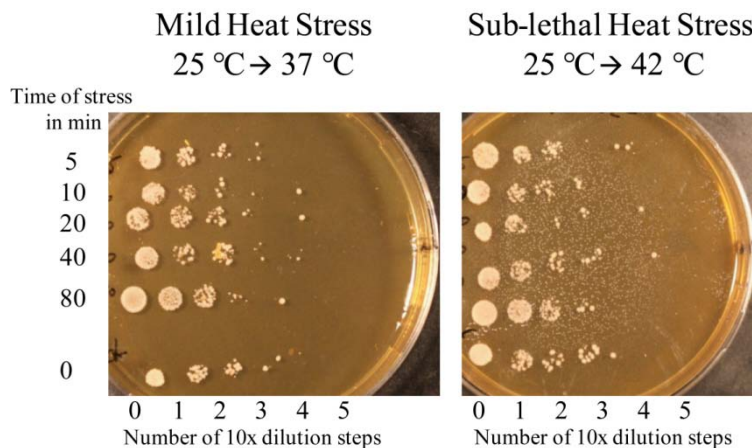


Figure 20 Survival assay of BY4741 wt yeast exposed to temperature stress. Serial 10x dilutions of cultures exposed to mild heat shock (left) and sub-lethal heat shock (right) for the indicated durations were prepared and spotted on YPD.

Microarrays were carried out with biological duplicates or triplicates enabling a statistically well-founded data analysis. Biological replicates were cross-correlated in order to identify potential outlier and were removed from data analysis if necessary. In general, the correlation between biological triplicates was very high (Pearson's $r > 0.900$). Data from different batches - in essence datasets from different experimental setups prepared on independent days - were quantile normalized which averaged the distribution of the intensities over all data points (Speed et al., 2003). This normalization procedure allows the comparison of microarray data of different batches and biological replicates.

4.3.1 The transcriptional response to mild heat stress

Mild heat stress elicits a transient heat shock response with distinct waves of transcription

A shift from 25°C to 37°C yields vast and swift alterations in transcription. Differentially regulated genes at the selected thresholds (see chapter 3.11) are listed in Table S1. Three hundred genes with at least a \log_2 -fold induction of 1 at 5 min after onset of stress are rapidly up-regulated (Figure 21A, red). In addition, down-regulation of 262 genes with at least a \log_2 -fold decrease of 1 in RNA level coincides in this time frame (Figure 21A, blue). All rapidly up- and down-regulated genes peak between 10 min and 15 min and gradually decline towards lower values thereafter. A second wave of transcriptional regulation is observable with slower kinetics and lower fold-changes in general. For these genes, differential regulation starts after 5 min and peaks between 10 and 20 minutes (Figure 21A, black and green). Here, too, regulation is bi-directional, with 294 up- and 280 down-regulated transcripts at the selected cutoff values. The decline towards basal RNA levels starting after 20 min - with the exception of two transcripts that remain high over the entire duration of stress - indicates an adaptation of baker's yeast to mild heat stress conditions by establishing new steady state transcriptional levels. Hence, the transcriptional response of wt baker's yeast to conditions of mild heat shock peaks between 10 min and 15 min and is transient, the cells adapt to a new steady state level of gene regulation starting after 20 min.

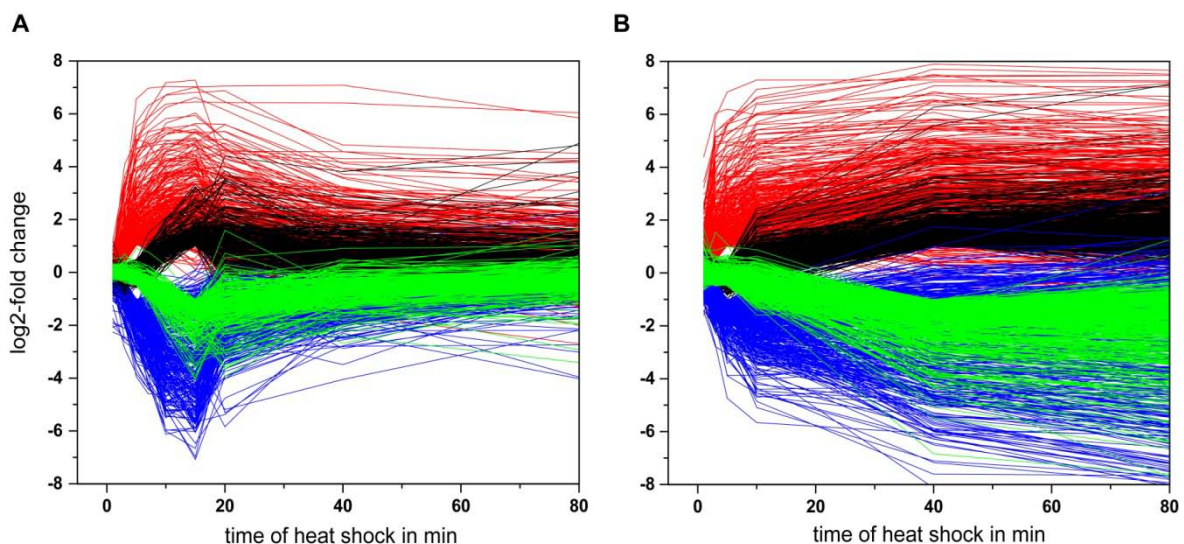


Figure 21 Kinetic profiles of transcriptional regulation of BY4741 wt baker's yeast under different types of heat stress.

A. Yeast cultures were submitted to mild heat stress (25°C → 37°C) for the indicated durations and total RNA levels were analyzed by microarrays. Plotted are \log_2 fold-changes of gene regulation over time relative to 0 min. B Kinetic profiles of gene regulation of yeast exposed to sub-lethal heat

stress (25°C → 42°C) and analyzed as in A. Red: early up-regulated genes; black: late up-regulated genes; blue: early down-regulated genes; green: late down-regulated genes. (Figure legend continued from previous page).

Gene ontology analysis of the transcriptional response to mild heat stress

The differentially regulated genes under mild 37°C heat stress were run through a Gene Ontology (GO) analysis using DAVID (Bioinformatics Resources 6.7; National Institute of Allergy and Infectious Diseases; NIH) and the GO Slim Mapper of the yeast genome database, in order to better display enriched pathways, biological processes, molecular functions or cellular components. Enriched GO terms of yeast stress included ‘responses to thermal stress’, as well as ‘abiotic stress’, terms involved in ‘protein folding’, ‘carbohydrate metabolism’, ‘protein catabolic processes’, and ‘generation of precursor metabolites and energy’ on the side of up-regulated genes. Enriched terms on the side of down-regulation mostly contain transcription-associated terms, such as ‘RNA-processing and modification’, ‘ribosomal RNA maturation’, but also translation related terms, such as ‘ribosome assembly’. Late down-regulated genes are annotated to GO terms associated with transcription and translation. ‘Regulation of translation’, ‘tRNA metabolic process’, and ‘nucleotide and nucleic acid biosynthetic processes’ are among these (Figure 22A, B).

Early up-regulation of molecular chaperones and energy metabolism

The appearance of the GO terms ‘protein refolding’ and ‘response to heat and abiotic stimulus’ can be attributed to the many molecular chaperones and co-chaperones being induced in transcription shortly after the onset of stress. These include *hsp26*, *hsp42*, *hsp12*, *hsp82*, *hsp104*, *ssa1*, *ssa4*, *hsp78*, *mdj1* and *aha1*. A more detailed analysis of the heat induced transcriptional regulation of the molecular chaperones is presented later (see chapter 4.3.4, Table 16). Proteins unfold at high temperatures and the results are the accumulation of protein aggregates. Therefore, the augmented demand for molecular chaperones as a protective mechanism is intuitive, as chaperones may serve to restore balance to cellular protein homeostasis by aiding in protein folding and maintenance of particular protein conformation. Further up-regulated clusters include carbohydrate metabolism related genes, such as genes from the glycolysis pathway, transporters for carbohydrate uptake, and genes of the trehalose metabolic machinery.

A GO analysis regarding the localization of the encoded proteins of early up-regulated genes was also conducted (Figure 22C). Of the 300 encoded proteins, 219 localize to the cytoplasm, 81 each to membrane and nucleus, 70 to mitochondria, 20 each to the vacuole

and ER, eight to the cytoskeleton, four to the peroxisome and two to the extracellular region.

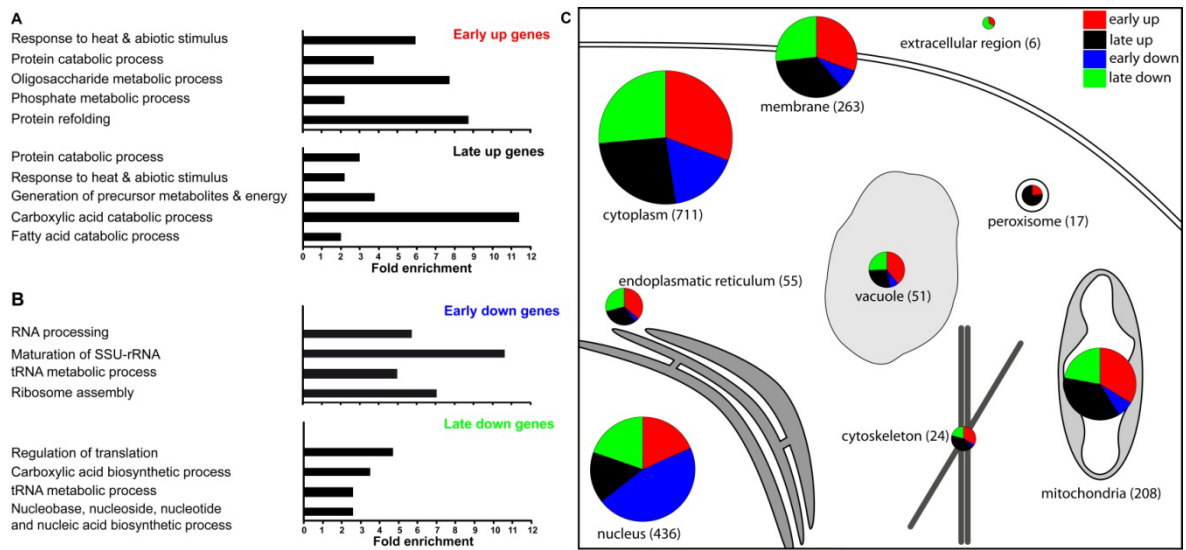


Figure 22 Gene Ontology (GO) analysis of differentially regulated genes from wt Saccharomyces cerevisiae after mild heat stress.

GO analysis of differentially regulated genes was carried out using the DAVID functional annotation clustering tool from the NIH (<https://david.ncifcrf.gov/>) and the GO Slim Mapper of the yeast genome database (www.yeastgenome.org). A: GO analysis of differentially up-regulated genes according to biological process or molecular function. Plotted is the fold-enrichment of a GO term compared to all entries associated with the term. Fold enrichment is shown for selected significantly over-represented GO biological process terms (EASE score <0.05). B: GO analysis of differentially down-regulated genes according to biological process or molecular function. Analysis was carried out as in A. C: GO analysis of differentially regulated genes according to cellular component. Early up-, late up-, early down-, and late down-regulated genes were assigned to the localization of their respective proteins. The size of the circle indicates the number of genes assigned to the respective component. The p-values for all listed GO terms was <0.05.

Late up-regulation shifts to detoxification and mitochondria associated processes

With an overall slower transcriptional response and with lower fold-changes, 294 genes are up-regulated significantly starting at 10 min after onset of heat shock and peaking at 15 min before re-establishing the new steady state levels (Figure 21). The clusters ‘heat stress - and abiotic stress response’ were enriched for this group. Additionally, the late up-regulated group shows an enrichment of genes involved in the breakdown of fatty acids and carboxylic acids, in general, implicating more mitochondria-related processes (Figure 22A). This is also evident from a GO analysis when clustering genes to ‘cellular components’ (Figure 22C). For late up-regulated genes, 187 localize to the cytoplasm when translated, 90 to membrane, 76 to mitochondria, 70 to the nucleus, 17 to the ER, 14

to the vacuole, 13 to the peroxisome, ten to the cytoskeleton, and none to the extracellular region. Compared to early up-regulated genes, an increase in mitochondria and peroxisomal proteins can be seen with approximately 75% of all differentially regulated peroxisomal genes being in the late up group. For the compartment mitochondria, approximately 30% of the differentially regulated genes lie in the late up-regulated group. The assignment to the cellular compartments is an agreement with the GO-biological process terms, ‘fatty acid catabolic process’ and ‘generation of energy precursors’.

Early down-regulation affects nuclear processes

GO analysis of the 262 early down-regulated genes reveals an enrichment in processes associated with the nucleus and nucleolus, such as ‘RNA-processing’ and ‘ribosome biogenesis and assembly’ (Figure 22B). This transcriptional down-regulation of genes encoding ribosomal biogenesis and assembly proteins coincides with a heat-induced pause of translational initiation and elongation processes (Shalgi et al., 2013), resulting in a global decrease of protein biosynthesis: a hallmark of the stress response described first in the 1980s (Ashburner and Bonner, 1979; Lindquist, 1980). This serves to relieve the accumulation of newly synthesized proteins during stress. As a result, the up-regulated heat shock messages are transcribed and translated, while other genes show a down-regulation on the RNA and protein level.

Considering the cellular localization of the respective proteins, 119 are in the cytoplasm, 22 in the membranes, 16 in the mitochondria and only four in the vacuole, two in the ER and one to the cytoskeleton. However, the majority of the genes, namely 200, localize to the nucleus, which represents roughly 50% of all differentially regulated genes assigned to the compartment ‘nucleus’ (Figure 22C). In summary, early down-regulated genes show enrichment for RNA-related processes occurring in the nucleus and nucleolus.

Late down-regulation shifts to translation related processes

With slower kinetics and lower \log_2 -fold-changes, the 280 late down-regulated genes, which possess differential regulation starting after 10 min of heat stress, contain further genes, encoding for ribosomal subunits and for proteins involved in the process of translation (Figure 22A). The GO analysis to cellular component yields 186 genes assigned to the cytoplasm, 85 to the nucleus, 70 to the membrane, 46 to the mitochondria, 16 to the ER, 13 to the vacuole, five to cytoskeleton, four to the extracellular region and none to peroxisome (Figure 22C). Compared to early down-regulation a shift from genes assigned

to the nucleus in the direction of the cytoplasm is present for the late down-regulated transcripts.

4.3.2 The transcriptional response to sub-lethal heat stress

Sub-lethal heat stress results in a lasting heat stress response

The more severe, yet still sub-lethal, heat shock from 25°C to 42°C, yields a different picture of gene regulation (Figure 21B). In this case, fold-changes are elicited more rapidly, indicating a faster transcriptional heat-stress response. The overall amplitudes and changes in the transcriptomic profile are larger and more prolonged, clearly visible with high fold-changes over the entire time course. This observation is in accordance with the literature, where a dose-dependent transcriptional regulation has been described for a variety of stresses, among them thermal stress. In those studies, a heat shock from 25°C to 37°C elicited a swifter and more pronounced response compared to a shift from 29°C to 33°C (Gasch et al., 2000; Jelinsky and Samson, 1999).

The most obvious difference from the transient response observed after mild heat stress is that the amplitude of gene regulation stays high over the entire course of time. Possible explanations may be that either yeast cells cannot adapt to heat stress of this magnitude, or new steady state RNA-levels are obtained at an even later period in time - beyond 80 min. The latter seems less likely since the overall tendency of fold-changes do not point towards starting mRNA values, but rather suggest even increasing \log_2 fold-changes (fcs).

Gene ontology analysis of the transcriptional response to sub-lethal heat stress

The same GO analysis as described above for the mild heat-stress response was carried out for the transcriptional response to 42°C. Here, 403 genes are early up-, 468 early down-, 385 late up- and 661 genes are late down-regulated (Table S2). The higher number of genes attributed to each category concurs with the overall faster and higher transcriptional response of wt baker's yeast compared to mild 37°C stress.

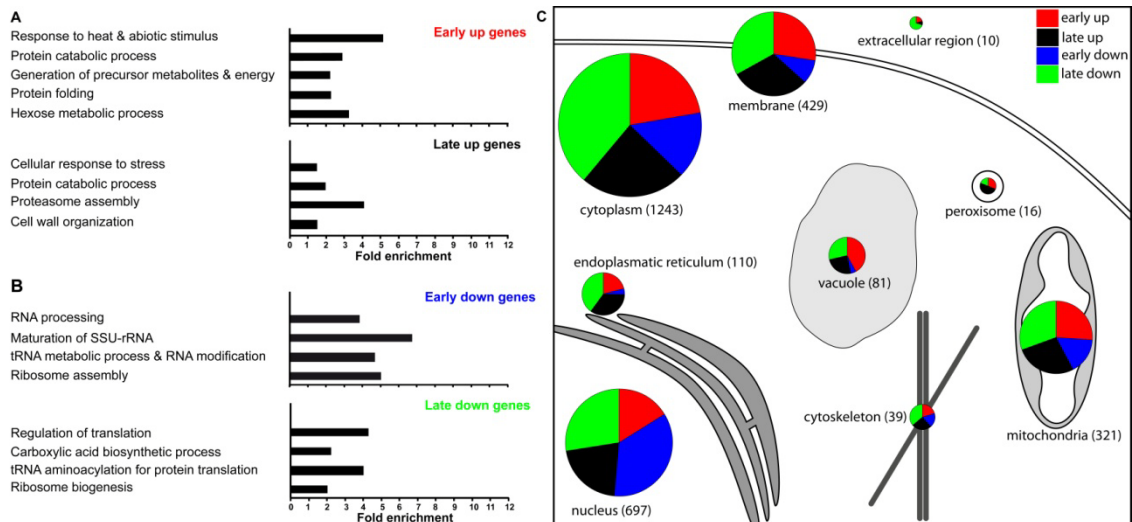


Figure 23 GO analysis of differentially regulated genes of BY4741 baker's yeast exposed to sub-lethal heat stress.

GO analysis of early- and late up- and down- regulated genes was carried out using the DAVID functional annotation tool (<https://david.ncifcrf.gov/>) and the GO Slim Mapper of the yeast genome database. A: GO analysis of the differentially up regulated genes clustered to biological processes. B: GO analysis of the differentially down regulated genes clustered to biological processes. C: GO analysis according to cellular component. Red: early up-regulated genes, black: late up-regulated genes, blue: early down-regulated genes, green: late down-regulated genes. The total number of genes attributed to the respective cellular compartment is shown in parenthesis. The p-values for all listed GO terms was <0.05 .

While sub-lethal heat stress produces a higher number of regulated genes, the enriched GO terms are similar to those obtained for mild heat stress (Figure 23A, B). Terms associated with stress responses, protein refolding, protein catabolism, and carbohydrate metabolism are still most enriched on the side of up-regulation, while RNA and translation linked terms are down-regulated. Changes in comparison to mild heat shock can be exposed, when for example, 'generation of metabolite precursors and energy' are shifted from the cluster of 'late up' genes into 'early up' group. In addition, 'proteasome assembly' appears as an enriched biological process. GO analysis to cellular compartment, in general, reflects the distribution found for mild heat stress.

In summary, these findings show that baker's yeast is capable of coping with mild heat stress on the transcriptional level by a rapid and transient response, obtaining a new steady state of its transcriptomic profile compared to unstressed control conditions. Sub-lethal heat shock evokes an even swifter transcriptional response with higher fold-changes, which is long-lasting. No adaptation to new steady state levels exists.

4.3.3 Origin of transcriptional waves

Basal levels of RNA and location of genes in the genome

Possible explanations for the observed two-wave kinetics of transcriptional gene regulation may be the localization of the genes within the yeast genome. RNA is transcribed by a RNA-polymerase II multi-protein complex. In order for this to occur, the RNA-polymerase machinery must be able to bind the DNA and initiate transcription. The DNA, therefore, must be uncondensed and accessible. The question arose: Do the genes activated and repressed under heat-stress conditions cluster to certain chromosomal regions of the yeast genome which may contribute to the coordinated transcription?

Inspecting the chromosomal loci of the genes, an even distribution over all 16 yeast chromosomes without any visible clustering of genes to certain chromosomal locations exists. No gene was found to be encoded in the mitochondrial DNA (Figure 24A). Hence, the grouping of the genes to sites of high or low transcriptional activity cannot be presented as a factor causing the two transcriptional waves of regulation.

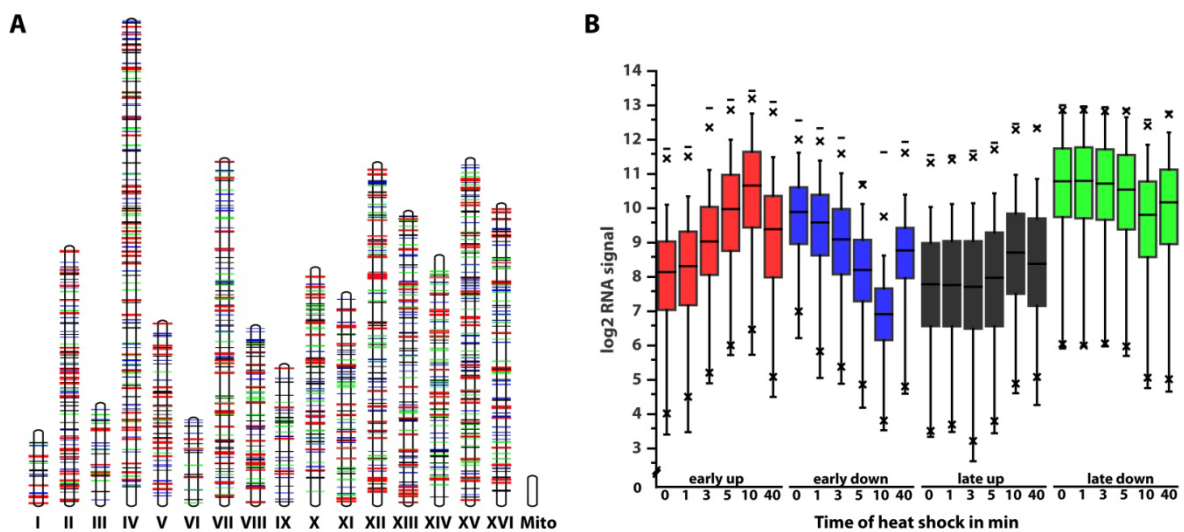


Figure 24 Distribution of differentially regulated genes over the yeast genome and their median RNA levels.

A: Chromosomal localizations of the differentially regulated genes after mild heat stress were obtained and mapped to their locations on the 16 yeast chromosomes. Localizations are color coded in early up (red), early down (blue), late up (black) and late down (green) genes. Thickness of the bars represents the length of the loci. B: A Box-plot with median \log_2 -RNA levels of the differentially regulated genes after mild heat stress. Plotted is the median \log_2 transcript levels over time color coded as in (A). The whiskers indicate maximum and minimum RNA signal of the dataset, the expansion of the box represents the values where 50% of the data resides with the upper and lower quartiles.

Furthermore, the initial starting levels of transcripts can have an influence on the kinetics. Here, higher starting levels would mean that more messages would have to be synthesized or degraded to obtain a \log_2 -fold change of 1, compared to transcripts with an initial lower transcript level.

Box-plotting the median RNA-levels for the mild heat-stress kinetics of early-, late- up- and down-regulated genes shows that the initial RNA value for up-regulated genes is nearly identical (Figure 24B, red & black), with the median \log_2 RNA signal lying around 8. The median transcript level of early up-regulated genes increases to a \log_2 -signal around 10 within 5 min of mild heat shock, while late up-regulated genes merely show an increase from 7.8 to 8.0 in the same time frame. Therefore, ‘early up’ genes are synthesized rapidly after heat stress peaking at 10 min to 15 min, while ‘late-up’ mRNAs are synthesized with slower kinetics and synthesis rates.

Focusing on the side of down-regulation, the median \log_2 -RNA signals for early and late down-regulated genes differ strongly (Figure 24B, blue & green). Unstressed, genes of the ‘early down’ category possess a median \log_2 -RNA signal of approximately 10, those of the ‘late down’ group of around eleven. This difference in basal RNA levels for early and late down-regulated genes may contribute to the observed different kinetics of down-regulation, since more copies of the ‘late down’ would have to be processed in order to elicit the same fold change as ‘early down’ genes.

Consensus sequence motifs of gene regulators

Another aspect of gene regulation lies in the transcription factor binding sites within the promoter sequences. Therefore, it was checked whether the differentially regulated genes show distinct patterns in the binding sites for the main regulators of the stress response, Hsf1, Msn2 and Msn4. The TF-consensus sequences annotated in the ‘yeastract database’ were retrieved, yielding five heat shock element (HSE) patterns for Hsf1 binding and five stress responsive elements (STREs) for Msn2- and Msn4 binding. They were searched for in the 1000 bps upstream from the start codon of all differentially regulated genes (Figure 25).

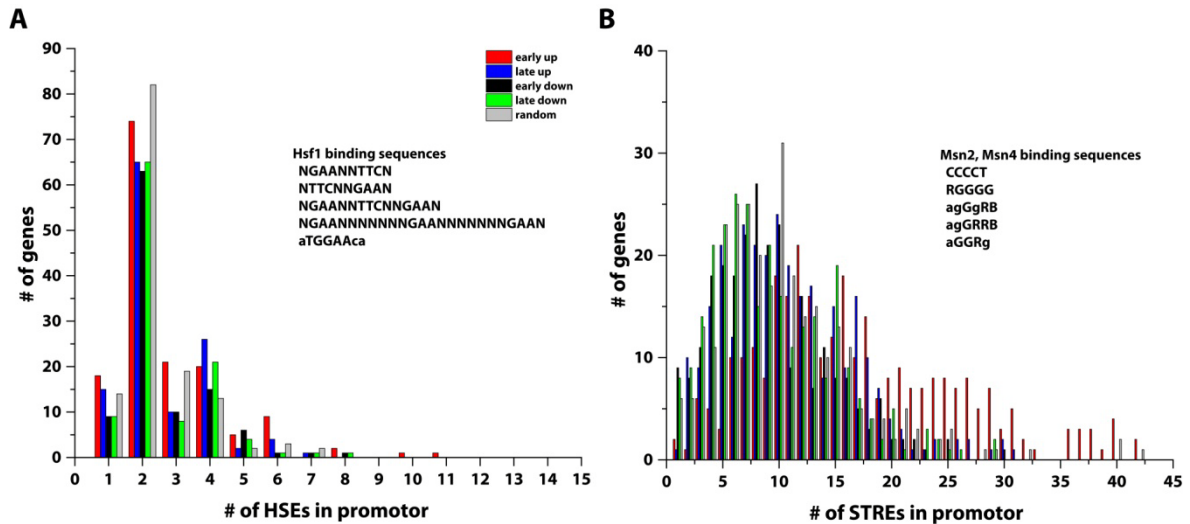


Figure 25 Number of TF-binding sites in promoters of differentially regulated genes.

A: The listed TF-consensus sequences for Hsf1 were searched for in the 1000 bp sequence upstream of the ATG-codon of all differentially regulated genes. Plotted is the number of genes over their number of HSEs in their promoters. B: The listed TF-consensus sequences for Msn2 and Msn4 were searched for in the 1000 bp sequence upstream of the ATG-codon of all differentially regulated genes. Bars are color-coded in early up- (red), early down- (blue), late up- (black) and late down- genes (green). Consensus sequences are represented according to the IUPAC frequency table.

With regard to the number of HSEs in the promoters of up and down-regulated genes after heat shock, it can be stated that the vast majority, approximately 25% of the genes, possess one to four motifs, with two being the most prominent number. Comparing early- and late-regulated genes, the distribution of genes harboring a specific number of HSEs within their upstream sequences is similar. For genes with heat-shock induced rapid expression, a small number of genes possess eight to ten identifiable HSEs. This is not the case for late up-regulated or down-regulated genes in general. For control purposes, a random selection of 300 genes was run through the same search, and the distribution of HSE number within their promoters displays similar numbers and types of HSEs (Figure 25A). The number of identified STREs is markedly higher than for the HSEs, with genes possessing up to 42 motifs within the 1000 bp upstream sequence. The majority of genes with differential regulation under heat shock conditions hold four to 15 STREs in their upstream regions, tailing off towards lower and higher STRE number. As an exception the early up-regulated genes show more genes with a higher number of STREs (>17), and less with a number in the range of one to 16 compared to late regulated genes or early down-regulated genes. A random selection of 300 genes displays an overall similar tendency as to early down- or late regulated genes (Figure 25B). It must be mentioned that, due to the short length and

variable positions of the Hsf1, Msn2 and Msn4 consensus sequences, their identification within a stretch of 1000 bps does not define a definite binding site for the gene regulator. Hence, above-described tendencies must be considered with caution. Although the number and type of HSE and STREs in the promoter region indicate that the regulation by Hsf1 and Msn2/4 may contribute to the transcriptional waves, other factors, such as secondary transcriptional responses or transcript half-lives must exist.

4.3.4 The heat shock response and the molecular chaperone system

Heat shock causes misfolding and aggregation of proteins and the molecular chaperones are the main proteins responsible for protein refolding and aggregation suppression. This prompted a closer look on the regulation of the molecular chaperones of yeast under mild and sub-lethal heat stress.

The kinetics of the transcriptional regulation of molecular chaperones

A list comprising 63 yeast chaperones extended by a few selected co-chaperones and chaperone interacting genes was acquired (Gong et al., 2009), and a color-coded heat map table was generated from the respective microarray data.

Some of the molecular chaperone genes are up-regulated under temperature stress (Table 16, red) and others do not show any significant changes in their mRNA levels (Table 16, uncolored). Again other chaperones are down-regulated in their mRNA-levels and show negative fold-change values (Table 16, blue).

Most of the rapidly induced chaperone genes show elevated transcript levels already after 3 min and have their peak \log_2 -fold change at 10 min in the range of 1.5 to 7.0, after which they decline again towards lower value, yet still elevated compared to 0 min. Genes of this category include *hsp12*, *hsp30*, *ssa4*, *hsp78*, *apj1*, *hsp78*, *sse2*, *ssa3*, *aha1*, *hsp104* and *hsp82*. *hsp42* and *hsp12* are exceptions to this category in that they do not possess the decrease of \log_2 -fc values at 40 min and 80 min, but display values higher than 5.8 for all time points analyzed. These long-lasting, high fold-changes under mild heat stress, as for *hsp26* and *hsp12*, are more prominent when exposing baker's yeast to sub-lethal heat stress, where the fcs of nearly all of the up-regulated molecular chaperones remain high for the entire time period. For a number of genes, mild heat stress elicits negative \log_2 -fc values, as is the case for a few genes encoding J-proteins (*jjj1*, *jjj2* and *jjj3*) and *cns1*.

Heat stress at 42°C does not merely augment the transcriptional up-regulation of selected genes but also the down-regulation of molecular chaperones. Among them are above-mentioned J-protein genes, as well as genes encoding for components of the yeast cytosolic

chaperonin Cct ring/TriC complex (*cct3*, *cct6*, *cct7*, *cct8*), required for the assembly of cytoskeletal components (Young et al., 2004). This heat induced down-regulation of the chaperonin complex has also been reported previously (Eisen et al., 1998). Furthermore, the ribosome-associated Hsp70 protein genes *ssb1*, *ssb2*, *ssz1* along with the gene encoding for its interacting partner *zuo1* display strong down-regulation of more than four-fold after 40 min and 80 min of sub-lethal heat stress. Another ribosome-associated protein with reduced transcript levels has its genomic blueprint in *snl1*, which has also been proposed to contribute to protein synthesis (Verghese and Morano, 2012). Heat stress at 42°C also results in the down-regulation of genes of the heterohexameric prefoldin-complex, which has been shown to be involved in co-translational protein folding and chromatin-remodeling for transcription (Millan Zambrano et al., 2013; Vainberg et al., 1998).

Table 16 Heat map of fold-changes of molecular chaperone transcript levels of Saccharomyces cerevisiae under heat stress.

Displayed are the log₂ fold-changes of gene regulation after mild heat stress (25°C → 37°C, left) and sub-lethal heat stress (25°C → 42°C; right) compared to zero time. Red indicates up-regulation, blue indicates down-regulation (log₂-fc: -4 to 4).

Gene Symbol	log ₂ fold-changes of transcript levels compared to 0 min											
	Mild heat stress						Sub-lethal heat stress					
	1	3	5	10	40	80	1	3	5	10	40	80
HSP26	0.47	2.91	6.56	7.04	7.08	5.85	0.23	5.88	6.84	7.30	7.30	7.26
HSP12	0.14	2.20	5.49	6.37	6.41	6.04	-0.51	3.90	4.57	5.25	5.78	5.83
HSP30	-0.60	2.48	4.48	5.39	1.19	1.76	0.89	4.56	5.63	6.95	7.46	7.47
SSA4	0.31	3.64	4.67	5.00	3.60	2.46	1.07	4.86	4.93	5.00	5.02	5.20
HSP78	0.83	3.39	3.97	4.25	2.51	2.06	2.54	4.97	4.97	5.41	5.69	5.61
HSP42	1.21	3.57	3.86	4.03	2.06	0.99	4.38	6.04	6.20	5.97	6.35	6.37
SSE2	-0.09	1.44	3.04	3.96	2.55	1.79	0.46	2.79	2.86	3.79	4.76	4.55
SSA3	-0.04	0.40	1.42	2.79	2.22	0.49	0.08	1.41	2.24	3.53	4.91	4.84
APJ1	-0.30	2.24	2.82	2.77	-0.51	-1.36	0.89	3.31	3.66	4.15	4.85	4.26
AHA1	0.37	1.38	2.05	2.35	2.06	1.54	0.64	1.69	1.80	2.11	2.94	2.89
HSP104	0.50	1.85	2.17	2.27	1.67	1.45	2.21	3.14	3.06	3.18	3.27	3.40
HSP32	-0.03	-0.84	0.47	2.08	1.57	1.46	0.03	1.74	2.39	4.15	5.55	4.99
HSP82	0.39	1.44	1.74	1.82	1.81	1.51	2.05	2.91	2.96	2.97	3.31	3.34
MDJ1	0.02	1.11	1.54	1.73	0.43	0.20	0.64	2.05	2.13	2.27	2.51	2.48
CPR6	0.17	0.76	1.10	1.48	1.33	0.93	0.37	1.35	1.31	1.64	1.98	2.00
FES1	-0.23	0.89	1.33	1.47	-0.25	-0.97	0.54	1.97	1.85	2.09	2.19	1.90
HSP31	0.07	0.31	0.82	1.41	1.42	0.19	-0.15	0.25	0.63	0.96	3.45	3.97
SSA1	0.28	0.85	1.02	1.32	1.30	0.80	1.12	1.93	1.61	2.18	2.38	2.43
HLJ1	-0.02	0.24	0.52	1.00	-0.16	-0.88	0.05	0.65	0.59	1.10	1.82	1.45
HCH1	0.13	0.35	0.62	0.85	0.90	0.79	0.10	0.62	0.63	0.92	1.39	1.39
HSP10	0.15	0.36	0.50	0.79	0.87	0.83	-0.10	0.47	0.57	0.68	1.02	0.92
ECM10	0.13	-0.07	0.20	0.77	-0.02	0.13	-0.41	-0.43	-0.59	-0.91	-0.43	0.43

4. Results

log ₂ fold-changes of transcript levels compared to 0 min												
Time of stress in minutes												
Gene Symbol	Mild heat stress						Sub-lethal heat stress					
	1	3	5	10	40	80	1	3	5	10	40	80
JAC1	0.15	0.08	0.14	0.69	0.79	0.98	-0.44	-0.22	-0.27	-0.13	0.71	0.66
STI1	-0.04	0.19	0.40	0.67	0.44	0.14	0.34	0.75	0.88	0.88	1.09	1.10
SIS1	-0.05	0.31	0.58	0.62	0.05	-0.31	0.34	0.85	1.02	0.93	1.34	1.28
CDC37	0.02	0.08	0.14	0.59	0.83	0.18	-0.13	0.26	0.18	0.68	1.19	1.25
ERJ5	0.10	0.06	0.23	0.58	0.39	-0.05	0.04	0.24	0.31	0.70	1.90	2.21
SSD1	0.09	0.24	0.26	0.52	0.16	0.23	0.77	0.40	0.40	0.61	1.86	2.50
SSQ1	0.00	-0.07	0.07	0.51	0.21	-0.20	0.14	-0.05	-0.10	0.11	0.10	0.49
KAR2	0.01	0.16	0.29	0.49	0.33	0.22	0.18	0.35	0.45	0.51	0.67	0.62
SSC1	0.02	0.17	0.28	0.48	0.29	0.26	0.24	0.47	0.32	0.55	0.86	0.80
SSE1	-0.06	0.09	0.23	0.40	0.29	0.14	0.05	0.29	0.01	0.40	0.46	0.35
CWC23	0.11	-0.05	0.07	0.39	0.26	0.41	-0.34	-0.07	-0.21	0.40	1.75	1.34
JID1	-0.42	0.18	0.39	0.35	-0.42	-0.53	0.53	0.71	1.35	1.20	1.31	1.72
YDJ1	-0.06	0.18	0.26	0.34	0.07	-0.19	-0.02	0.27	0.29	0.32	0.54	0.52
MDJ2	-0.28	0.07	-0.14	0.33	-0.27	0.38	-0.24	-0.32	-0.31	-0.85	-0.58	-0.83
LHS1	0.13	0.10	0.02	0.31	0.53	0.22	0.14	0.03	0.11	0.26	2.02	2.82
HSP60	0.01	0.14	0.25	0.30	0.35	0.20	0.08	0.24	0.46	0.30	0.72	0.69
CAJ1	0.00	0.05	0.16	0.26	0.20	-0.16	-0.07	0.00	-0.06	0.08	-0.35	-0.49
SWA2	-0.04	-0.14	-0.16	0.25	0.11	-0.01	-0.13	-0.13	-0.07	0.06	1.53	1.61
SCJ1	0.01	0.01	0.08	0.17	0.55	0.37	-0.05	0.11	0.39	0.51	1.84	2.30
JEM1	-0.03	-0.15	-0.47	0.17	0.53	-0.14	-0.10	-0.47	-0.79	-0.19	1.99	2.69
HSC82	-0.02	0.03	0.04	0.13	0.20	0.07	0.04	0.02	0.15	0.10	0.29	0.28
SBA1	-0.07	-0.13	0.04	0.07	0.21	-0.22	-0.02	0.04	0.13	0.08	0.73	0.86
HSP150	-0.07	-0.08	-0.10	0.06	0.57	0.41	0.02	-0.06	-0.04	0.20	0.90	0.96
SSA2	-0.06	0.09	0.07	0.05	0.17	0.14	0.01	-0.16	0.15	-0.10	0.00	0.15
GIM4	0.07	0.10	0.07	-0.03	0.20	0.23	-0.13	0.05	0.07	0.37	-0.22	-0.11
SSB1	0.02	-0.02	-0.01	-0.05	-0.25	-0.04	0.09	-0.03	0.09	0.04	-3.22	-3.76
CPR7	0.08	0.03	0.04	-0.06	0.22	0.28	-0.11	-0.06	-0.19	-0.44	-0.76	-0.75
XDJ1	-0.32	-0.46	-0.50	-0.08	0.16	0.31	-0.26	-0.55	-0.58	-0.69	-0.37	0.03
SSB1///SSB2	0.01	0.04	0.01	-0.16	-0.24	0.02	0.05	0.00	0.07	-0.01	-2.08	-2.57
SLS1	0.02	-0.24	-0.39	-0.20	-0.35	0.08	-0.39	-0.53	-0.76	-1.25	-2.16	-2.85
SSB2	0.05	0.02	0.05	-0.21	-0.24	0.12	0.14	0.03	0.14	0.03	-3.41	-3.86
MCX1	0.01	-0.06	-0.25	-0.28	-0.45	-0.58	-0.01	0.03	0.09	-0.18	-0.44	-1.43
CCT4	-0.05	-0.18	-0.29	-0.28	-0.01	-0.38	-0.09	-0.37	-0.33	-0.38	-0.48	-0.43
DJP1	-0.11	-0.25	-0.27	-0.29	-0.41	-0.18	-0.08	-0.42	-0.88	-0.80	-0.97	-0.43
SEC63	-0.05	-0.06	-0.24	-0.35	-0.13	-0.42	0.26	-0.03	-0.17	-0.24	0.01	0.65
SSZ1	-0.04	-0.02	-0.19	-0.38	-0.63	-0.23	0.04	-0.07	-0.15	-0.21	-2.01	-2.39
ZUO1	-0.05	-0.09	-0.10	-0.45	-0.48	-0.23	-0.02	-0.08	0.06	-0.25	-2.70	-3.45
JJ2	-0.15	-0.49	-1.13	-0.47	-0.43	-0.74	-0.08	-1.24	-1.72	-2.18	-1.38	-0.31
PFD1	0.15	0.05	-0.14	-0.48	0.34	-0.22	-0.27	-0.11	-0.23	-0.48	-1.26	-1.56
GIM5	-0.04	-0.01	-0.08	-0.50	-0.38	-0.35	-0.19	-0.04	-0.08	-0.08	-1.38	-1.78
TCP1	-0.07	-0.13	-0.30	-0.51	-0.12	-0.31	0.02	-0.10	-0.15	-0.40	-0.75	-0.27
YKE2	0.00	-0.01	-0.26	-0.51	0.13	0.05	-0.37	-0.10	-0.23	-0.35	-0.31	-0.44
GIM3	-0.04	-0.12	-0.25	-0.52	0.01	-0.22	-0.19	-0.11	-0.16	-0.47	-1.16	-2.02

log ₂ fold-changes of transcript levels compared to 0 min												
Time of stress in minutes												
Gene Symbol	Mild heat stress						Sub-lethal heat stress					
	1	3	5	10	40	80	1	3	5	10	40	80
CCT5	-0.03	-0.07	-0.26	-0.54	-0.02	-0.09	-0.03	-0.14	-0.40	-0.75	-0.46	0.24
CCT3	-0.05	-0.17	-0.33	-0.65	-0.49	-0.41	0.05	-0.18	-0.30	-0.55	-1.10	-0.53
PAC10	0.06	-0.09	-0.21	-0.66	-0.33	-0.36	-0.60	-0.20	-0.19	-0.47	-1.68	-2.78
CCT6	-0.08	-0.14	-0.41	-0.66	-0.23	-0.29	0.04	-0.34	-0.41	-1.02	-0.41	0.31
SNL1	0.02	-0.04	-0.14	-0.66	-0.83	-0.38	-0.06	-0.08	-0.21	-1.00	-1.61	-2.34
CCT8	-0.04	-0.23	-0.51	-0.68	-0.34	-0.49	0.07	-0.28	-0.44	-0.94	-1.18	-0.78
CCT2	-0.11	-0.10	-0.47	-0.80	-0.43	-0.33	-0.06	-0.17	-0.28	-0.74	-0.79	-0.65
CCT7	0.01	-0.14	-0.47	-1.05	-0.55	-0.66	0.04	-0.31	-0.70	-1.10	-1.20	-0.82
PAM18	-0.05	-0.28	-0.70	-1.25	-0.04	0.01	-0.41	-0.68	-1.07	-1.79	-2.08	-2.44
CNS1	-0.27	-0.46	-0.89	-1.97	-0.93	-0.38	-0.32	-0.64	-0.80	-1.16	-2.21	-2.61
JJJ1	-0.09	-0.36	-0.97	-2.19	-0.95	0.12	-0.77	-1.20	-1.21	-1.98	-3.78	-3.82
JJJ3	-0.40	-1.32	-2.37	-3.40	-0.41	0.40	-1.41	-2.06	-3.02	-3.79	-1.75	-3.99

Absolute changes of molecular chaperone transcripts

Due to the fact that the analysis of fold-changes compared to the unstressed wt does not take the actual initial mRNA-level into account, the mRNA-signals of molecular chaperones listed in Table 16 of unstressed yeast, as well as after 10 min of mild heat stress, the time of the maximal transcriptional heat stress response, were plotted. This enables the identification of heat shock proteins with a high initial level of transcription and those that are hardly present under physiological temperatures at all (Figure 26). Nine chaperones possess very low basal expression and are strongly up-regulated after 10 min of mild heat stress, also explaining why these genes possess the highest log₂-fc values of all molecular chaperones (Figure 26A). This group comprises the *hsp26*, *hsp42*, *hsp12*, *ssa4*, *hsp78*, *hsp30*, *apj1*, *sse2* and *ssa3*. Although all these genes share the very low basal expression and the high mRNA level after 10 min of stress, the final levels obtained differ. While *hsp26*, *hsp42*, *ssa4*, *hsp78* and *hsp12* all reach values higher than 7,000, *hsp30*, *apj1*, *sse2* and *ssa3* reach values ranging from 2,000 to 6,000. This combination of very low basal and very high heat-induced expression is indicative of the important role the product of these genes play in maintaining proteostasis under stress-conditions.

With a high basal expression (1,000 < signal < 4,000), but also strongly up-regulated, *aha1*, *hsp82*, *mdj1*, *hsp104*, *cpr6*, *ssa1*, *hch1*, *hsp10*, *fes1* and *sis1* make up another group (Figure 26C). Here, the final transcript levels reach values between 5,000 and 10,000, in general, bringing the messenger levels into the same range as those of the two sHsps.

A third category is best described with genes possessing very high basal transcription, yet still showing higher mRNA levels after thermal stress. This group encompasses *kar2*, *ssc1*, *sse1*, *sti1*, *ydj1* and *hsp60* (Figure 26B). The high basal expression of these two later categories suggests the need of the respective proteins for proteostasis under permissive conditions and an enhanced demand of higher levels under elevated temperatures.

Eight molecular chaperones possess very high basal expression with the mean signals in the range of 4,000 to 8,000 and show close to no change after mild heat stress. *Sba1*, *hsp150*, *hsc82*, *ssa2*, *ssb1*, *ssb2* and *ssz1* belong to this class (Figure 26E). Next to a number of *hsp70* genes, *hsc82*, a close structural and functional homolog to *hsp82*, is assigned to this group. They have been described to be expressed constitutively at higher basal expression levels compared to *hsp82*, as is the case here (Gross et al., 1990).

Again other genes are expressed at rather low basal levels (signal 200 to 300) and are up-regulated merely to a weak extent by thermal stress (Figure 26D). The list of genes in this category includes *hlj1*, *hsp31*, *cdc37*, *ssd1*, *cwc23*, *erj5*, *scj1*, *lhs1* and *caj1*. Many of these genes encode for co-chaperones of the J-protein type that modulate the activity of other chaperones.

Genes of the Cct/TriC complex, which contributes to folding of roughly 5% to 10% of all yeast proteins in its central cavity (Kim et al., 2013), *cct*-genes, *cns1*, *sec63* and *gim3* exhibit high basal expression and are down-regulated weakly (Figure 26F).

The last group includes 22 genes with low basal expression levels (signal <1,500) that do not change upon mild heat stress or show very minor changes of their absolute mRNA level (Figure 26G).

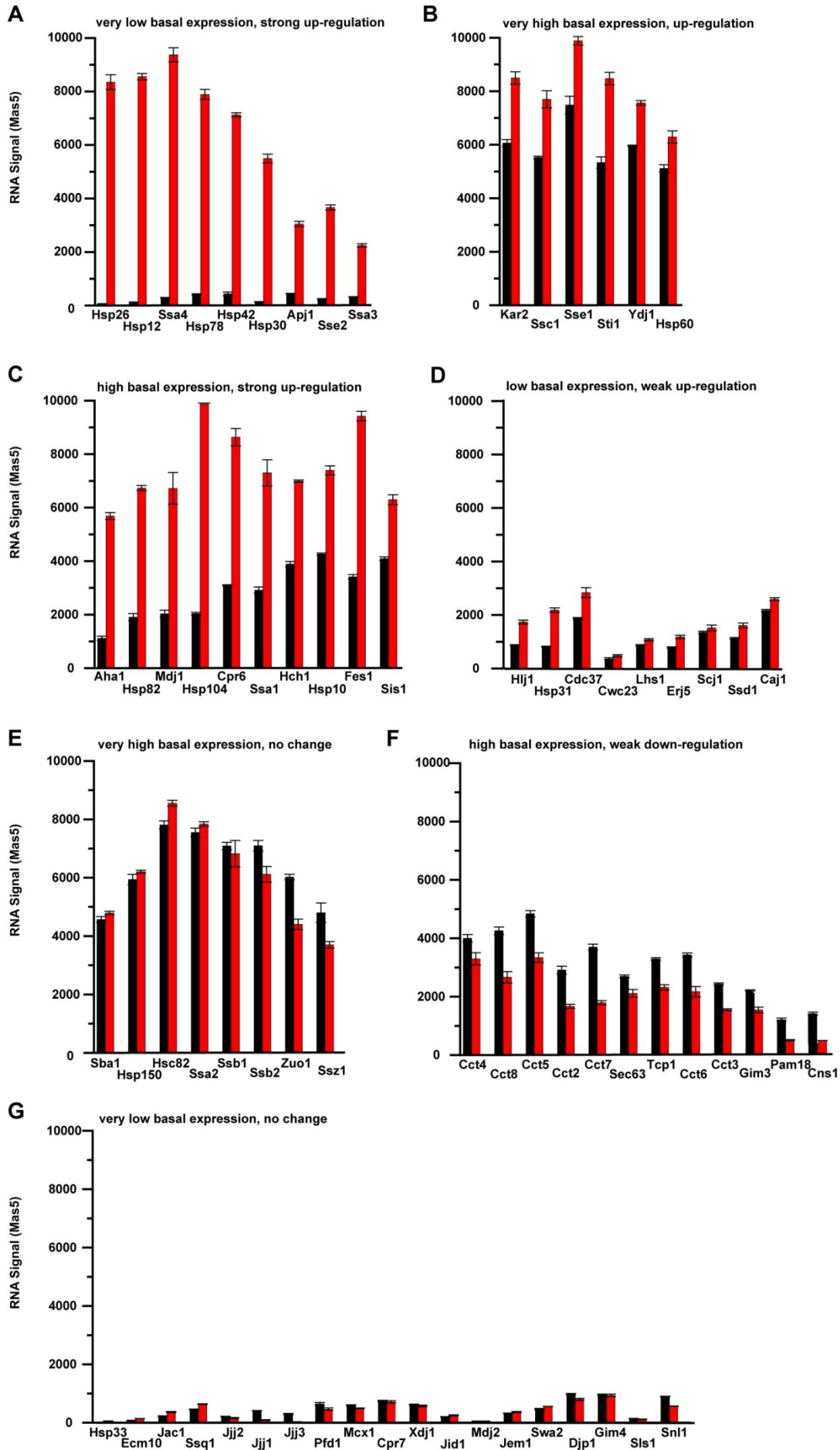
The necessity to analyze not only fold-changes, but also absolute mRNA values is best displayed by looking at the mRNA levels of *jjj1*, *jjj2*, *jjj3* and *hsp33*. Their \log_2 -fcs suggest a high down- or up-regulation after thermal stress; however, when focusing on the absolute values, only small changes in transcript levels are displayed. Careful interpretation of the fold-changes of gene regulation is hence necessary.

A combined interpretation of the absolute values and the fold-changes clearly indicate which molecular chaperones are of high importance in the context of the heat stress response. In especially genes with a low transcript level in non-stress conditions and with a strong heat-responsive up-regulation must be mentioned. Furthermore, some molecular chaperones are also necessary for cellular proteostasis under permissive condition and their function is needed even more so under heat shock, therefore their expression is also elevated. Other chaperones are needed under physiological conditions, but their action and

function is not needed in elevated levels under heat shock, hence no regulation is visible. This nicely illustrates the different nature of the molecular chaperones, some functioning as housekeepers, some exclusively required under stress conditions and others for both physiological and stress conditions.

Figure 26 Expression levels of molecular chaperone genes under permissive growth conditions and 10 min of mild heat stress.

Plotted is the mRNA-signal of the respective genes before (black) and after heat shock (red). Genes were grouped according to their basal expression levels and direction of regulation into A: 'very low basal expression & strong up-regulation', B: 'very high basal expression & up-regulation', C: 'high basal expression & strong up-regulation', D: 'low basal expression weak up-regulation', E: 'very high basal expression & no change', F: 'high basal expression, weak down-regulation' and G: 'very low basal expression & no change'. See 3.11 for a detailed description of grouping into the respective category. Error bars indicate the standard deviation of three biological replicates. (Figure on next page).



4.3.5 Transcriptional regulation of selected pathways

Heat stress results in denaturation of cellular proteins, which are in need of refolding, sequestration or proteolytic removal. Among the differentially-regulated genes are also components of the proteolytic system involved in autophagy, a process where proteins are targeted for lysosomal degradation (Table 17), as well as genes contributing to the ubiquitin-proteasome mediated degradation of proteins (Table 18). The former in the context of heat shock describes a rather nonselective process in which cytosolic components, including proteins of non-native conformation and whole organelles, are engulfed in double-membrane structures and directed to lysosomes or, in the case of yeast, to the vacuole for degradation (Hecht et al., 2015). Indeed, a recent study linked the heat shock response directly to an augmentation of autophagy in mammalian cells, with the aim of unfolded and misfolded protein clearance (Dokladny et al., 2013). The latter describes the process in which a large multi-subunit complex, termed the proteasome, recognizes poly-ubiquitylated substrates, removes the ubiquitin chains, unfolds the clients and drives them through its inner pore, where it is proteolytically cleaved into peptides (Finley et al., 2012). Furthermore, a closer look was given to genes of the trehalose system (Table 19): The role of the trehalose system in the heat shock response and acquisition of thermotolerance is known (Gibney et al., 2015).

Heat stress activates genes of the autophagic system

Investigating the 29 autophagy-related (ATG) genes, as well as a few other selected autophagy maker genes, it becomes evident that many of the genes are up-regulated transcriptionally after mild temperature stress with \log_2 fold-changes in the range of 0.5 to 2.5, meaning increased RNA levels by a factor of 1.4 to 5.5 (Table 17). Furthermore, 40 minutes after heat shock, the transcriptional changes have already declined towards lower values, indicative of the adaptation of the organism to the environmental condition. 53% of the listed autophagy-related genes possess a, at least, two-fold increase in their mRNA levels at 10 min of 37°C temperature stress.

Sub-lethal heat stress, eliciting a transcriptional response more rapidly and with higher amplitude as described earlier, shows differential regulation at earlier points in time, with many autophagy messengers enriched by \log_2 -fc > 0.5 at 5 min and even increasing to maximal \log_2 -fcs around 5 at 80 min. This represents a 32-fold accumulation of the respective transcripts (*atg8*, *ams1*), which is indicative of an enhanced need for autophagic clearance of cellular debris under more severe conditions of stress.

Table 17 Heat map of the fold-changes of autophagy related genes of *Saccharomyces cerevisiae* after mild and sub-lethal heat stress.

Displayed are the log₂ fold-changes of gene regulation after mild heat stress (25° → 37°C, left) and sub-lethal heat stress (25° → 42°C, right) compared to zero time. Red indicates up regulation, blue indicates down regulation (log₂-fc: -4 to 4).

Gene Symbol	log ₂ fold-changes of transcript levels compared to 0 min											
	Mild heat stress						Sub-lethal heat stress					
	1	3	5	10	40	80	1	3	5	10	40	80
Associated genes												
AMS1	0.07	0.08	0.45	1.98	2.54	2.54	-0.46	0.27	0.60	2.45	4.80	5.54
LAP4	0.32	0.70	1.41	2.18	2.26	1.79	0.24	1.08	1.60	2.44	4.12	3.83
VPS30	0.15	0.28	0.53	1.03	0.73	0.23	0.29	0.67	1.07	1.55	1.82	1.79
Core Machinery												
ATG1	-0.18	-0.16	0.27	1.30	1.04	-0.06	0.16	-0.04	-0.10	1.05	2.73	3.64
ATG2	0.06	0.09	0.56	1.35	0.72	0.53	-0.18	0.46	0.31	0.31	0.98	1.30
ATG3	-0.30	0.06	0.45	0.81	0.06	-0.66	0.38	0.69	0.85	1.31	1.52	1.95
ATG4	0.01	0.15	0.45	0.79	-0.01	-0.30	0.46	0.52	0.27	-0.03	0.17	1.02
ATG5	-0.29	-0.57	-0.58	-0.23	0.10	0.50	-0.85	-0.64	0.14	1.48	1.68	0.16
ATG7	-0.22	0.36	1.11	1.98	0.14	-0.19	0.58	1.21	1.17	1.33	1.88	2.15
ATG8	0.05	0.96	1.86	2.74	1.65	0.74	0.61	2.29	2.63	3.40	4.30	4.73
ATG9	0.06	0.25	0.70	1.32	0.86	0.28	-0.04	0.65	0.42	0.47	0.72	1.33
ATG10	0.03	0.02	0.28	-0.04	0.13	-0.10	-0.37	0.04	0.63	0.68	-0.89	-1.66
ATG12	-0.03	0.14	0.37	0.63	0.41	0.03	-0.27	0.01	0.03	0.08	0.31	0.09
ATG13	0.27	0.47	0.70	0.96	0.43	0.29	0.09	0.44	0.53	0.59	1.40	1.64
ATG14	0.27	0.47	1.12	1.78	0.67	0.11	-0.23	0.40	0.30	0.35	1.87	1.62
ATG15	0.08	0.00	0.07	0.58	0.18	0.08	1.06	0.11	-0.34	-0.23	0.35	2.38
ATG16	0.09	1.04	1.51	2.20	1.45	0.30	1.48	0.77	0.79	0.77	0.90	1.81
ATG18	-0.02	0.25	0.32	0.51	-0.11	0.27	0.09	0.16	0.30	-0.09	-0.11	-0.07
ATG22	-0.08	-0.02	-0.04	0.09	0.44	0.52	0.34	0.52	0.77	0.64	0.85	1.74
Selective Autophagy Specific												
ATG11	0.11	-0.17	-0.06	-0.03	0.47	0.61	-0.50	-0.52	-0.29	0.16	1.01	1.22
ATG19	0.28	0.49	0.94	1.60	1.13	1.11	0.33	0.53	0.71	0.96	2.48	2.06
ATG20	0.00	0.51	0.96	1.38	0.49	-0.47	0.62	0.97	1.08	1.72	1.51	1.71
ATG21	0.17	0.29	0.68	0.90	0.28	-0.22	0.08	0.46	0.51	0.74	0.89	0.71
ATG23	-0.15	-0.30	-0.18	0.27	0.34	0.69	0.00	0.31	0.16	0.23	0.80	1.05
SNX4//ATG24	0.00	0.14	0.57	1.13	0.27	-0.44	0.28	0.67	0.38	1.11	2.01	2.44
ATG26	0.22	0.53	0.75	1.03	0.49	0.57	0.26	0.81	0.76	0.84	0.97	1.08
ATG27	0.06	-0.01	-0.03	-0.22	0.09	-0.23	-0.01	-0.07	0.02	0.22	0.27	-0.32
ATG32	0.03	0.17	0.01	-0.41	-0.68	-0.23	0.03	-0.01	0.39	0.37	-0.08	0.33
ATG33	0.17	0.34	0.83	1.32	1.28	0.72	0.13	0.62	0.82	0.71	1.33	2.04
Nonselective Autophagy Specific												
ATG17	0.05	0.05	0.19	0.81	0.65	0.30	-0.24	0.00	-0.61	-0.68	1.33	2.14
ATG29	0.35	0.78	1.14	2.49	0.88	-0.29	1.35	1.17	0.70	1.59	2.14	3.88
CIS1//ATG31	0.43	0.55	1.00	1.85	1.88	1.90	-0.11	0.16	0.35	0.63	1.93	2.46

Heat stress induces the ubiquitin-proteasomal-degradation system (UPS)

Genes involved in the 26S-proteasome mediated degradation process of poly-ubiquitinated proteins after heat shock were acquired, and a heat map with the transcriptional regulation compared to the unstressed control was generated (Table 18). A general statement can be made: Under conditions of mild heat shock, only a few genes of the UPS are differentially regulated.

Ubi4 which encodes ubiquitin, the basic building block for the poly-ubiquitin branches, is significantly up-regulated already three minutes after onset of stress. Under mild heat shock conditions, *ubi4* transcript levels reach a maximum after 10 min (\log_2 -fc of 3.2) and decrease only slightly at 40 min of heat shock. After 80 min the *ubi4*- transcript levels are lower compared to untreated control conditions.


Rpn4 is a transcription factor that re-localizes to the nucleus upon heat stress and regulates the expression of genes encoding proteasomal subunits, among others (Xie and Varshavsky, 2001). The *rpn4*-locus itself is activated rapidly after heat stress with more than two-fold induction already after three min of stress, reaching basal values after 40 min and is down-regulated at 80 min, perhaps due to the transcriptional feedback loop in which the 26S-proteasome itself degrades Rpn4 (Xie and Varshavsky, 2001). Shifting the focus to *rpn4* targets, some of the transcript levels of subunits from the proteasome core particle, and the lid and base from the regulatory particle (*sem1*, *rpn7*, *rpn12*, *rpn11*, *rpn9*, *rpn8*, *rpn2*, *rpt2*, *pre3*, *pre9*, *pre6*, *pre1*, *prs3*) are marginally elevated at 10 and 40 min, which is shortly after the peak of *rpn4* transcript level itself. It must be noted that the \log_2 -fcs are rather low, lying in the range of 0.25 and 1.12. After 80 min transcriptional repression of these genes is detectable with negative fold-changes or no measured differences.

Additionally, the gene for the sole *S. cerevisiae* ubiquitin-activating enzyme *uba1* is slightly enriched in its transcript level at 10 and 40 min, and messenger numbers of a few of the ubiquitin conjugating enzymes (*ubc5*, *ubc7*, *ubc8*) are also elevated. Furthermore, many *loci* of de-ubiquitinating enzymes are differentially regulated after thermal stress, some being activated (*ubp2*, *ubp4*, *ubp9* and *ubp15*) and others repressed (*ubp1*, *ubp8*, *ubp10*, *ubp12* and *ubp13*) in their expression. De-ubiquitinylases hydrolyze the isopeptide bond from ubiquitylated proteins and hence influence their proteasomal degradation.

Sub-lethal stress yields similar tendencies of gene regulation (Table 18, right), however with more pronounced effects and without the re-establishment of a new steady state level. For instance, the *ubi4* locus is up-regulated over the entire course of time. Additionally, the regulator Rpn4 is transcriptionally induced close to two-fold at 1 min of stress, four-fold at

5 min and even six-fold at 80 min of 42°C heat stress. The most evident difference in gene regulation of proteasomal degradation-associated-genes lies in the high \log_2 -fc values at 40 min and 80 min, indicating a sustained need for proteasomal degradation of proteins under the given experimental conditions of 42°C of heat stress.

Table 18 Heat map of fold-changes of ubiquitin-proteasomal degradation associated genes of Saccharomyces cerevisiae after mild and sub-lethal heat stress.

Displayed are the \log_2 fold-changes of gene regulation after mild heat stress (25°C → 37°C, left) and sub-lethal heat stress (25°C → 42°C, right) compared to zero time: Red indicates up regulation, blue indicates down regulation (\log_2 -fc: -4  4).

\log_2 fold-changes of transcript levels compared to 0 min												
Time of stress in minutes												
Gene Symbol	Mild heat stress						Sub-lethal heat stress					
	1	3	5	10	40	80	1	3	5	10	40	80
Selected associated genes												
RPN4	0.18	1.14	1.17	0.90	-0.08	-1.10	0.98	1.79	2.00	2.09	2.63	2.58
UBI4	0.33	1.40	2.49	3.20	2.72	-1.65	0.32	2.46	2.84	3.45	3.68	3.61
RPN14	-0.02	0.14	0.54	0.95	0.27	-0.21	-0.34	0.22	0.28	0.48	1.40	0.93
BLM10	-0.11	-0.22	-0.28	-0.50	-0.11	-0.47	-0.22	-0.23	-0.27	-0.51	-1.27	-1.12
DDI1	0.09	0.02	0.06	-0.35	-0.25	0.11	-0.20	0.04	-0.07	-0.23	-1.67	-1.43
DSK2	-0.03	-0.01	0.06	-0.05	0.26	-0.24	0.27	0.04	0.01	-0.11	0.42	1.11
ECM29	0.08	0.12	0.10	0.89	1.42	0.23	-0.07	-0.05	-0.31	-0.09	1.59	2.26
HUL5	0.10	0.19	0.41	0.79	0.67	0.32	0.01	0.37	0.50	0.62	1.52	1.89
RAD23	-0.03	-0.11	-0.25	-0.38	-0.02	-0.31	0.12	0.01	-0.05	-0.12	0.36	0.73
UFD4	0.07	0.05	0.08	0.32	0.35	0.29	0.11	0.21	-0.03	-0.14	0.46	0.82
Core particle												
SCL1	-0.06	-0.06	-0.01	0.11	0.28	-0.35	-0.05	0.02	-0.09	-0.06	0.76	0.78
PRE8	-0.01	-0.10	-0.05	-0.01	0.28	-0.10	-0.07	-0.04	-0.07	-0.15	1.12	1.38
PRE9	-0.05	-0.10	-0.04	0.10	0.59	-0.02	-0.02	-0.06	-0.27	-0.31	0.44	0.49
PRE6	0.04	-0.01	0.02	0.28	0.52	0.25	0.02	-0.01	0.06	-0.02	0.78	0.89
PUP2	-0.01	-0.04	-0.12	0.06	0.39	0.07	-0.09	-0.10	-0.15	-0.22	0.90	1.16
PRE5	0.04	0.00	0.06	0.10	0.17	-0.17	-0.03	0.05	-0.05	0.05	0.58	0.69
PRE10	0.00	-0.02	-0.03	0.10	0.36	-0.23	-0.07	-0.10	-0.07	-0.37	0.55	0.80
PRE3	-0.01	0.06	0.08	0.41	0.71	0.24	0.05	0.06	0.09	0.09	0.61	1.04
PUP1	0.06	0.04	0.02	-0.14	0.29	-0.50	-0.04	0.09	-0.23	-0.49	0.18	0.51
PUP3	-0.03	-0.05	0.02	0.18	0.32	-0.16	0.14	0.09	0.04	-0.16	0.76	1.10
PRE1	0.02	-0.05	0.02	0.16	0.47	-0.08	-0.14	-0.05	-0.15	-0.35	0.90	1.11
PRE2	-0.06	-0.06	-0.01	0.11	0.28	-0.35	-0.05	0.02	-0.09	-0.06	0.76	0.78
PRE7//PRS3	0.02	-0.03	0.08	0.35	0.47	0.10	-0.08	0.12	0.16	0.38	1.26	1.21
PRE4	-0.06	-0.13	-0.17	0.12	0.29	-0.32	-0.09	-0.05	-0.10	-0.12	1.23	1.49
Regulatory particle lid												
SEM1	0.29	-0.02	0.25	0.38	1.12	0.40	-0.40	0.04	-0.17	0.21	1.09	1.32
RPN6	-0.12	-0.12	-0.12	0.25	0.35	-0.34	0.07	-0.01	-0.12	0.01	0.96	1.14
RPN5	-0.09	-0.04	-0.11	0.20	0.28	-0.35	0.10	0.02	-0.10	0.13	0.98	1.14
RPN3	0.01	-0.09	-0.15	0.14	0.16	-0.44	0.07	-0.02	-0.11	-0.06	0.75	0.97
RPN7	0.01	0.01	0.02	0.44	0.59	-0.04	0.33	0.12	0.23	0.22	1.01	1.43

log ₂ fold-changes of transcript levels compared to 0 min												
Time of stress in minutes												
Gene Symbol	Mild heat stress						Sub-lethal heat stress					
	1	3	5	10	40	80	1	3	5	10	40	80
RPN12	0.02	-0.05	-0.08	0.18	0.55	0.10	-0.04	-0.01	-0.22	-0.30	1.03	1.11
RPN11	-0.09	-0.12	-0.04	0.28	0.33	-0.40	0.12	0.07	0.06	0.19	1.43	1.60
RPN9	-0.09	-0.09	-0.12	0.29	0.45	-0.12	-0.01	-0.05	-0.14	0.01	1.29	1.26
RPN8	0.02	0.00	0.03	0.28	0.54	-0.43	-0.09	-0.02	-0.24	-0.17	0.88	1.03
Regulatory particle base												
RPN1	-0.02	-0.07	-0.20	-0.11	0.25	-0.25	0.11	-0.04	-0.13	-0.27	0.76	0.94
RPN2	0.00	-0.02	0.02	0.22	0.37	0.15	-0.13	0.02	0.01	0.09	1.23	1.20
RPN10	-0.01	-0.07	-0.11	-0.14	0.05	-0.33	-0.03	-0.12	-0.18	-0.61	0.19	0.34
RPN13	0.03	0.00	0.08	0.29	0.25	-0.39	0.08	0.22	0.13	0.24	0.63	0.88
RPT1	-0.04	-0.07	-0.16	0.03	0.25	-0.08	0.02	-0.07	-0.12	-0.24	0.67	0.96
RPT2	-0.03	-0.04	0.09	0.37	0.34	-0.33	0.06	0.20	0.13	0.13	0.99	1.18
RPT3	-0.11	-0.18	-0.09	0.10	-0.01	-0.72	0.18	0.03	-0.03	0.06	1.05	1.54
RPT4	0.04	-0.01	-0.07	0.10	0.32	-0.04	-0.05	0.00	-0.05	-0.12	0.84	1.17
RPT5	-0.10	-0.10	-0.26	0.01	-0.02	-0.50	0.09	-0.04	-0.23	-0.23	0.55	0.90
RPT6	-0.08	-0.10	-0.08	0.00	0.07	-0.34	0.01	0.01	0.04	-0.18	0.69	0.91
SAN1	-0.06	-0.13	-0.17	0.12	0.29	-0.32	-0.09	-0.05	-0.10	-0.12	1.23	1.49
Ubiquitin activating and conjugating enzymes												
UBA1	0.02	-0.03	0.08	0.35	0.47	0.10	-0.08	0.12	0.16	0.38	1.26	1.21
UBC1	-0.03	0.01	0.13	0.14	0.34	0.19	-0.08	0.18	0.29	0.30	0.09	-0.30
UBC2//RAD6	-0.04	-0.07	-0.16	0.03	0.25	-0.08	0.02	-0.07	-0.12	-0.24	0.67	0.96
UBC3//CDC34	-0.01	-0.05	0.04	0.10	0.02	-0.48	-0.13	0.10	0.12	0.07	-0.55	-0.32
UBC4	-0.01	0.08	0.24	0.45	0.26	0.08	0.01	0.33	0.30	0.45	0.47	0.50
UBC5	-0.05	0.07	0.35	0.95	0.91	0.47	-0.42	-0.17	-0.10	-0.24	0.81	1.60
UBC6	-0.01	-0.05	0.04	0.10	0.02	-0.48	-0.13	0.10	0.12	0.07	-0.55	-0.32
UBC7	0.10	0.19	0.41	0.79	0.67	0.32	0.01	0.37	0.50	0.62	1.52	1.89
UBC8	0.04	0.64	1.40	2.11	1.62	0.44	0.54	1.29	1.52	1.29	1.94	2.81
UBC9	0.09	0.02	0.06	-0.35	-0.25	0.11	-0.20	0.04	-0.07	-0.23	-1.67	-1.43
UBC10//PEX4	-0.03	0.01	0.13	0.14	0.34	0.19	-0.08	0.18	0.29	0.30	0.09	-0.30
UBC11	-0.99	-1.32	-1.86	-3.20	-1.63	-2.14	-0.25	-0.60	-0.22	-1.11	-2.87	-2.10
UBC12	0.03	0.03	0.35	0.39	-0.11	0.06	-0.37	-0.06	0.23	-0.10	0.12	-0.17
UBC13	0.14	0.10	0.19	0.20	0.31	0.45	-0.11	0.12	0.21	0.25	0.46	0.85
Deubiquitylases												
UBP1	-0.02	-0.16	-0.71	-1.44	-0.41	-0.38	-0.23	-0.51	-0.60	-0.94	-1.17	-1.19
UBP2	0.10	0.20	0.48	0.76	0.84	0.28	0.51	0.64	0.67	0.59	0.55	1.24
UBP3	0.00	0.11	0.00	0.01	0.12	0.26	0.06	-0.09	-0.36	-0.34	0.23	0.43
UBP4//DOA4	0.26	0.62	0.96	1.60	0.97	0.58	0.91	0.94	1.29	1.73	2.65	3.36
UBP5	-0.28	-0.22	0.14	0.10	0.20	0.00	0.09	0.01	0.09	1.08	1.75	1.58
UBP6	0.00	0.00	0.05	0.47	0.28	-0.18	0.04	0.20	0.22	0.46	1.52	1.59
UBP7	-0.01	0.04	0.09	0.31	0.17	-0.39	0.15	-0.16	-0.08	-0.28	-0.41	0.03
UBP8	-0.07	-0.11	-0.48	-0.54	-0.39	-0.66	0.19	-0.28	-0.21	-0.51	-0.47	-0.10
UBP9	0.10	0.01	0.47	1.50	0.47	0.47	-0.10	0.16	0.28	1.22	1.87	2.61
UBP10	-0.21	-0.51	-1.23	-2.40	-0.70	-0.11	-0.38	-0.62	-0.74	-1.11	-1.76	-1.85
UBP11	-0.32	0.05	0.46	0.63	0.10	0.02	-0.16	0.30	0.17	-0.17	-0.46	-0.29

log ₂ fold-changes of transcript levels compared to 0 min												
Time of stress in minutes												
Gene Symbol	Mild heat stress						Sub-lethal heat stress					
	1	3	5	10	40	80	1	3	5	10	40	80
UBP12	-0.05	-0.11	-0.43	-0.51	0.05	-0.15	-0.18	-0.55	-0.88	-1.13	-0.66	-0.27
UBP13	-0.05	-0.14	-0.61	-0.80	-0.14	-0.62	0.36	-0.23	-0.58	-0.63	-0.97	-0.94
UBP14	-0.02	-0.05	-0.17	-0.30	-0.11	-0.13	0.26	-0.08	0.16	0.09	-0.52	-0.66
UBP15	0.12	0.17	0.69	1.19	0.99	0.13	0.15	0.61	0.34	0.58	0.75	1.01
UBP16	0.02	0.06	0.12	0.07	-0.03	0.95	-0.18	-0.06	-0.21	0.03	0.03	0.13
YUH1	0.04	-0.04	0.12	0.52	0.55	0.33	-0.20	0.08	0.39	0.67	1.48	1.13
OTU1	-0.10	-0.13	0.09	0.95	1.48	0.66	0.36	-0.04	0.22	0.21	0.85	2.13
OTU2	-0.20	-0.47	-0.78	-1.30	-0.45	-0.13	-0.36	-0.63	-0.76	-1.47	-1.51	-1.57

Heat shock induces the trehalose system

The up-regulated genes of carbohydrate metabolism comprise those annotated to GO term ‘trehalose metabolic process’. Trehalose is a storage form of glucose, and it was shown that high levels of trehalose protect cells from temperature stress (Verghese et al., 2012). The disaccharide is thought to operate as a compatible solute stabilizing membranes and proteins by acting as a chemical chaperone. Trehalose buffers unfavorable interactions the displacement of water, and by binding to polar regions of lipids and proteins (Gibney et al. 2015; Singer & Lindquist 1998).

Table 19 Heat map of the fold-changes of the gene regulation of the trehalose network. Displayed are the log₂ fold-changes of gene regulation after mild heat stress (25°C → 37°C, left) and sub-lethal heat stress (25°C → 42°C, right) compared to zero time. Red indicates up regulation, blue indicates down regulation (log₂-fc: -4 to 4).

log ₂ fold-changes of transcript levels compared to 0 min												
Time of stress in minutes												
Gene Symbol	Mild heat stress						Sub-lethal heat stress					
	1	3	5	10	40	80	1	3	5	10	40	80
TPS3	0.22	0.53	1.01	1.57	0.76	0.50	0.44	0.88	0.83	0.89	1.78	1.83
TPS2	0.28	1.75	2.50	2.85	1.18	0.62	1.84	2.55	2.90	3.16	3.59	3.33
TPS1	0.27	1.17	1.72	2.26	1.31	0.75	1.37	2.02	2.30	2.61	3.28	3.23
TSL1	0.69	3.20	3.96	4.19	3.17	2.61	3.43	5.12	5.36	5.62	5.81	5.74
NTH1	0.37	1.24	1.91	2.70	1.84	1.54	1.47	2.11	2.29	2.86	4.18	4.29
NTH2	0.19	0.98	1.64	2.23	1.40	1.23	0.33	1.12	1.44	1.80	2.50	2.73
ATH1	0.29	0.65	1.45	2.39	2.32	1.51	0.33	0.99	1.30	2.11	2.92	3.66

All members of this cluster (*tps1*, *tps2*, *tps3*, *tsl1*, *nth1*, *nth2* and *ath1*) are highly heat-stress induced (Table 19). Within three to ten minutes of mild heat shock, log₂-fc values of 1.01 to 3.96 are reached, not only for the trehalose-synthase complex subunits (*tps1*, *tps2*, *tps3* and *tsl1*), but also for trehalose degrading neutral trehalases (*nth1*, *nth2*) and acid

trehalase (*ath1*). Compared to trehalose producing subunits -with the exception of *tsl1*-, *nth1*, *nth2* and *ath1* remain elevated at later times of mild heat shock and are up-regulated slightly later. This effect is more prominent for stress at 42°C where the genes encoding degrading subunits are induced significantly starting at 3 min to 5 min, while synthesizing subunits possess \log_2 fcs >1 already after 1 min, with *tps3* being an exception.

4.3.6 Transcriptional regulators of the mild heat shock response

In order to gain a deeper insight into the transcriptional regulation of wt baker's yeast heat shock response, all yeast transcription factors (TFs) were tested for enrichment of their respective targets among the differentially regulated genes. To this end, all known targets of the TFs, based on DNA-binding plus expression evidence annotated in the freely accessible 'yeastract database' (www.yeastract.com), were searched in either up- or down-regulated genes, furthermore differentiating between early and late regulated genes. The analysis was carried out for the kinetics of mild heat shock (37°C) because it reflects the gene regulation at 42°C.

Regulators of up-regulated genes are stress response transcription factors

A list was compiled with the 10 TFs that show a significant enrichment of their targets in either early or late up-regulated genes (Table 20).

Table 20 Enriched transcription factors (TF) in early up and late up-regulated genes after mild heat stress in wt baker's yeast.

The number of targets, as well as the p-value in the respective dataset, was retrieved using DNA-binding and expression evidence annotated in the yeastract database (September 2015). The ten most significant regulators for early and late genes are listed in their rank of significance from top to bottom. The p-value was calculated as described in 3.11. Significance: $p < 0.01$. For comparison, the respective p-value in a random dataset with an equivalent number of genes is also noted.

TF	# targets in dataset 'early up'	p-value early up	# targets in dataset 'late up'	p-value late up	# targets in genome	p-value in random dataset of equivalent number
Regulators of early up-regulated genes						
Msn2	184	$2.9 e^{-77}$	53	0.12	1187	0.28
Msn4	129	$1.9 e^{-52}$	38	0.063	739	0.32
Hsf1	126	$1.8 e^{-62}$	61	$1.4 e^{-12}$	571	0.23
Aft1	150	$5.5 e^{-50}$	84	$2.3 e^{-10}$	1114	0.34
Pdr1	110	$1.5 e^{-41}$	30	0.25	653	0.46
Sok2	128	$1.5 e^{-36}$	62	0.00024	1034	0.003
Gis1	66	$1.4 e^{-38}$	38	$6.6 e^{-14}$	223	0.51
Rpn4	128	$1.2 e^{-36}$	58	0.0019	1032	0.031
Sko1	90	$1.2 e^{-27}$	26	0.47	627	0.055
Hot1	35	$4.1 e^{-29}$	4	0.25	74	0.11
Regulators of late up-regulated genes						
Gis1	66	$1.4 e^{-38}$	38	$6.6 e^{-14}$	223	0.51
Hsf1	126	$1.8 e^{-62}$	61	$1.4 e^{-12}$	571	0.23
Aft1	150	$5.5 e^{-50}$	84	$2.3 e^{-10}$	1114	0.34
Hac1	13	0.09	21	0.00013	208	0.19
Sok2	128	$1.5 e^{-36}$	62	0.00024	1034	0.003
Hap3	11	0.14	17	0.0015	1032	0.031
Rtg2	1	0.029	2	0.0017	6	0.033
Rpn4	128	$1.2 e^{-36}$	58	0.0019	1032	0.031
Rtg1	5	0.55	13	0.0019	129	0.286
Hap2	13	0.064	17	0.002	197	0.013

For genes rapidly regulated in wt baker's yeast ('early' category, up- or down-regulated), the calculated p-values indicate a high enrichment of their annotated targets, while the TFs with enriched targets in the 'late' regulated genes have higher p-values, indicating lower significance.

Among the regulators with enriched targets in the 300 rapidly and strongly up-regulated genes are Msn2, Msn4 and Hsf1. Msn2 and Msn4 are the main mediators of the 'general stress-response' (GSR), initiating a stress response pathway upon exposure toward various types of stress, such as heat, oxidative stress, osmotic shock, acidic pH, starvation and others (Martinez-Pastor et al., 1996). Of the 300 early up-regulated genes, 184 are putative Msn2 targets and 129 of Msn4, while only 53 or 38 of the Msn2 and Msn4 targets are identified in the late up-regulated genes. Hsf1 regulates the transcriptional 'heat stress response' (HSR) with the two response systems having a high overlap in their target genes (Morano et al., 2011). Hot1 is an activator of Hog1, which is known to regulate the 'osmotic stress response' pathway, e.g. when exposing yeast to an environment with high osmolarity (Tamas and Hohmann, 2003). Here too, an overlap to the environmental stress response has been identified (Gasch, 2002). While Aft1 is a regulator of iron uptake and storage also implicated in oxidative stress responses, Pdr1 regulates, among others, genes involved in the export of drugs from the cell, as well as hexose transporters in the cellular membrane (Mamnun et al., 2002; Toledano et al., 2003). Another regulator with enriched targets is Sko1, with 90 of its 627 putative targets in the yeast genome found to be up-regulated early. Sko1 is involved in osmotic as well as oxidative stress responses (Toledano et al., 2003).

Of all the listed regulators with enriched targets in the early up category, the p-values are considerably lower than those obtained for a random dataset of 300 genes, demonstrating that their enrichment is not merely due to chance. Almost all listed regulators with enriched targets in the 'early up' category are not significantly enriched in the 'late up' category. This points to a selective mechanism in the first minutes of heat stress which most probably triggers adaptation to the stress.

With regard to the late up-regulated genes, the targets of Gis1, Hsf1, Aft1 and Rpn4 are also significantly enriched, while for others (e.g. Hap2, Thi2, Hac1) the higher p-values indicate a lower level of significance of their target enrichment among the regulated genes. Hac1 is a transcriptional activator of the Unfolded Protein Response (UPR) pathway, explaining why its targets are up-regulated after temperature stress.

Regulators of down-regulated genes target ribosome synthesis and stress responses

As for up-regulation, a list was compiled with the 10 TFs that show enrichment of their target genes among the early- or late down-regulated genes (Table 21)

Table 21 Enriched transcription factors (TF) in early down and late down-regulated genes after mild heat stress in wt baker's yeast.

The number of targets, as well as the p-value in the respective dataset was retrieved using DNA-binding and expression evidence annotated in the yeasttract database (September 2015). The ten most significant regulators for early and late genes are listed in their rank of significance from top to bottom. The p-value was calculated as described in 3.11. Significance: $p < 0.01$. For comparison, the respective p-value in a random dataset with an equivalent number of genes is also listed

TF	# targets in dataset 'early down'	p-value early down	# targets in dataset 'late down'	p-value late down	# targets in genome	p-value in random dataset of equivalent number
Regulators of early down-regulated genes						
Sfp1	195	$4.7 e^{-64}$	165	$3.0 e^{-34}$	2183	0.00017
Stb5	62	$5.4 e^{-27}$	8	0.95	339	0.055
Gln3	83	$2.2 e^{-25}$	53	$1.8 e^{-07}$	667	0.55
Pdr3	65	$3.2 e^{-18}$	37	0.00058	547	0.78
Adr1	33	$7.8 e^{-05}$	17	0.55	443	0.64
Mss1	10	$8.2 e^{-05}$	2	0.57	68	0.11
Msn2	72	$2.9 e^{-07}$	63	0.00079	1187	0.29
Met4	73	$1.6 e^{-06}$	67	0.00038	1260	1
Ino4	43	$4.2 e^{-05}$	38	0.004	637	0.0097
Rsc30	5	0.00015	1	0.23	21	0.047
Regulators of late down-regulated genes						
Sfp1	195	$4.7 e^{-64}$	165	$3.0 e^{-34}$	2183	0.00017
Yap1	63	0.23	128	$1.7 e^{-19}$	1824	0.63
Gcn4	65	0.00019	93	$6.4 e^{-13}$	1260	0.034
Gln3	83	$2.2 e^{-25}$	53	$1.8 e^{-07}$	667	0.55
Bas1	7	0.27	21	$3.9 e^{-07}$	152	0.0013
Rap1	60	0.0057	99	$3.0 e^{-08}$	1502	0.12
Arr1	35	0.053	55	$8.0 e^{-07}$	743	0.004
Leu3	9	0.99	39	$1.7 e^{-05}$	495	0.54
Ste12	72	0.18	103	$3.5 e^{-06}$	2142	0.086
Msn1	4	0.28	13	$1.8 e^{-05}$	87	0.097

Sfp1, a stress-activated TF involved in activation and repression of the transcription of ribosomal proteins and ribosomal biogenesis genes, is the most significant regulator on the side of down-regulation (Marion et al., 2004). From its annotated and putative targets 195 are found in the 262 early down-regulated genes. Even within the 280 genes down-regulated in the timeframe 10 min until 20 min of heat shock ('late down'), 165 are thought to be regulated by Sfp1 (Table 21).

Stb5, with 62 of its 339 targets in the yeast genome identified in the early down-regulated genes, is involved in regulation of drug resistance as well as oxidative stress, potentially

linking it to stress response more generally (Larochelle et al., 2006). Pdr3, a homolog of Pdr1, regulates the same pathways of pleiotropic drug response. While Pdr1's targets are mainly up-regulated, the targets of Pdr3 are enriched among the early down-regulated genes. Sixty-five of its 547 targets are identified in the 265 down-regulated genes (Mamnun et al., 2002). Msn2, one of the two main regulators of the GSR, also significantly represses transcription of 72 of the 265 early down-regulated genes.

In the group of genes with a maximum of transcriptional down-regulation between 10 to 20 min ('late down'), Sfp1-targets are also most significantly enriched in the late down genes. Next is Yap1 with 128 of differentially regulated targets. This regulator is involved in the oxidative stress response, controlling the expression of a number of anti-oxidant proteins (Toledano et al., 2003). Gcn4 and Bas1 are the next major regulators among the late down-regulated genes and are involved in the general amino acid control network. This network is required for the production of translation precursors, such as purines, ribosomal proteins, and amino acids. In addition, Gcn4 and Bas1 regulate genes involved in multiple stress responses (Arndt et al., 1987; Natarajan et al., 2001). Rap1 is a transactivator of ribosomal protein genes (Lieb et al., 2001). Therefore, the appearance of 99 of its targets among the 'late down genes' reflects the cells' reduced need for the production and assembly of ribosomes for protein biosynthesis.

In summary, as is also evident from the clustering of the differentially-regulated genes into GO categories (Figure 22), TFs regulating stress response pathways are the most prominent gene regulators on the side of increased mRNA production, while TFs involved in regulation of ribosomal protein genes and amino acid biosynthesis are most significant on the side of mRNA reduction after heat stress.

4.4 Transcriptional heat stress response in the genetic background of TF deletions

The investigation of the responsible regulators of the differentially-regulated genes under heat shock suggest Msn2, Msn4, Hsf1, Rpn4 and Sko1 to be involved in the regulation of the transcriptional heat-stress response (see chapter 4.3.6). For this reason, the response was examined in the genetic background of transcription factor deletions.

Due to the fact that Msn2 and Msn4 regulate the general stress response and many of the early-up regulated genes of the wt transcriptional response are regulated by these TFs, the transcriptional heat stress response in the *msn2-msn4* null-background was investigated. The *rpn4* deletion was chosen due to its high number of targets in general and within the differentially regulated genes, and due to its role in regulation of genes encoding for proteasomal degradation (Xie and Varshavsky, 2001). Furthermore, the *rpn4* transcript level itself is up-regulated two-fold within the first 5 minutes in wt baker's yeast. Another transcription factor focused on was Sko1, owing to its involvement in oxidative and osmotic stress responses and its high number of differentially regulated targets in wt yeast's transcriptional heat stress response.

The null mutants $\Delta rpn4$, $\Delta sko1$ and the double deletion strain $\Delta msn2\Delta msn4$ were subjected to mild heat stress by shifting cells in the early logarithmic growth phase from 25°C to 37°C for up to 40 min. Deletion of the respective gene regulators did not affect yeast viability under the experimental conditions tested (Figure 27).

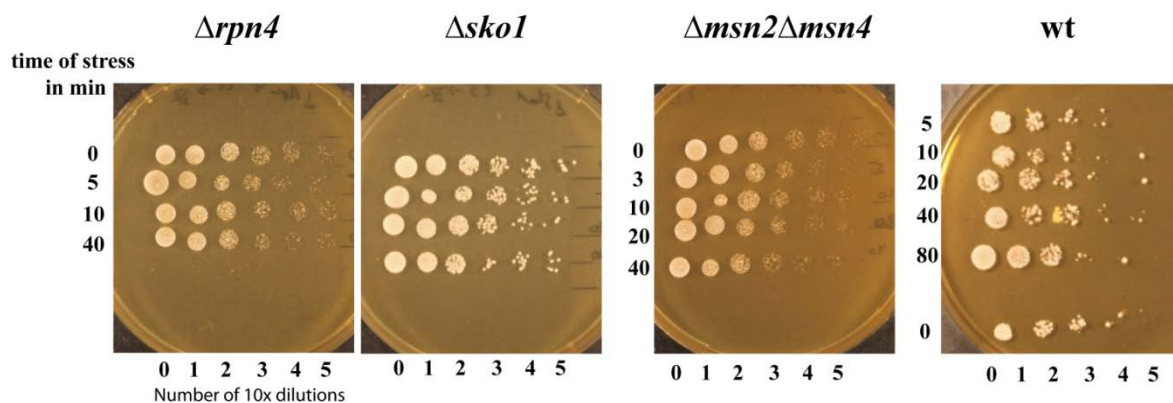


Figure 27 Survival assays of wt and TF-deletion strains used for microarray analysis. Cultures were grown at 25°C in YPD into the logarithmic growth phase ($OD_{595}=0.5$) and shifted to 37°C. At indicated time points a 10x dilution series was prepared and cells spotted on YPD agar.

Microarray analysis was carried out for time points up to 40 min, the time range of maximal gene regulation and re-establishment of steady state transcription in wt yeast. All cultures were prepared in biological triplicates. Data normalization and analysis were carried out as for the kinetic response of the wt strain. In principle, the mean mRNA signals were calculated from normalized data of the biological triplicates for the wt and null mutant and \log_2 transformed. Ratios of $\frac{KO}{WT}$ were calculated for each gene and point in time, as well as fold-changes of transcript level compared to the unstressed control. A list of genes was generated with up- and down-regulated genes in the KO mutant at a selected cutoff of two-fold differential regulation ($\log_2 = |1|$). Genes below noise-level, defined at a MAS5-mRNA signal of 40, were omitted from the analysis.

4.4.1 *Rpn4* deletion has broad effects on the transcriptome

In the genetic background of *rpn4* deletion, 186 messages are up- or down-regulated by a \log_2 -value of at least 1, which approximates 3.3% of all *S. cerevisiae* genes. 386 transcripts, or 6.8% of the genome, are altered in their transcription at the selected thresholds after 5 min of mild heat shock, while the number rises to 526 genes (9.2% of the genome) after 10 min of increased temperature stress and drops down again to 357 genes (6.2% of the genome) at 40 min (Table S3).

In order to examine the effect *rpn4* disruption has on gene regulation, annotated targets of Rpn4 were retrieved from the yeast genome database. Selected targets included those based on microarray expression studies. Putative targets based on computational combinatorial analysis were omitted from this network. By these criteria, 29 activated and 20 repressed targets by Rpn4 were obtained and the Rpn4 gene regulatory network designed (Figure 28).

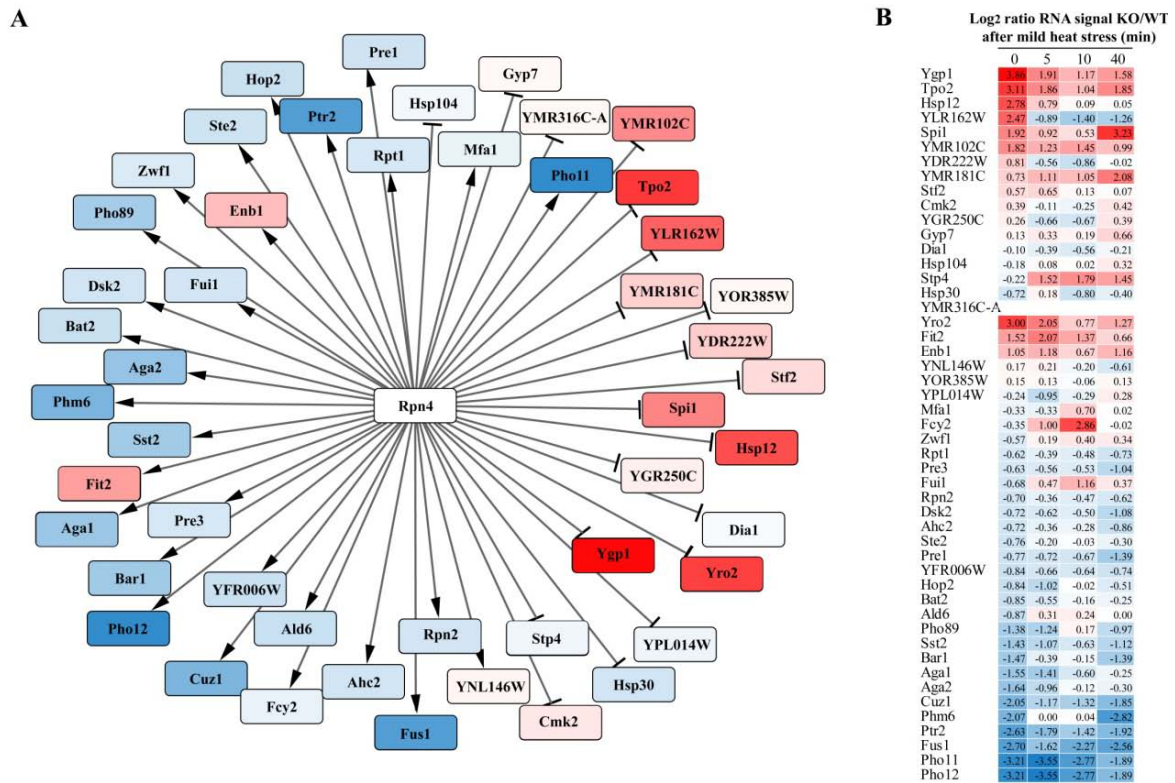


Figure 28 Gene regulation network of *Rpn4*.

A: Regulation of *Rpn4* targets in the $\Delta rpn4$ mutant under permissive conditions. Targets were obtained from the SGD, based solely on expression evidence. Arrows as edges indicate *Rpn4* being annotated as an activator, \top -shaped edges indicate *Rpn4* is annotated as repressor. Nodes are color coded according to their log₂ ratios compared to wt yeast. Red indicates higher transcript level, blue indicates reduced transcript levels in the KO strain. **B:** Heat map of gene regulation of *Rpn4* targets in a $\Delta rpn4$ mutant strain exposed to mild heat stress (25°C → 37°C). Log₂-ratios of transcripts compared to wt levels under equal duration of stress are noted. (-4 +4)

Where *Rpn4* is a trans-activator, deletion of *rpn4* pilots the transcript levels towards lower values in 24 out of 29 cases. This equals close to 83% (Figure 28A). For these targets the log₂-ratios lie in the range of -0.57 to -3.21. For two targets (*mfa1*, *fcy2*), the ratios are merely slightly reduced and lie at -0.33 and -0.35; and for two targets, the transcript ratio is actually elevated in the KO strain (*enb1*, *fit2*). On the side of targets repressed by *Rpn4*, a deletion of *rpn4* and, consequently, the removal of the transcriptional repressor, results in elevated mRNA levels in nine out of the 20 targets (Figure 28A). For these 45% of *Rpn4*-repressed targets, the log₂-ratios lie within the range of 0.57 to 3.86. A total number of 7, or 35% of the repressed target genes, display only weak or no changes in their transcript levels under non-stress conditions (*stp4*, *dia1*, *hsp104*, *gyp7*, *YPL014w*, *YOR385w*, *cmk2*); and only one (*hsp30*) has a decreased level in the *rpn4*-KO - contrary to its annotated *Rpn4*-inhibited character. All in all, the gene regulation for these 49 targets is in good

agreement with the annotated function of Rpn4 as an activator and repressor of transcription (Xie and Varshavsky, 2001).

For these 49 genes, the differences in transcript levels between the *rpn4* deletion strain and wt baker's yeast diminish when exposed to 37°C heat stress for 5 min and 10 min and are restored close to unstressed values after 40 min of stress (Figure 28B). This indicates a transcriptional response to heat in wt yeast, which adjusts the mRNA levels to those present in the *rpn4*Δ yeast from the start.

Analysis of the kinetic transcriptional response of Δrpn4 yeast

As stated above, the influences on the transcriptome go beyond these 49 listed targets of Rpn4. Plotting the transcriptional regulation of the *rpn4*-deletion strain against that of the wt yeast strain points out the differences in gene regulation (Figure 29). After 5 min of stress, most genes show similar regulation in wt and Δ*rpn4* yeast. This can be derived from the fact that they lie close to the diagonal of the diagram, which represents the line of perfect correlation between KO and wt gene regulation. Nevertheless, already at 5 min, genes show deviations from the diagonal, especially on the side of down-regulated transcripts after heat shock. This indicates differential regulation between the KO and wt strains, in that these messengers are down-regulated to a stronger extent in the wt yeast (Figure 29A). Also on the side of up-regulation, transcripts deviate from the diagonal, however, to a lower number. After 10 min of heat shock, the effect of differential regulation between the KO and wt strain is more pronounced. Here, especially transcripts that show \log_2 -fcs in the wt in the range of -3 to -6, meaning an eight to 64-fold down-regulation, are down-regulated weaker in the *rpn4*-disrupted background, where the \log_2 -fcs lies in the range of 0 to -3 (Figure 29B). After 40 min of heat shock, the differences in gene regulation between KO and wt strain are reduced again. The \log_2 -fcs of most transcripts move towards the diagonal again, however, as stated above, 357 genes still possess a fold-change by a factor ≥ 2 (Figure 29C).

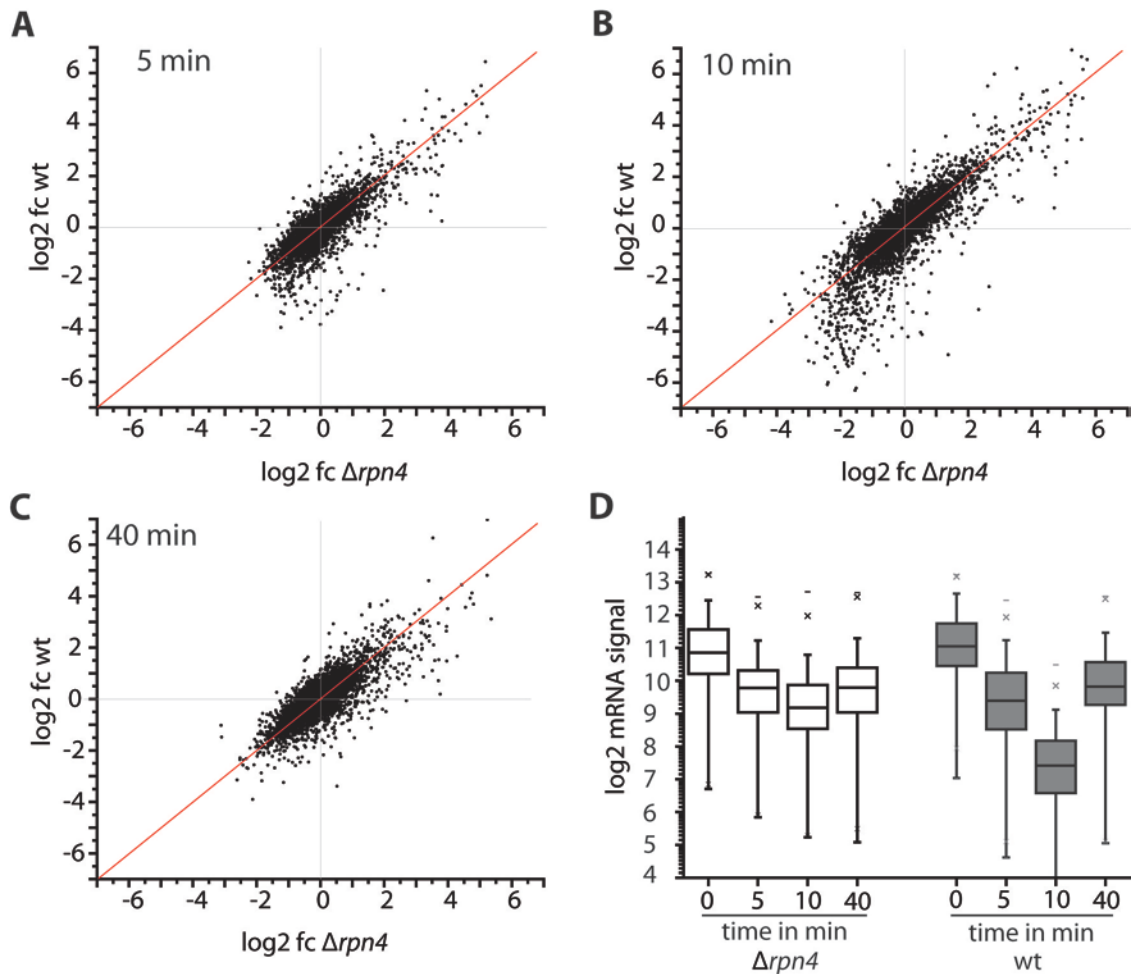


Figure 29 Gene regulation in the *rpn4*-deletion strain compared to wt yeast. Yeast was exposed to 37°C stress and RNA levels determined for times of 5, 10 and 40 min by microarrays. Fold-changes versus unstressed zero time were calculated, the mean value for three biological replicates determined, and \log_2 -transformed. Genes lying below a mean RNA-MAS5 signal of 30 were omitted from the analysis. **A:** Fold-changes of gene regulation of $\Delta rpn4$ yeast plotted against wt yeast after 5 min of 37°C. **B:** Gene regulation of $\Delta rpn4$ vs. wt yeast after 10 min of heat stress. **C:** Gene regulation of $\Delta rpn4$ vs. wt yeast after 40 min of heat shock. **D:** Box plot of mean RNA levels of genes that showed less down-regulation in $\Delta rpn4$ yeast compared to wt. One box plot each is prepared for wt and $\Delta rpn4$ yeast for 0, 5, 10 and 40 min of 37°C stress. Displayed is the median RNA signal with the upper and lower quartiles. The whiskers indicate the maximum and minimum value in the data. Outliers are marked with 'x', strong outliers by '-'.

The transcripts that showed less down-regulation in the *rpn4* null mutant were analyzed with respect to their RNA level, in order to exclude any artifacts due to gene-chip signals close to the limits of detection. Therefore, the RNA-signals of the 189 genes were box-plotted for the $\Delta rpn4$ and wt strains (Figure 29D). The plots for 0 min are very similar for both yeast strains with a median \log_2 -RNA signal at 11. After 5 min of stress, the median signal drops to just below 10 for the $\Delta rpn4$ strain and closer to 9 for the wt strain. At 10 min, this discrepancy in the median RNA signal is much more pronounced: While the

deletion strain still has a median \log_2 -RNA-signal in the range of 9, meaning an absolute RNA signal near 500, the wt possesses a median \log_2 -RNA signal of 7, or 128 on the absolute scale. This lies well within the detection range between six to 14 of the utilized yeast genome 2.0 microarrays (Handbook Affymetrix, 2014).

GO analysis of genes with differential kinetic regulation

In order to gain more insight on the genes differentially regulated over time in the KO compared to wt yeast, they were put into a GO analysis search, and enriched clusters were noted (Table 22). Significantly enriched biological processes of ‘ribosome biogenesis & assembly’, ‘maturation of SSU-rRNA’ and ‘tRNA modification’ are obtained. After 40 min, the most significant GO terms are related to ‘abiotic stress response’ and carbohydrate metabolism, a clear shift away from ribosomal biogenesis perhaps due to adaptation of both yeast strains to the high ambient temperatures.

Table 22 GO analysis of genes with differential regulation in Δ rpn4 yeast under heat shock compared to wt regulation.

Genes with a more than two-fold different regulation at the indicated times of stress were submitted to GO analysis. Only the most enriched GO terms with a p value < 0.001 are listed.

GO ID	GO term	# genes identified in cluster	Enrichment score	p-value
5 min				
GO:0042254	Ribosome biogenesis	34	5.80	<0.0000001
GO:0030490	Maturation of SSU-rRNA	13	2.82	0.000009
10 min				
GO:0042254	Ribosome biogenesis	118	43.83	<0.0000001
GO:0030490	Maturation of SSU-rRNA	41	16.32	<0.0000001
GO:0042255	Ribosome assembly	23	5.70	<0.0000001
GO:0006400	tRNA modification	17	4.50	0.000012
40 min				
GO:0009628	Response to abiotic stimulus	29	4.95	<0.000001
GO:0005996	Monosaccharide metabolic process	13	1.93	0.000613

4.4.2 *Sko1* deletion has minor effects on the transcriptome

Disruption of the *sko1*-locus alters the transcription of 76 genes two-fold compared to wt when grown at 25°C. Five minutes of 37°C stress increases the number to 102 genes, 175 genes are altered after 10 min of stress, and 100 after 40 min (Table S4). Hence, the effect of *sko1*-disruption is not as prominent as for *rpn4* deletion. Focusing on the *Sko1* targets and based on SGD expression evidence only, 14 transcript levels were examined more closely (Figure 30). From the ten genes repressed in their expression by *Sko1*, six possess elevated signals with \log_2 -ratios between 0.70 and 3.03 in KO strain compared to wt (YLR162W, *fre4*, *gre2*, *thi4*, YML131W and *cwp1*). Only two of the *Sko1*-repressed target genes are unaffected in their transcription (*nog2*, YLR297W), and *hpf1* is the sole target with a reduced signal in the knockout strain, lying -0.40x lower on the \log_2 -scale in the *sko1*-null mutant. YOL150C was not probed for on the microarray. From the four targets activated by *Sko1*, *gcv1* mRNA level increases by a \log_2 -factor of 0.82 in the KO, *akr2* is unchanged; and for *pcl1* and *ptr2*, a disruption of the activator *Sko1* brings forth a drop in their mRNA levels, by a \log_2 -factor of -0.36 and -0.84. Heat shock, in general, leads to a reduction in the discrepancies between KO mutant and wt yeast, meaning transcript levels merge towards similar values at 5 min and 10 min of heat stress for most of the genes. Only *fre2* and *nog2* expose even higher ratios under heat shock. At 40 min of stress, ratios similar to those under physiological conditions are present (Figure 30B).

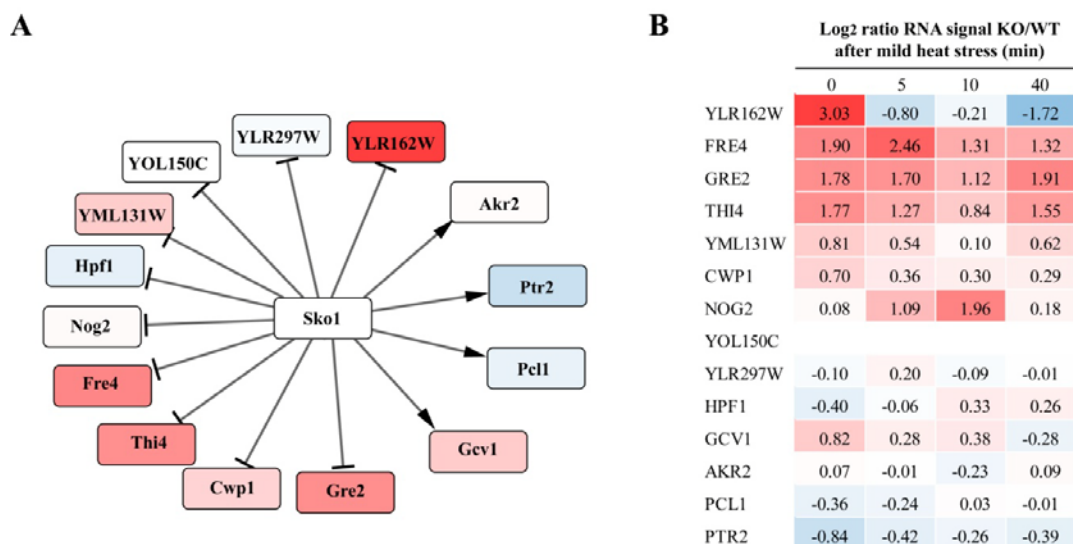



Figure 30 Gene regulation network of *Sko1*.

A: Regulation of *Sko1* targets in the $\Delta rpn4$ mutant under permissive conditions. Targets were obtained from the SGD, based solely on expression evidence. Arrows as edges indicate *Rpn4* being annotated as an activator, \top -shaped edges indicate *Rpn4* is annotated as repressor. Nodes are color coded according to their \log_2 ratios compared to wt yeast. Red indicates higher transcript

level, blue indicates reduced transcript levels in the KO strain (-4  +4). B: Heat map of gene regulation of *Sko1* targets in a $\Delta sko1$ mutant strain exposed to mild heat stress (25°C \rightarrow 37°C). Log₂-ratios of transcripts compared to wt levels under equal duration of stress are noted. (Figure legend continued from previous page).

As for the *rpn4*-deletion strain, the kinetics of fold-changes of gene regulation of the $\Delta sko1$ -strain under mild heat stress were compared to those of wt baker's yeast. The differences in gene regulation between *sko1*-null mutant and wild type are not as pronounced as for the $\Delta rpn4$ yeast. This can also be derived from the diagrams in which the log₂-fcs of gene regulation of the $\Delta sko1$ strain are plotted against those of the wt strain (Figure 31). After 5 min of 37°C heat shock, the vast majority of genes show the same transcriptional regulation for both yeast strains, the points in the diagram lie near the diagonal of the diagram. However - as was the case for $\Delta rpn4$ yeast - a number of genes showed deviation from the diagonal, indicating differential gene regulation in the KO strain compared to wt (Figure 31A). After 10 min, the deviations from the diagonal are more pronounced, especially for the genes on the side of down-regulation that move towards the right of the diagonal. This means they possess weaker down-regulation in the KO strain compared to wt yeast (Figure 31B). These discrepancies are no longer present at the last time measured, where fold-changes in general are lower and differences between KO and wt strain transcriptional regulation are less (Figure 31C).

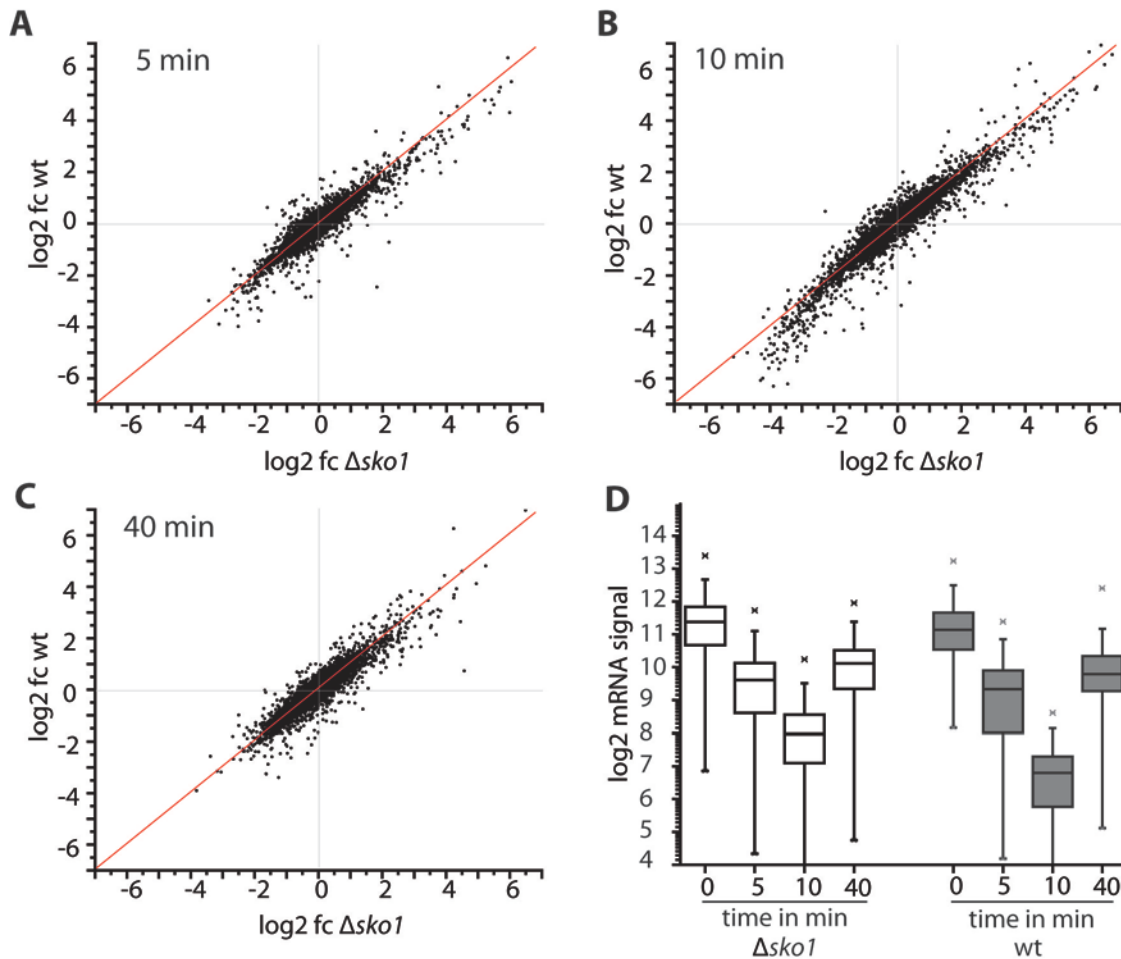


Figure 31 Gene regulation in the *sko1*-deletion strain compared to wt yeast. Yeast was exposed to 37°C stress and RNA levels determined for time points 5, 10 and 40 min by microarrays. Fold-changes versus unstressed zero time were calculated, the mean value for three biological replicates determined and log₂-transformed. Genes lying below a mean RNA-MAS5 signal of 30 were omitted from the analysis. **A:** Fold-changes of gene regulation of $\Delta sko1$ yeast plotted against wt yeast after 5 min of 37°C. **B:** Gene regulation of $\Delta sko1$ vs. wt yeast after 10 min of heat stress. **C:** Gene regulation of $\Delta sko1$ vs. wt yeast after 40 min of heat shock. **D:** Box plot of mean RNA levels of genes that showed less down-regulation in $\Delta sko1$ yeast compared to wt. One box plot each is prepared for wt and $\Delta sko1$ yeast for 0, 5, 10 and 40 min of 37°C stress. Displayed is the median RNA signal with the upper and lower quartiles. The whiskers indicate the maximum and minimum value in the data. Outliers are marked with 'x', strong outliers by '-'

Comparing the RNA-levels of the 89 transcripts that possess weaker down-regulation in $\Delta sko1$ yeast after 10 min at 37°C with those of wt *S. cerevisiae*, shows that from the same RNA-levels initially, the drop in mRNA is more pronounced for the wt, i.e. from a median log₂-signal of eleven to eight for the *sko1*-null yeast and to seven for wt yeast. After 40 min, the median log₂-RNA signals again are restored to around ten for both strains (Figure 31D). This again leads to the conclusion that the observed effects lie within the detection range of the microarrays and, therefore, are not due to limitations of the employed method.

GO analysis of differentially regulated genes in $\Delta sko1$ cells

Table 23 GO analysis of genes with differential regulation in $\Delta sko1$ yeast under heat shock compared to wt regulation.

Genes with a more than two-fold different regulation at the indicated times of stress were submitted to GO analysis. Only the most enriched GO terms are listed, the p-values are notes. Significance: $p < 0.05$.

GO ID	GO term	# genes identified in cluster	Enrichment score	p-value
5 min				
GO:0008643	Carbohydrate transport	4	3.42	0.001065
GO:0055085	Transmembrane transport	5	1.31	0.032427
10 min				
GO:0042254	Ribosome biogenesis	30	8.51	<0.000001
GO:0006364	rRNA processing	22	3.23	<0.000001
GO:0009266	Response to temperature stimulus	14	2.96	0.000081
40min				
GO:0009628	Response to abiotic stimulus	10	2.55	0.000672

Five minutes of stress yields only 33 genes with a regulation at least two-fold different from wild-type values. These genes are involved in transport processes, especially in the uptake of sugar across the membrane. These are the only GO terms obtained with a significant p-value < 0.05 . One hundred genes have differential kinetic regulation at the second point in time. Close to one third of the genes are enriched for nuclear proteins involved in ribosome biogenesis or rRNA processing. Also, the biological process of ‘response to temperature stimulus’ is among the significant GO terms, showing that *Sko1* does participate in the regulation of heat stress response associated genes. At the last point of time measured, only 45 genes remain that are enriched in genes involved in ‘response to abiotic stimulus’. In conclusion, *sko1* disruption results in genes with differential kinetic regulation in the context of heat shock. These include many genes of ribosome biogenesis, as was the case for the transcriptional response of $\Delta rpn4$ yeast.

4.4.3 *Msn2/4* deletion has vast influences on the transcriptome

Deletion of the two regulators of the general stress response affects the basal transcription of 298 genes, roughly 5.2 % of the 5,717 genes probed for in the microarrays. This number is even augmented under temperature stress where 531 genes (9.3%) show differential regulation compared to wt yeast after 3 min of exposure to 37°C and even 716 genes (12.5%) after 10 min of stress, the point in time where the transcriptional response of *S. cerevisiae* is at its maximum. After 20 min, the number decreases to 580 genes (10.2%) and drops further down to 255 after 40 min (4.5%). Hence, the deletion of the two regulators of the general stress response has broad effects on gene regulation in baker's yeast.

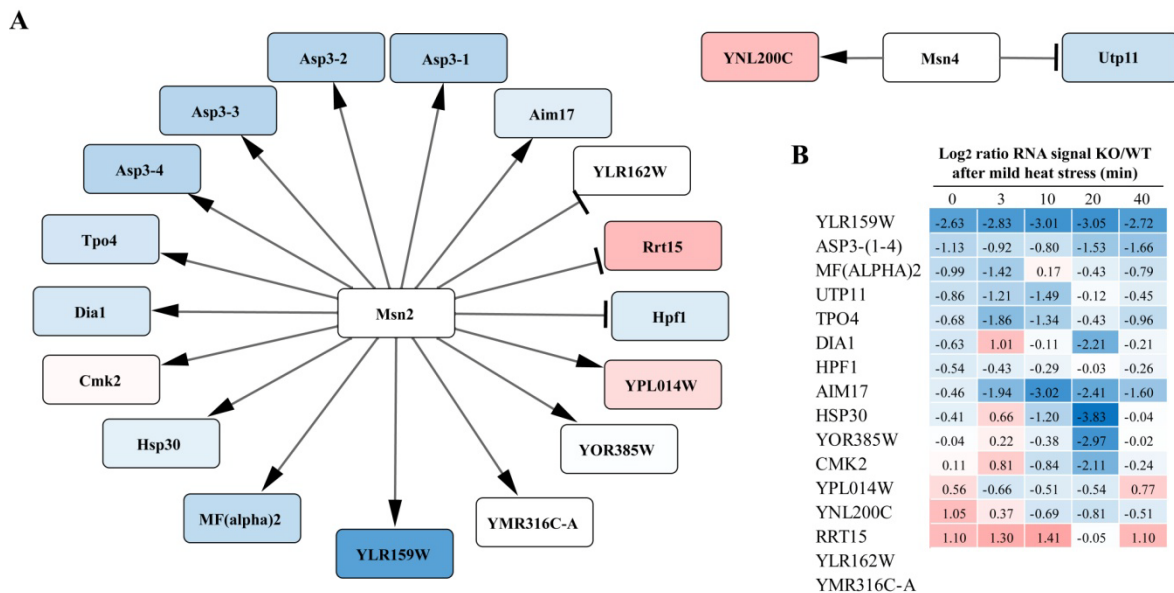


Figure 32 Gene regulation network of *Msn2* and *Msn4*.

A: Regulation of *Msn2* and *Msn4* targets in the $\Delta msn2\Delta msn4$ mutant under permissive conditions. Targets were obtained from the SGD, based solely on expression evidence. Arrows as edges indicate *Msn2* or *Msn4* being annotated as an activator, \top -shaped edges indicate the TF is a repressor. Nodes are color-coded according to their log₂ ratios compared to wt yeast (-4 to +4). Red indicates higher transcript level, blue indicates reduced transcript levels in the KO strain.

B: Heat map of gene regulation of *Msn2* and *Msn4* targets in a $\Delta msn2\Delta msn4$ mutant strain exposed to mild heat stress (25°C → 37°C). Log₂-ratios of transcripts compared to wt levels under equal duration of stress are noted.

Based on expression evidence 20 genes are listed in the yeast genome database as targets of *Msn2* and *Msn4*, with 16 genes being activated and four being repressed. These genes are focused on with respect to their transcription level under permissive and heat shock conditions (Figure 32). Ten of the 16 activated targets, or 62.5 %, possess lower transcript

levels in the KO strain with \log_2 ratios between -0.41 and -2.63. Two genes are unaffected in their basal transcription (YOR385W, Cmk2) and two show higher mRNA signals in the KO strain - with the \log_2 ratios lying at 1.05 and 0.56 (YNL200C, YPL014W). Of the four repressed target genes, only one (Rrt15) has a higher basal transcript level, roughly a two-fold increase in mRNA level in the *msn2-msn4* deletion strain, while Utp11 and Hpf1 actually have less mRNA compared to wt yeast. The latter is contrary to expectations, where a knock-out of the transcriptional inhibitors would result in higher transcript levels. One transcript each for activated and repressed targets was not probed for by the gene chips (YMR316C-A, YLR162W), therefore, no statement can be made on their regulation in the null-mutant.

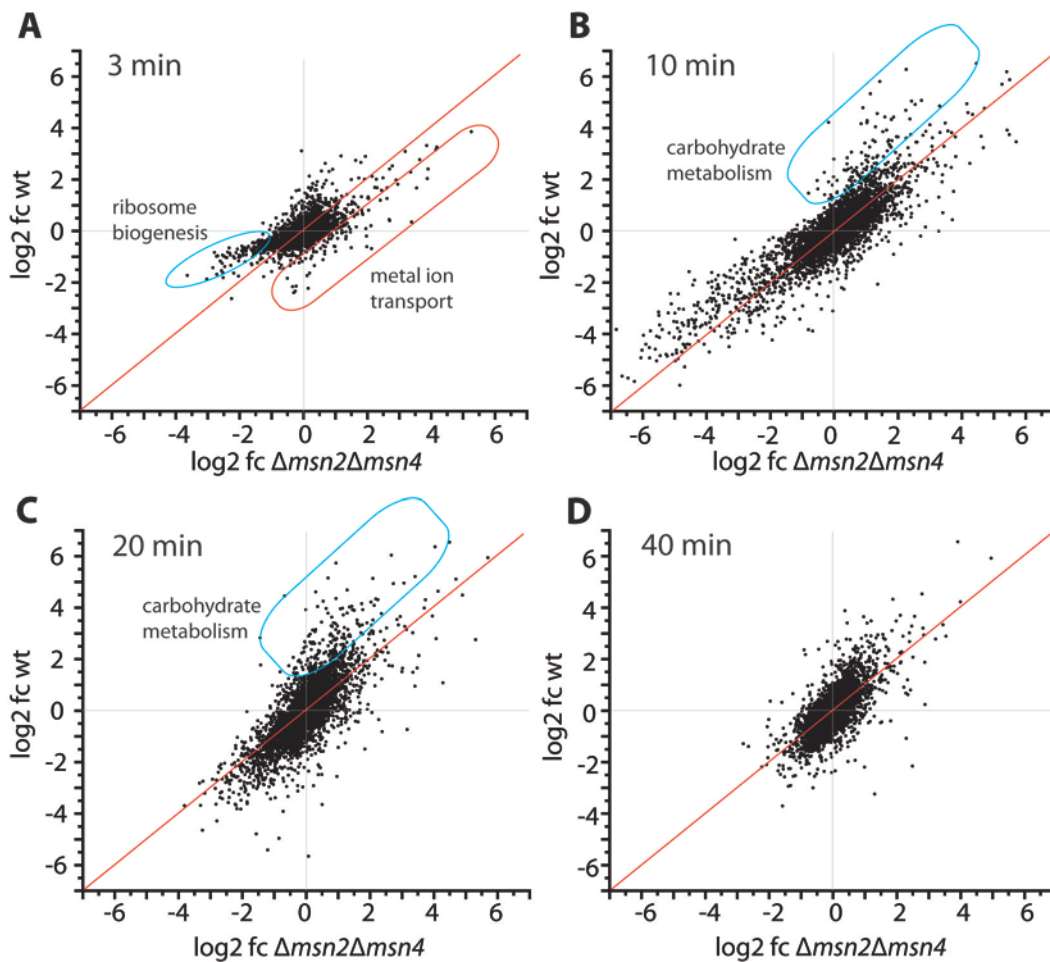


Figure 33 Gene regulation in the *msn2msn4*-deletion strain compared to wt yeast.

Yeast was exposed to 37°C stress and RNA levels determined for time points 3, 10, 20 and 40 min by microarrays. Fold-changes versus unstressed zero time were calculated, the mean value for 3 biological replicates determined and \log_2 -transformed. Genes lying below a mean RNA-MAS5 signal of 30 were omitted from the analysis. A: Fold-changes of gene regulation of $\Delta msn2\Delta msn4$ yeast plotted against wt yeast after 3 min of 37°C. B: Gene regulation of $\Delta msn2\Delta msn4$ vs. wt yeast after 10 min of heat stress. C: Gene regulation of $\Delta msn2\Delta msn4$ vs. wt yeast after 20 min of heat

shock. D: Gene regulation of $\Delta msn2\Delta msn4$ vs. wt yeast after 40 min of heat shock. Gene with strong differential regulation after heat shock are marked in boxes and noted with the most significant GO term. (Figure legend continued from previous page).

A plot of the fold-changes of gene regulation of $\Delta msn2\Delta msn4$ yeast exposed to mild heat shock against those of wt, exposes differences in heat-induced gene regulation already appearing after three minutes (Figure 33A). Although fold-changes remain low at 3 min, as evident in the point clustering around the origin of the coordinate system, there are 54 genes that show stronger down-regulation in the KO strain, with \log_2 fold-changes ranging from -1.5 to -4.0. The respective values in the wt strain are more than two-fold lower (Figure 33A, blue circle). A GO analysis of this selection revealed ‘ribosome biogenesis’ to be the most significant GO term with 33 of the selected genes clustering to this process. In addition to the more down-regulated genes in the KO, there are some with higher up-regulation compared to wt (Figure 33A, red circle). A GO analysis of these 65 genes yielded metal ion transport to be the most significant GO term, although only seven genes cluster to this process. The stronger down-regulation of genes in the KO strain for the ribosome biogenesis cluster is still present at 10 min of stress and, furthermore, another set of genes comes up which possess stronger up-regulation in the wt strain (Figure 33B, blue box). These 54 genes are enriched for processes involving carbohydrate metabolism, with one fourth of the genes annotated to this term. This group of genes also depicts higher up-regulation in the wt at 20 min of stress (Figure 33C). 40 min of heat shock displays an adaptation of both yeast strains to the high temperature of 37°C, as the \log_2 fold-changes of gene regulation for both strains decrease to lower values. In addition, the deviations from the diagonal at 3 min and 10 min, as described above, are not present anymore.

In conclusion, deletion of the main mediator of the general stress response *Msn2/4* has extensive consequences on the transcriptome of baker’s yeast exposed to heat shock. Genes with differential regulation are involved in energy metabolism, ion homeostasis, and, most significantly, in ribosome biogenesis. Therefore, besides specific changes in the transcriptional profile, deletion of *rpn1*, *sko1* and *msn2/4* all have in common altered kinetic transcription of ribosome biogenesis factors, suggesting an altered need for protein biosynthesis compared to wt yeast.

4.5 Transcriptional heat stress response in *hsp12* and *sHsp* deletion yeast

The kinetic stress response to 37°C was not only investigated for wt yeast or transcription factor KO strains, but also for two other selected knockout strains: the *hsp12*- null mutant and the *hsp26/42* null strain. These strains were chosen because both baker's yeast sHsps genes and *hsp12* are among the most highly induced genes after thermal stress. Furthermore, the fold-changes *hsp12* and *hsp26* remained high over the entire time period in the transcriptional response of wt yeast (see Table 16). With only very low basal expression under physiological conditions, they represent the two most highly induced of all 5,717 yeast genes analyzed by gene chip. The need for these two genes to remain highly up-regulated leaves room for speculation. Hsp12, an intrinsically unstructured protein, is dispensable for growth under non-stress conditions, but it is directed towards specific cellular membranes upon a variety of stresses, including heat shock. Upon binding of lipids in the plasma membrane, endosomes and possibly also of vacuoles, Hsp12 adopts helical structure and is thought to stabilize membrane integrity (Welker et al., 2010). In the context of the heat shock response, cellular integrity is crucial for proteostasis, since leaky membranes may result in the uncontrolled loss and uptake of molecules (Verghese et al., 2012). Hsp26, the heat stress inducible sHsp of baker's yeast, fulfills its cyto-protective function by inhibiting the irreversible aggregation of proteins under stress (Haslbeck et al., 1999). The need for the long-lasting transcriptional up-regulation may be explained by the experimental setup with persisting thermal stress, where protein biosynthesis starts again at later points in time, and newly synthesized proteins may be prone to aggregate at 37°C. In this respect, Hsp26 would aid in aggregation suppression and support the Hsp104- and Hsp70-mediated (re)-folding of the proteins. Interestingly, *hsp42* showed a behavior different from *hsp26* in that it was rapidly up-regulated to levels comparable to *hsp26* at 10 min to 15 min but declined after 20 min almost to RNA levels of un-stressed cells.

Due to their strong up-regulation and their roles in cellular homeostasis, the heat stress response was investigated in their null-background.

To check for a growth phenotype, cultures in early exponential growth were shifted from 25°C to 37°C for up to 80 min and a drop dilution assay carried out (Figure 34).

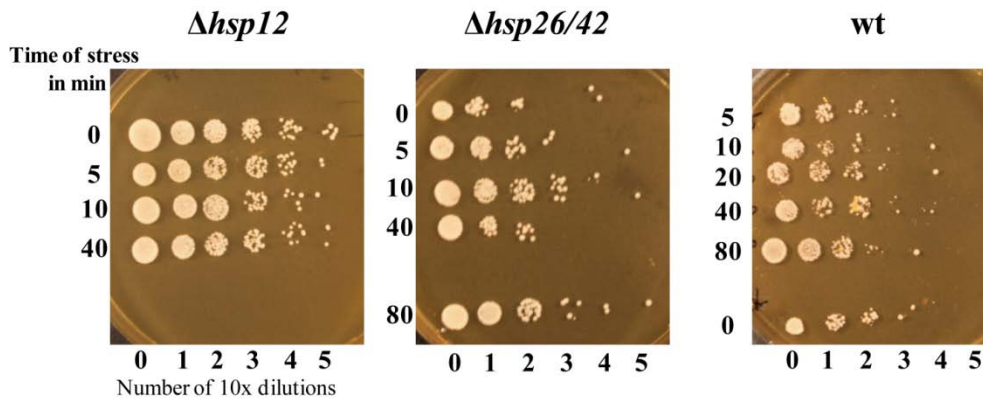


Figure 34 Survival assay of $\Delta hsp12$, $\Delta hsp26/42$ and wt yeast under mild heat stress. Log-phase cultures grown at 25°C were shifted to 37°C and 10x dilution series were prepared at the indicated times of stress. Cells were spotted on YPD-plates and incubated for three days to allow surviving cells to form colonies.

No growth phenotype after exposure to 37°C for up to 40 min could be detected for either strain. Therefore, disruption of *hsp12* or of the small heat shock protein system in *S. cerevisiae* does not render the cells more susceptible to mild heat shock.

Data normalization and selection of differentially-regulated genes was carried out as for the investigation of the transcriptional response of TF-KO strains (see chapter 4.4).

4.5.1 *Hsp26/42* deletion results in vast transcriptional changes

The deletion of the small heat shock protein genes *hsp26* and *hsp42* resulted in the differential regulation of 156 genes (2.7 % of the genome) for unstressed, 267 (4.7 %) for 5 min, 381 (6.7 %) for 10 min, and 268 (4.7 %) for 40 min of 37°C stress, compared to wt yeast treated identically (Table S5). Hence, the deletion mutant exhibited an altered transcriptome under permissive conditions, which was further augmented under temperature stress.

Gene regulation networks of differentially regulated genes

In a network analysis, as carried out by Papsdorf *et al.* (Papsdorf *et al.*, 2015), differentially regulated genes in the KO strain were separated into up- and down-regulated genes, and put to cluster analysis resulting in interconnected networks (Figure 35 & 36). This was carried out for 0 min and 10 min, since 5 min reflects the transcriptional state of 10 min, and 40 min is closer to unstressed control condition.

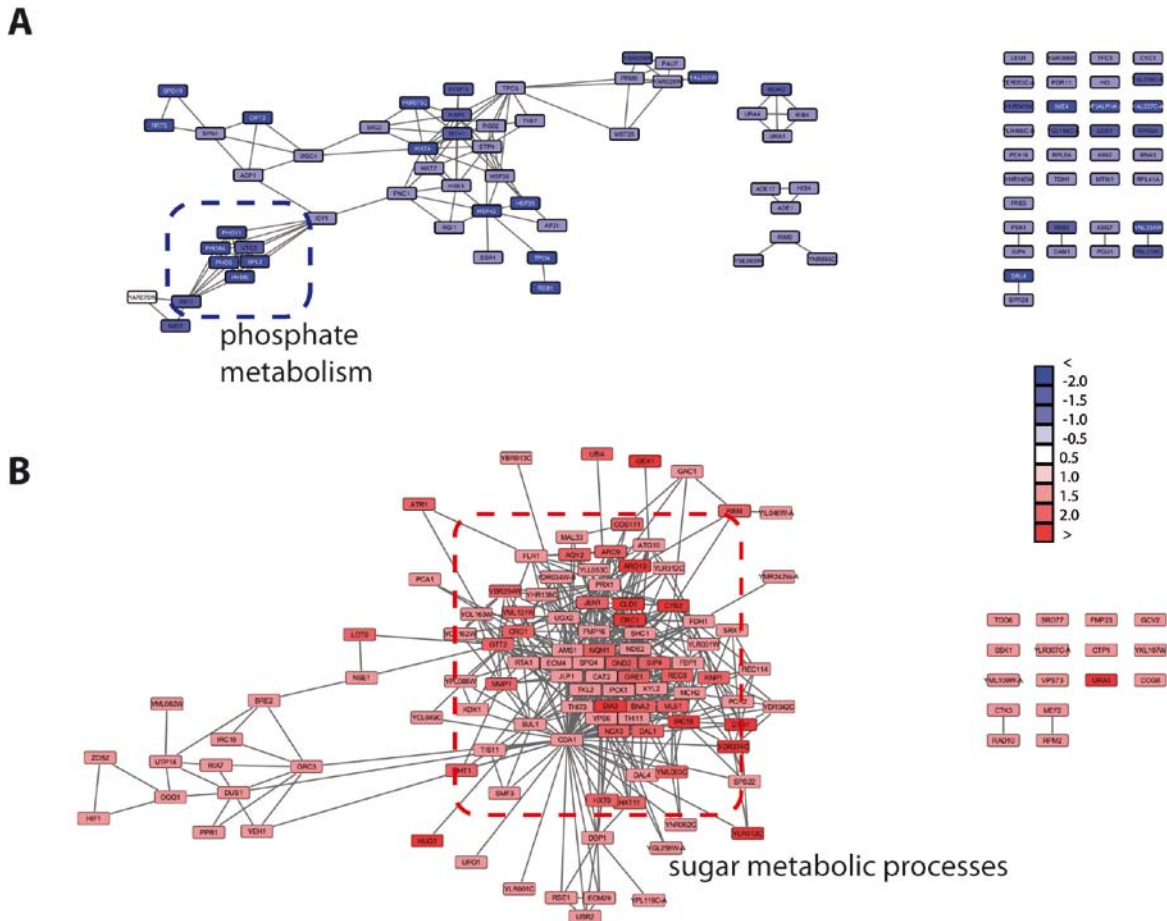


Figure 35 Networks of genes differentially regulated in $\Delta hsp26\Delta hsp42$ compared to *wt* under physiological temperatures. A: Network of down-regulated genes in the KO strain. B: Network of up-regulated genes. Detectable clusters are marked with a dashed box. Genes are colored stepwise according to their \log_2 ratios. The regulatory network was generated as described elsewhere (Papsdorf et al., 2015).

The networks for up- and down-regulated transcripts in the KO strain under physiological temperature where 156 genes were altered in their mRNA levels reveal that genes with reduced transcripts do not form clusters; and a large fraction of the hits actually cannot be integrated into the network at all. Only a small cluster for phosphate metabolism was identified, possibly indicating a phosphate imbalance in the double deletion strain (Figure 35A). On the side of up-regulated transcripts in the deletion strain, more genes are interconnected in the network. One cluster of genes involved in carbohydrate metabolic process can be identified, suggesting an increased energy metabolism in yeast (Figure 35B). To visualize the effects of heat stress, the same network analysis was carried out for 10 min of stress.

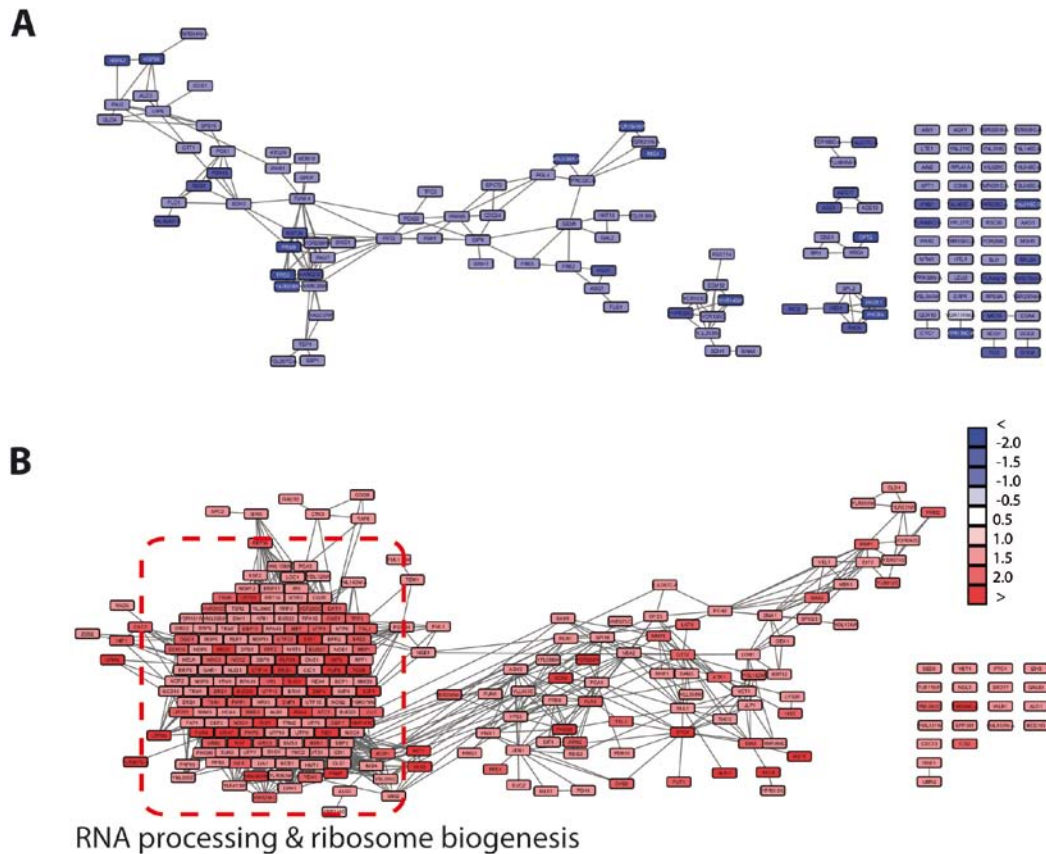


Figure 36 Networks of genes differentially-regulated in $\Delta hsp26\Delta hsp42$ compared to wt at 10 min of 37°C heat stress. A: Network of down-regulated genes in the KO. B: Network of up-regulated genes. A detectable cluster is marked with a dashed box. Genes are colored stepwise according to their \log_2 ratios.

After 10 min of heat stress, 381 transcripts differ by a factor of two in the sHsp-KO strain and again more are up-regulated in the KO strain than down-regulated. In the network of down-regulated transcripts, many genes were unable to be matched into the network, and only loose clustering of the genes is visible (Figure 36A). The regulation network of genes with higher mRNA levels shows one very prominent cluster, encompassing a large fraction of the differentially up-regulated genes after 10 min of heat shock. The GO term annotated to these genes, according to functional annotation of the DAVID database, is RNA-processing and ribosome biogenesis (Figure 36B).

Although the transcriptional down-regulation of genes encoding for ribosome synthesis is in common for wt yeast and the sHsp null mutant, the decrease of the mRNA-levels for the deletion strain is not as prominent. This means higher levels of messengers exist at 5 min and 10 min of heat shock, possibly indicating more ribosome assembly and perhaps even a higher level of protein biosynthesis.

UPS and autophagy are elevated in *Δhsp26/42* yeast

Since small heat shock proteins are capable of suppressing the aggregation of proteins under stress conditions, a closer investigation of selected biological processes was carried out. The UPS and autophagy systems were investigated because a lack of the sHsps as aggregations suppressors may result in enhanced accumulation of misfolded proteins in need of controlled degradation.

Ubiquitin proteasome system

Among the most prominent differences in transcript levels between the *Δhsp26Δhsp42* KO mutant and wt yeast, *ubi4* was found, which was enriched 1.73 log₂-fold in the deletion mutant. This suggests the possibility of an overall enhanced activity of the ubiquitin-proteasomal degradation system (UPS) in the absence of the two baker's yeast sHsps, which prompted an analysis of the transcript levels of 76 genes (see Table 18 for list of genes) of the UPS. The respective transcript levels were compared to those of wt yeast (Figure 37A, C).

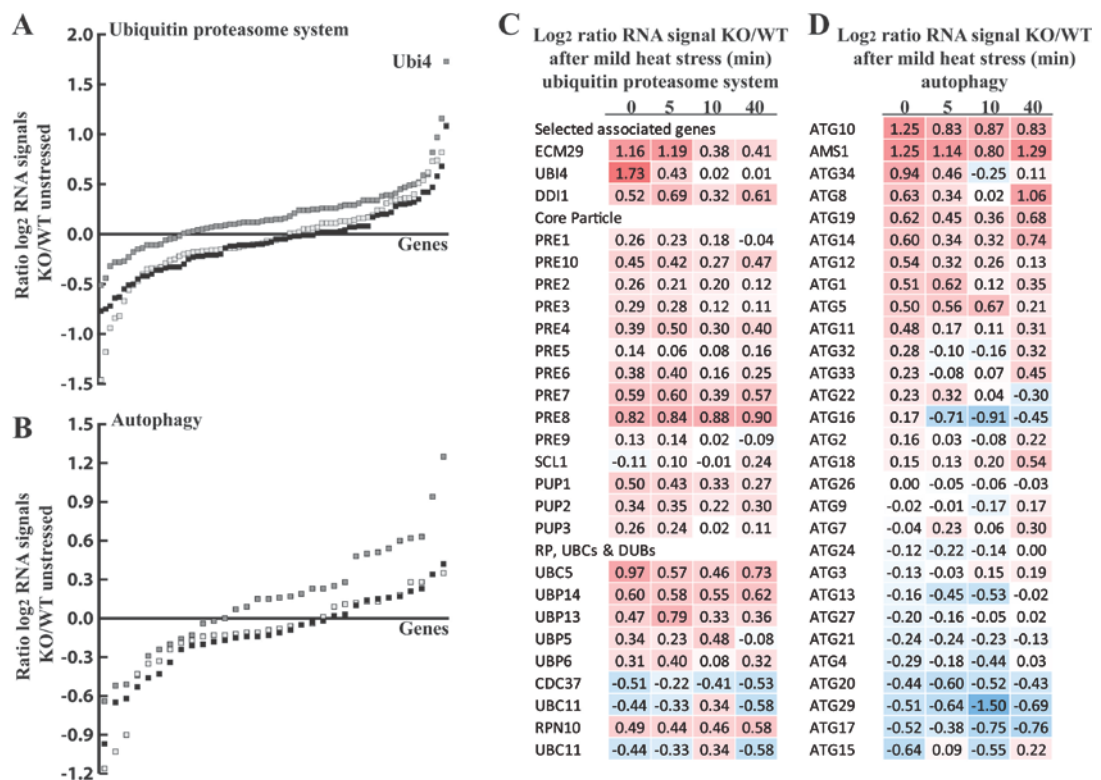


Figure 37 Elevated ubiquitin-proteasomal degradation machinery in *Δhsp26/42* baker's yeast.

A: Plot of the $\log_2 \frac{KO}{WT}$ ratios of the mRNA signals of 76 ubiquitin-proteasome related genes (grey) and comparison to two randomly selected lists of 76 genes (black & white). One square represents one gene. Red indicates enriched, blue diminished transcript levels in the KO strain (\log_2 ratio: -3 to +3). B: Same as in A, but with 34 autophagy related genes. C: \log_2 ratios $\frac{KO}{WT}$ over time

after mild heat stress (25°C → 37°C) for selected genes associated with proteasomal degradation with elevated or diminished levels in the KO strain. D: Same as in C with 29 autophagy related genes. Ubi4: Ubiquitin; RP: Regulatory Particle; UBCs: Ubiquitin Conjugating Enzymes; DUBs: De-ubiquitylases. (Figure legend continued from previous page).

In general, genes encoding for the proteasome core particle (*pre1*, *pre2*, *pre3*, *pre4*, *pre6*, *pre7*, *pre8*, *pre10*, *pup1*, *pup2*, *pup3*), as well as nine proteasomal degradation associated genes (e.g. *ecm29*, *hul5*), possess slightly elevated mRNA levels (Figure 37C), while only three are diminished compared to wt levels. In order to visualize this, the \log_2 ratios $\frac{\text{mRNA signal KO}}{\text{mRNA signal WT}}$ of all 76 UPS genes were plotted, and compared to the ratios of two sets of 76 randomly selected genes. While the random genes evenly distribute to positive and negative values (Figure 37A, black & white), the proteasomal genes in the null background shift towards higher values (Figure 37, grey). This means an increased number of the genes have elevated UPS transcript levels compared to wt yeast.

The kinetics of the transcriptional regulation of the deletion mutant compared to wt show that, over time, the initial discrepancies of UPS associated genes weaken. However, they remain slightly elevated for the entire examined time period up to 40 min (Figure 37C). This suggests increased levels of ubiquitylated proteins and perhaps also higher proteasomal degradation activity under permissive conditions in the sHsp double deletion strain in order to maintain proteostasis. In this context, thermal stress would activate the UPS in the wt, which is already activated in the sHsp deletion strain, and it leads to fewer discrepancies between KO and wt UPS transcript levels under heat stress.

Because genes involved in the UPS indicated an elevated activity and the *ubi4* locus was among the most prominent elevated transcript levels in the *hsp26-hsp42* double null mutant, cell lysates of wt, single sHsp, and double-deletion strains were probed directly for Ubi4, mono- and poly-ubiquitylated protein conjugates (Figure 38).

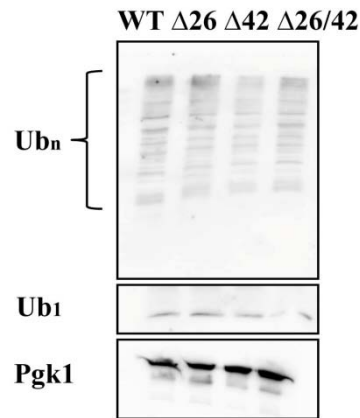


Figure 38 Immunoblot for ubiquitin-levels in S. cerevisiae wt and sHsp-deletion mutants. Clarified cell lysates of wt and sHsps deletion mutant were probed for free ubiquitin (Ub₁) and mono- or poly-ubiquitinated conjugates (Ub_n). Yeast 3-phosphoglycerate kinase (Pgk1) served as loading control.

Neither in the *hsp26* and *hsp42* single deletion strain nor in the *hsp26-hsp42* double knockout strain were detectable increases in free ubiquitin (Ub₁) and mono- or poly-ubiquitinated protein (Ub_n)-conjugates obtained. On the mRNA level a 3.3-fold higher signal was present in the sHsp-double KO strain, with a mean mRNA signal of 5,470 in the double mutant and 1,650 in wt *S. cerevisiae*. Hence, the changes on mRNA level could not be transferred to the protein level in this specific case, or the differences on the protein level were so subtle that they are not measurable by simple immuno-blotting.

Autophagic system

Next to proteasomal degradation, autophagy is part of the tripartite proteostasis system. Therefore, the same analysis as described above for the UPS was carried out for genes involved in autophagy (Figure 37B, D). For the 33 autophagy related genes, the \log_2 ratios $\frac{\text{mRNA signal KO}}{\text{mRNA signal WT}}$ were plotted and compared to the ratios of two random selections of an equal number of genes. Here too, deletion of the two sHsps gives way towards slightly elevated transcript levels of autophagy-related genes. These differences are maintained over the entire course of the experimental setup.

In summary, gene regulation indicates slightly up-regulated autophagy and UPS in $\Delta hsp26\Delta hsp42$ *S. cerevisiae*. However, initial investigations on the degree of ubiquitinylation of proteins did not display accumulation of free ubiquitin or conjugated proteins. This is in accordance with the data of the proteome stress sensors, where Fluc-GFP reporters indicated only a weakly elevated level of proteome stress (see chapter 4.21).

The most significant change of having higher transcript levels of ribosome biosynthesis and RNA processing was also present in the transcription factor deletion strains.

4.5.2 *Hsp12* deletion affects ion homeostasis

In order to analyze effects of the disruption of *hsp12* (the most rapidly and highly up-regulated gene in wt yeast under thermal stress) on the gene regulation of baker's yeast, microarrays were utilized also. Again, the same data normalization and selection criteria were used as for the wt, TF-KO and $\Delta hsp26/42$ strains were used.

In the unstressed sample at zero time, 100 genes fall within the selection criteria, with 66 genes having higher and 34 possessing lower transcript levels in the KO strain (Table S6). After five minutes, 135 genes (2.4% of all genes) show a two-fold increase or decrease in transcript level, 168 (2.9%) do so at 10 min, and after 40 minutes, this number falls to 116 (2.0%). Hence, *hsp12*-disruption, in general, has less influence on the yeast transcriptome under physiological and stress conditions compared to the *sHsp*-double deletion strain, affecting only up to 3% of all yeast genes at any given point in time of the experimental setup.

GO analysis of differentially regulated genes


Table 24 GO analysis of the differentially regulated genes in $\Delta hsp12$ yeast at physiological conditions.

Genes with a ≥ 2 -fold change of mRNA level in the KO strain compared to wt level were submitted to GO analysis using the DAVID funcat tool. The most significant GO terms of identified clusters are listed with GO ID, GO term, number of genes identified within the term, EASE enrichment score and p-value. Significance: $p < 0.01$

GO ID	GO term	# genes identified in cluster	Enrichment score	p-value
GO:0006879	Cellular iron ion homeostasis	8	4.80	<0.000001
GO:0006811	Ion transport	18	4.80	<0.000001
GO:0031224	Intrinsic to membrane	39	3.39	0.000062
GO:0015749	Monosaccharide transport	4	1.60	0.007309

A GO analysis, clustering genes to cellular components, biological processes or molecular function, revealed an over-representation of genes involved in 'ion transport', 'cellular iron ion homeostasis', 'intrinsic to membrane', as well as in 'monosaccharide transport' (Table 24). Genes involved in ion homeostasis (*gex1*, *ccc2*, *fet5*, *tpo2*, *jen1*, *fre1*, *ctr3*, *pho84*, *aqr1*, *fre7*, *enb1*, *ctr1*, *tpo3*, *opt2*, *fre5*, *fit1*, *arn1*, *fre4*, *fit2*, *fit3*) include many copper and iron uptake genes localized to the cellular membrane and cell wall. These include

siderophore-iron-chelate transporters and glycosylated proteins, anchored in the cellular membrane, that function in retaining siderophore-iron. The characteristic of these genes, encoding for proteins localized to the membrane, also explain why the term ‘intrinsic to membrane’ is over-represented.

Table 25 Heat map of the transcript levels of genes involved in iron homeostasis in *S. cerevisiae*. Listed are the ratios of the transcript levels of the respective genes in the KO vs. wt on the \log_2 scale. Color code is 0  4<.

Difference in RNA level of $\Delta hsp12$ strain compared to wt (\log_2 scale)									
Gene Symbol	Time of stress in min				Gene Symbol	Time of stress in min			
	0	5	10	40		0	5	10	40
ARN1	1.70	2.23	2.22	2.55	FMP23	1.22	1.19	0.77	0.60
ARN2	2.70	3.36	3.54	3.41	FRE3	1.50	1.26	0.88	1.03
CCC2	1.16	1.37	0.82	1.20	FRE4	1.34	3.05	2.53	0.64
DDR2	1.97	1.08	0.29	1.63	FRE5	2.05	2.06	1.15	1.74
ENB1	1.83	1.98	1.48	1.86	HMX1	1.80	2.91	2.55	2.63
FIT1	1.49	1.77	2.30	2.10	TIS11	2.44	2.88	1.27	2.83
FIT2	2.26	2.39	1.37	0.72	YLR126C	1.06	0.76	0.66	0.86
FIT3	1.96	1.80	1.43	1.16					

In a heat map that displays the difference in transcript level between the $\Delta hsp12$ knockout and wt *S. cerevisiae* for the genes involved in iron ion homeostasis, the transcript levels for all listed genes is higher in the KO. Therefore, disruption of the *hsp12* locus results in elevated transcript levels of iron uptake proteins, indicating an imbalance in iron homeostasis (Table 25).

Kinetics of gene regulation in heat shocked $\Delta hsp12$ yeast

To investigate potential differences in heat-induced transcription over time, the fold-changes in gene regulation of the KO yeast were plotted against the fold-changes of wt yeast (Figure 39).

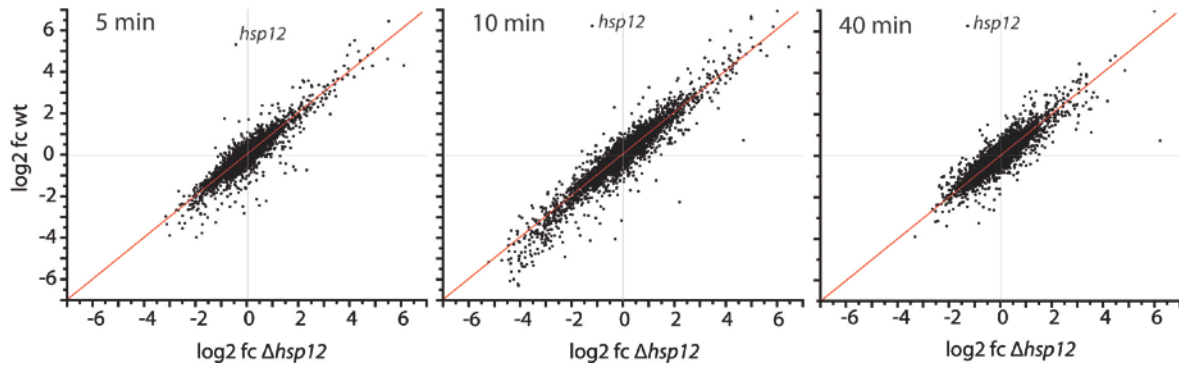


Figure 39 Gene regulation in the hsp12-deletion strain compared to wt yeast.

Yeast was exposed to 37°C stress and RNA levels determined for time points 5, 10 and 40 min by microarrays. Fold-changes versus unstressed zero time were calculated, the mean value for three biological replicates determined, and log₂-transformed. Genes lying below a mean RNA-MAS5 signal of 30 were omitted from the analysis. Left: Fold-changes of gene regulation of $\Delta hsp12$ yeast plotted against wt yeast after 5 min of 37°C. Middle: Gene regulation of $\Delta hsp12$ vs. wt yeast after 10 min of heat stress. Right: Gene regulation of $\Delta hsp12$ vs. wt yeast after 40 min of heat shock.

Comparing the transcriptional regulation over time of $\Delta hsp12$ under temperature stress to that of wt yeast, genes with differential regulation in the KO exist. Deviations from the diagonals in the plots point out differentially regulated genes (Figure 39). Forty-eight genes show stronger down-regulation in the wt compared to $\Delta hsp12$ yeast at 5 min of stress, and 132 do so at 10 min, where more points located in the bottom left of the diagram deviate from the diagonal of the coordinate system. Another 30 minutes later, these deviations are reduced in number to 60, and the gene regulation of the KO strain again resembles the wt more. Of these genes with different regulation in the KO strain, GO analysis reveals, ‘ion transport’, ‘membrane-associated’ terms, and ‘ribosomal biogenesis’ as enriched processes (Table 26).

Table 26 GO analysis of genes with differential kinetic regulation in $\Delta hsp12$ compared to wt yeast. Genes with differential \log_2 -fc values above 1 or below -1 in the $\Delta hsp12$ strain were submitted to the analysis. GO terms from enriched clusters are listed with their ID, name, number of identified genes in the cluster, EASE enrichment score and p-value. The DAVID functional annotation tool was used (<https://david.ncifcrf.gov/>) for the analysis. Level of significance: $p < 0.05$

GO ID	GO term	# genes identified in cluster	Enrichment score	p-value
5 min				
GO:0006811	Ion transport	7	2.34	0.005800
GO:0005886	Plasma membrane	13	2.34	0.000006
GO:0055085	Transmembrane transport	7	1.74	0.014000
10 min				
GO:0042254	Ribosome biogenesis	28	5.19	<0.000001
GO:0006364	rRNA processing	20	5.19	0.000001
GO:0009266	Response to temperature stimulus	14	1.94	0.000764
GO:0051540	Metal cluster binding	5	1.87	0.001683
40 min				
GO:0046914	Transition metal ion binding	16	2.73	0.000716
GO:0031225	Anchored to membrane	4	1.73	0.011659
GO:0006811	Ion transport	8	1.57	0.005620

In the kinetic response to heat, *hsp12*-KO yeast exhibits gene regulation different from the wild type in ion transport or, more general, in transmembrane transport, which has already been the case in permissive conditions. At the maximum of the transcriptional response to heat at 10 min, genes differentially regulated in the KO cluster to processes involved in rRNA-processing and ribosome biogenesis, which has also been the case for the sHsps-KO yeast under stress (see Figure 36B). After 40 min, GO terms associated with membranes or ion homeostasis are the most enriched of the biological processes or cellular components.

4.6 Proteomic investigations on *S. cerevisiae* under heat shock

The transcriptional reprogramming of *S. cerevisiae* to changes in ambient temperature is only one aspect of the stress response, since they merely serve as proxies for the actual biomolecules carrying out the protective functions and reactions: the proteins. By means of a combination of metabolic labeling and mass spectrometry analysis, the influence of two heat shock temperatures on the proteome and phospho-proteome of baker's yeast was to be investigated, and the correlation to the transcriptomic changes assessed. As carried out for the transcriptional investigation, two heat-shock scenarios were investigated: a mild heat shock, shifting cells from 25°C to 37°C, and a sub-lethal heat shock, transferring yeast from 25°C to 42°C. In a first experimental setup, the selected duration of stress was 10 min, representing the time of maximum transcriptional heat shock response. Because translation is a tightly regulated and slower process compared to RNA synthesis, a time of 30 min was chosen, to allow the transcriptional response to manifest itself on the protein level.

To investigate the influence of heat stress on the proteome, a stable isotope labeling with amino acids in cell culture approach was applied (Cox and Mann, 2008). In principle, yeast cultures were grown overnight at 25°C in medium containing heavy atom labeled amino acids (R0/K0, R6/K4 or R10/K6) to allow for a full incorporation into the proteome. Fresh, labeled medium was inoculated with these overnight cultures and cultivated for eight hours into the mid-logarithmic growth phase (see chapter 3.13). A label-swapping approach was carried out to allow for the analysis of three biological replicates. The investigation of the proteome and phospho-proteome was carried out in collaboration with the chair of Prof. S. Sieber from the Department of Organic Chemistry II of the TUM, Germany.

4.6.1 The cellular proteome after 10 min of heat stress

An initial SILAC-MS investigation of the proteome and phospho-proteome after 10 min of thermal stress allowed the quantification of 2,462 proteins for 37°C and 2,457 for 42°C in all three replicates, covering approx. 42 % of the entire yeast proteome, with 5,917 proteins listed in the SGD as of October 2015. The number of identified class-1 phosphorylation (P-) sites, meaning sites with a localization probability >0.75, was near 2,000 for each replicate, however, the overlap between all three replicates was merely 1,304 for 37°C and 1,305 for 42°C, respectively (Figure 40).

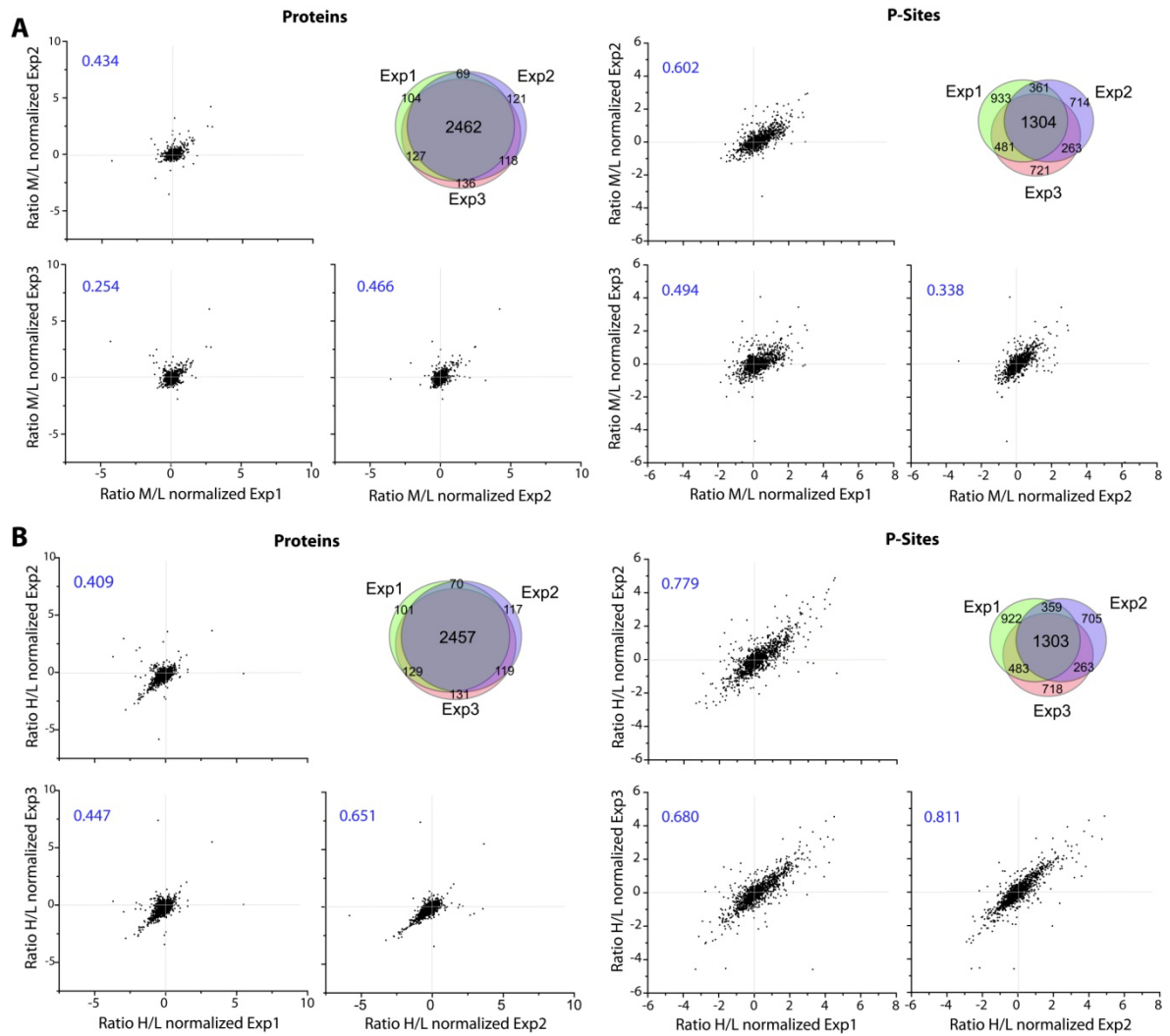


Figure 40 Number of quantified proteins and correlation of label swap replicates after 10 min of heat shock.

A: Mild heat shock (25 \rightarrow 37°C). Left: Correlation of protein ratios of label-swapped replicates. The number of quantified proteins and the overlap in the replicates is shown in the Venn-Diagram. The Pearson's r correlation coefficient between the replicates is noted in blue. Right: Number of identified class-I phosphorylation (P-) sites and correlation between label swapped replicates. B: Sub-lethal heat shock (25 \rightarrow 42°C). Quantified proteins, class-I P-sites and correlation between replicates displayed as in A. For ratios L=25°C, M=37°C and H=42°C. Exp1, Exp2 and Exp3 are the replicates with label-swap.

Incubation of baker's yeast for 10 min of 37°C yielded a vast and swift transcriptional response, but had only very limited effect on the proteome. The \log_2 ratios of the proteins after heat shock compared to unstressed cells (M/L) gather close to the origin of the coordinate system and are indicative of very little fold-changes in the protein amounts. To assess the quality of the data, correlation statistics was carried out. The correlation coefficients r between the ratios of the three label swap-replicates, calculated according to (Pearson, 1895), are 0.254, 0.434 and 0.466, and, hence, display a weak positive

correlation. Label-swap replicates were used because they allowed for the simultaneous mass-spectrometry analysis of three independent biological replicates. For the quantified 1304 class-1 P-sites correlation is slightly stronger, yet still also weak with coefficients of 0.338, 0.494 and 0.602 between replicates. Additionally, more of the identified P-sites show ratios with higher or lower values compared to the changes on the protein level (Figure 40A). At 42°C, r-values are 0.409, 0.447 and 0.651, suggesting moderate positive correlation between label-swap replicates. The ratios between stressed and unstressed protein levels (H/L) cluster primarily around the origin of the coordinate system but also display a tailing towards the bottom left, indicative of a reduced amount of these proteins after 10 min of sub-lethal heat stress. This is in contrast to mild heat shock, where this tailing towards negative ratios is not as prominent. The correlation between the 1,303 class-1 P-sites quantified after 10 min of 42°C stress is strong and positive with r-values at 0.680, 0.779 and 0.811. Also, the ratios which show tailing towards higher and lower values, suggest a stronger regulation of the *S. cerevisiae* heat shock response on the phospho-proteome when exposed to 42°C compared to 37°C (Figure 40B).

10 min of mild heat shock has only little effect on the proteome

Submitting wt baker's yeast to 37°C for the short period of 10 min elicited very little effect on the cellular proteome. Only 28 proteins were found to be enriched and no protein showed two-fold reduction at the selected threshold of a two-fold increase- or decrease and the criteria that the direction of change was to be the same in all three replicates (Table S7). Many of the molecular chaperones are found among the proteins (Hsp82, Hsp12, Ssa4, Ssa3, Hsp78, Hsp104, Hsp42, Fes1) thus chaperones are among the first proteins to be synthesized under heat stress, demonstrating their importance in cellular proteostasis under heat shock. Along with the other 20 proteins the biological process 'response to temperature stimulus' is the most enriched GO term with a score of 9.47, followed by 'protein catabolic process' with a score of 3.23 and 'protein folding' with a low score of 1.82 (Table 27).

As stated above in the correlation plots, 10 min stress of 42°C results in a different picture: Here, merely four proteins (Tma10, YPR036W, Ssa4 and Gnp1) are two-fold enriched, most likely as a result of less ribosomal protein biosynthesis at this high temperature. On the other hand, 58 proteins were quantitated to a two-fold lower extent after the short 42°C stress (Table S7). Nuclear proteins involved in 'ribosome biogenesis' and 'RNA processing' are enriched with a score of 12.96, and 'ribosome assembly' with a score of

4.33 (Table 27). Next to the decreased ribosomal activity at elevated temperatures, the reduction in these proteins involved in ribosome biogenesis may explain why fewer proteins have elevated levels under sub-lethal heat stress compared to mild heat shock.

Table 27 GO analysis of enriched or diminished proteins and P-sites after 10 min of heat shock in baker's yeast.

The GO functional annotation database (DAVID) was used to identify enriched GO terms. Listed are enriched GO terms, the number of proteins identified within the respective cluster, the enrichment score and p-value. For the analysis of P-sites, the respective proteins were put into the GO analysis.

GO-ID	GO-Term	# of proteins identified	Enrichment score	p-value
Enriched proteins 10 min 37°C				
GO:0009266	Response to temperature stimulus	16	9.47	<0.0000001
GO:0030163	Protein catabolic process	8	3.23	0.00139500
GO:0006457	Protein folding	7	1.82	0.00000954
Diminished Proteins 10 min 42°C				
GO:0042254	Ribosome biogenesis	28	12.96	<0.0000001
GO:0006396	RNA processing	26	12.96	<0.0000001
GO:0042255	Ribosome assembly	9	4.22	0.00000036
Proteins with enriched diminished P-sites 10 min 37°C				
GO:0005991	Trehalose metabolic process	4	1.90	0.00010800
GO:0007039	Vacuolar protein catabolic process	5	1.90	0.02051000
Protein with diminished P-sites 10 min 42°C				
GO:0051301	Cell division	35	12.47	<0.00000001
GO:0000902	Cell morphogenesis	18	9.53	0.00000215
GO:0051726	Regulation of cell cycle	21	1.92	0.00000023

Influence of 10 min heat stress on protein phosphorylation

Phosphorylation of serine, threonine, and tyrosine residues is one type of post-translational modification of proteins that contributes to the regulation of protein function. Therefore, the SILAC-MS screen carried out here also encompassed the quantification of class-1 phosphorylation sites. Of the 1,304 quantified class-1 P-sites after 10 min of 37°C heat shock, 57 had a more than or equal to two-fold higher ratio of phosphorylation compared to unstressed cells, and only seven showed an increase in their de-phosphorylated state. These P-sites were distributed over 52 proteins (Table S8). A GO-analysis of the combined 64 proteins revealed two clusters: 'Trehalose metabolic process' and 'vacuolar protein catabolic process', both with an enrichment score of 1.90. In the case of 10 min 42°C heat shock, 148 P-sites with at least two-fold enrichment and 75 with at least two-fold reduction compared to unstressed control condition were found on 169 proteins. For these, the GO

analysis revealed biological processes of ‘cell division’ and ‘cell morphogenesis’, as well as ‘regulation of cell cycle’ as the most significant GO terms with enrichments scores of 12.47, 9.63 and 1.92 (Table 27). Hence, the main sites for phosphorylation and dephosphorylation under sub-lethal heat shock conditions are on proteins involved in cell proliferation.

4.6.2 The cellular proteome after 30 min of stress

A second SILAC-MS experiment with wt baker’s yeast exposed to heat for 30 minutes was carried out to analyze the cellular proteome and phospho-proteome after prolonged exposure to elevated ambient temperature. This experiment was able to quantify approximately 3,400 proteins in each replicate with a high overlap of 3,284 proteins for 37°C stress and 3,275 for 42°C in all three replicates. This high number of quantified proteins represents coverage of 55.5 % of all yeast proteins. In addition, the number of class-1 P-sites quantified in all replicates was nearly doubled to 2,617 for 37°C and 2,611 for 42°C compared to the 10 min dataset (Figure 41).

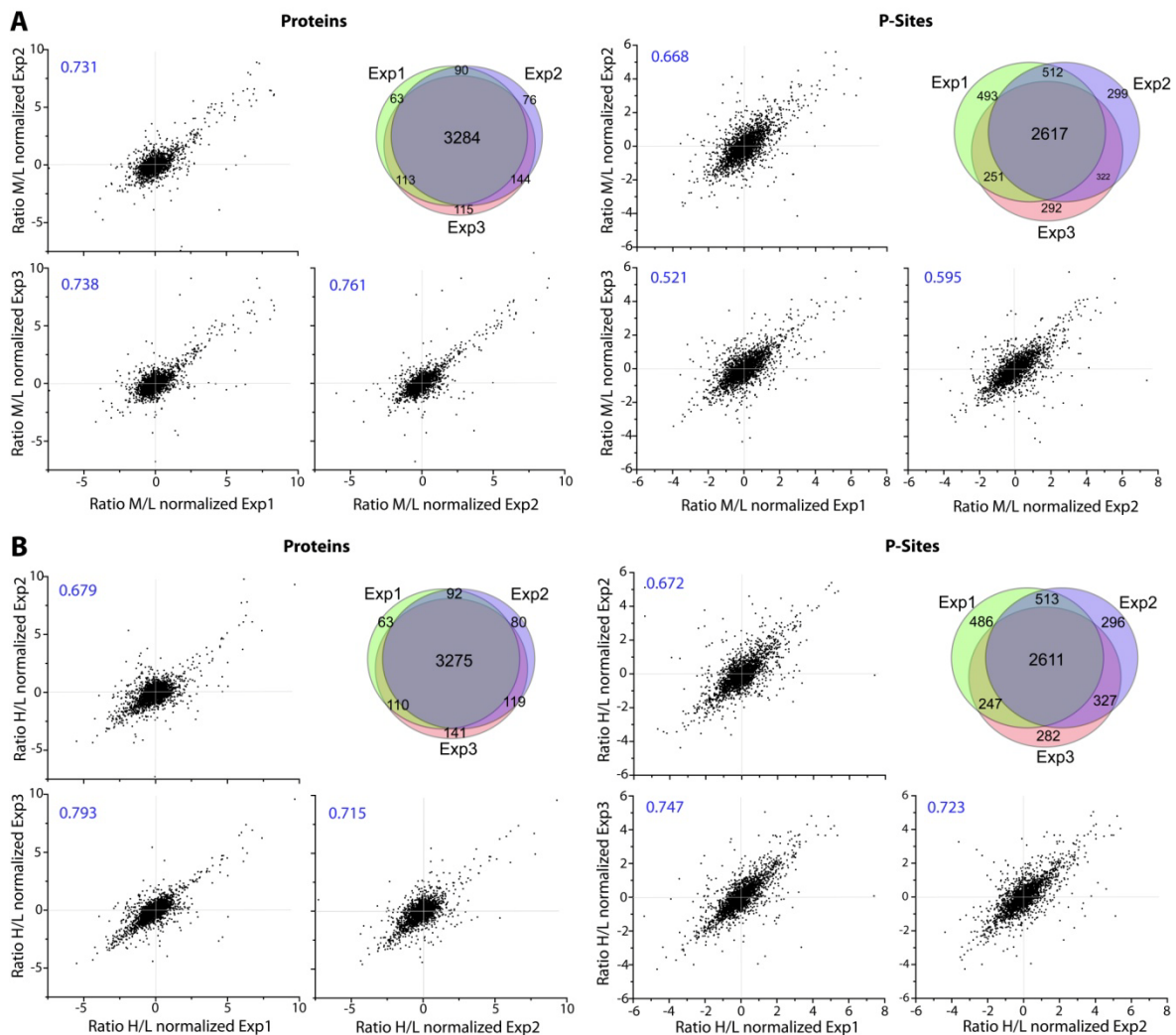


Figure 41 Number of quantified proteins and correlation of label swap replicates after 30 min of heat shock.

A: Mild heat shock (25 → 37°C). Left: Correlation of protein ratios of label-swapped replicates. The number of quantified proteins and the overlap in the replicates is shown in the Venn-Diagram. The Pearson's r correlation coefficient between the replicates is noted in blue. Right: Number of identified class-I phosphorylation (P-) sites and correlation between label swapped replicates. B: Sub-lethal heat shock (25 → 42°C). Quantified proteins, class-I P-sites and correlation between replicates displayed as in A. For ratios L=25°C, M=37°C and H=42°C. Exp1, Exp2 and Exp3 are the replicates with label-swap. (Figure on previous page).

In a quality assessment of the replicates, the calculated protein ratios of stressed cells compared to unstressed controls, Pearson's r -coefficients lie at 0.731, 0.738, and 0.761, indicating a strong correlation. The distribution of the \log_2 ratios in the correlation plots demonstrates a tailing towards the top right of the coordinate system, representing an increased protein amount after 30 min of 37°C treatment due to protein biosynthesis. For the P-sites, regulation goes in both directions, phosphorylation and de-phosphorylation, visible where the quantified P-sites distribute to both top right and bottom left in the correlation plot (Figure 41A). At 42°C of stress, correlations between the replicates lie above 0.679 and, hence, a strong positive correlation can be concluded. Here too, a fraction of the proteins is enriched in their levels with \log_2 ratios >1 indicating their heat stress induced biosynthesis. Sub-lethal heat stress for 30 min, as was the case for 10 min, again resulted in proteins with diminished levels in stressed yeast. The quantified P-sites also show a strong positive linear correlation with r -values >0.672 . As was the case for 37°C, P-sites with enriched and decreased phosphorylation compared to unstressed control exist with an even distribution towards higher and lower ratios (Figure 41B).

In conclusion, 30 min of heat stress exhibits more changes on the total proteome and phospho-proteome compared to a 10-minute stress. However, it must be noted that the overall higher number of quantified proteins and class-1 P-sites may contribute to the higher number of differential class-1 P-sites.

Investigations on proteins with heat-induced change in their quantity

In order to analyze which proteins are affected by heat shock, proteins that showed the same positive, strong correlation and showed a change in their quantity by at least two-fold in average were selected. For 30 min at 37°C, 149 proteins were enriched two-fold and 69 proteins showed a two-fold reduction in their quantity (Table S9). These hits were used to build a protein interaction network using the String-v10 database (Szklarczyk et al., 2015). The network was generated using annotated protein-protein interactions inferred only from

experimental evidence and with a high confidence score (>0.700) to minimize the probability of integrating false interactions into the network. For illustrative purposes, proteins that do not possess at least one interaction with another protein in the generated network are not displayed (Figure 42).

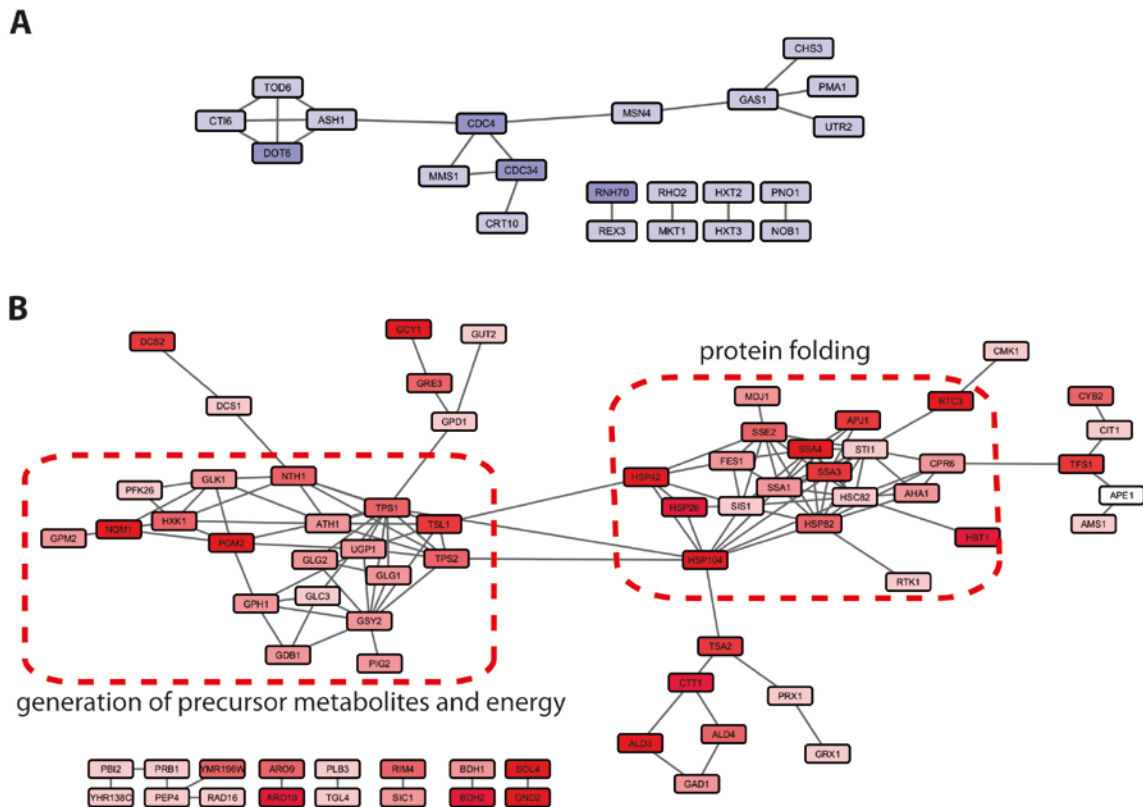


Figure 42 Protein networks of enriched and diminished proteins after 30 min of mild heat shock in baker's yeast.

Proteins that displayed changes in amount upon temperature stress were used to build an interaction network using the STRING-v10 database (<http://string-db.org/>) and selecting high stringency (>0.700) interactions inferred from experimental evidence only. The resulting networks were exported to cytoscape for color-coding of the nodes and visualization of the clusters. A. Interaction network of proteins with at least two-fold reduction after heat shock. B. Network of proteins enriched at least two-fold after 30 min of mild heat shock. Degree of enrichment of diminishment is color coded stepwise from $-4 >$ $4 <$ in 1-increment steps. Identified clusters according to the DAVID funcat tool (<https://david.ncifcrf.gov>) are marked with a box.

For the 69 proteins with diminished levels after 30 min of mild heat stress, 21 could be integrated into a network (Figure 42A), albeit with only a low number of edges between the protein nodes. Consequentially, no clusters within the proteins reduced in quantity can be identified. For the 149 proteins with enhanced levels, 76 proteins could be incorporated into a protein network (Figure 42B). Here, more edges, meaning protein-protein interactions, were identified. GO analysis revealed two clusters of biological processes to

be enriched. The first, protein folding, contains Hsp90-Hsp70-co-chaperone system, the sHsp-system, and the Hsp104 disaggregase. This is in accordance with the 10 min data, where the protein folding and refolding machinery was up-regulated on the protein level. Another cluster of proteins is involved in carbohydrate metabolism and is coined 'generation of precursor metabolites and energy'. The cluster also engulfs the enzymes of the trehalose system found after 10 min of mild heat shock.

All in all, 30 min of mild heat stress results in a specific biosynthesis of proteins of the molecular chaperone system, serving to protect the cell from heat induced unfolding of proteins. In addition, proteins involved in the production of molecules usable for the generation of energy are synthesized. Diminished proteins after 30 min of heat shock do not follow any recognizable pattern.

30 min of sublethal heat shock results in more diminished proteins

Treating yeast cells with the harsh 42°C stress has less effect on up-regulated proteins compared to 37°C stress. Ninety-three proteins were enriched two-fold or more in their cellular levels. Of them, 67 were also identified among the 149 enriched proteins after 30 min of mild stress (Table S10). These proteins cluster to protein folding processes and trehalose metabolic process, as visible in the protein network (Figure 43B). The 26 proteins enriched more than two-fold only in the 42°C dataset do not show any enriched GO terms.

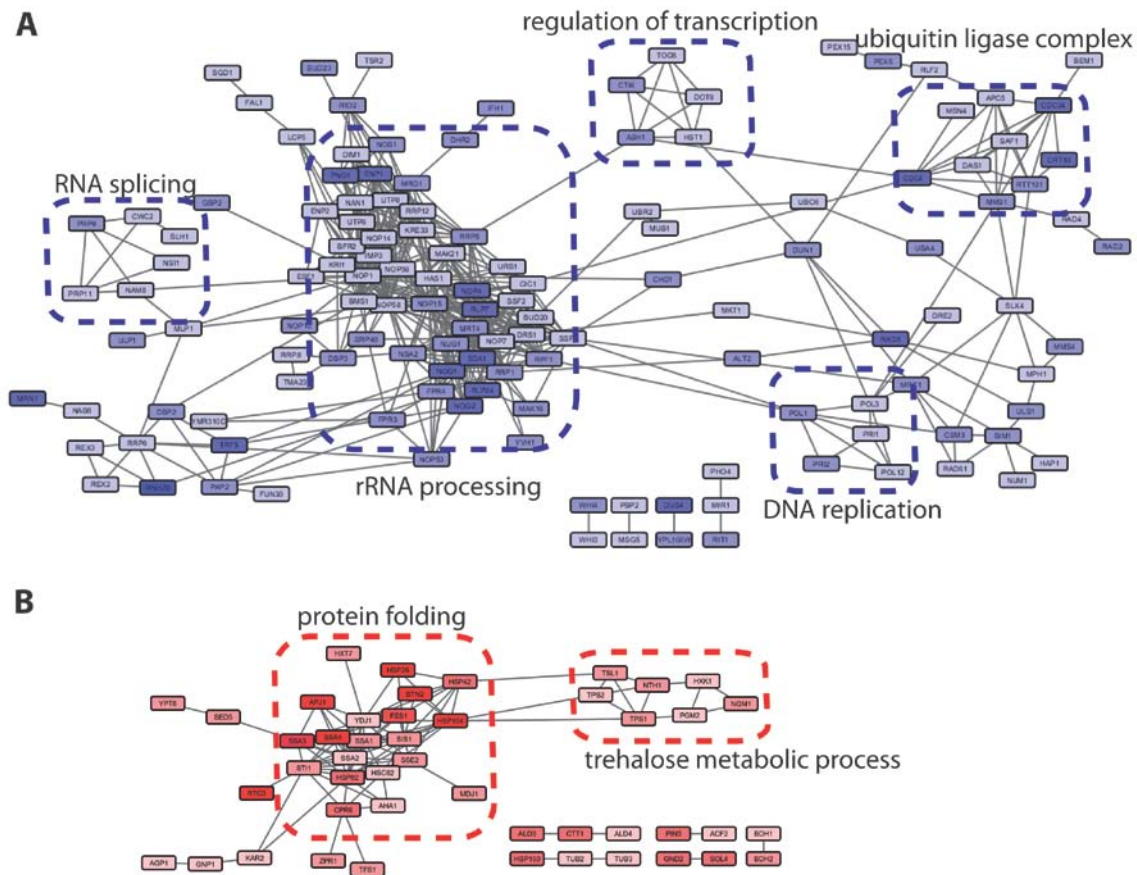


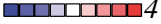
Figure 43 Protein networks for enriched and diminished proteins after 30 min of 42°C heat shock. Proteins that displayed changes in amount upon temperature stress were used to build an interaction network using the STRING-v10 database (<http://string-db.org/>) and selecting high stringency (>0.700) interactions inferred from experimental evidence only. The resulting networks were exported to cytoscape for color-coding of the nodes and visualization of the clusters. **A.** Interaction network of proteins with at least two-fold reduction after heat shock. **B.** Network of proteins enriched at least two-fold after 30 min of mild heat shock. Degree of enrichment of diminishment is color coded stepwise from >-4 (blue) to 4 (red) in 1-increment steps. Identified clusters according to the DAVID funcat tool (<https://david.ncifcrf.gov>) are marked with a box.

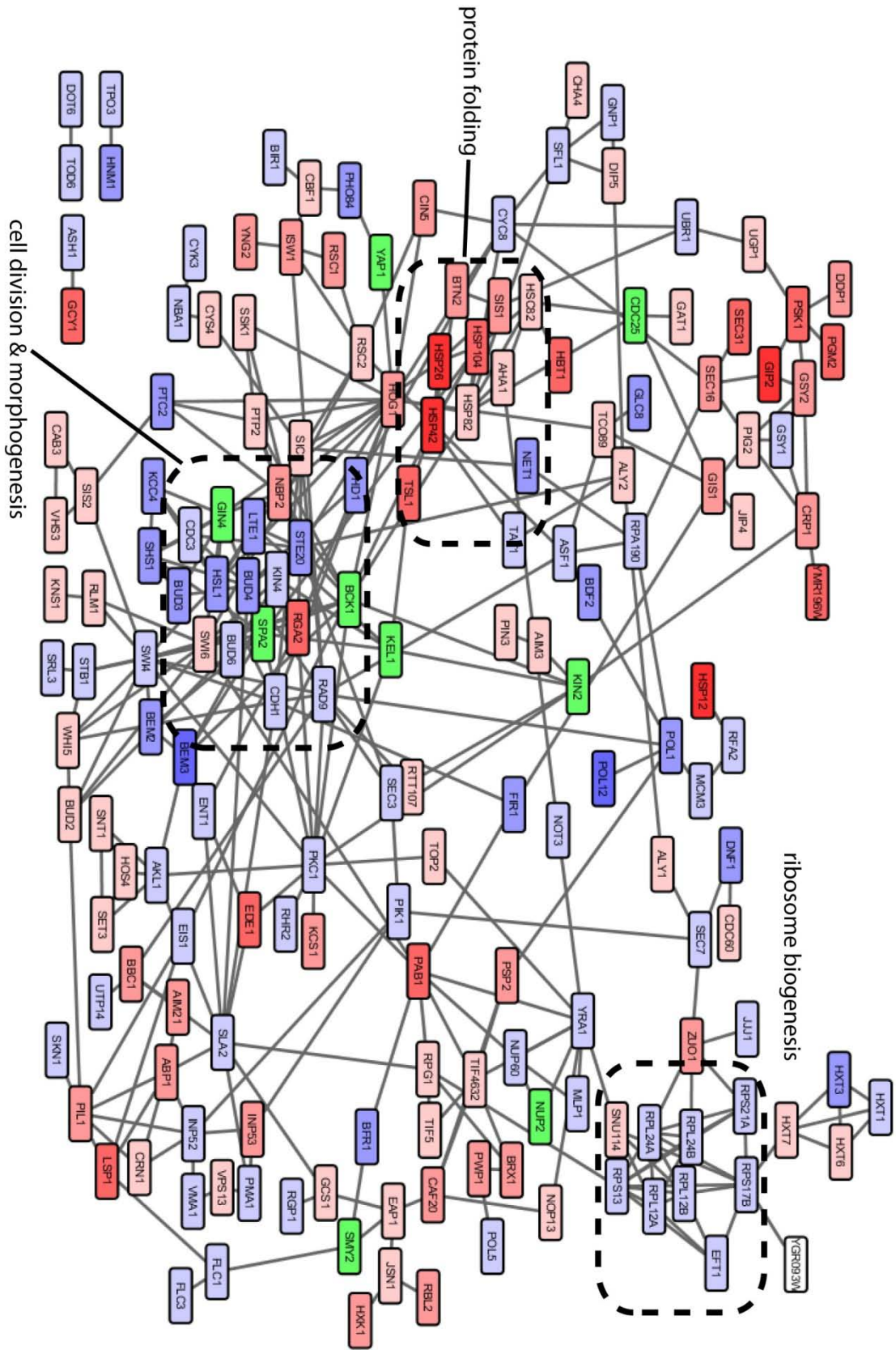
Prolonged sub-lethal heat shock affects the cellular proteome to a higher extent on the side of proteins with reduced levels. Two hundred twenty-four proteins were found to be decreased in their quantity by at least two-fold (Table S10). Twenty-nine of those were also found among the 69 proteins decreased after 37°C stress. Again, a protein network was generated to display any interactions among them and reveal clusters of proteins affected by 30 min sub-lethal heat shock (Figure 43). One cluster is made up of nine proteins that match up to an ‘ubiquitin ligase complex’, also involved in cell cycle regulation by targeting key substrates for degradation. The other four clusters also describe processes taking place inside the nucleus. Six proteins gather to a small cluster described

with the GO term ‘RNA-splicing’, and five proteins make up the cluster ‘regulation of transcription’. The third cluster with six proteins is ‘DNA-replication’. By far the most interactions are found between 54 proteins that make up a cluster with the term ‘rRNA-processing’. Hence, 30 min of sub-lethal heat stress results in a reduction of proteins that contribute to the processing of primary ribosomal RNA into mature rRNA. These terms were also among the enriched terms in the transcriptional response of baker’s yeast.

Influence of 30 min heat stress on the phospho-proteome


30 min of 37°C yielded 383 quantified P-sites with a two-fold decrease or increase in their phosphorylation state compared to untreated control conditions when applying the same selection criteria for class-1 P-sites as for the dataset after 10 min of 42°C heat stress. Of these P-sites, 165 P-sites were reduced in their ratios, meaning they were de-phosphorylated after heat shock and 218 possessed a heat-induced increase in their phosphorylation state. All 383 P-sites are distributed over 259 different proteins (Table S11). The severe heat shock of 42°C for 30 min elicited more class-1 P-sites: 195 P-sites with a decrease in their phosphorylation state and 408 with an increase. This resulted in combination in 603 identified P-sites within the borders of the selection criteria applied. These P-sites are localized on 305 different proteins (Table S12). In order to gain insight into which biological processes are regulated by means of (de-) phosphorylation, proteins with identified P-sites were used to create a protein interaction network, using the STRING10-database. As was the case for the total proteome networks described above, protein-protein interactions were inferred from experimental evidence only, with a high confidence score of >0.700. This enabled a graphical representation of interconnected cellular processes after 30 min of mild or sub-lethal heat shock (Figure 44 & 45).

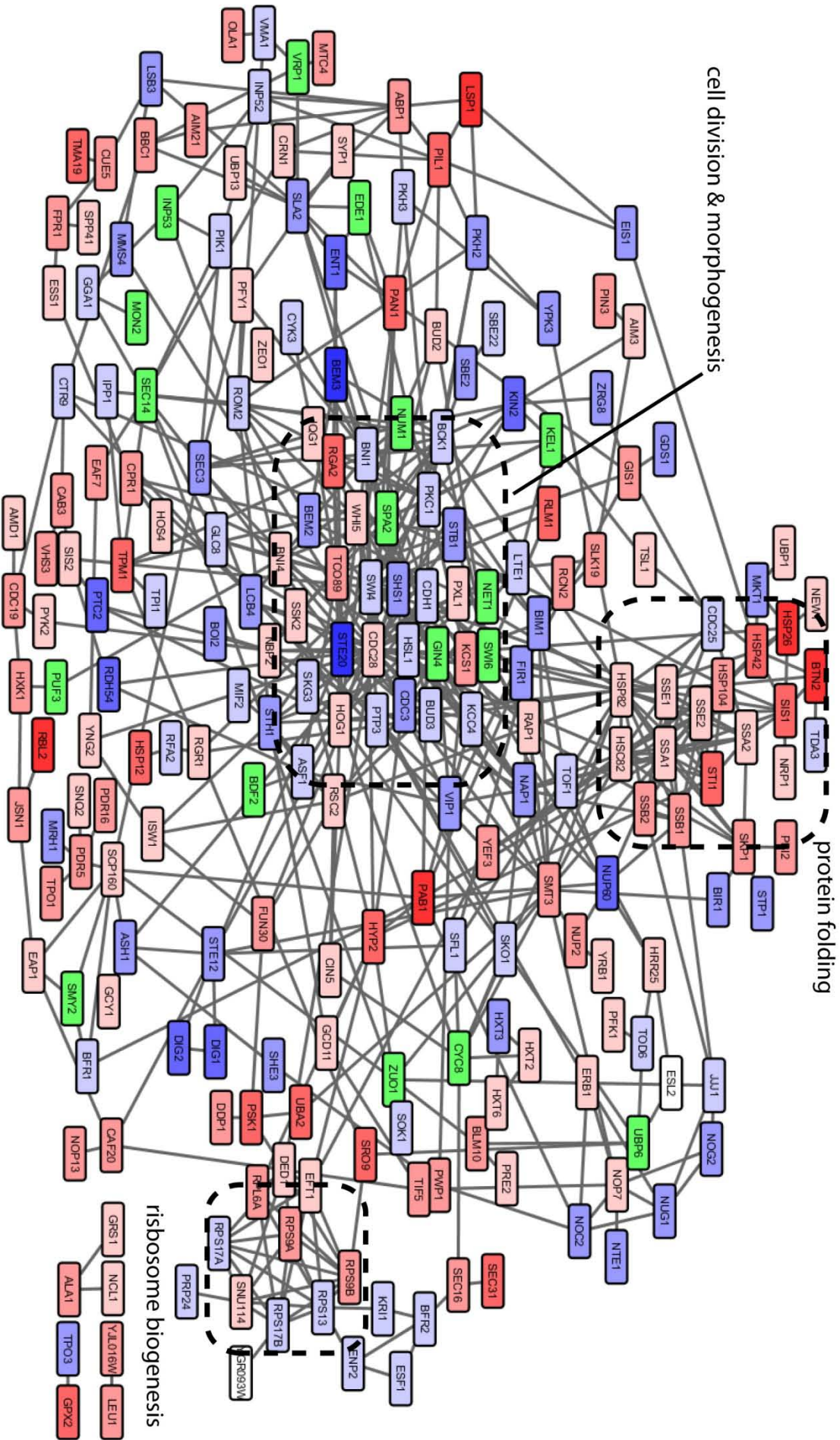
Figure 44 Interaction network of proteins with differentially regulated P-sites after 30 min of 37°C. Proteins with a two-fold increase or decrease in their phosphorylation state in all three replicates were selected. The network was generated using the STRING-v10 db (experimental evidence, high stringency score >0.700). Illustration was carried out in Cytoscape. Interaction between proteins is indicated with edges. Nodes are color coded in a 1-increment fashion, with blue indicating decrease and red showing an increase in phosphorylation state of the protein >-4  $4<$. In the case of multiple P-sites for a protein, the P-site with the highest fold change was used for coloration. Proteins containing P-sites with both directions of change in the phosphorylation state are colored green. Clusters of genes are marked with a black box. (Figure on next page).



Of the 259 proteins with differential P-sites after 30 min of 37°C, 169 could be mapped into the protein network (Figure 44). For illustrative purposes, proteins without at least one interaction partner in the network are not displayed. While many proteins were found to be differentially phosphorylated, a rather loose network is obtained, visible with only a low degree of clustering of the nodes in the protein network. Nonetheless, three clusters of genes were identified: The first cluster is localized in the top right corner and is composed of nine proteins, seven of which are ribosomal subunits. These proteins show a heat induced increase in their de-phosphorylated state and are best described with the GO term ‘ribosome biogenesis’. The second cluster contains proteins of the molecular chaperone system, in particular: the two yeast Hsp90 proteins (Hsp82, Hsc82), the two sHsps (Hsp26 and Hsp42), the disaggregase Hsp104, a few co-chaperones of the Hsp90-Hsp70 system (Aha1, Sis1), along with a subunit of the trehalose synthesis machinery (Tsl1). All members of this group show a strong increase in their phosphorylated state. ‘Protein folding’ is the GO term that describes this cluster of genes. The third cluster involves 17 proteins that contribute to cell division and morphogenesis. Most of the proteins here possess a higher percentage of de-phosphorylation after stress or have multiple P-sites with opposing characteristics regarding their phosphorylation state. In conclusion, regulation by a change in the phosphorylation pattern affects the same biological processes that showed a heat-induced accumulation or reduction in proteins.

Of the 218 proteins with a change in total protein quantity after 30 min of mild heat shock, 45 proteins (20.8%) also possessed differential phosphorylation. Thirty-six are among the 149 proteins enriched in level, nine among the 69 proteins quantified with an at least two-fold lower abundance. Hence, 24.2% of proteins enriched on the total protein level also possessed differential phosphorylation, and only 13.4% of the proteins with diminished levels did so.

Figure 45 Interaction network of proteins with differentially regulated P-sites after 30 min of 42°C. Proteins with a two-fold increase in decrease in their phosphorylation state in all three replicates were selected. The network was generated using the STRING-v10 db (experimental evidence, high stringency score >0.700). Illustration was carried out in Cytoscape. Protein interactions are indicated by edges. Nodes are color coded in 1-increment steps, with blue indicating decrease and red showing an increase in phosphorylation state of the protein >-4  4<. Where there are multiple P-sites for a protein, the P-site with the highest fold-change was used for coloring. Proteins with P-sites with both directions of change in the phosphorylation state are colored green. Clusters of genes are marked with a black box. (Figure on next page).



The phospho-proteome after 30 min of sub-lethal heat shock

The interaction network of proteins with differential phosphorylation after 30 min of 42°C stress, basically reflect the network obtained for mild heat shock. Even though more proteins could be integrated in the network, the same three clusters of ‘ribosome biogenesis’, ‘protein folding’ and ‘cell division and morphogenesis’ show up (Figure 45). This time the protein folding machinery also contains the cytosolic Hsp70 proteins (Ssa and Ssb) that exhibit more phosphorylation after stress. The identified subunits of the ribosome are different from those found under mild heat shock condition and show a bidirectional phosphorylation pattern. This may be due to the stringent selection criteria of a two-fold change in P-state, where proteins lying just marginally below this threshold are not included in the analysis. This also why the Hsp70 proteins are not found in the protein network at 37°C: They lie just below a two-fold increase in P-state. For example, Ssa1_T416, Ssa3_T416, Ssa4_T417 possess an increase of 1.87 fold. The cluster of proteins for ‘cell division and morphogenesis’ contains more proteins compared to mild heat shock.

High temperature does lead to cell cycle stop (Johnston and Singer, 1980; Kühl and Rensing, 2000). Perhaps this suggests that under severe heat shock a condition, *S. cerevisiae* achieves a cell cycle arrest more readily, compared to heat shock at lower temperatures. A high number of proteins could be integrated into the interaction network, nevertheless they do not cluster to any specific process, but rather are loosely connected to only a few other nodes. This also demonstrates that heat stress elicits changes in the phosphorylation state of diverse proteins involved in various cellular processes and pathways.

Of the 305 proteins with differential phosphorylation after 30 min of 42°C, 43 were among the proteins with a two-fold increase or decrease in their levels. Twenty-two are among the 93 up-regulated proteins and 21 among the 224 proteins with reduced levels. In other words, 13.6% of all proteins that were affected by heat shock are also differentially phosphorylated, 23.7% on the side of up-regulated proteins. 9.4% on the side of proteins with decreased levels.

In general, the proteins accumulated after heat shock, as well as the proteins with reduced quantity correlate with the changes on the transcriptional level. The molecular chaperones and proteins involved in energy metabolism, as well as the enzymes of the trehalose system, are the most prominent proteins accumulated. These were also the genes induced rapidly and strongly on the transcriptional level. In especially proteins of nuclear processes

were identified of having reduced quantity after heat shock, which was also the case for the transcriptional down-regulation.

5. Discussion

5.1 The small heat shock proteins of baker's yeast

The small heat shock proteins are a ubiquitous class of molecular chaperones found through all kingdoms of life. So far, only a handful of organisms have been identified that lack even a single representative of this diverse class of molecular chaperones. Their main function - in the context of cellular proteostasis - lies in the suppression of protein aggregation (Hilton et al., 2013). With this function in mind, the term 'molecular sponges' of the cellular proteostasis network has been brought forth. These molecular sponges, of highly dynamic nature yet with defined structural elements, such as a dimeric building block, trap proteins during the process of unfolding and prevent the potentially deleterious consequences of protein aggregation (Hilton et al., 2013). sHsps act without ATP-hydrolysis and - in a concerted action with ATP-dependent chaperones of the Hsp70 family, or with Hsp104 in yeast - the sHsp-holdases contribute to the protein disaggregation and refolding processes.

Saccharomyces cerevisiae has a two-component sHsp system consisting of Hsp26 and Hsp42. Studies have mainly focused on the characterization of their activities as molecular chaperones and on the structural investigation of Hsp26. Only in the recent past has Hsp42 been linked to protein trafficking processes in the cell (Escusa-Toret et al., 2013; Roth and Balch, 2013; Specht et al., 2011). Studies on deletion strains of baker's yeast small heat shock proteins were unable to elicit a phenotype (Escusa-Toret et al., 2013; Petko and Lindquist, 1986; Stratil, 2010), a surprising finding given their highly stress-induced nature and their role in proteostasis.

One aspect of this study focused on finding novel potential genetic interaction partners of the small heat shock proteins of *S. cerevisiae*. This task was undertaken by synthetic genetic arrays (SGA), often referred to as synthetic lethal screens. The SGAs aimed at identifying genes that result in a growth phenotype or lethality when deleted in combination with one or both sHsps. The pathways in which the obtained genetic interactors lie were to suggest new roles of the small heat shock proteins in cellular processes.

The deletion of 66 different genes resulted in a synthetic genetic interaction in combination with disruption of both yeast small heat shock proteins. Slightly less interactors were found in combination with a *hsp42* deletion and just over half the number in combination with Δ *hsp26*. The vast majority of genes with a synthetic interaction in combination with disruption of one of the two sHsp resulted in a synthetic growth defect. Roughly 87% in

both cases were of this non-lethal type. Only approx. 10% of the genes yielded a lethal interaction. Interestingly, an overlap between the genetic interactors of the three SGAs existed. 48% of the genetic interactors of *hsp26* were also among those for the double deletion strain and 42% of the *hsp42* hits were found as interactors in the double KO. For the $\Delta hsp26\Delta hsp42$ knockout strain, 40% of the genetic interactions were of the lethal type. This points to an additive deleterious effect of *hsp26* and *hsp42* deletion.

In silico functional annotation of all hits identified protein trafficking processes to be enriched among the genetic interactors. More specifically the trafficking process of the endomembrane system including the transport of cargo from the Golgi to the vacuole was affected. This was the case for all three SGA screens, suggesting that both small heat shock proteins contribute to the process. From the combined list of 103 genetic interactors, almost one fifth of the genes cluster to vacuolar transport (*bro1*, *pep1*, *pep7*, *pep12*, *snf7*, *snf8*, *vps4*, *vps9*, *vps15*, *vps16*, *vps24*, *vps25*, *vps28*, *vps32*, *vps33*, *vps36*, *stp22*). Vacuoles are not only storage compartments in yeast but are also a major site of protein degradation; they contain seven proteases identified as of today (Hecht et al., 2015), potentially linking the small heat shock proteins to vacuolar protein degradation.

An additional cluster of *hsp42* interactors is made up by six genes that did not appear in the *hsp26* SGA. These genes (*pex2*, *pex4*, *pex8*, *pex10*, *pex12*, *pex14*) are assigned to protein transport into the peroxisome. For *Pex14*, a physical interaction with *Hsp42* has been reported (Tarassov et al., 2008). This points to a potential role of *Hsp42* in protein trafficking to the peroxisome. To be more exact, all these proteins comprise part of the translocon complex of the peroxisomal membrane, responsible for protein translocation into the matrix (Heiland and Erdmann, 2005).

Molecular chaperones have been implicated in protein trafficking (Bukau et al., 2006; Hartl et al., 2011). Also, the small heat shock proteins have been shown to be involved in protein sequestration processes (Escusa-Toret et al., 2013; Roth and Balch, 2013; Specht et al., 2011). Therefore an appearance of protein trafficking processes is in the scope of the reported biological functions of molecular chaperones. As of today, a specific role for *Hsp26* and *Hsp42* in the process of protein transport through the endomembrane system or into the peroxisome has not yet been put forth. Due to the fact that no direct physical contact of *Hsp26* or *Hsp42* with vacuolar sorting proteins has been identified as of yet, it appears more likely that the sHsps contribute to the process of substrate-transport to the vacuole, rather than for the vacuolar protein sorting components itself. Because of the known physical interaction of *Hsp42* with the *Pex14* component of the peroxisomal

importeur complex, Hsp42 could also function in the correct assembly of the complex. However, also the shuttle of Hsp42-substrates to the translocation complex is imaginable. A next step that could shed more light on how the genetic interactors connect with the small heat shock protein system of baker's yeast lays in the investigation of direct physical contact between the respective proteins. Previous analysis of this kind showed a limited overlap between genetic interactors and true physical contact, ranging from 1% in the case of Hsp90 genetic interactors (Zhao et al., 2005) to 20% in the case of the co-chaperone Sba1 (Echtenkamp et al., 2011). Studies on direct physical contact could help to pinpoint a more precise role of the sHsps in protein trafficking and protein translocation into the peroxisomes.

In microarray analysis, the mRNA levels of the genetic interactors were monitored in the sHsp deletion background. No change compared to wild-type levels were detected in physiological conditions, after heat shock (37°C, 42°C and 50°C), and in the stationary phase. This implies that only when both components - the sHsp and the protein trafficking processes - are impaired, a deleterious consequence to yeast is exhibited. Nevertheless, the data suggests a role for the sHsps of baker's yeast in directing proteins to vacuolar degradation processes or for protein translocation into peroxisomes.

Protein aggregation has been linked to several neuropathies, such as Alzheimer's disease and Huntingtons's disease. In these diseases, mutations in the genome cause a protein to become more aggregation-prone than its wild-type version, and, hence, they are often addressed as protein misfolding disorders. It has been suggested, that sequestration of misfolding and aggregated proteins in the cell could also be a central part of protein quality control; next to refolding, degradation, and inclusion formation (Roth and Balch, 2013). Two aggregation models were investigated here with respect to the contribution of Hsp26 and Hsp42 to protein aggregation: a non-toxic model based on the aggregation-prone protein firefly luciferase (Fluc) and the toxic model of poly-Q aggregation. In the first model, Fluc was used as a sensor of the state of proteome stress inside sHsp-deletion mutants. These sensors have successfully been utilized in mammalian cells and *C. elegans* in studies on age-related protein aggregation (Gupta et al., 2011; Walther et al., 2015). Luciferase requires a concerted action of Hsp40, Hsp70 and Hsp90 in the refolding process (Minami and Minami, 1999). Consequently, an imbalance of proteostasis may titrate the chaperones away from luciferase refolding and result in enhanced luciferase aggregation. For this purpose, GFP-fused wild-type Fluc and two mutants of increasing instability, FlucSM and FlucDM were introduced into the yeast strains and monitored

microscopically. FlucSM displayed GFP foci formation in the double-KO strain under permissive conditions, but a homogeneous signal in wt and single-sHsp mutants. After heat shock, FlucSM remained soluble only for the wt strain. The even more instable FlucDM mutant had an overall lower expression level at 25°C and also showed foci formation in the single-KO strains in 5% to 10% of the cells. Heat shock led to aggregation of FlucDM also in wt cells. All in all, the destabilized Fluc-GFP reporters are suitable sensors of proteome stress in yeast cells. They indicated a higher level of proteome stress in sHsp-disrupted yeast. Deletion of both sHsp displayed a slightly higher tendency of FlucDM aggregation, which suggests a higher level of proteome stress in yeast lacking the sHsp-system.

The destabilized Fluc-GFP mutants, hence, serve as useful tools to investigate the state of proteome stress in *S. cerevisiae*. An interesting observation was the type of aggregates formed. In wt and $\Delta hsp26$ cells, FlucGFP formed large foci, usually with one or two per cell. $\Delta hsp42$ and $\Delta hsp26/42$ yeast harbored more granular-like aggregates. This is in contrast to published data, where it was reported that the formation of peripheral inclusions is abolished in $\Delta hsp42$ cells, and only one large nuclear-associated inclusion is formed (Escusa-Toret et al., 2013; Specht et al., 2011). The reason for this discrepancy is unclear and can only be speculated on. A first thought is that proteasome-inhibition may have an influence on the formation of cellular inclusions, since all of the studies worked in presence of the proteasome inhibitor MG-132. A very recent study excludes this option, where $\Delta hsp42$ cells expressing a FlucDM-GFP with a nuclear localization sequence formed one large inclusion without any peripheral deposits, showing the formation of the large inclusions is not dependent on proteasome inhibition (Miller et al., 2015). In the work presented here, a constitutively active GPD promotor on a high copy 2 μ -plasmid was used. This resulted in a high level of Fluc-GFP expression, perhaps to an extent that overloaded the cell and resulted in peripheral aggregates in the absence of Hsp42. A low-copy plasmid with inducible expression of the reporter protein could be better suited to analyze the aggregation process of firefly luciferase in the absence of *S.cerevisiae*'s sHsps. However, the formation of many inclusions of smaller size fits well with the supposed role in the formation of Q-bodies - dynamic cytosolic inclusions of proteins considered to be precursors of larger inclusions. Q-body formation and maturation was proposed to occur with the help of Hsp104 and Hsp42: Hsp104 disaggregates existing Q-bodies and Hsp42 is responsible for a subsequent coalescing with other existing Q-bodies, thus contributing to the formation of larger cytosolic inclusions (Escusa-Toret et al., 2013; Roth and Balch, 2013). Additional studies are warranted to elucidate the observed effects in this thesis.

PolyQ56-expressing yeast cells displayed a strong phenotype of *pica* (polyQ-induced cycle arrest) cells in accordance with the toxic nature of the polyQ56 protein (Kaiser et al., 2013; Papsdorf et al., 2015). Microscopic analysis on polyQ56-YFP expressing yeasts showed the formation of large inclusions of poly-Q aggregates, mostly in the cellular periphery, in accordance with reports localizing amyloidogenic polyQ proteins to insoluble protein deposits (IPOD) (Kaganovich et al., 2008; Ogrodnik et al., 2014). In the sHsp deletion strains no differences in toxicity or cellular localization of the polyQ56 aggregates was identified, large YFP-Q56 foci persisted. Studies on polyQ toxicity with endogenous Hsp26-GFP or Hsp42-GFP fusion did not yield conclusive results in combination with polyQ56 intoxication. Both GFP fusion proteins showed foci formation in pQ0 and pQ56 cells. No difference between the non-toxic and toxic state was observed. This may be due to the large GFP-tag fused to the C-Terminus of the respective sHsp. N- and C-terminal extensions are important for oligomerization and functional activity of sHsp (Basha et al., 2006), a large tag of approx. 28kDa likely affects structural and functional properties of the sHsps. Smaller tags, such as the FLAsH-tag (6 aa long), could be used as an alternative to GFP-fusion (Adams et al., 2002).

In conclusion, the Fluc-GFP reporters indicate that removal of the entire sHsp-system of *S.cerevisiae* raises the level of proteome stress slightly, however, not to a degree that is detrimental to the cell's survival.

5.2 The transcriptional heat shock response

Organisms are constantly exposed to changes in their environment. These can be of diverse kind: an increase or drop in temperature, exposure to toxic substances or radiation, fluctuating nutrient levels or a change in osmolarity, just to name a few. Adaptation to these environmental fluctuations is key for cellular survival. Evolution has put forth effective protective mechanisms that help cells to cope with their ever changing surroundings and life depends on these ancient protective mechanisms. These include the initiation of a stimulus-specific transcriptional response, as well as the initiation of a common transcriptional response, coined the environmental stress response (Gasch and Werner-Washburne, 2002). The induction of cytoprotective genes is central in this process. The heat shock proteins (Hsps) are part of the battery of protective genes and the molecular chaperones comprise a subset of the Hsps. They assist in protein folding, protein refolding, and suppression of protein aggregation. The heat shock response goes beyond the induction of Hsps. Many genes involved in metabolic processes or signaling processes have also been reported to be induced. Investigations on the transcriptional response of baker's yeast to heat stress started some decades ago, with a general description of the genes involved and a basic kinetic analysis (Causton et al., 2001; Gasch et al., 2000). It must be noted that not all of the aforementioned studies analyzed the entire list of *S. cerevisiae* ORFs known today or used yeast strains of different genetic background for their studies. Furthermore, the selection of points in time for kinetic studies on the transcriptional response was limited and in most cases started when the transcriptional response was already in full throttle. Hence, many studies have focused on the investigation of the heat shock response, but the data is distributed over a large number of scientific reports hindering an exact comparison of the results. A comprehensive approach that encompasses all aspects in one study has not been accomplished as of today.

Using state-of-the-art microarrays probing for 5,717 yeast ORFs, the *S. cerevisiae* transcriptome dynamics were investigated here in detail with high temporal resolution for the conditions of mild and sub-lethal heat shock. The heat stress response within the first few minutes was explored meticulously, gaining information that was lacking as of yet.

The kinetic response to mild heat shock possessed a rapid initiation of a transcriptional response with measurable fold-changes of gene regulation already 1 min after heat shock. This regulation was further augmented until 15 min of stress, where the transcriptional response was at its maximum. Put in numbers, approx. 300 genes each were up- or down-regulated more than two-fold by a time of 5 min. Furthermore, the kinetic analysis revealed

differential regulation for roughly 600 genes at later points in time and with lower changes in mRNA level. This indicates diverse transcriptional waves of gene regulation, information that was only hinted on previously due to the limited data in the first few minutes of heat shock (Gasch et al., 2000).

The *in silico* functional annotation of differentially-regulated genes revealed the molecular chaperones to be among the fastest and highest up-regulated genes after heat shock. These include the sHsps (*hsp26*, *hsp42*), *hsp12*, genes of the Hsp70 system (*ssa1*, *ssa4*), the stress-induced Hsp90 isoform (*hsp82*), co-chaperones of the Hsp70 and Hsp90 systems (*aha1*, *fes1*, *sis1*) and the disaggregase *hsp104*. This is in accordance with the literature and the recognized understanding that under (heat) shock conditions the expression of molecular chaperones - as keepers of cellular proteostasis - is specifically induced (Gasch, 2002; Gasch et al., 2000; Morano et al., 2012; Richter et al., 2010). Components of the chaperone system are generally up-regulated, with the exception of TRiC (Figure 46).

Besides the molecular chaperones, many genes of proteins with metabolic function were found among the rapidly up-regulated genes. These include carbohydrate transporters and glycolytic enzymes (*hxt1*, *hvk1*), and the entire set of the trehalose metabolic machinery (*tps1*, *tps2*, *tps3*, *tsl1*, *nth1*, *nth1*, *ath1*). Trehalose, a disaccharide, has been shown to serve as a cytoprotective chemical chaperone, accumulated under heat stress conditions (Singer and Lindquist, 1998a). Furthermore, high levels of trehalose interfere with protein refolding, also explaining why genes for trehalose-degradation proteins are also up-regulated under stress conditions (Gibney et al., 2015; Singer and Lindquist, 1998b; Vergheze et al., 2012). The differential regulation of genes involved in carbohydrate metabolism may be explained with the increased demand of the cell for ATP, since many energy-consuming processes are active under stress. These include processes chaperoned by ATP-dependent Hsps, the biosynthesis of Hsps, and also proteolytic degradation steps aimed at removing denatured proteins from the cytosol. An additional speculation has been brought forth regarding the role of the carbohydrate metabolic genes in the context of heat shock: In combination with signaling genes, they may serve in sensing the metabolic health of the cells and in regulating growth processes. For instance, while the molecular chaperones, especially Hsp104, may serve in sensing and regulating protein refolding, Tps2, along with glycolytic enzymes (e.g. Pfk1) or enzymes of gluconeogenesis (e.g. Pyc1) could regulate glycolytic flux. In the context of heat shock, these enzymes (along with others) prime the cells for growth resume after the stress has subsided (Gibney et al., 2013).

Furthermore, it must be mentioned that many genes with differential up- or down-regulation under conditions of heat shock, are still uncharacterized and still require an investigation of their function.

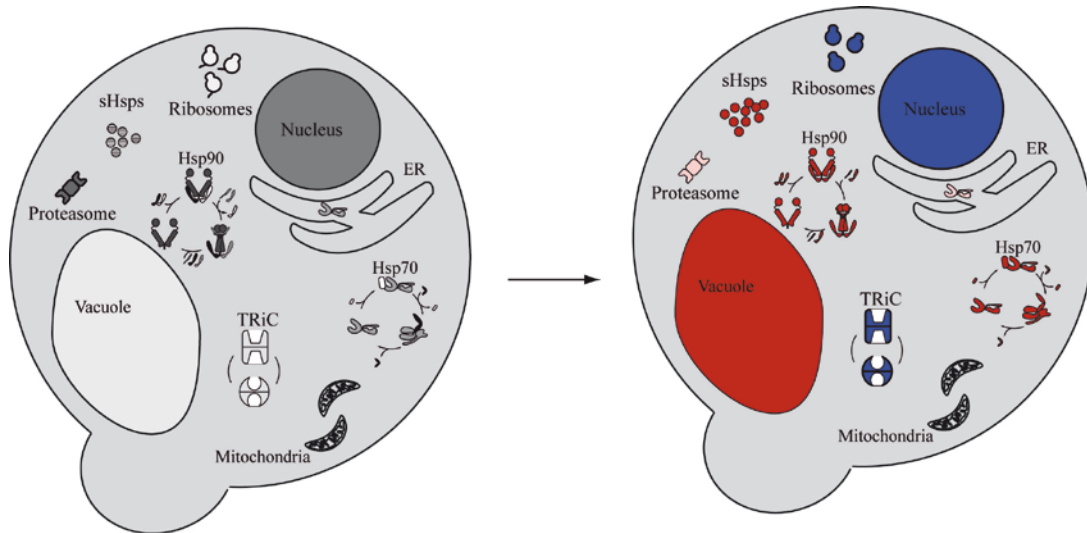


*Figure 46 Effects of heat shock on molecular chaperone gene transcription of *S. cerevisiae*. Left: Cell under non-stress conditions with basal transcription of the sHsps, the proteasome-system, the Hsp90 system, the TRiC complex, the Hsp70 system, and ribosomes. Right: Cell after heat shock. Red indicates a heat-induced up-regulation of the transcripts, blue indicates down-regulation (dark red: $fc > 1$, light red: $fc > 0.5$, blue: $fc < -1$). Heat shock results in a strong up-regulation of the small heat shock proteins (sHsp), as well as of the Hsp90-system, the Hsp70 system and also of autophagy-associated genes (indicated by a red vacuole) and the ubiquitin-proteasome-system (red proteasome). Down-regulated after heat shock are the chaperonin system (TRiC), ribosomal subunits and assembly factors (ribosomes), as well as nuclear processes involved in DNA-replication and RNA-processing (blue nucleus).*

With identical kinetics and fold-changes of gene-regulation but on the side of down-regulation, genes involved in RNA-metabolism, such as RNA-processing and splicing, tRNA processing, and ribosome biogenesis are repressed considerably upon heat stress. The consequence is a global stop in protein biosynthesis - with the exception of the heat shock proteins - described as the hallmark of the heat shock response (Figure 46) (Ashburner and Bonner, 1979; Lindquist, 1980).

GO analysis of the differentially regulated of the later transcriptional wave implicates more peroxisomal and mitochondria-related processes up-regulated in the heat stress response, as well as a shift from RNA-related processes towards protein translation-related terms on the side of down-regulation. The slight delay in the down-regulation of ribosomal proteins has also been indicated previously (Gasch et al., 2000). The appearance of peroxisomal and mitochondrial genes can be explained by the overlapping stress response systems of

baker's yeast, where a significant cross-talk between the systems exists (Verghese et al., 2012). Therefore, heat shock does not only elicit a heat stress response but also a heat-induced, secondary oxidative stress response (Davidson and Schiestl, 2001; Morano et al., 2012).

In this study, the kinetics of the transcriptional heat stress response to sub-lethal heat shock was also analyzed. In general, the transcriptional response reflects that observed under mild heat shock. Nevertheless, two observations differ: The fold-changes of gene regulation are obtained at even earlier times, and the transcriptional response is long-lasting with high fold-changes maintained over the entire course of time. Mild heat stress resulted in a decline in transcript levels after 20 min of stress and the adaptation to a new steady level of transcription. The dose dependency of the transcriptional response is known: a shift from 25°C to 37°C was shown to result in higher and longer lasting transcriptional changes, compared to a shift from 29°C to 33°C (Gasch, 2002). The lasting response at 42°C heat shock without re-establishment of a new steady state level of the transcriptional profile has not been demonstrated before and can be considered a new finding. Perhaps this can be explained with the severity of the stress with 42°C lying just below the temperature limit of yeast: A constant exposure to such a severe stress may result in lasting protein unfolding and aggregation, overloading the cellular proteostasis system, therefore, the transcriptional up-regulation of protective factors remains constantly high, while factors of ribosome biogenesis and, consequently, protein biosynthesis remain constantly down-regulated.

Selected processes involved in the protein quality control system were also addressed. Mild heat stress only had little influence on the transcript levels of UPS genes but activated the transcription of 50% of the autophagy-related genes to more than two-fold (Figure 46). The 42°C stress resulted in augmented transcript levels of the genes of the UPS and autophagy, especially after prolonged exposure to the elevated temperatures. The enhanced need of these two protein clearance mechanisms under conditions of proteotoxic stress, are in agreement with their function within the proteostasis network of the cell to increase the removal of potentially toxic protein aggregates (Bejarano and Cuervo, 2010; Kim et al., 2013).

The transcriptional response to heat was also investigated in the genetic background of deletion mutants. Disruption of *hsp12* led to changes in gene regulation of metal ion homeostasis. More specifically, many membrane-localized or membrane-associated copper and iron transporter and chelators were differentially up-regulated in the KO strain.

A decade old study indeed identified *hsp12* to be up-regulated under excess of copper and a Δ *hsp12* mutant was more sensitive to copper intoxication (van Bakel et al., 2005). Copper and iron ions are tightly connected with the generation of reactive oxygen species, in essence oxidative stress (Liochev and Fridovich, 1999). The conclusion that can be drawn from this is that Hsp12 - in accordance with its function as a membrane stabilizing protein (Welker et al., 2010) - protects the cellular membrane from damage caused by copper and ion induced oxidative stress. Further investigation on the exact role of Hsp12 in ion homeostasis could be carried out in the future.

Deletion of both small heat shock proteins yielded broad changes on the transcriptional profile of the cell. Genes involved in autophagy and UPS were elevated marginally under non-stress conditions already, perhaps indicative of slightly higher level of proteome stress in the absence of the sHsp system. This would fit well with the observed effects of the destabilized luciferase-GFP reporters. The transcription of genes involved in carbohydrate metabolism is also elevated compared to wt. One can speculate that this may be due to a higher requirement of ATP to fuel the elevated level of protein degradation processes.

Microarray analysis on yeast with transcription factor deletions was also carried out. Rpn4, Sko1 and Msn2/4 were chosen due to the enrichment of their targets among the regulated genes in the wt response and their known function in regulation of proteasomal degradation, oxidative and osmotic stress response or of the general stress response (Martinez-Pastor et al., 1996; Rep et al., 2001; Xie and Varshavsky, 2001). Surprisingly, Msn2/4 disruption led to approx. 300 transcripts with significantly altered levels compared to wt yeast under non-stress conditions. As mediators of the general stress response, it had been reported that Msn2/4 disruption does not affect gene regulation under permissive conditions (Stansfield, 2007), however, it had also been stated that disruption of *msn2/4* leads to altered basal gene transcription (Grably et al., 2002; Gutin et al., 2015).

In accordance with their function and the number of known and putative targets, the *msn2/4* deletion had the most profound effect on gene regulation, followed by *rpn4*- and, lastly, *sko1*-disruption. All strains share the same clusters of differentially regulated genes: ribosome biogenesis, RNA-processing and energy metabolism. One can speculate that these gene deletion strains have a stronger imbalance of the proteostasis system with more protein aggregation and less re-folding. As a potential compensatory mechanism, a higher demand of energy-consuming protein biosynthesis is required, hence the higher transcript levels of above-mentioned gene clusters.

5.3 Heat stress and the proteome

The transcriptional studies of the heat shock response were expanded to the analysis of the heat shock effects on the level of proteins, since they are the entities carrying out the functions in the cellular environment. In a SILAC-based mass-spectrometry approach, 10 min and 30 min of heat shock at either 37°C or 42°C were investigated. In this thesis, approx. 2,500 proteins were quantified for the short time of stress and almost 3,330 proteins for the prolonged heat shock. This equals roughly 40% to 50% of the yeast proteome (Kumar et al., 2002).

A short exposure to 37°C resulted in only minor effects on the proteome, just over 20 proteins increased more than two-fold in quantity. Short sub lethal stress at 42°C had an opposite effect, only a handful of proteins were accumulated and approx. 50 showed reduced quantity at the selected two-fold cutoff. The longer heat shock affected more proteins: Six times more proteins were increased in quantity and close to 70 proteins were decreased after mild heat shock compared to the short time of stress. Sub-lethal stress at 42°C, again, had fewer proteins with increased quantity and three times more with reduced levels. The decrease in number of proteins synthesized at 42°C can be attributed to translational pausing induced by intracellular proteotoxic stress, which is also caused by heat (Liu et al., 2013; Shalgi et al., 2013). Another reason lies in the proteins with reduced quantity: They show a strong enrichment for rRNA processing, ribosomal subunits or ribosome assembly factors. Less ribosomes consequently also mean a reduced capacity for protein biosynthesis. At this point, it cannot be determined whether the reduction in the quantity of the proteins is due to controlled degradation processes or due to heat-induced aggregation. The experimental setup, in which insoluble material is removed from the analysis by means of centrifugation, currently does not allow the discrimination between both possibilities. A recent mass-spectrometry-based study that analyzed the heat induced aggregated portion of the yeast proteome, quantified 982 proteins and found 18% of the quantified proteins to move into the insoluble fraction after short exposure to 46°C. The study further showed that the proteins retained their fidelity and are resolubilized when physiological temperatures are restored (Wallace et al., 2015). Here, in this thesis, 30 out of the 224 proteins with reduced quantity were also found among the aggregator fraction in above-described study and are mostly proteins of ribosome biogenesis, potentially localized to heat shock granules (Buchan and Parker, 2009; Wallace et al., 2015). An additional mass-spectrometry analysis, quantifying proteins in the soluble and insoluble fraction, could complement the results in this thesis and shed more light into the degree of

protein degradation or aggregation. It is likely that a combination of both processes is responsible for the reduction in quantity for the close to 230 proteins after 30 min of 42°C stress. In published proteomic studies, the half-lives of baker's yeast proteins were measured (Belle et al., 2006; Christiano et al., 2014). The studies differ in the measured half-lives from a few minutes to several hours, however similar tendencies were stated: proteins of cell cycle regulation are short-lived, while ribosome subunits are supposedly long-lived. In this thesis, also ribosomal proteins were found among the proteins with heat-induced reduction of their quantity. Since these proteins are reported to be long-lived, this points to their aggregation, or controlled aggregation into stress granules (Wallace et al., 2015), more than to their controlled degradation. Other proteins identified here with a reduction in quantity, such as proteins involved in RNA-processing or in DNA-replication, could be due to degradation processes, since they were reported to have short half-lives (Belle et al., 2006; Christiano et al., 2014).

Proteins that are specifically accumulated under heat shock conditions contain many of the molecular chaperones. These include both sHsps, Hsp12, the heat inducible Hsp70s, Hsp82, and co-chaperones Aha1, Mdj1, Sti1, Sis1, and Fes1. This heat-induced, specific accumulation of the 'molecular chaperome' (Brehme et al., 2014) is in accordance with literature (Finka et al., 2015; Richter et al., 2010). Furthermore, proteins involved in energy metabolism (including the enzymes involved in trehalose biosynthesis and degradation) are specifically accumulated after heat shock.

All in all, the general proteome changes correlate well with changes on the transcriptional level. However, the transcriptional reprogramming affects many more genes compared to the changes elicited on the protein level. A reason for this could be that an initial stress elicits a swift and vast transcriptional response, not entirely needed for survival of the stressor. The differential regulation of these genes rather primes the cell's transcriptional profile for the appearance of a potential secondary stress. This could also explain the overlapping nature of the diverse stress response pathways (Gasch and Werner-Washburne, 2002; Morano et al., 2012). Speculating further, the appearance of the potential secondary stress would result in a translation of these messages and the respective proteins to be accumulated.

In addition to total protein quantity, the influence of heat shock on the phospho-proteome was also investigated. Posttranslational modifications (PTMs), the reversible covalent modifications of proteins, can be considered an additional, highly versatile means of regulating protein activity, phosphorylation representing one of the most prevalent types of

PTMs (Humphrey et al., 2015). Here, the phospho-proteome was investigated in combination with the total proteome analysis described above.

The short exposure to elevated temperatures elicited less P-sites with a differential change in their phosphorylation state compared to the longer duration of stress. Furthermore, the effects were more pronounced for the stress of higher temperature compared to mild heat shock. Differential P-sites were mostly found in three cellular processes: protein folding, cell division and morphogenesis, and ribosome assembly. These GO terms also were found among the differential changes on the total proteome and on the transcriptional level. Heat stress is known to slow down or even stop the cell cycle (Li and Cai, 1999), therefore an in- or decrease in the phosphorylation state of cell cycle regulator and proteins is intuitive. A recent study also found cell morphogenesis and cell cycle regulation proteins to be major sites for heat-induced (de-) phosphorylation (Kanshin et al., 2015).

5.4 X-ray tomography

Besides the induction of a transcriptional response, heat stress can have profound consequences on cellular integrity, architecture and morphology and these have been summarized in a recent review (Richter et al., 2010). In this thesis, the consequences of heat stress on the inner cellular morphology of *S. cerevisiae* were investigated by means of X-ray tomography. This method has a number of benefits: At the employed energy range of the X-ray microscope, organic material absorbs one order of magnitude stronger than water-rich structures. Hence, these carbon-rich structures yield images of high contrast, while water-rich structures will appear more transmissive (Larabell and Nugent, 2010; Schneider et al., 2010). Furthermore, cell preparation is carried out similar to cryo-EM preparation by flash freezing in temperatures below -170°C enabling a preservation of the ultra-structure without the necessity of staining procedures. And lastly, whole cells can be investigated without preparation of thin sections.

X-ray microscopy of unstressed BY4741wt yeast and reconstruction of the tomograms enabled the visualization of several sub-cellular structures and organelles: the nucleus and therein lying nucleolus, lipid droplets of different sizes, the vacuoles in various sizes and shapes, and a tubular network of the mitochondria. This is in accordance with published reports that utilized X-ray tomography to study the cell division cycle of *S. cerevisiae* and *S. pombe* (Gu et al., 2007; Uchida et al., 2011). Non-stressed yeast displayed an intact cellular morphology with undamaged organelles and no visible formation of aggregation in the cytosol. Heat stress for 10 min at 37°C or 42°C did not have any influence on the

cellular morphology, at least as far as can be determined by X-ray microscopy. Only the harmful stimulus at 50°C was able to elicit a change in the inner architecture of the cell. Here, a fragmentation of the mitochondria was observed, a swelling of the vacuole, and an accumulation of aggregates in the cytosol. The heat-induced fragmentation of mitochondria is known (Welch and Suhan, 1985), as is the formation of one large swollen vacuole (Meaden et al., 1999). The accumulation of visible aggregates in the cytosol can be explained with protein aggregation in general and, more specifically, with the appearance of stress granules: cytosolic agglomerates of mRNA, ribosomal proteins and translation factors, among other proteins (Buchan and Parker, 2009).

The investigation of the morphological consequences of heat on yeast was expanded to yeasts with gene deletions in *hsp26*, *hsp42*, *hsp26/42* or *hsp12*. The same effects of heat as for wild-type yeast were observed: The yeast strains displayed an undamaged cellular interior for temperatures up to 42°C but showed impaired inner structures when exposed to the harmful 50°C stimulus. KO-specific effects, such as the reported crumpled cell wall of *hsp12*, *hsp26* and *hsp42* deletion strains, were not retrieved (Haslbeck et al., 2004; Welker et al., 2010). A number of reasons can be brought forth: First, the different genetic backgrounds of the utilized yeast strains, and secondly, the utilized method. The raisin-like surface morphology was observed by scanning electron microscopy, a method that requires full dehydration and metal coating of the samples (Weston et al., 2010). This can introduce artifacts and influence cellular surface morphology. In X-ray microscopy, frozen cells are imaged under native-like conditions without any staining procedures.

It must be noted that, due to the time required for projection image series acquisition (approx. 1 h per tomogram) and the limited beam time obtained at the U41-TXM microscope (BessyII, Berlin), only two or three reconstructable tilt series were able to be obtained per yeast strain and condition. A statistic foundation of the results requires the acquisition of more tomograms.

In summary, X-ray microscopy as carried out here gave a nice overview of the entire inner cellular morphology of baker's yeast in a natural-like surrounding. For a more detailed analysis of the consequences of heat shock on inner morphology of yeast, an expansion to other microscopic methods could be helpful.

Serial block-face-scanning electron microscopy (SBF-SEM) poses a promising alternative technique. This method uses scanning electron microscopy to investigate thin sections of resin-embedded yeast cells in 100 nm increments. The spatial resolution obtained is equal to that of X-ray microscopy (in the low tens of nanometers) but SBF-SEM enables the

acquisition of thin sections of multiple cells at once, a clear benefit for obtaining a high number of replicas. However, the advantage of investigating yeast in a frozen state is no longer given (Miyazaki et al., 2014). Cryo-electron tomography (cryo-ET) could also represent an alternative for future analysis of yeast's inner cellular morphology. Sample preparation for cryo-ET on baker's yeast is similar to that of X-ray tomography. However, thin sections of the sample must be prepared in order to render them transparent for the electron beam, and, consequently, not the entire cellular volume is visualized. In the past, this has been carried out with a cryo-ultramicrotome. More recently, cryo-focused ion beam (cryo-FIB) milling has become the method of choice for preparing thin sections of any desired thickness (Asano et al., 2015). Cryo-ET has successfully been used for the investigation of macromolecular complexes; hence the spatial resolution lays more than one order of magnitude higher compared to X-ray microscopy (Asano et al., 2015; Beck et al., 2004).

6. Appendix

6.1 Microarray data on the heat shock response

Table S1 List of early and late up- & down regulated genes in baker's yeast after mild heat stress (25 → 37°C). Yeast Genome 2.0 microarrays from Affymetrix were utilized. See chapter 3.11 for classification of genes into 'early' and 'late' categories.

Table S1 List of early & late up- regulated genes, early & late down-regulated genes of Saccharomyces cerevisiae after mild heat stress from 25°C to 37°C.

Selection criteria are described in material and methods (see 3.11). The total number of genes attributed to this category is in parenthesis. Genes are listed with their official gene name.

Category (# of genes)	Genes				
	YAL005C	YAL017W	YAL028W	YAL060W	YAL061W
	YBL029C-A	YBL064C	YBL075C	YBL078C	YBL086C
	YBR001C	YBR018C	YBR045C	YBR053C	YBR054W
	YBR056W	YBR066C	YBR072W	YBR085C-A	YBR101C
	YBR126C	YBR128C	YBR132C	YBR139W	YBR157C
	YBR169C	YBR183W	YBR214W	YBR230C	YBR280C
	YBR285W	YBR298C	YCL040W	YCR021C	YCR061W
	YCR091W	YDL021W	YDL022W	YDL079C	YDL110C
	YDL124W	YDL130W-A	YDL146W	YDL181W	YDL199C
	YDL204W	YDL214C	YDL222C	YDL247W	YDL247W
	YDR001C	YDR003W	YDR003W-A	YDR034W-B	YDR043C
	YDR070C	YDR074W	YDR096W	YDR151C	YDR171W
	YDR214W	YDR216W	YDR247W	YDR258C	YDR342C
	YDR358W	YDR379C-A	YDR479C	YDR516C	YEL011W
	YEL012W	YEL024W	YEL039C	YEL060C	YER033C
	YER035W	YER037W	YER053C	YER053C-A	YER054C
	YER062C	YER067W	YER079W	YER096W	YER103W
	YER150W	YFL014W	YFL016C	YFL030W	YFL054C
	YFR015C	YFR017C	YFR053C	YGL037C	YGL045W
	YGL059W	YGL096W	YGL104C	YGL227W	YGL229C
Early up (300)	YGR008C	YGR019W	YGR023W	YGR052W	YGR053C
	YGR070W	YGR088W	YGR127W	YGR130C	YGR131W
	YGR161C	YGR194C	YGR197C	YGR205W	YGR210C
	YGR211W	YGR243W	YGR248W	YGR249W	YGR250C
	YGR287C	YGR288W	YGR289C	YHL008C	YHL021C
	YHL024W	YHL028W	YHR007C-A	YHR016C	YHR087W
	YHR097C	YHR104W	YHR138C	YHR140W	YHR157W
	YHR161C	YHR171W	YHR198C	YIL029C	YIL045W
	YIL097W	YIL101C	YIL107C	YIL111W	YIL113W
	YIL136W	YIL155C	YIR014W	YIR016W	YIR017C
	YIR018C-A	YIR039C	YJL042W	YJL048C	YJL057C
	YJL066C	YJL070C	YJL082W	YJL132W	YJL133C-A
	YJL141C	YJL144W	YJL155C	YJL161W	YJL163C
	YJL164C	YJR008W	YJR046W	YJR059W	YJR115W
	YJR127C	YKL035W	YKL091C	YKL093W	YKL103C
	YKL109W	YKL133C	YKL142W	YKL148C	YKL150W
	YKL151C	YKL171W	YKR011C	YKR058W	YKR067W
	YLL019C	YLL026W	YLL039C	YLL041C	YLR006C
	YLR080W	YLR102C	YLR149C	YLR151C	YLR168C
	YLR174W	YLR176C	YLR177W	YLR178C	YLR216C
	YLR251W	YLR258W	YLR260W	YLR270W	YLR312C

Category (# of genes)	Genes				
	YLR327C	YLR345W	YLR406C-A	YLR438W	YLR446W
	YML054C	YML100W	YML120C	YML128C	YML130C
	YMR031C	YMR053C	YMR068W	YMR081C	YMR085W
	YMR104C	YMR105C	YMR169C	YMR194C-B	YMR196W
	YMR250W	YMR251W-A	YMR261C	YMR262W	YMR291W
	YNL006W	YNL007C	YNL008C	YNL011C	YNL063W
	YNL077W	YNL125C	YNL160W	YNL194C	YNL200C
	YNL274C	YNL305C	YNR001C	YNR002C	YNR014W
	YNR034W	YNR034W-A	YNR068C	YNR069C	YOL016C
	YOL032W	YOL048C	YOL052C-A	YOL083W	YOL084W
	YOL104C	YOL117W	YOR020W-A	YOR028C	YOR032C
	YOR049C	YOR052C	YOR054C	YOR065W	YOR100C
	YOR137C	YOR152C	YOR161C	YOR173W	YOR178C
	YOR185C	YOR186W	YOR220W	YOR267C	YOR273C
	YOR289W	YOR292C	YOR317W	YOR347C	YOR374W
	YOR386W	YPL003W	YPL014W	YPL017C	YPL087W
	YPL123C	YPL186C	YPL196W	YPL203W	YPL230W
	YPL239W	YPL240C	YPL247C	YPL250C	YPL264C
	YPR026W	YPR154W	YPR158W	YPR160W	YPR184W
	YAL010C	YAL054C	YAR042W	YBL001C	YBL005W-A
	YBL019W	YBL045C	YBL049W	YBL059C-A	YBL080C
	YBL091C-A	YBR013C	YBR014C	YBR022W	YBR024W
	YBR062C	YBR076W	YBR077C	YBR089C-A	YBR108W
	YBR111C	YBR117C	YBR170C	YBR193C	YBR201W
	YBR223C	YBR240C	YBR273C	YCL044C	YCL064C
	YCR005C	YCR009C	YCR015C	YCR038C	YCR100C
	YCR101C	YDL024C	YDL057W	YDL085W	YDL107W
	YDL119C	YDL180W	YDL200C	YDL223C	YDL233W
	YDL244W	YDL246C	YDL248W	YDR019C	YDR032C
	YDR055W	YDR059C	YDR063W	YDR130C	YDR131C
	YDR169C	YDR242W	YDR248C	YDR282C	YDR286C
	YDR287W	YDR306C	YDR307W	YDR314C	YDR319C
	YDR330W	YDR369C	YDR377W	YDR423C	YDR453C
	YDR505C	YDR506C	YDR511W	YDR512C	YDR513W
	YEL019C	YEL057C	YEL062W	YER014W	YER078W-A
	YER087W	YER134C	YER139C	YER142C	YER143W
	YER162C	YER163C	YER175C	YER179W	YFL020C
Late up (294)	YFL044C	YFL060C	YFL064C	YFL065C	YFR033C
	YGL004C	YGL018C	YGL062W	YGL090W	YGL117W
	YGL146C	YGL154C	YGL180W	YGL185C	YGL191W
	YGL196W	YGL205W	YGL248W	YGL249W	YGL259W
	YGR016W	YGR028W	YGR067C	YGR153W	YGR174C
	YGR223C	YGR235C	YGR236C	YGR256W	YGR268C
	YGR284C	YHL010C	YHL030W	YHL042W	YHL048C-A
	YHR022C	YHR028C	YHR043C	YHR051W	YHR071W
	YHR102W	YHR116W	YHR159W	YHR160C	YHR202W
	YIL001W	YIL009C-A	YIL014C-A	YIL033C	YIL071C
	YIL072W	YIL073C	YIL117C	YIL157C	YIL160C
	YIR024C	YIR025W	YIR036C	YJL003W	YJL013C
	YJL030W	YJL031C	YJL036W	YJL045W	YJL091C
	YJL206C	YJR005C-A	YJR022W	YJR053W	YJR062C
	YJR078W	YJR106W	YKL007W	YKL016C	YKL065C
	YKL086W	YKL094W	YKL100C	YKL107W	YKL138C-A
	YKL187C	YKL208W	YKL217W	YKL218C	YKR009C
	YKR016W	YKR091W	YKR097W	YLL006W	YLL040C
	YLR012C	YLR047C	YLR053C	YLR054C	YLR070C
	YLR133W	YLR205C	YLR240W	YLR245C	YLR267W

Category (# of genes)	Genes				
	YLR273C	YLR284C	YLR307W	YLR324W	YLR361C
	YLR395C	YLR408C	YLR414C	YLR423C	YML007C-A
	YML029W	YML050W	YML068W	YML070W	YML095C
	YML129C	YMR009W	YMR020W	YMR022W	YMR023C
	YMR025W	YMR041C	YMR052W	YMR092C	YMR107W
	YMR118C	YMR159C	YMR173W	YMR175W	YMR182W-A
	YMR184W	YMR198W	YMR244C-A	YMR253C	YMR256C
	YMR271C	YMR278W	YMR297W	YMR311C	YMR322C
	YNL009W	YNL012W	YNL033W	YNL037C	YNL055C
	YNL117W	YNL122C	YNL130C	YNL155W	YNL202W
	YNL208W	YNL237W	YNL265C	YNL293W	YNR019W
	YOL031C	YOL069W	YOL107W	YOL131W	YOL156W
	YOL159C	YOR003W	YOR012W	YOR022C	YOR025W
	YOR035C	YOR040W	YOR059C	YOR124C	YOR134W
	YOR155C	YOR162C	YOR177C	YOR208W	YOR221C
	YOR245C	YOR350C	YOR357C	YOR358W	YOR382W
	YOR383C	YPL060W	YPL097W	YPL109C	YPL113C
	YPL119C	YPL119C-A	YPL147W	YPL148C	YPL150W
	YPL154C	YPL162C	YPL224C	YPL249C	YPR001W
	YPR006C	YPR024W	YPR047W	YPR055W	YPR081C
	YPR093C	YPR098C	YPR107C	YPR151C	YPR159C-A
	YAL025C	YAL037W	YAL059W	YBL014C	YBL028C
	YBL042C	YBL054W	YBL081W	YBR034C	YBR061C
	YBR104W	YBR141C	YBR247C	YBR267W	YBR271W
	YCL036W	YCL054W	YCR016W	YCR035C	YCR047C
	YCR054C	YCR057C	YCR072C	YDL031W	YDL060W
	YDL063C	YDL129W	YDL150W	YDL167C	YDL227C
	YDR020C	YDR021W	YDR075W	YDR083W	YDR087C
	YDR101C	YDR110W	YDR184C	YDR198C	YDR280W
	YDR281C	YDR299W	YDR312W	YDR324C	YDR339C
	YDR398W	YDR399W	YDR412W	YDR449C	YDR492W
	YDR496C	YDR514C	YER002W	YER056C	YER075C
	YER127W	YFL002C	YFL023W	YFR001W	YFR032C
	YFR055W	YGL028C	YGL029W	YGL056C	YGL063W
	YGL064C	YGL078C	YGL169W	YGL171W	YGL209W
	YGL236C	YGL246C	YGR030C	YGR040W	YGR079W
	YGR081C	YGR093W	YGR128C	YGR140W	YGR158C
	YGR159C	YGR187C	YGR251W	YGR271C-A	YGR283C
Early down (262)	YHL026C	YHR040W	YHR048W	YHR052W	YHR062C
	YHR065C	YHR066W	YHR070W	YHR085W	YHR088W
	YHR148W	YHR149C	YHR169W	YHR187W	YHR196W
	YHR197W	YIL019W	YIL079C	YIL091C	YIL096C
	YIL103W	YIL104C	YIL127C	YJL010C	YJL025W
	YJL033W	YJL069C	YJL098W	YJL122W	YJL125C
	YJL148W	YJL157C	YJL162C	YJL194W	YJR041C
	YJR055W	YJR063W	YJR097W	YJR147W	YKL009W
	YKL021C	YKL074C	YKL078W	YKL082C	YKL099C
	YKL125W	YKL172W	YKR024C	YKR044W	YKR045C
	YKR056W	YKR060W	YKR063C	YKR079C	YKR081C
	YKR099W	YLL011W	YLL035W	YLR002C	YLR003C
	YLR009W	YLR015W	YLR042C	YLR051C	YLR063W
	YLR068W	YLR073C	YLR129W	YLR146C	YLR196W
	YLR213C	YLR214W	YLR215C	YLR222C	YLR223C
	YLR243W	YLR363W-A	YLR401C	YLR405W	YLR407W
	YLR409C	YLR435W	YML005W	YML018C	YML027W
	YML043C	YML080W	YML082W	YML113W	YML123C
	YMR014W	YMR093W	YMR127C	YMR185W	YMR187C

Category (# of genes)	Genes				
	YMR211W	YMR239C	YMR268C	YMR310C	YNL002C
	YNL022C	YNL024C	YNL050C	YNL061W	YNL062C
	YNL065W	YNL075W	YNL095C	YNL110C	YNL113W
	YNL119W	YNL124W	YNL141W	YNL162W-A	YNL164C
	YNL182C	YNL186W	YNL207W	YNL218W	YNL221C
	YNL240C	YNL254C	YNL282W	YNL289W	YNL299W
	YNL308C	YNL313C	YNR015W	YNR024W	YNR038W
	YNR053C	YOL010W	YOL019W	YOL041C	YOL054W
	YOL080C	YOL101C	YOL124C	YOL128C	YOL144W
	YOL152W	YOR004W	YOR056C	YOR078W	YOR119C
	YOR145C	YOR154W	YOR206W	YOR213C	YOR252W
	YOR272W	YOR274W	YOR287C	YOR294W	YOR295W
	YOR302W	YOR315W	YOR337W	YOR339C	YOR340C
	YOR342C	YOR359W	YPL012W	YPL030W	YPL068C
	YPL093W	YPL108W	YPL130W	YPL146C	YPL157W
	YPL183C	YPL193W	YPL201C	YPL202C	YPR112C
	YPR124W	YPR137W	YPR143W	YPR144C	
	YAL033W	YAL035W	YAL036C	YAR015W	YAR050W
	YAR071W	YBL009W	YBL029W	YBL052C	YBL071W-A
	YBL076C	YBL082C	YBL106C	YBR040W	YBR048W
	YBR073W	YBR079C	YBR084W	YBR092C	YBR093C
	YBR115C	YBR187W	YBR208C	YBR219C	YBR244W
	YBR248C	YBR249C	YBR263W	YBR275C	YBR296C
	YCL024W	YCL025C	YCR034W	YCR051W	YCR059C
	YDL051W	YDL082W	YDL121C	YDL131W	YDL171C
	YDL205C	YDL212W	YDL229W	YDL229W	YDL241W
	YDR037W	YDR042C	YDR045C	YDR078C	YDR097C
	YDR106W	YDR119W	YDR121W	YDR126W	YDR138W
	YDR144C	YDR156W	YDR211W	YDR234W	YDR297W
	YDR300C	YDR321W	YDR345C	YDR384C	YDR395W
	YDR408C	YDR414C	YDR418W	YDR429C	YDR471W
	YDR488C	YDR502C	YEL026W	YEL036C	YEL042W
	YEL076C-A	YER025W	YER036C	YER043C	YER055C
	YER073W	YER086W	YER104W	YER110C	YER118C
	YER131W	YER165W	YER171W	YFL022C	YFL034C-A
	YFL034C-B	YFR018C	YGL009C	YGL016W	YGL032C
Late down (280)	YGL120C	YGL148W	YGL234W	YGL261C	YGR061C
	YGR072W	YGR082W	YGR083C	YGR094W	YGR096W
	YGR141W	YGR152C	YGR156W	YGR173W	YGR195W
	YGR217W	YGR234W	YGR264C	YGR285C	YGR286C
	YHL011C	YHR007C	YHR020W	YHR042W	YHR072W
	YHR100C	YHR127W	YHR128W	YHR154W	YHR165C
	YHR175W-A	YHR204W	YHR205W	YHR208W	YHR216W
	YIL008W	YIL011W	YIL069C	YIL121W	YIL176C
	YJL076W	YJL080C	YJL111W	YJL130C	YJL177W
	YJL186W	YJL200C	YJL216C	YJR007W	YJR016C
	YJR031C	YJR072C	YJR112W	YKL004W	YKL029C
	YKL047W	YKL110C	YKL113C	YKL156W	YKL182W
	YKL205W	YKR013W	YKR025W	YKR026C	YKR043C
	YKR102W	YKR104W	YLL022C	YLL054C	YLL061W
	YLR017W	YLR040C	YLR048W	YLR056W	YLR057W
	YLR059C	YLR083C	YLR106C	YLR172C	YLR183C
	YLR291C	YLR318W	YLR342W-A	YLR343W	YLR359W
	YLR372W	YLR406C	YLR420W	YLR430W	YLR432W
	YLR433C	YLR448W	YLR449W	YLR451W	YML014W
	YML022W	YML023C	YML026C	YML075C	YML106W
	YML125C	YMR006C	YMR016C	YMR061W	YMR143W

Category (# of genes)	Genes				
	YMR146C	YMR177W	YMR194W	YMR217W	YMR241W
	YMR243C	YMR266W	YMR301C	YMR305C	YMR308C
	YMR312W	YMR321C	YNL066W	YNL067W	YNL087W
	YNL096C	YNL102W	YNL142W	YNL209W	YNL217W
	YNL220W	YNL247W	YNL251C	YNL255C	YNL277W-A
	YNL300W	YNR043W	YNR044W	YNR046W	YOL024W
	YOL028C	YOL029C	YOL052C	YOL092W	YOL097W-A
	YOL120C	YOL123W	YOL137W	YOL139C	YOR021C
	YOR047C	YOR051C	YOR093C	YOR108W	YOR168W
	YOR188W	YOR190W	YOR207C	YOR222W	YOR224C
	YOR229W	YOR271C	YOR298W	YOR335C	YOR355W
	YOR361C	YOR390W	YPL016W	YPL019C	YPL079W
	YPL081W	YPL160W	YPL163C	YPL192C	YPL237W
	YPL241C	YPL245W	YPL246C	YPL263C	YPL273W
	YPL274W	YPL279C	YPR033C	YPR035W	YPR037C
	YPR058W	YPR118W	YPR145W	YPR163C	YPR169W
	YAL025C				

Table S2 List of early & late up-regulated genes, early & late down-regulated genes of *Saccharomyces cerevisiae* after sub-lethal heat stress from 25°C to 42°C.

Selection criteria are described in material and methods (see 3.11). The total number of genes attributed to this category is in parenthesis. Genes are listed with their official gene name.

Category (# of genes)	Genes				
	YAL005C	YAL017W	YAL028W	YAL060W	YAL061W
	YAR027W	YBL029C-A	YBL064C	YBL075C	YBL078C
	YBL086C	YBR001C	YBR005W	YBR045C	YBR053C
	YBR054W	YBR098W	YBR101C	YBR114W	YBR126C
	YBR132C	YBR139W	YBR147W	YBR157C	YBR161W
	YBR169C	YBR182C	YBR183W	YBR208C	YBR214W
	YBR230C	YBR285W	YBR287W	YBR298C	YBR299W
	YCL040W	YCR011C	YCR021C	YBR056W	YBR056W-A
	YBR066C	YBR072W	YBR083W	YBR085C-A	YBR085W
	YCR061W	YDL020C	YDL021W	YDL022W	YDL025C
	YDL110C	YDL113C	YDL114W	YDL124W	YDL130W-A
	YDL142C	YDL146W	YDL214C	YDL234C	YDL247W
	YDR001C	YDR003W	YDR034W-B	YDR042C	YDR043C
	YDR069C	YDR070C	YDR074W	YDR089W	YDR096W
Early up (403)	YDR151C	YDR171W	YDR173C	YDR182W-A	YDR214W
	YDR216W	YDR246W-A	YDR247W	YDR256C	YDR258C
	YDR259C	YDR273W	YDR342C	YDR358W	YDR379C-A
	YDR380W	YDR516C	YEL011W	YEL012W	YEL039C
	YEL060C	YER020W	YER033C	YER035W	YER037W
	YER039C	YER046W	YER053C	YER053C-A	YER054C
	YER062C	YER067W	YER079W	YER081W	YER096W
	YER103W	YER150W	YER158C	YER185W	YFL014W
	YFL016C	YFL054C	YFR015C	YFR017C	YFR053C
	YGL006W	YGL010W	YGL035C	YGL036W	YGL037C
	YGL045W	YGL096W	YGL104C	YGL166W	YGL179C
	YGL237C	YGR008C	YGR019W	YGR023W	YGR052W
	YGR055W	YGR070W	YGR088W	YGR121C	YGR127W
	YGR130C	YGR131W	YGR136W	YGR138C	YGR142W
	YGR146C	YGR149W	YGR161C	YGR194C	YGR205W
	YGR211W	YGR236C	YGR237C	YGR243W	YGR248W

Category (# of genes)	Genes				
	YGR249W	YGR250C	YGR289C	YHL008C	YHL021C
	YHL024W	YHR004C	YHR007C-A	YHR016C	YHR022C
	YHR050W-A	YHR054C	YHR056C	YHR075C	YHR082C
	YHR087W	YHR096C	YHR097C	YHR104W	YHR136C
	YHR137W	YHR138C	YHR157W	YHR161C	YHR171W
	YHR209W	YIL045W	YIL055C	YIL056W	YIL066C
	YIL097W	YIL107C	YIL111W	YIL113W	YIL117C
	YIL119C	YIL136W	YIL155C	YIR014W	YIR016W
	YIR017C	YIR039C	YJL047C-A	YJL048C	YJL052W
	YJL057C	YJL066C	YJL070C	YJL082W	YJL089W
	YJL094C	YJL103C	YJL106W	YJL108C	YJL133C-A
	YJL141C	YJL144W	YJL149W	YJL153C	YJL155C
	YJL164C	YJL165C	YJL170C	YJL213W	YJR008W
	YJR036C	YJR046W	YJR047C	YJR059W	YJR061W
	YJR091C	YJR115W	YJR149W	YKL026C	YKL035W
	YKL043W	YKL086W	YKL091C	YKL093W	YKL096W
	YKL103C	YKL109W	YKL124W	YKL133C	YKL142W
	YKL150W	YKL151C	YKL162C	YKL163W	YKL193C
	YKL201C	YKR011C	YKR039W	YKR058W	YKR067W
	YKR091W	YLL019C	YLL026W	YLL028W	YLL039C
	YLL041C	YLR006C	YLR054C	YLR064W	YLR108C
	YLR120C	YLR142W	YLR149C	YLR152C	YLR168C
	YLR174W	YLR176C	YLR177W	YLR178C	YLR216C
	YLR219W	YLR251W	YLR254C	YLR258W	YLR270W
	YLR297W	YLR312C	YLR327C	YLR343W	YLR345W
	YLR350W	YLR438W	YLR446W	YML054C	YML091C
	YML100W	YML120C	YML128C	YML130C	YMR009W
	YMR031C	YMR034C	YMR040W	YMR081C	YMR085W
	YMR087W	YMR101C	YMR102C	YMR104C	YMR105C
	YMR110C	YMR135C	YMR136W	YMR139W	YMR169C
	YMR194C-B	YMR195W	YMR196W	YMR210W	YMR250W
	YMR251W-A	YMR262W	YMR280C	YMR291W	YMR315W
	YMR316W	YNL006W	YNL007C	YNL008C	YNL015W
	YNL036W	YNL037C	YNL042W-B	YNL063W	YNL077W
	YNL125C	YNL144C	YNL160W	YNL194C	YNL200C
	YNL270C	YNL274C	YNL305C	YNR001C	YNR002C
	YNR014W	YNR019W	YNR034W	YNR034W-A	YNR068C
	YOL016C	YOL032W	YOL048C	YOL052C-A	YOL084W
	YOL091W	YOL117W	YOL154W	YOR020W-A	YOR028C
	YOR032C	YOR036W	YOR049C	YOR052C	YOR054C
	YOR062C	YOR137C	YOR152C	YOR161C	YOR173W
	YOR178C	YOR185C	YOR186W	YOR219C	YOR220W
	YOR227W	YOR230W	YOR267C	YOR273C	YOR289W
	YOR292C	YOR297C	YOR317W	YOR344C	YOR347C
	YOR374W	YPL003W	YPL005W	YPL014W	YPL054W
	YPL057C	YPL061W	YPL087W	YPL111W	YPL120W
	YPL123C	YPL135W	YPL170W	YPL203W	YPL223C
	YPL230W	YPL239W	YPL240C	YPL247C	YPL250C
	YPL264C	YPR015C	YPR026W	YPR030W	YPR036W-A
	YPR061C	YPR065W	YPR151C	YPR154W	YPR158W
	YPR160W	YPR184W	YPR194C		
	YAL010C	YAL014C	YAL018C	YAL031C	YAL068C
	YAL068C	YAR010C	YAR020C	YAR023C	YAR029W
Late up (468)	YBL001C	YBL007C	YBL019W	YBL022C	YBL041W
	YBL043W	YBL045C	YBL085W	YBL098W	YBL101C
	YBL107C	YBL108C-A	YBL108C-A	YBR004C	YBR007C
	YBR013C	YBR016W	YBR022W	YBR070C	YBR071W

Category (# of genes)	Genes				
	YBR077C	YBR093C	YBR107C	YBR111C	YBR117C
	YBR128C	YBR137W	YBR148W	YBR168W	YBR170C
	YBR201W	YBR279W	YBR284W	YBR301W	YBR301W
	YCL004W	YCL010C	YCL026C-A	YCL026C-B	YCL047C
	YCL050C	YCL067C	YCR033W	YCR036W	YCR039C
	YCR095C	YCR096C	YCR099C	YCR104W	YDL024C
	YDL035C	YDL045W-A	YDL057W	YDL059C	YDL069C
	YDL070W	YDL089W	YDL091C	YDL099W	YDL107W
	YDL115C	YDL160C	YDL173W	YDL181W	YDL197C
	YDL218W	YDL223C	YDL238C	YDL243C	YDL243C
	YDL244W	YDL246C	YDL248W	YDR005C	YDR019C
	YDR022C	YDR031W	YDR058C	YDR067C	YDR077W
	YDR082W	YDR123C	YDR131C	YDR168W	YDR169C
	YDR178W	YDR183W	YDR200C	YDR208W	YDR210W
	YDR236C	YDR242W	YDR248C	YDR249C	YDR251W
	YDR262W	YDR285W	YDR293C	YDR295C	YDR303C
	YDR306C	YDR311W	YDR314C	YDR319C	YDR320C
	YDR334W	YDR363W-A	YDR376W	YDR394W	YDR423C
	YDR427W	YDR434W	YDR453C	YDR476C	YDR478W
	YDR503C	YDR511W	YDR518W	YDR525W-A	YDR528W
	YDR540C	YEL005C	YEL020C	YEL020W-A	YEL023C
	YEL049W	YEL049W	YEL057C	YEL058W	YEL059C-A
	YEL070W	YER024W	YER027C	YER045C	YER048W-A
	YER051W	YER058W	YER066W	YER069W	YER095W
	YER098W	YER109C	YER143W	YER144C	YER182W
	YFL020C	YFL029C	YFL031W	YFR004W	YFR010W
	YFR026C	YFR033C	YFR039C	YFR041C	YFR047C
	YFR050C	YFR052W	YGL004C	YGL007C-A	YGL047W
	YGL058W	YGL062W	YGL071W	YGL073W	YGL090W
	YGL091C	YGL093W	YGL094C	YGL117W	YGL122C
	YGL125W	YGL126W	YGL127C	YGL128C	YGL131C
	YGL133W	YGL157W	YGL178W	YGL180W	YGL191W
	YGL197W	YGL248W	YGL261C	YGL261C	YGR028W
	YGR032W	YGR048W	YGR062C	YGR087C	YGR097W
	YGR109W-B	YGR109W-B	YGR144W	YGR153W	YGR168C
	YGR170W	YGR188C	YGR201C	YGR235C	YGR255C
	YGR258C	YGR270W	YGR294W	YGR294W	YHL002W
	YHL009W-B	YHL030W	YHL042W	YHL048C-A	YHR001W-A
	YHR008C	YHR030C	YHR037W	YHR044C	YHR051W
	YHR102W	YHR112C	YHR146W	YHR198C	YIL001W
	YIL014C-A	YIL023C	YIL031W	YIL048W	YIL049W
	YIL073C	YIL075C	YIL089W	YIL108W	YIL120W
	YIL135C	YIL139C	YIL152W	YIL165C	YIL170W
	YIR002C	YIR007W	YIR024C	YIR025W	YJL003W
	YJL030W	YJL031C	YJL035C	YJL056C	YJL060W
	YJL062W-A	YJL073W	YJL074C	YJL088W	YJL091C
	YJL102W	YJL154C	YJL166W	YJL174W	YJL185C
	YJL219W	YJL219W	YJR022W	YJR052W	YJR078W
	YJR099W	YJR106W	YJR117W	YJR151C	YJR155W
	YKL016C	YKL020C	YKL023W	YKL048C	YKL050C
	YKL061W	YKL067W	YKL073W	YKL074C	YKL079W
	YKL089W	YKL094W	YKL098W	YKL106W	YKL129C
	YKL165C	YKL167C	YKL178C	YKL179C	YKL188C
	YKL189W	YKL195W	YKL206C	YKL213C	YKL218C
	YKR019C	YKR050W	YKR061W	YKR076W	YLL009C
	YLL025W	YLL033W	YLL056C	YLL057C	YLR001C
	YLR028C	YLR034C	YLR046C	YLR053C	YLR080W

Category (# of genes)	Genes				
	YLR092W	YLR099C	YLR099W-A	YLR107W	YLR119W
	YLR121C	YLR156W	YLR157W-D	YLR159W	YLR161W
	YLR164W	YLR213C	YLR227C	YLR231C	YLR240W
	YLR247C	YLR248W	YLR250W	YLR307C-A	YLR324W
	YLR332W	YLR352W	YLR423C	YLR455W	YLR457C
	YML011C	YML013W	YML029W	YML032C	YML042W
	YML070W	YML092C	YML095C	YML101C	YML118W
	YMR002W	YMR004W	YMR013C	YMR025W	YMR028W
	YMR035W	YMR036C	YMR067C	YMR158C-A	YMR170C
	YMR182W-A	YMR189W	YMR197C	YMR200W	YMR214W
	YMR256C	YMR265C	YMR278W	YMR281W	YMR284W
	YMR297W	YMR303C	YMR311C	YNL012W	YNL042W
	YNL054W	YNL073W	YNL076W	YNL084C	YNL092W
	YNL100W	YNL103W	YNL115C	YNL128W	YNL133C
	YNL155W	YNL192W	YNL230C	YNL234W	YNL237W
	YNL241C	YNL293W	YNL322C	YNR035C	YNR047W
	YNR064C	YNR073C	YOL023W	YOL031C	YOL036W
	YOL043C	YOL055C	YOL058W	YOL071W	YOL073C
	YOL088C	YOL100W	YOL107W	YOL110W	YOL114C
	YOL133W	YOL148C	YOL151W	YOL159C	YOL159C-A
	YOR005C	YOR007C	YOR009W	YOR012W	YOR019W
	YOR023C	YOR035C	YOR037W	YOR059C	YOR064C
	YOR075W	YOR076C	YOR089C	YOR097C	YOR107W
	YOR162C	YOR172W	YOR192C-C	YOR193W	YOR238W
	YOR250C	YOR269W	YOR299W	YOR303W	YOR328W
	YOR336W	YOR388C	YPL001W	YPL006W	YPL015C
	YPL024W	YPL034W	YPL036W	YPL055C	YPL060W
	YPL070W	YPL071C	YPL088W	YPL089C	YPL110C
	YPL141C	YPL149W	YPL150W	YPL162C	YPL168W
	YPL177C	YPL221W	YPL222W	YPL224C	YPL258C
	YPR006C	YPR024W	YPR046W	YPR047W	YPR049C
	YPR055W	YPR081C	YPR093C	YPR107C	YPR108W
	YPR109W	YPR127W	YPR137C-A	YPR148C	YPR167C
	YPR174C	YPR175W	YPR191W	YPR193C	YPR196W
	YAL011W	YAL025C	YAL059W	YBL004W	YBL014C
	YBL028C	YBL042C	YBL052C	YBL054W	YBL059W
	YBL060W	YBL066C	YBL081W	YBR034C	YBR061C
	YBR088C	YBR104W	YBR141C	YBR146W	YBR153W
	YBR172C	YBR192W	YBR196C-A	YBR213W	YBR244W
	YBR247C	YBR257W	YBR259W	YBR267W	YBR271W
	YCL029C	YCL036W	YCL054W	YCR014C	YCR015C
	YCR016W	YCR020W-B	YCR035C	YCR047C	YCR054C
	YCR057C	YCR072C	YCR081W	YCR086W	YCR106W
	YCR107W	YCR107W	YDL030W	YDL031W	YDL038C
	YDL039C	YDL060W	YDL063C	YDL104C	YDL105W
Early down (385)	YDL127W	YDL129W	YDL167C	YDL179W	YDL189W
	YDL201W	YDL209C	YDL227C	YDR014W	YDR020C
	YDR021W	YDR030C	YDR060W	YDR065W	YDR075W
	YDR083W	YDR101C	YDR104C	YDR110W	YDR120C
	YDR184C	YDR194C	YDR198C	YDR240C	YDR243C
	YDR280W	YDR299W	YDR312W	YDR324C	YDR351W
	YDR370C	YDR398W	YDR399W	YDR412W	YDR414C
	YDR420W	YDR449C	YDR451C	YDR496C	YDR514C
	YDR545W	YEL029C	YEL065W	YER001W	YER007W
	YER028C	YER056C	YER075C	YER124C	YER127W
	YER154W	YER175C	YER187W	YFL001W	YFL002C
	YFL023W	YFL050C	YGL014W	YGL028C	YGL029W

Category (# of genes)	Genes				
	YGL063W	YGL064C	YGL078C	YGL101W	YGL113W
	YGL143C	YGL169W	YGL171W	YGL236C	YGL246C
	YGR030C	YGR041W	YGR058W	YGR079W	YGR081C
	YGR082W	YGR093W	YGR109C	YGR128C	YGR140W
	YGR150C	YGR154C	YGR159C	YGR177C	YGR215W
	YGR221C	YGR271C-A	YGR272C	YGR274C	YGR283C
	YHL014C	YHL026C	YHR011W	YHR040W	YHR052W
	YHR058C	YHR065C	YHR066W	YHR085W	YHR088W
	YHR094C	YHR109W	YHR118C	YHR120W	YHR144C
	YHR148W	YHR149C	YHR166C	YHR167W	YHR169W
	YHR184W	YHR187W	YHR196W	YHR197W	YIL071C
	YIL079C	YIL091C	YIL092W	YIL096C	YIL103W
	YIL104C	YIL127C	YIL158W	YIR042C	YJL010C
	YJL025W	YJL046W	YJL058C	YJL069C	YJL077W-B
	YJL087C	YJL098W	YJL122W	YJL125C	YJL147C
	YJL148W	YJL157C	YJL162C	YJL194W	YJR003C
	YJR041C	YJR043C	YJR055W	YJR063W	YJR097W
	YKL009W	YKL021C	YKL068W	YKL068W-A	YKL078W
	YKL099C	YKL125W	YKL172W	YKR024C	YKR044W
	YKR056W	YKR060W	YKR063C	YKR077W	YKR079C
	YKR081C	YKR086W	YKR099W	YLL011W	YLL034C
	YLL038C	YLL062C	YLR008C	YLR009W	YLR015W
	YLR042C	YLR051C	YLR052W	YLR063W	YLR067C
	YLR068W	YLR073C	YLR129W	YLR143W	YLR146C
	YLR180W	YLR186W	YLR196W	YLR214W	YLR215C
	YLR222C	YLR273C	YLR320W	YLR323C	YLR336C
	YLR355C	YLR363W-A	YLR401C	YLR405W	YLR409C
	YLR419W	YLR435W	YLR467W	YML005W	YML006C
	YML018C	YML027W	YML043C	YML080W	YML093W
	YML099C	YML113W	YMR014W	YMR093W	YMR106C
	YMR127C	YMR132C	YMR167W	YMR168C	YMR187C
	YMR199W	YMR211W	YMR224C	YMR225C	YMR227C
	YMR267W	YMR268C	YMR300C	YMR309C	YMR310C
	YNL002C	YNL022C	YNL053W	YNL062C	YNL065W
	YNL075W	YNL078W	YNL095C	YNL110C	YNL113W
	YNL119W	YNL124W	YNL141W	YNL162W-A	YNL164C
	YNL182C	YNL201C	YNL204C	YNL218W	YNL221C
	YNL227C	YNL234W	YNL249C	YNL250W	YNL254C
	YNL256W	YNL282W	YNL289W	YNL299W	YNL308C
	YNL313C	YNR024W	YNR038W	YNR053C	YOL019W
	YOL021C	YOL034W	YOL041C	YOL054W	YOL080C
	YOL095C	YOL112W	YOL124C	YOL126C	YOR004W
	YOR056C	YOR078W	YOR104W	YOR119C	YOR140W
	YOR143C	YOR144C	YOR145C	YOR149C	YOR154W
	YOR156C	YOR166C	YOR204W	YOR213C	YOR232W
	YOR233W	YOR243C	YOR252W	YOR274W	YOR279C
	YOR287C	YOR294W	YOR295W	YOR315W	YOR337W
	YOR340C	YOR342C	YOR359W	YOR396W	YPL012W
	YPL029W	YPL030W	YPL038W-A	YPL040C	YPL043W
	YPL052W	YPL068C	YPL093W	YPL108W	YPL146C
	YPL157W	YPL174C	YPL175W	YPL183C	YPL193W
	YPL209C	YPL211W	YPL216W	YPL252C	YPL254W
	YPL267W	YPR018W	YPR031W	YPR083W	YPR112C
	YPR120C	YPR124W	YPR137W	YPR143W	YPR144C
Late down (661)	YAL020C	YAL021C	YAL029C	YAL033W	YAL035W
	YAL036C	YAL058W	YAR002W	YAR015W	YAR018C
	YAR068W	YAR073W	YAR075W	YBL002W	YBL003

Category (# of genes)	Genes				
	YBL027W	YBL027W	YBL032W	YBL068W	YBL072C
	YBL072C	YBL076C	YBL082C	YBL087C	YBL087
	YBL106C	YBL113W-A	YBR029C	YBR031W	YBR038W
	YBR048W	YBR048W	YBR074W	YBR079C	YBR084C-A
	YBR084C-A	YBR084W	YBR092C	YBR115C	YBR121C
	YBR181C	YBR187W	YBR189W	YBR191W	YBR191W
	YBR202W	YBR205W	YBR210W	YBR220C	YBR242W
	YBR248C	YBR249C	YBR251W	YBR252W	YBR254C
	YBR255C-A	YBR261C	YBR263W	YBR265W	YBR275C
	YBR281C	YCL005W-A	YCL009C	YCL024W	YCL025C
	YCL028W	YCL037C	YCL059C	YCL064C	YCR017C
	YCR020C-A	YCR028C-A	YCR034W	YCR037C	YCR043C
	YCR051W	YCR052W	YCR053W	YCR059C	YCR060W
	YCR087C-A	YCR092C	YDL014W	YDL040C	YDL043C
	YDL051W	YDL061C	YDL061C	YDL064W	YDL066W
	YDL082W	YDL083C	YDL083C	YDL083C	YDL121C
	YDL130W	YDL131W	YDL133C-A	YDL136W	YDL157C
	YDL171C	YDL184C	YDL191W	YDL205C	YDL213C
	YDL229W	YDL229W	YDR012W	YDR023W	YDR025W
	YDR025W	YDR035W	YDR037W	YDR045C	YDR046C
	YDR051C	YDR064W	YDR091C	YDR093W	YDR097C
	YDR119W	YDR121W	YDR127W	YDR135C	YDR143C
	YDR144C	YDR146C	YDR156W	YDR161W	YDR170C
	YDR190C	YDR211W	YDR226W	YDR239C	YDR267C
	YDR297W	YDR300C	YDR321W	YDR341C	YDR345C
	YDR365C	YDR367W	YDR384C	YDR395W	YDR418W
	YDR418W	YDR424C	YDR428C	YDR429C	YDR447C
	YDR447C	YDR450W	YDR450W	YDR450W	YDR454C
	YDR461W	YDR465C	YDR471W	YDR488C	YDR492W
	YDR500C	YDR538W	YEL026W	YEL036C	YEL046C
	YEL054C	YEL054C	YER007C-A	YER019C-A	YER025W
	YER031C	YER036C	YER043C	YER055C	YER056C-A
	YER057C	YER073W	YER074W	YER074W	YER086W
	YER090W	YER102W	YER102W	YER110C	YER117W
	YER117W	YER118C	YER120W	YER131W	YER146W
	YER165W	YER170W	YER171W	YER174C	YFL004W
	YFL007W	YFL022C	YFL026W	YFR005C	YFR006W
	YFR031C-A	YFR031C-A	YFR031C-A	YFR032C-A	YGL009C
	YGL016W	YGL027C	YGL031C	YGL032C	YGL040C
	YGL055W	YGL056C	YGL070C	YGL084C	YGL092W
	YGL097W	YGL099W	YGL100W	YGL116W	YGL120C
	YGL123W	YGL147C	YGL148W	YGL189C	YGL195W
	YGL202W	YGL213C	YGL226C-A	YGL234W	YGL255W
	YGL257C	YGR001C	YGR004W	YGR027C	YGR029W
	YGR031W	YGR034W	YGR035C	YGR049W	YGR054W
	YGR061C	YGR068C	YGR072W	YGR074W	YGR078C
	YGR083C	YGR085C	YGR085C	YGR094W	YGR095C
	YGR105W	YGR108W	YGR116W	YGR118W	YGR118W
	YGR123C	YGR124W	YGR155W	YGR157W	YGR169C-A
	YGR173W	YGR181W	YGR195W	YGR214W	YGR234W
	YGR262C	YGR264C	YGR285C	YGR286C	YHL001W
	YHL003C	YHL006C	YHL011C	YHL033C	YHL033C
	YHL039W	YHR010W	YHR013C	YHR019C	YHR020W
	YHR023W	YHR025W	YHR032W	YHR041C	YHR042W
	YHR060W	YHR063C	YHR064C	YHR067W	YHR068W
	YHR072W-A	YHR089C	YHR092C	YHR100C	YHR117W
	YHR121W	YHR128W	YHR141C	YHR152W	YHR170W

Category (# of genes)	Genes				
	YHR204W	YHR208W	YHR216W	YIL003W	YIL004C
	YIL008W	YIL009W	YIL011W	YIL016W	YIL018W
	YIL018W	YIL018W	YIL020C	YIL039W	YIL043C
	YIL064W	YIL069C	YIL069C	YIL090W	YIL094C
	YIL115C	YIL121W	YIL123W	YIL126W	YIL131C
	YIL132C	YIL133C	YIL134W	YIL148W	YIR035C
	YJL008C	YJL014W	YJL039C	YJL051W	YJL080C
	YJL110C	YJL121C	YJL130C	YJL134W	YJL137C
	YJL138C	YJL145W	YJL177W	YJL179W	YJL183W
	YJL184W	YJL186W	YJL190C	YJL191W	YJL198W
	YJL200C	YJL207C	YJR016C	YJR069C	YJR072C
	YJR074W	YJR092W	YJR094W-A	YJR111C	YJR112W
	YJR112W-A	YJR123W	YJR124C	YJR134C	YJR135W-A
	YJR143C	YJR150C	YKL004W	YKL006W	YKL024C
	YKL027W	YKL029C	YKL047W	YKL081W	YKL122C
	YKL154W	YKL156W	YKL180W	YKL182W	YKL184W
	YKL211C	YKL214C	YKL216W	YKR013W	YKR025W
	YKR026C	YKR043C	YKR059W	YKR070W	YKR074W
	YKR075C	YKR092C	YKR093W	YKR094C	YLL022C
	YLL045C	YLL048C	YLL063C	YLR005W	YLR017W
	YLR022C	YLR032W	YLR043C	YLR048W	YLR049C
	YLR056W	YLR060W	YLR061W	YLR074C	YLR083C
	YLR141W	YLR150W	YLR153C	YLR154C	YLR172C
	YLR175W	YLR183C	YLR185W	YLR188W	YLR195C
	YLR229C	YLR244C	YLR249W	YLR262C-A	YLR285C-A
	YLR285W	YLR286C	YLR291C	YLR305C	YLR321C
	YLR325C	YLR333C	YLR335W	YLR342W-A	YLR344W
	YLR351C	YLR353W	YLR359W	YLR367W	YLR372W
	YLR384C	YLR388W	YLR388W	YLR389C	YLR412W
	YLR413W	YLR420W	YLR426W	YLR430W	YLR432W
	YLR433C	YLR438C-A	YLR441C	YLR448W	YLR449W
	YLR450W	YML014W	YML017W	YML019W	YML022W
	YML023C	YML024W	YML026C	YML026C	YML026C
	YML052W	YML056C	YML063W	YML064C	YML073C
	YML074C	YML086C	YML094W	YML098W	YML106W
	YML126C	YMR006C	YMR012W	YMR016C	YMR030W-A
	YMR032W	YMR038C	YMR061W	YMR079W	YMR080C
	YMR129W	YMR131C	YMR142C	YMR143W	YMR143W
	YMR143W	YMR146C	YMR147W	YMR183C	YMR194W
	YMR208W	YMR215W	YMR217W	YMR221C	YMR230W
	YMR230W	YMR230W-A	YMR235C	YMR241W	YMR242C
	YMR242C	YMR242C	YMR243C	YMR246W	YMR247C
	YMR260C	YMR277W	YMR290C	YMR301C	YMR305C
	YMR307W	YMR308C	YMR312W	YMR321C	YNL010W
	YNL024C-A	YNL038W	YNL058C	YNL067W	YNL069C
	YNL096C	YNL102W	YNL108C	YNL123W	YNL132W
	YNL145W	YNL148C	YNL149C	YNL153C	YNL162W
	YNL166C	YNL189W	YNL209W	YNL220W	YNL246W
	YNL247W	YNL255C	YNL259C	YNL262W	YNL280C
	YNL300W	YNL301C	YNL302C	YNL307C	YNL316C
	YNL327W	YNR003C	YNR018W	YNR021W	YNR041C
	YNR044W	YNR046W	YNR050C	YNR067C	YOL005C
	YOL022C	YOL040C	YOL052C	YOL056W	YOL059W
	YOL092W	YOL097C	YOL120C	YOL123W	YOL127W
	YOL139C	YOL143C	YOR016C	YOR021C	YOR038C
	YOR045W	YOR046C	YOR051C	YOR058C	YOR063W
	YOR073W	YOR091W	YOR096W	YOR106W	YOR108W

Category (# of genes)	Genes				
	YOR112W	YOR129C	YOR142W	YOR167C	YOR168W
	YOR175C	YOR207C	YOR210W	YOR217W	YOR222W
	YOR224C	YOR229W	YOR234C	YOR237W	YOR246C
	YOR247W	YOR251C	YOR271C	YOR276W	YOR278W
	YOR281C	YOR293W	YOR310C	YOR312C	YOR312C
	YOR312C	YOR320C	YOR335C	YOR355W	YOR356W
	YOR361C	YOR375C	YOR382W	YPL050C	YPL063W
	YPL079W	YPL081W	YPL090C	YPL112C	YPL122C
	YPL127C	YPL143W	YPL145C	YPL160W	YPL163C
	YPL199C	YPL226W	YPL227C	YPL235W	YPL246C
	YPL249C-A	YPL253C	YPL263C	YPL265W	YPL273W
	YPL274W	YPR010C	YPR016C	YPR033C	YPR035W
	YPR037C	YPR041W	YPR043W	YPR051W	YPR057W
	YPR058W	YPR063C	YPR069C	YPR074C	YPR102C
	YPR118W	YPR119W	YPR132W	YPR132W	YPR138C
	YPR163C				

Table S3 Differentially regulated genes in *Arpn4* strain compared to *wt*.

Genes with at least two-fold higher or lower RNA level in the *KO* compared to *wt* at the respective point in time were selected. See material and methods for exact selection criteria. Time of stress is noted; the total number of genes identified is in parenthesis. Genes are listed with their official gene name.

Time of stress (# of genes)	Gene IDs				
	YHR047C	YNR044W	YGL032C	YFL030W	YGL156W
	YOL058W	YJL088W	YHL047C	YDR380W	YHR137
	YJL170C	YGR224W	YIL015W	YAL060W	YAL061W
	YGR142W	YDR270W	YGR110W	YIL111W	YOR303W
	YPR158W	YKL096W	YML054C	YOR173W	YOL052C-A
	YDL024C	YDL174C	YBL043W	YKR076W	YOL158C
	YOR382W	YOR383C	YBR008C	YDR070C	YBR047W
	YJL161W	YGR243W	YKR049C	YOL152W	YCL027W
	YBR018C	YDR019C	YMR189W	YAL044C	YCR098C
	YCL040W	YGR256W	YGL121C	YDL021W	YOL151W
	YOR185C	YIR038C	YKL109W	YLR205C	YER062C
	YFL014W	YBR072W	YCR020W-B	YER039C	YHR094C
	YMR011W	YHR092C	YDR343C	YDR342C	YLR099C
	YNL037C	YHR216W	YJL082W	YMR081C	YER142C
0 min (185)	YBR297W	YJL102W	YHR015W	YLL061W	YDR277C
	YJL116C	YGR043C	YFL044C	YKR097W	YPL058C
	YDR406W	YNL231C	YBL005W	YKR046C	YGR239C
	YDR281C	YAR071W	YHR215W	YBR093C	YML123C
	YBR296C	YNL279W	YIL117C	YDR055W	YKR093W
	YIL121W	YOR107W	YIL119C	YDL133C-A	YDL184C
	YDL133C-A	YDL184C	YFR052W	YER021W	YDL007W
	YFR032C	YOR049C	YGR213C	YGR161C	YPL274W
	YIL113W	YBL102W	YIL099W	YDR515W	YGR197C
	YGR248W	YJR159W	YDL246C	YER150W	YHR136C
	YPL130W	YHR184W	YLR452C	YDL130W-A	YGL184C
	YBR083W	YLR136C	YBR117C	YGR138C	YOR273C
	YGR019W	YDL169C	YPL019C	YAR009C	YPR137C-A
	YAR010C	YAR068W	YBL005W-B	YCL021W-A	YCR061W
	YCR102C	YPL087W	YDL124W	YER188C-A	YNL160W
	YGR109W-A	YHR029C	YHR048W	YHR050W-A	YHR112C

Time of stress (# of genes)	Gene IDs				
5 min (362)	YHR140W	YIL014C-A	YIL169C	YIR035C	YKL070W
	YKL071W	YKL183C-A	YKR075C	YLL056C	YLR040C
	YLR042C	YLR046C	YLR149C	YLR156W	YLR346C
	YLR460C	YML131W	YMR102C	YMR230W-A	YNL042W-B
	YNL200C	YOL013W-A	YOL038C-A	YOR152C	YOR192C-C
	YOR289W	YOR338W	YPL113C	YPR015C	YIR039C
	YBR054W	YNL237W	YER033C		
	YMR251W	YCL058C	YBR117C	YBR040W	YMR107W
	YDL039C	YIL150C	YOR384W	YML047C	YMR175W
	YLR307W	YOR068C	YDL085W	YPL223C	YBL043W
	YNL093W	YCR010C	YMR174C	YBR240C	YJL116C
	YBL049W	YKR097W	YOR338W	YHR015W	YDL244W
	YML095C	YGR066C	YCR098C	YKL071W	YLR267W
	YBR033W	YPR151C	YNR056C	YGL158W	YLR063W
	YGL121C	YOR376W-A	YGR110W	YDL049C	YCL036W
	YJR097W	YOR100C	YGR256W	YNL162W-A	YML054C
	YDL222C	YEL070W	YHR048W	YGR109W-A	YDR030C
	YBR267W	YCL018W	YNR069C	YOL104C	YML043C
	YBL054W	YDR106W	YBR296C	YBR141C	YNL065W
	YHR184W	YIL169C	YDL169C	YDL039C	YMR187C
	YLR156W	YNL237W	YGR239C	YDR545W	YPR002W
	YGR079W	YGL156W	YNL270C	YDL223C	YML080W
	YGR146C-A	YDR021W	YER187W	YOR359W	YDR453C
	YBR184W	YOL013W-A	YOL128C	YDR246W-A	YIL104C
	YDL127W	YDL247W	YMR271C	YIL099W	YER188C-A
	YNL299W	YIL014C-A	YKR024C	YGR153W	YGR043C
	YHR096C	YER175C	YOL058W	YGL236C	YPL038W-A
	YBR297W	YCR047C	YOR178C	YBL029W	YHR085W
	YCR020W-B	YOR302W	YJL161W	YGR138C	YNL119W
	YHR210C	YLR205C	YNR004W	YPL222W	YNL164C
	YNL234W	YPL068C	YGL209W	YJL194W	YBL081W
	YKR099W	YIL101C	YHL026C	YDL204W	YMR081C
	YDR070C	YOL083W	YDR019C	YHR066W	YPR194C
	YLL062C	YKR056W	YKR075C	YER060W	YDL246C
	YGR030C	YBR257W	YDL021W	YDL048C	YOL101C
	YOR289W	YLR042C	YOL019W	YCL027W	YHR050W-A
YCR072C	YHR157W	YER058W	YOR328W	YPL089C	
YGL263W	YPL229W	YLR073C	YDR501W	YIL029C	
YBL005W	YLR142W	YHR169W	YDR182W-A	YDR075W	
YIR018C-A	YOR205C	YBR241C	YER075C	YCR102C	
YLR313C	YNL124W	YPL113C	YHR140W	YNR053C	
YAR031W	YLR136C	YPR156C	YKL132C	YBR056W-A	
YNL195C	YLR407W	YER169W	YDR515W	YAR068	
YIL091C	YLR460C	YHR156C	YFR027W	YDR449C	
YLR149C	YJL213W	YHL047C	YBR034C	YLR107W	
YIL144W	YBR006W	YNL042W-B	YJL163C	YLR040C	
YMR158C-A	YOR092W	YNL053W	YGR289C	YER127W	
YLL061W	YGR286C	YKL068W-A	YHL040C	YKR076W	
YJL122W	YHR196W	YPL093W	YKR049C	YKR046C	
YCL026C-B	YJL047C-A	YOR078W	YGL056C	YHL036W	
YPL026C	YDR173C	YER142C	YPL274W	YMR189W	
YHR043C	YAL039C	YHR136C	YHL035C	YLR099C	
YHR052W	YLR346C	YMR090W	YMR013C	YPL241C	
YMR078C	YMR093W	YCR061W	YLR356W	YOR303W	
YHR154W	YNR034W-A	YOR049C	YDL085C-A	YLR452C	
YBR054W	YIL119C	YBL098W	YLR342W-A	YNR044W	
YGL028C	YBR105C	YDR270W	YDR391C	YNL200C	

Time of stress (# of genes)	Gene IDs				
	YOR120W	YPR184W	YOL158C	YNL292W	YIL136W
	YGL010W	YBR066C	YOR173W	YOL014W	YPL266W
	YKL185W	YDR055W	YOR073W	YCL021W-A	YOR347C
	YDL148C	YGR123C	YCR018C	YMR006C	YDR406W
	YMR319C	YOL126C	YMR196W	YNR068C	YKL151C
	YHL039W	YMR181C	YDL174C	YML128C	YPL245W
	YOR192C-C	YAR073W	YBR008C	YBR093C	YKL014C
	YGR224W	YEL065W	YJL050W	YGR173W	YGR088W
	YGL062W	YDR365C	YHR092C	YNL231C	YIL121W
	YGR035C	YLR214W	YOL052C-A	YAL061W	YBR073W
	YMR102C	YKL029C	YGR103W	YNL036W	YCR087C-A
	YPR124W	YOR108W	YNL015W	YDL121C	YOL151W
	YDR043C	YLR178C	YGR055W	YOR382W	YCL059C
	YCR043C	YML131W	YGR159C	YNL175C	YPL170W
	YMR250W	YGR248W	YNL132W	YJL144W	YGR281W
	YBR244W	YNL155W	YCL064C	YOR383C	YPL019C
	YGL157W	YEL011W	YHR047C	YPR160W	YDR516C
	YNL160W	YKL109W	YLL056C	YER062C	YHR208W
	YDL133C-A	YHR216W	YGL009C	YDL171C	YNL077W
	YNL008C	YGR197C	YOR028C	YPR158W	YKR093W
	YDL020C	YNL006W	YOR273C	YPL239W	YPL250C
	YDL020C	YOL104C	YPR194C	YHR015W	YPR159C-A
	YHR184W	YOL013W-A	YCR098C	YDR545W	YLR462W
	YGR109W-A	YBL111C	YGR224W	YCR020W-B	YNR069C
	YIL169C	YER188C-A	YDR314C	YDR253C	YLR081W
	YGR146C-A	YJL107C	YOR376W-A	YLL005C	YBR184W
	YMR001C-A	YEL070W	YGL007C-A	YPR193C	YBL097W
	YPR156C	YCR102C	YLR042C	YCL027W	YPL171C
	YOR378W	YGR174W-A	YDR246W-A	YBL005W-A	YER187W
	YHR153C	YCR107W	YNL012W	YLL062C	YGL263W
	YLL061W	YAR073W	YPL038W-A	YHR044C	YGR188C
	YIL160C	YAR023C	YIR015W	YLR460C	YIL166C
	YHR210C	YDL246C	YGR153W	YHL048C-A	YNR057C
	YDL129W	YGR109C	YPL241C	YBR021W	YPL166W
	YJL019W	YMR251W	YDR179C	YHR050W-A	YNL117W
	YOR339C	YNL009W	YKL061W	YGL254W	YGL090W
	YBR297W	YNR004W	YIR042C	YLR313C	YJL162C
	YDR123C	YAR031W	YGL251C	YMR168C	YLR040C
10 min (526)	YDR501W	YNL042W-B	YJR097W	YHR136C	YCL036W
	YKL050C	YKL078W	YIR018C-A	YNL249C	YJR011C
	YDR515W	YGR288W	YJL089W	YLR329W	YDR540C
	YBR056W-A	YHR124W	YBL111C	YCR099C	YKL132C
	YOR284W	YLR068W	YPL201C	YIL096C	YLR103C
	YIL144W	YHR154W	YPL113C	YFR027W	YMR182C
	YPR179C	YFL023W	YOR287C	YMR158C-A	YIL119C
	YOR195W	YIL103W	YDL063C	YAL034W-A	YKL071W
	YOL152W	YNL299W	YHR197W	YIL104C	YAL016C-B
	YER071C	YLL034C	YIL029C	YGL169W	YKL134C
	YNL162W-A	YHR156C	YDR021W	YKL014C	YJR041C
	YHL036W	YEL064C	YOR348C	YMR006C	YMR175W
	YLR142W	YBR093C	YMR042W	YPL223C	YOL080C
	YER028C	YCR047C	YNL132W	YMR078C	YBL063W
	YOR108W	YGR271C-A	YHR070W	YHR216W	YMR013C
	YDL085C-A	YDL049C	YNR003C	YOR134W	YLR132C
	YGL236C	YKL015W	YBR141C	YFR032C	YLR381W
	YNL182C	YJL047C-A	YLR063W	YAR071W	YBL054W
	YBR281C	YOL069W	YDL167C	YMR014W	YDL024C

Time of stress (# of genes)	Gene IDs				
	YBR238C	YML080W	YOR340C	YKL001C	YAL025C
	YLR401C	YAR035W	YCL021W-A	YBL098W	YHR040W
	YDR365C	YGL029W	YCL054W	YDL127W	YBL100W-A
	YNL313C	YJL098W	YGR128C	YML113W	YCR087C-A
	YGR283C	YDL201W	YCL026C-B	YDL039C	YBL042C
	YMR239C	YER143W	YDL121C	YCR057C	YPR112C
	YDR412W	YMR310C	YJL213W	YIL079C	YML093W
	YOR073W	YCR010C	YOR119C	YER142C	YIL121W
	YFL044C	YPL068C	YDL085W	YHR066W	YLR002C
	YJL102W	YGL016W	YLR267W	YLL012W	YPR192W
	YOL144W	YGL010W	YPL034W	YNL119W	YDL060W
	YHR043C	YLL056C	YKR024C	YHR092C	YKR060W
	YBR008C	YDR184C	YHR169W	YAL059W	YOL058W
	YBR247C	YIL127C	YBL043W	YBL081W	YHL026C
	YLR129W	YPL263C	YLR409C	YNL075W	YBR073W
	YBR267W	YJL031C	YIL146C	YKL163W	YDR120C
	YGL121C	YOR302W	YER118C	YPR151C	YOR056C
	YDL133C-A	YCL059C	YDL031W	YGR081C	YIL091C
	YER082C	YMR230W-A	YOR206W	YLR222C	YOR004W
	YCR075C	YPL012W	YOR294W	YBR104W	YDR075W
	YLR073C	YGR066C	YGR138C	YPL183C	YPR144C
	YOR272W	YOR341W	YER075C	YNL164C	YLL011W
	YDR300C	YLR154W-E	YLR196W	YGR030C	YJL116C
	YML043C	YHR148W	YCR072C	YDR324C	YOL124C
	YMR271C	YHR088W	YBL005W-B	YNL141W	YBR244W
	YHR085W	YHR208W	YPL151C	YNL248C	YOL019W
	YPL030W	YOR192C-C	YKR056W	YGR256W	YJR111C
	YGR239C	YJL157C	YJR063W	YHL030W	YDR299W
	YOR101W	YJL069C	YLR223C	YJR101C-A	YOR100C
	YCR043C	YGL078C	YNL308C	YDR492W	YDR101C
	YPL211W	YNL149C	YPR061C	YKL125W	YAR068W
	YNL124W	YPL252C	YKR099W	YPL229W	YPR143W
	YOL010W	YNL053W	YDR195W	YPL043W	YKL093W
	YPR137W	YPR002W	YNL234W	YIL099W	YDR496C
	YIL101C	YGR187C	YOR359W	YHR196W	YLR276C
	YDL169C	YNL111C	YER175C	YCR097W	YLR262C-A
	YER158C	YDR449C	YER049W	YDL039C	YOL041C
	YMR107W	YER002W	YPL170W	YKR075C	YHR069C
	YJL122W	YKR081C	YER127W	YPL163C	YHR047C
	YHL040C	YGL009C	YER169W	YOR092W	YBR117C
	YML054C	YPL222W	YHL008C	YNL078W	YLR051C
	YML091C	YPL093W	YCR034W	YJR016C	YAR009C
	YLL027W	YPL273W	YOR253W	YML131W	YDL048C
	YKL172W	YBL005W	YNL077W	YKL082C	YLR407W
	YDR399W	YOR078W	YGL158W	YDR321W	YAR010C
	YLR046C	YDR398W	YDR527W	YDR453C	YLR186W
	YHR052W	YGR201C	YOL077C	YGL056C	YJL148W
	YNL186W	YNL113W	YNL155W	YPL026C	YAR015W
	YLR009W	YMR093W	YOR145C	YOR338W	YKR093W
	YMR120C	YNL237W	YNL065W	YOR028C	YNL110C
	YJL161W	YNL002C	YHL047C	YOR328W	YAL039C
	YGR079W	YLR359W	YIL087C	YLR346C	YKR046C
	YNL301C	YLR099C	YDR070C	YHR020W	YDR210W
	YKR076W	YGL028C	YNR053C	YDR072C	YPL250C
	YHR094C	YDR019C	YGL156W	YGL209W	YOR342C
	YKL009W	YOR062C	YGR197C	YHR175W	YLR074C
	YLR356W	YHL035C	YNL112W	YMR189W	YMR169C

Time of stress (# of genes)	Gene IDs				
	YKR049C	YHR143W	YDL223C	YDL208W	YMR230W
	YMR230W	YPL239W	YBR034C	YAR075W	YKL185W
	YOL126C	YHR096C	YBR158W	YOR049C	YGR044C
	YOR303W	YPL081W	YEL054C	YDL222C	YLR205C
	YGR043C	YER056C	YOL121C	YBR105C	YJR073C
	YNL195C	YFL034C-A	YLR136C	YNL209W	YOR293W
	YDL182W	YMR102C	YDL174C	YLR355C	YEL065W
	YDL204W	YMR181C	YJL190C	YLL023C	YBL100W-B
	YGR035C	YDR055W	YNL231C	YGL157W	YGR159C
	YPR184W	YLR300W	YGL062W	YPL135W	YOR173W
	YOR120W	YOL151W	YNL036W	YOR383C	YML128C
	YDR406W	YOR153W	YAL061W	YOR382W	YNL160W
	YOR049C	YBR117C	YMR107W	YGL158W	YAL061W
	YER150W	YNR014W	YHR096C	YDL222C	YDR070C
	YGR088W	YLR136C	YDL204W	YPR192W	YJL116C
	YDR406W	YIL101C	YNL195C	YGR043C	YLR205C
	YHL047C	YNL277W	YFR017C	YDL223C	YOR302W
	YOL126C	YOR338W	YNL194C	YNL237W	YPL223C
	YOR134W	YOL052C-A	YPL230W	YGR239C	YPR184W
	YMR181C	YHR087W	YKL093W	YLR174W	YOR178C
	YOR032C	YGR248W	YGR052W	YOL084W	YGL209W
	YOR173W	YMR095C	YDL039C	YHR007C-A	YHL040C
	YGR161C	YBL005W	YOL151W	YGL156W	YOR303W
	YGR138C	YNR002C	YIL099W	YKL071W	YDL024C
	YOR120W	YIL011W	YGR201C	YAR068W	YML054C
	YDL085W	YDL227C	YGL184C	YGR066C	YPR151C
	YIL136W	YHR139C	YHR022C	YIL113W	YNL234W
	YMR096W	YJL078C	YMR291W	YOR161C	YMR319C
	YML128C	YDR453C	YNL160W	YFR015C	YNL112W
	YER158C	YNL093W	YHL035C	YPL017C	YER054C
	YBR214W	YLR149C	YIL055C	YJR115W	YMR105C
	YMR196W	YKR049C	YAL039C	YDL048C	YER028C
	YIL066C	YEL065W	YGL121C	YNR034W-A	YOR328W
	YBL049W	YPL186C	YER088C	YFL021W	YGR256W
40 min (357)	YFL054C	YPL229W	YLR164W	YJL141C	YOR344C
	YBR105C	YJL163C	YDL174C	YIL087C	YLL052C
	YER169W	YPL222W	YDL039C	YLL053C	YPL159C
	YIL155C	YBR054W	YKR039W	YDL129W	YDR277C
	YPL247C	YHR033W	YDR074W	YGR079W	YOR062C
	YIL042C	YKL163W	YBR157C	YMR250W	YLR178C
	YEL039C	YDR391C	YBR241C	YOL059W	YER035W
	YKL107W	YJL089W	YAL034C	YLR099C	YDR516C
	YLR258W	YLL019C	YDL110C	YCR010C	YPR061C
	YDR034W-B	YNL117W	YOL158C	YJL088W	YOL047C
	YLR177W	YCL025C	YKL038W	YIR018W	YKL151C
	YMR058W	YGR138C	YOR316C	YNL042W	YNL277W-A
	YMR136W	YDR270W	YJL026W	YHR143W	YJL144W
	YJR047C	YNL274C	YLR156W	YKR098C	YNL180C
	YJL149W	YHR097C	YER033C	YHL027W	YKR075C
	YNL240C	YLR219W	YER053C	YOR348C	YGR236C
	YPR127W	YML058W-A	YIL056W	YDR001C	YPL068C
	YJL161W	YOR152C	YLL027W	YAL040C	YLR270W
	YDR171W	YPL134C	YPR160W	YNL014W	YOR383C
	YGL071W	YLR156W	YDL169C	YLR466C-B	YKL008C
	YEL011W	YBR114W	YMR090W	YER096W	YMR271C
	YCR061W	YNL130C	YMR078C	YBR129C	YAR031W
	YJL179W	YOL101C	YOL090W	YFR042W	YIL172C

Time of stress (# of genes)	Gene IDs				
	YLR200W	YLR183C	YHR132W-A	YDR068W	YDR065W
	YOR315W	YJL001W	YDR210W	YCL002C	YDL121C
	YJL031C	YDR342C	YGL230C	YER021W	YCL030C
	YGL101W	YLR421C	YGL047W	YDR427W	YOL155W-A
	YMR314W	YGL254W	YKL138C-A	YPL241C	YER067W
	YCR075C	YMR276W	YLR313C	YNL202W	YPL255W
	YFL048C	YLR103C	YCL026C-B	YJL102W	YBR111W-A
	YML007W	YLR452C	YPL052W	YFR050C	YDL007W
	YJL173C	YER071C	YBL100W-B	YFR027W	YGR109C
	YCR090C	YJR057W	YCR043C	YBL005W-B	YFR055W
	YHR121W	YOR195W	YKL196C	YKL161C	YLL056C
	YOL013W-A	YFR052W	YDL003W	YJL045W	YML108W
	YJR067C	YPL267W	YIL138C	YJR118C	YDR031W
	YAR008W	YDR248C	YLR287C	YGR286C	YKR083C
	YGR135W	YNL012W	YJL218W	YHR043C	YEL070W
	YGR197C	YCL021W-A	YGR271C-A	YIL015W	YBR184W
	YER012W	YOL038C-A	YFR004W	YBL107C	YDR363W-A
	YCL055W	YOL152W	YNL042W-B	YDR179C	YJL011C
	YOR261C	YCR020W-B	YDR545W	YCR098C	YBR244W
	YGL010W	YKL015W	YNL149C	YFL044C	YHR153C
	YHR154W	YGL263W	YML123C	YER187W	YGR153W
	YHL030W	YNL155W	YDR365C	YAR071W	YKR093W
	YLR040C	YHR015W	YDL133C-A	YPL113C	YBL005W-B
	YDR515W	YHR184W	YAR009C	YHR137W	YER142C
	YOL104C	YCL027W	YDR281C	YDR380W	YDL246C
	YLR042C	YHR136C	YPR194C	YAR073W	YHR216W
	YGR224W	YDL020C			

Table S4 Differentially regulated genes in *Ask1* strain compared to wt.

Genes with at least two-fold higher or lower RNA level in the KO compared to wt at the respective point in time were selected. See material and methods for exact selection criteria. Time of stress is noted; the total number of genes identified is in parenthesis. Genes are listed with their official gene name.

Time of stress (# of genes)	Gene name				
0 min (76)	YGL192W	YGL262W	YHL043W	YJR150C	YBR090C
	YBL008W-A	YOL104C	YAR069C	YIR028W	YOR100C
	YEL070W	YMR081C	YPL223C	YMR118C	YBR033W
	YMR175W	YPR194C	YCL073C	YIL169C	YMR322C
	YEL039C	YBL043W	YLR377C	YKL178C	YBR296C
	YJL027C	YDL243C	YAL063C-A	YHR096C	YDR034C-A
	YGR213C	YCR021C	YPL130W	YGR110W	YDR281C
	YHR136C	YJL088W	YOL052C-A	YDR277C	YMR323W
	YBR117C	YJL116C	YBR093C	YGR043C	YKR075C
	YER053C-A	YER067W	YIL014C-A	YDR342C	YAR071W
	YOL152W	YJL108C	YHR092C	YKL109W	YIL117C
	YJR047C	YDR380W	YDL181W	YBR054W	YFL014W
	YJL133C-A	YML123C	YAR073W	YGR144W	YNR060W
	YOR161C	YDL133C-A	YPL019C	YDR222W	YBL005W-B
	YHR033W	YAR009C	YHR216W	YNL160W	YOL151W
	5 min (102)	YGL192W	YGL188C-A	YNL042W-B	YPR078C
YHR126C		YAL064W-B	YJR150C	YJR053W	YIL170W
YDR545W		YNR066C	YIR027C	YAL037C-A	YOR134W
YGL240W		YMR118C	YOL104C	YEL070W	YDL218W

Time of stress (# of genes)	Gene name				
	YDL220C	YNL117W	YHR139C	YBR296C	YJL027C
	YCL073C	YNR069C	YPR194C	YDL243C	YMR251W
	YOR177C	YDR034C-A	YMR322C	YMR107W	YDL039C
	YOR107W	YCR107W	YKL217W	YOR338W	YHR136C
	YPR156C	YGL263W	YDR179C	YMR323W	YML123C
	YCR102C	YER071C	YBR093C	YJL116C	YBR117C
	YIL144W	YBR267W	YNL237W	YDL039C	YML043C
	YGR249W	YDL223C	YMR303C	YOR348C	YNL065W
	YBR208C	YDL085C-A	YAR071W	YGR079W	YDL222C
	YGR043C	YLR205C	YNL234W	YLL025W	YHR096C
	YAR073W	YGR144W	YJR047C	YJR115W	YDL048C
	YMR169C	YNR053C	YGL209W	YNR060W	YBR034C
	YKR075C	YPL019C	YHL047C	YBL005W-B	YDL133C-A
	YLR136C	YHL035C	YAR009C	YNR034W-A	YHR216W
	YHR033W	YBR054W	YGR088W	YLR214W	YOR382W
	YBL100W-B	YNL036W	YER053C-A	YHR094C	YOL052C-A
	YOL151W	YNL160W			
	YFR012W	YNR062C	YML066C	YDL220C	YLR341W
	YCR045C	YBL054W	YFR032C	YDL039C	YDR536W
	YLR377C	YPL201C	YOR287C	YNL279W	YHR066W
	YPL277C	YCR072C	YDL218W	YNR066C	YDL167C
	YCR047C	YDR021W	YNL117W	YIL160C	YOR107W
	YHL009W-A	YGL029W	YEL069C	YNL299W	YBR021W
	YAL025C	YNL182C	YMR014W	YBR141C	YPL152W-A
	YOR294W	YPR108W-A	YKR024C	YGL192W	YHR197W
	YOR359W	YJL116C	YGR087C	YIL091C	YBR267W
	YDR545W	YGL078C	YGL259W	YGR283C	YDR184C
	YLR222C	YCL018W	YDR496C	YMR322C	YGR249W
	YPR159C-A	YDL039C	YBR117C	YMR310C	YNL119W
	YCR107W	YHR148W	YLR401C	YKR056W	YOR338W
	YOR348C	YOL015W	YGL209W	YCR014C	YNL065W
	YKR099W	YLR462W	YPL093W	YDR449C	YJL122W
	YDR101C	YER038C	YHR196W	YMR323W	YML043C
	YCR098C	YOL144W	YOR004W	YHR085W	YLR081W
	YDL031W	YMR107W	YJL069C	YBL111C	YNR069C
	YDR299W	YEL070W	YGR079W	YDR545W	YHR184W
	YNR060W	YBL005W-A	YMR303C	YLR196W	YNR053C
	YKL217W	YPR194C	YIL172C	YGL258W-A	YOR032C
	YKR081C	YOR315W	YMR001C-A	YCR020W-B	YHR153C
	YLR009W	YOL104C	YBR184W	YGR159C	YJL157C
	YKL163W	YOR030W	YHR044C	YHL048C-A	YHR052W
	YGR188C	YDR398W	YMR093W	YPL038W-A	YDR492W
	YAL068C	YDR179C	YCR102C	YNR004W	YKL187C
	YPR156C	YNL053W	YDR453C	YAR029W	YJR011C
	YPL166W	YJL108C	YDL048C	YNL110C	YKL093W
	YHL047C	YDL223C	YJR115W	YLR205C	YBR034C
	YGL263W	YIL144W	YER056C	YER071C	YKL009W
	YHR154W	YHR136C	YOL152W	YHR094C	YDL204W
	YDL222C	YHR033W	YDR070C	YAL016C-B	YGR043C
	YMR169C	YML123C	YBR093C	YAR073W	YHR096C
	YDR365C	YJR047C	YAR071W	YOL151W	YDL133C-A
	YNL036W	YHR216W	YBL005W-B	YAR009C	YBL100W-B
	YGL192W	YPL130W	YNL034W	YMR251W	YDR545W
	YFR012W	YOR376W-A	YHR136C	YDR536W	YLR053C
	YCL073C	YEL070W	YFR032C	YPR194C	YDR281C
	YCL058C	YGL263W	YPR156C	YDL039C	YJR153W
	YOR348C	YOR107W	YAR073W	YDR179C	YMR322C
10 min (175)					
40 min (100)					

Time of stress (# of genes)	Gene name				
	YDL214C	YNR060W	YBR093C	YDR534C	YKR083C
	YGR087C	YJR005C-A	YOL152W	YER071C	YBR117C
	YNR014W	YHR043C	YDL039C	YEL039C	YKL220C
	YMR323W	YGR271C-A	YML123C	YGR052W	YAR071W
	YDL085C-A	YGR144W	YDL133C-A	YOR302W	YDR070C
	YDR031W	YDL204W	YHR216W	YMR303C	YOL084W
	YNL237W	YDL222C	YDL227C	YKL043W	YGL255W
	YLR205C	YJL108C	YGR088W	YHR022C	YJL116C
	YLR136C	YBR021W	YDL246C	YGR256W	YHR096C
	YDL223C	YBL005W-B	YAR009C	YCL026C-B	YLR327C
	YGR138C	YOL126C	YER067W	YMR169C	YKL163W
	YMR300C	YDR453C	YHL040C	YCL030C	YHR033W
	YDR399W	YGR248W	YOR161C	YER150W	YBL042C
	YLR359W	YKL216W	YGR043C	YBL100W-B	YOL151W
	YBR054W	YOL052C-A	YHR087W	YHR094C	YNL160W

Table S5 Differentially regulated genes in $\Delta hsp26\Delta hsp42$ strain compared to wt.

Genes with at least two-fold higher or lower RNA level in the KO compared to wt at the respective point in time were selected. See material and methods for exact selection criteria. Time of stress is noted; the total number of genes identified is in parenthesis. Genes are listed with their official gene name.

Time of stress (# of genes)	Gene name				
	YML123C	YHR136C	YAR071W	YOR049C	YBR093C
	YPR194C	YKR075C	YHR092C	YOR273C	YAL037W
	YOL126C	YPL019C	YIL169C	YAR029W	YAR073W
	YKL109W	YHR216W	YJR047C	YPL081W	YBR033W
	YAL016C-B	YDR277C	YJL170C	YDL048C	YDL227C
	YOR344C	YLR466C-B	YKL216W	YAL005C	YAR009C
	YIL013C	YAR015W	YMR120C	YKL183C-A	YHL028W
	YER053C-A	YJR048W	YDR342C	YAR028W	YOR313C
	YAR033W	YAR031W	YOL143C	YNL077W	YLR466C-B
	YJR153W	YGL209W	YLR420W	YPR156C	YMR195W
	YAL001C	YGL009C	YGL037C	YAR020C	YBL005W-B
	YDL133C-A	YER067W	YCR021C	YAL031C	YAL034W-A
	YJL052W	YCL030C	YHR140W	YLR231C	YCL025C
	YFR053C	YAL017W	YAL049C	YHL033C	YIL169C
	YHR160C	YCL027W	YDR258C	YDR380W	YML058W-A
0 min (186)	YGR110W	YDL024C	YLL062C	YHR137W	YGR256W
	YLL060C	YLR011W	YML116W	YLL039C	YJL116C
	YHR209W	YLL061W	YBR203W	YBR284W	YLL052C
	YKL217W	YML131W	YJR078W	YGR043C	YLR004C
	YGL104C	YOL162W	YLL012W	YDL244W	YLR312C
	YLR031W	YLL053C	YKL086W	YML095C	YLR070C
	YLL042C	YGL156W	YKL161C	YDL169C	YML088W
	YDR042C	YBR013C	YHR138C	YDR070C	YBR008C
	YMR189W	YBR047W	YIR039C	YML080W	YJL102W
	YKR076W	YLR014C	YHL030W	YLR015W	YCL049C
	YKR097W	YBL064C	YLR034C	YML093W	YOL163W
	YBL106C	YGR213C	YBR295W	YLR007W	YLL022C
	YLL035W	YLR136C	YLL033W	YLR024C	YML049C
	YML060W	YML071C	YML042W	YML081W	YLL034C
	YPL119C	YML091C	YLL057C	YLR001C	YBR291C
	YBR297W	YML112W	YPL088W	YDR034W-B	YML082W

Time of stress (# of genes)	Gene name				
5 min (268)	YGL192W	YAR035C-A	YLR154W-F	YAR066W	YNL130C-A
	YNL018C	YAL064W-B	YNL018C	YHR021W-A	YJR150C
	YBR072W	YJR114W	YMR279C	YLR462W	YPR194C
	YAL063C-A	YDR545W	YMR018W	YAL037W	YFR032C
	YCL042W	YOR293C-A	YIL169C	YOR376W-A	YAR023C
	YJR153W	YML123C	YCL018W	YOR313C	YAR029W
	YCR014C	YOL013W-A	YLL066W-B	YGL007C-A	YJL219W
	YER188C-A	YHR140W	YPL038W-A	YAR020C	YIL013C
	YOR049C	YPR156C	YAR031W	YHR136C	YAL016C-B
	YBL109W	YAR033W	YBL111C	YDL039C	YOR289W
	YMR107W	YLR466C-B	YLR466C-B	YAR068W	YLL057C
	YLR329W	YPL054W	YAL034W-A	YDL244W	YOR100C
	YAR042W	YJL170C	YLR267W	YLR031W	YHL028W
	YOL162W	YJL213W	YMR075W	YDL024C	YAL010C
	YOR338W	YGR256W	YKL217W	YIL144W	YJL116C
	YAL032C	YBR093C	YMR187C	YDR031W	YAL002W
	YML087C	YAL031C	YAL024C	YML095C	YJR097W
	YHR043C	YDL169C	YML043C	YKL161C	YGR110W
	YDR042C	YMR194C-B	YPL014W	YDL227C	YGL156W
	YBL060W	YBR141C	YML118W	YNL065W	YAR071W
	YPL171C	YOR287C	YLR231C	YAR019C	YPR002W
	YJR048W	YAL058W	YNL095C	YDL085C-A	YAL008W
	YBR203W	YBR284W	YOR304C-A	YNR034W-A	YAL028W
	YGR088W	YAR028W	YGR079W	YAL009W	YAL061W
	YGR043C	YBR230W-A	YHR085W	YDL039C	YAL046C
	YAL055W	YER028C	YCR047C	YHR209W	YLR024C
	YAL041W	YAR073W	YAL034C	YLL052C	YDR406W
	YBL106C	YKR024C	YBR021W	YBL054W	YML099C
	YBR297W	YJR047C	YHR066W	YOR173W	YLR015W
	YBR238C	YNR060W	YLR014C	YBR267W	YML054C
	YAL001C	YGR283C	YER037W	YKR056W	YML113W
	YOR328W	YKL078W	YER053C-A	YML080W	YLL062C
	YLR026C	YLR142W	YML096W	YCR072C	YGL209W
	YLL055W	YAL017W	YNR053C	YBR257W	YNL124W
	YML058W-A	YBL014C	YML097C	YBR047W	YCL054W
	YAL049C	YLL035W	YIL169C	YPL052W	YKL029C
	YML060W	YML088W	YPL019C	YBR271W	YLL012W
	YLL004W	YLL060C	YHL040C	YAR027W	YML109W
	YKR076W	YJL069C	YBL055C	YPL088W	YFR055W
	YHL047C	YJL122W	YBL042C	YHR196W	YOR294W
	YML076C	YML114C	YPL081W	YML112W	YLL022C
	YLL053C	YLL051C	YJL047C-A	YLR136C	YML049C
	YHR216W	YPR112C	YML102W	YBR061C	YBR247C
	YHR148W	YHR052W	YBR125C	YAR015W	YLR420W
	YML082W	YBR004C	YAL060W	YLL011W	YOR004W
	YDL133C-A	YOL155C	YLR011W	YBR034C	YML119W
	YDL031W	YDR101C	YAR009C	YJL052W	YLL061W
YMR120C	YKR075C	YPL093W	YLR023C	YLR002C	
YDR496C	YCL030C	YLR003C	YLR196W	YLR007W	
YAR002C-A	YHL030W	YLL036C	YML116W	YMR105C	
YOL143C	YKL216W	YLL034C	YML093W	YLL008W	
YOR273C	YBL004W	YDR380W	YLR009W	YLR034C	
YBR157C	YHL033C	YBR008C	YEL065W	YLR214W	
YML131W	YNL036W	YDL182W			
10 min (381)	YML123C	YPR194C	YAL016C-B	YAR009C	YAR071W
	YPR159C-A	YHR140W	YPR156C	YAR029W	YPL038W-A
	YAR031W	YAR033W	YBR093C	YIL169C	YJR153W

Time of stress (# of genes)	Gene name				
	YLR466C-B	YDR545W	YLR466C-B	YAR023C	YHR022C
	YAR073W	YHR216W	YAL063C-A	YHR043C	YJR047C
	YHL033C	YMR120C	YOR376W-A	YOR049C	YAR015W
	YIL144W	YDR031W	YDR406W	YLR462W	YAL037W
	YCR020W-B	YOR289W	YAL034W-A	YPL166W	YDL085C-A
	YAL017W	YGR174W-A	YBL111C	YGL007C-A	YJL213W
	YMR001C-A	YDR179C	YHL028W	YBL109W	YIL169
	YIL119C	YJR133W	YAL008W	YHL048C-A	YGR088W
	YLR231C	YAL032C	YAR028W	YIL029C	YNR034W-A
	YJR048W	YAL028W	YDL133C-A	YAR042W	YMR075W
	YAL049C	YAR020C	YCR014C	YMR169C	YAR003W
	YAL047C	YAL031C	YKL061W	YDL154W	YEL069C
	YHR136C	YMR158C-A	YBL111C	YJL170C	YER071C
	YPL060W	YDL214C	YHR044C	YNL146C-A	YAL001C
	YCR101C	YOL155C	YLR218C	YCR100C	YNL211C
	YMR174C	YOL013W-A	YBR033W	YOR386W	YER188C-A
	YAL009W	YAL024C	YER039C-A	YER124C	YHR184W
	YGR035W-A	YGL205W	YOR384W	YCL027W	YAL048C
	YNL202W	YCR107W	YAL010C	YPR192W	YLL066W-B
	YAL046C	YLR081W	YAR050W	YLL066W-B	YAR002C-A
	YBL005W-B	YGR121W-A	YAL061W	YOR040W	YMR133W
	YBL044W	YBR230W-A	YNL128W	YAL041W	YDR357C
	YPL081W	YKL220C	YOR389W	YPL186C	YAL055W
	YHR054C	YHR001W-A	YDR545W	YAL060W	YCL018W
	YPR108W-A	YLR359W	YFR032C-B	YOR315W	YEL061C
	YBR285W	YIL013C	YAR027W	YAR033W	YOL143C
	YER180C-A	YAL011W	YKL183C-A	YLR156W	YAL015C
	YNR004W	YLR024C	YDR361C	YJL010C	YLR016C
	YBR293W	YML071C	YGR158C	YNL002C	YLR026C
	YLR414C	YMR229C	YBR250W	YPL274W	YHR052W
	YLR413W	YML094W	YDL063C	YLL048C	YBR125C
	YOL080C	YNR053C	YIL162W	YOR001W	YNL075W
	YLR023C	YNL112W	YHR089C	YJR115W	YLR063W
	YDR312W	YER006W	YOR340C	YLL052C	YLR276C
	YKR075C	YDR161W	YML109W	YML118W	YGL055W
	YGR110W	YPR144C	YOR328W	YBL106C	YLR074C
	YDR492W	YML051W	YML075C	YLR175W	YDR120C
	YML076C	YNL023C	YLR032W	YLR435W	YBR060C
	YHR065C	YMR093W	YML086C	YML131W	YLR205C
	YHR085W	YLR007W	YML081W	YGL169W	YJL122W
	YDR412W	YLR031W	YML049C	YML108W	YML119W
	YEL065W	YNL313C	YCL054W	YNR064C	YNL061W
	YGR128C	YLR401C	YMR049C	YIL103W	YNL110C
	YML125C	YML064C	YNL248C	YLR018C	YOR056C
	YLR180W	YOL041C	YIL096C	YLR017W	YJR063W
	YPL171C	YJL047C-A	YBR050C	YER082C	YPL043W
	YLL053C	YBR142W	YNL308C	YLL062C	YBR061C
	YBL055C	YHR040W	YLR121C	YKL217W	YBR005W
	YJL033W	YML114C	YML056C	YDL182W	YJR070C
	YDR398W	YDR299W	YLL036C	YNL095C	YBR295W
	YNL117W	YLL055W	YBR004C	YGR079W	YLL051C
	YOR272W	YJL198W	YLR014C	YNL036W	YBR104W
	YDR101C	YPL266W	YGL029W	YPR002W	YDR042C
	YML095C	YNL062C	YDR449C	YLL057C	YOL144W
	YKR056W	YBR034C	YIL127C	YMR014W	YJL069C
	YPL088W	YOL077C	YKL009W	YOR359W	YPR015C
	YBL082C	YML112W	YCR057C	YLR142W	YDL024C

Time of stress (# of genes)	Gene name				
	YML060W	YMR128W	YOL162W	YOR206W	YBR271W
	YBR157C	YLL035W	YHL047C	YBR056W-A	YML113W
	YDL060W	YPL093W	YOR202W	YLL012W	YPL211W
	YML102W	YGR159C	YHR196W	YDR021W	YKL078W
	YOR004W	YLR015W	YNL182C	YDL201W	YBR117C
	YLR011W	YLL022C	YNL065W	YBR238C	YJR041C
	YLR012C	YLR222C	YGR283C	YLR003C	YBR008C
	YBL042C	YLR196W	YLL008W	YLR409C	YNL299W
	YNR060W	YFL023W	YLR002C	YDR184C	YKR081C
	YBR247C	YLL061W	YLL060C	YML116W	YML054C
	YJR097W	YKR024C	YDL031W	YMR310C	YBL004W
	YML080W	YPR112C	YER028C	YIL091C	YML058W-A
	YLL011W	YJL116C	YBR267W	YBL039C	YOR338W
	YBR141C	YHR197W	YDR496C	YML082W	YDL039C
	YHR148W	YJR005C-A	YOR294W	YMR107W	YML093W
	YBR021W	YHR094C	YLR009W	YBR296C	YGL078C
	YLL034C				
	YGL192W	YNL018C	YPL130W	YLR341W	YAR035C-A
	YIL169C	YOR049C	YPR194C	YCL018W	YER153C
	YDR545W	YOR376W-A	YAL037W	YDR281C	YAR050W
	YFR032C	YLR462W	YLR053C	YAR023C	YCR107W
	YML123C	YBL111C	YHR007C-A	YHR136C	YCL058C
	YJR153W	YPR156C	YOL013W-A	YLR466C-B	YDL129W
	YLR466C-B	YPL038W-A	YJL219W	YAR029W	YCR020W-B
	YIL013C	YBR294W	YCR107W	YAL016C-B	YHR044C
	YAL061W	YNL117W	YDL227C	YAR035W	YIL172C
	YLR030W	YAR031W	YNL202W	YHR153C	YIL029C
	YKL107W	YOL131W	YLL046C	YAR033W	YLL038C
	YDR179C	YAL034W-A	YAR073W	YAL047C	YLL057C
	YNL277W	YHR043C	YJL088W	YCL027W	YDL039C
	YMR006C	YAR003W	YOL069W	YJL219W	YOL162W
	YGR230W	YJL170C	YKL217W	YMR075W	YMR169C
	YBR182C	YBR203W	YBL111C	YAL031C	YLR012C
	YDR182W-A	YLR054C	YBR117C	YAL025C	YAL024C
	YAL010C	YEL061C	YBR297W	YAR028W	YER071C
	YER061C	YAR042W	YLR174W	YJR005C-A	YJL153C
	YCR102C	YHR140W	YAR008W	YAL056W	YBL106C
40 min (268)	YDL024C	YML087C	YAL059W	YGR271C-A	YBR284W
	YAR033W	YAR071W	YML095C	YBR238C	YER053C-A
	YIL139C	YHR154W	YLL063C	YDL085C-A	YLL052C
	YDR031W	YAL033W	YBR296C	YLR231C	YLR070C
	YML118W	YOR289W	YLL062C	YNR034W-A	YKL086W
	YJL213W	YAL019W	YNL141W	YHR216W	YHL024W
	YLL061W	YGR110W	YDR222W	YIL169C	YAL041W
	YDL133C-A	YAL001C	YLR205C	YDL039C	YAL008W
	YAL017W	YOL058W	YAL046C	YOR273C	YGL045W
	YLR121C	YGR108W	YLR136C	YJR080C	YKL043W
	YLR031W	YLL035W	YHR054C	YLR015W	YOR338W
	YBL046W	YBR085W	YMR316W	YBR212W	YLR026C
	YCR097W	YJR048W	YLR413W	YAR007C	YLL018C-A
	YML054C	YJL047C-A	YBR295W	YBR005W	YDR089W
	YLR014C	YML058W-A	YLL022C	YOL155C	YML088W
	YBR021W	YBR194W	YML113W	YHL040C	YLL060C
	YKL006C-A	YAL049C	YLL019C	YMR246W	YPR002W
	YPL019C	YDR441C	YLR016C	YML119W	YBR047W
	YJR025C	YLR262C-A	YML120C	YAR009C	YLL058W
	YLL053C	YCL030C	YKL163W	YLR006C	YBR056W-A

Time of stress (# of genes)	Gene name				
	YJL116C	YBL089W	YBR227C	YML082W	YML102W
	YAR015W	YAR027W	YGL156W	YBL082C	YML114C
	YML076C	YBR008C	YBR241C	YKL029C	YAL007C
	YCL049C	YML049C	YBR267W	YCL026C-B	YBL016W
	YLL034C	YLR011W	YML064C	YLR002C	YDR342C
	YDR399W	YML112W	YBL005W-B	YBR125C	YLL012W
	YAR002C-A	YLR001C	YML071C	YLL036C	YLR003C
	YML107C	YLR023C	YML093W	YAL023C	YLL027W
	YML091C	YML053C	YML051W	YLR005W	YOL151W
	YBL078C	YLL056C	YLR359W	YBL042C	YMR011W
	YML057W	YER150W	YLL029W	YLL031C	YLR009W
	YML131W	YML075C	YOL121C	YPL111W	YLR034C
	YLL040C	YDR380W	YLR438W	YHR137W	YBL064C
	YBL075C	YML125C	YER103W		

Table S6 Differentially regulated genes in Δ hsp12 strain compared to wt.

Genes with at least two-fold higher or lower RNA level in the KO compared to wt at the respective point in time were selected. See material and methods for exact selection criteria. Time of stress is noted; the total number of genes identified is in parenthesis. Genes are listed with their official gene name.

Time of stress (# of genes)	Gene name				
0 min (100)	YHL047C	YDL181W	YLR136C	YNL117W	YOR382W
	YOR384W	YJL037W	YOL052C-A	YKL178C	YOR383C
	YMR251W	YCL073C	YOL158C	YLR205C	YNL160W
	YDR380W	YFL011W	YHL035C	YJR078W	YOR100C
	YFL012W	YHL040C	YFR053C	YLR377C	YIR028W
	YOR381W	YDR534C	YIR027C	YBR203W	YDR342C
	YKL221W	YJL103C	YLL052C	YAR068W	YAL063C-A
	YNR060W	YBR047W	YGR256W	YBR054W	YHR092C
	YIL014C-A	YHR015W	YOL058W	YDR270W	YDL244W
	YGR043C	YKL217W	YEL024W	YFL030W	YOL083W
	YBR299W	YPL171C	YLR327C	YHR176W	YLR126C
	YFL059W	YLL053C	YGL146C	YML054C	YER058W
	YHR137W	YBR072W	YLR312C	YGR110W	YJR079W
	YMR189W	YHR136C	YML123C	YAR071W	YBR093C
	YAR073W	YHR216W	YOL155C	YIL169C	YFR032C
	YFL014W	YPL019C	YPR194C	YPL130W	YBL043W
	YDR281C	YDL171C	YGL009C	YOR107W	YCR005C
	YAR009C	YCR021C	YJL133C-A	YKR075C	YBL005W-B
	YBR033W	YER153C	YNR056C	YJL144W	YPR156C
	YIL117C	YKR093W	YER081W	YOL013W-A	YPR036W-A
5 min (135)	YFL014W	YML123C	YAR071W	YHR136C	YBR093C
	YAR073W	YHR216W	YPR194C	YIL169C	YDL171C
	YPR156C	YCL018W	YOL155C	YGL009C	YAR009C
	YBL005W-B	YOR028C	YGR138C	YPL019C	YOL013W-A
	YDR179C	YDL214C	YHR140W	YOR044W	YIL029C
	YPR035W	YNR056C	YJL012C	YNL277W-A	YOR293C-A
	YBR203W	YJR047C	YGL222C	YHL028W	YKL062W
	YDL133C-A	YHR050W-A	YIR018C-A	YLL025W	YPL189C-A
	YBR085W	YAL016C-B	YKL221W	YHR015W	YOR120W
	YML095C	YGL062W	YLR411W	YJL127C	YDR476C
	YDL048C	YNR034W-A	YDR453C	YOL052C-A	YHR176W
	YJL037W	YDR019C	YIL014C-A	YJL103C	YLR377C

6. Appendix

	YNL160W	YOL058W	YKR024C	YPL052W	YNR053C
	YOL162W	YPL156C	YJL194W	YLR042C	YIL150C
	YDL181W	YCL026C-A	YNL279W	YDL220C	YBR047W
	YDR380W	YPL093W	YAR068W	YEL065W	YKL217W
	YBL043W	YOR381W	YGL236C	YFL041W	YML080W
	YHR177W	YCL027W	YEL057C	YGR256W	YFR023W
	YDL039C	YOR338W	YDR270W	YNL237W	YBR034C
	YDL218W	YGR043C	YPR124W	YOR381W-A	YBR267W
	YGR079W	YKL178C	YJR078W	YDL244W	YJL027C
	YBR054W	YOR177C	YLR214W	YFL012W	YJL116C
	YFL011W	YER028C	YNL036W	YNL065W	YCL073C
	YKR075C	YPL171C	YDR534C	YOR383C	YBR117C
	YOL152W	YDL039C	YOL158C	YNL117W	YGL209W
	YOR384W	YIR027C	YHL035C	YHL040C	YMR251W
	YOR382W	YLR136C	YLR205C	YNR060W	YHL047C
	YHL047C	YGL209W	YBL043W	YLR205C	YNR060W
	YER028C	YCR072C	YJR005C-A	YDR534C	YDL039C
	YBR117C	YHL040C	YJL116C	YKR024C	YGL078C
	YHR094C	YPL171C	YKR075C	YGR159C	YNL065W
	YDR496C	YHR148W	YLR222C	YMR310C	YOR359W
	YJL157C	YKL178C	YCL073C	YDL167C	YNL117W
	YPL093W	YDR449C	YNL036W	YMR251W	YHL035C
	YOR294W	YIL091C	YGR283C	YNR053C	YDL031W
	YNL299W	YCL026C-B	YAR068W	YBR267W	YOL158C
	YLR042C	YHR196W	YLR009W	YJL122W	YOR383C
	YCR047C	YKR056W	YPR002W	YOR382W	YMR014W
	YBR050C	YBR141C	YCL026C-A	YGR079W	YKL043W
	YBR296C	YJL108C	YLR136C	YGL029W	YOR338W
	YHR052W	YFL023W	YNL119W	YGR239C	YGR035C
	YJR078W	YOR303W	YDR399W	YOL058W	YDR019C
	YKL221W	YHR085W	YNL078W	YDR184C	YLR196W
10 min (169)	YBR034C	YOR384W	YOL019W	YJL069C	YKR081C
	YDR476C	YCL027W	YNL053W	YFL059W	YDL048C
	YLR401C	YDR453C	YDL127W	YGL236C	YJR147W
	YFR034C	YEL057C	YDL244W	YGR043C	YKL220C
	YAL063C-A	YGL016W	YPL018W	YCR097W	YIR015W
	YNR003C	YER071C	YGR088W	YPR035W	YJR047C
	YMR128W	YOL069W	YDR234W	YBR285W	YBR018C
	YPL189C-A	YAR015W	YMR279C	YHR140W	YGR138C
	YOR028C	YIL029C	YHR050W-A	YBR203W	YOL155C
	YOR178C	YNL194C	YCL018W	YGR245C	YJL200C
	YHL028W	YBR184W	YOR044W	YDL148C	YMR158C-A
	YGL158W	YJR153W	YAR029W	YCR098C	YHR043C
	YGR204C-A	YPR159C-A	YIL169C	YLR156W	YHR096C
	YPL166W	YCR020W-B	YDL133C-A	YAL016C-B	YGL009
	YMR001C-A	YHR136C	YDR179C	YBL005W-B	YJR016C
	YPR194C	YGL007C-A	YOL013W-A	YGR174W-A	YPL038W-A
	YAR009C	YDL171C	YBR093C	YOR032C	YAR071W
	YPR156C	YHR216W	YAR073W	YML123C	
	YJR005C-A	YHL047C	YLR136C	YLR205C	YDL227C
	YHL040C	YHR087W	YLL052C	YCL026C-B	YDR534C
	YOL158C	YNR034W-A	YKL220C	YAR068W	YHL035C
	YPL171C	YBR291C	YDL039C	YOL052C-A	YKL178C
40 min (116)	YOR120W	YLL053C	YHR092C	YGR234W	YOR306C
	YKL043W	YBR117C	YDR453C	YER150W	YER028C
	YGR248W	YDR441C	YNL237W	YMR058W	YJR078W
	YFR017C	YDR516C	YDR270W	YDL244W	YCR021C
	YJL219W	YER053C	YLR466C-B	YOR383C	YFR012W-A
	YFL012W	YER158C	YAL063C-A	YKL107W	YNL160W

6. Appendix

YDR391C	YML131W	YDL181W	YDL247W	YMR090W
YEL065W	YBR050C	YOR381W	YPL247C	YOR173W
YKR049C	YCL018W	YDR399W	YLL013C	YCR097W
YJL045W	YBR093C	YPL038W-A	YPL019C	YOR044W
YLR053C	YBR285W	YMR158C-A	YGL007C-A	YGL101W
YJR153W	YDR275W	YDR216W	YER187W	YDR031W
YER071C	YIL169C	YEL071W	YGR286C	YIL029C
YLR012C	YBL075C	YDL171C	YGR243W	YCR020W-B
YBR244W	YCL030C	YGL009C	YKL029C	YOL152W
YIL169C	YFR032C	YOL013W-A	YAL016C-B	YDR179C
YBL005W-B	YPR156C	YOR376W-A	YCR005C	YJL133C-A
YDL133C-A	YAR071W	YAR009C	YPR194C	YDR281C
YHR096C	YPR002W	YAR073W	YHR216W	YML123C
YHR136C				

6.2 Proteome data on the heat stress response

Table S7 Enriched and diminished proteins after 10 min of 37 and 42°C stress.

Two-fold higher or lower protein counts were set as threshold. Proteins are listed with their average fold change compared to unstressed control cells, standard deviation across three biological replicates and the p-value indicating significance of the fold change ($p < 0.05$).

Protein ID	\log_2 x/ 25°C	St. Dev.	p-value	Protein ID	\log_2 x/25°C	St. Dev	p-value
Enriched protein after 10min 37°C							
TMA10	4.34	1.66	0.010659	HBT1	1.10	0.27	0.001991
BDH2	2.66	0.21	0.000025	HXT7	1.05	0.08	0.000017
SSA4	2.58	0.12	0.000004	SOL4	0.99	0.32	0.006213
ARO10	1.56	0.47	0.004455	STF2	0.96	0.11	0.000117
PHM8	1.45	0.20	0.000233	HSP42	0.95	0.32	0.006401
CWP1	1.44	0.16	0.000092	PGM2	0.95	0.26	0.002989
HSP104	1.41	0.08	0.000008	YGR250C	0.83	0.18	0.001356
YBR085C-A	1.30	0.16	0.000149	FES1	0.82	0.05	0.000007
HSP78	1.29	0.07	0.000007	GNP1	0.82	0.24	0.003919
RTC3	1.25	0.28	0.001597	HSP12	0.78	0.30	0.010608
YPR036W-A	1.24	0.17	0.000239	AIM17	0.77	0.25	0.006105
CYC7	1.17	0.24	0.001006	HSP82	0.77	0.19	0.002333
SSA3	1.14	0.64	0.036896	PIR1	0.75	0.06	0.000036
HSP150	1.13	0.14	0.000139	MET3	0.75	0.36	0.022144
Enriched Proteins after 10 min 42°C							
TMA10	4.14	1.19	0.003815	SSA4	1.35	0.29	0.001351
YPR036W-A	1.66	0.29	0.000582	GNP1	1.08	0.08	0.000024
Diminished proteins after 10 min 42°C							
YER163C	-2.99	0.24	0.000027	NOP15	-1.26	0.35	0.000604
NOP4	-2.49	0.27	0.000087	NOP58	-1.23	0.08	0.003307
ETT1	-2.40	0.42	0.000588	MLP1	-1.23	0.16	0.000013
IOC4	-2.35	3.01	0.247663	SQS1	-1.22	0.21	0.000173
SDA1	-2.34	0.39	0.000504	NOP56	-1.20	0.05	0.000555
YDR131C	-2.12	0.30	0.000264	TOF1	-1.18	0.44	0.000002
RMT2	-2.12	0.22	0.000072	NGL2	-1.16	0.25	0.009823
CRT10	-2.11	0.31	0.000309	NUM1	-1.15	0.14	0.001219
MMS1	-1.97	0.31	0.000390	PNO1	-1.15	0.16	0.000127
PMU1	-1.95	0.09	0.000003	BIM1	-1.14	0.45	0.000254
SCP1	-1.92	0.23	0.000124	GOS1	-1.13	2.00	0.011715
MRN1	-1.87	0.27	0.000268	RPF2	-1.12	0.16	0.382358
PPM2	-1.87	0.03	0.000000	YLR126C	-1.11	0.07	0.000283
TSR4	-1.87	0.12	0.000012	CIC1	-1.11	0.25	0.000009
FAP7	-1.77	0.22	0.000150	RRP5	-1.09	0.19	0.001547
ALT2	-1.62	1.35	0.105908	GBP2	-1.09	0.15	0.000593
RKM3	-1.62	0.32	0.000968	NOC2	-1.09	0.12	0.000217
NOG1	-1.61	0.30	0.000711	NOP7	-1.07	0.25	0.000093
RNH70	-1.55	1.36	0.118898	YBR062C	-1.07	0.25	0.001675
RLP7	-1.53	0.22	0.000272	CDC45	-1.06	0.46	0.001657
MKT1	-1.47	0.23	0.000361	ECM16	-1.06	0.31	0.016445

Protein ID	\log_2 x/25°C	St. Dev.	p-value	Protein ID	\log_2 x/25°C	St. Dev.	p-value
FAU1	-1.47	0.08	0.000007	HAS1	-1.06	0.20	0.003882
NSA2	-1.40	0.14	0.000063	PRP43	-1.03	0.08	0.000809
NUG1	-1.39	0.21	0.000354	DPH1	-1.03	0.15	0.000026
PET127	-1.36	0.18	0.000205	DBP3	-1.02	0.14	0.000325
ENP1	-1.36	0.28	0.001116	SFB2	-1.01	0.23	0.000215
NOG2	-1.35	0.32	0.001810	STE23	-1.00	0.15	0.001576
YDR161W	-1.32	0.19	0.000256	BUD20	-1.00	0.13	0.000359
RPF1	-1.30	0.42	0.005970	RLP24	-1.30	0.23	0.000178

Table S8 Class-I P-sites with a differential phosphorylation state after 10 min 37°C and 42°C. P-sites with a change in the phosphorylation state of at least two-fold were selected. Proteins are listed with their P-sites, average fold change compared to unstressed control cells, standard deviation across three biological replicates and the p-value indicating significance of the fold change ($p < 0.05$). S= Serin, T= Threonine.

P-Site	\log_2 X/25°C	St. Dev.	p-value	P-Site	\log_2 X/25°C	St. Dev.	p-value
Quantified class I P-sites after 10 min 37°C							
SEC31_S1053	2.86	0.51	0.000617	RGT1_S205	1.17	0.31	0.002964
BTN2_S379	2.73	0.34	0.000147	SKO1_T113	1.16	0.85	0.076536
PAB1_S119	2.69	0.56	0.001108	UPC2_T122	1.13	0.38	0.006454
HSP104_S206	2.08	0.63	0.004708	SKY1_S4	1.13	0.39	0.007507
CIN5_S41	2.03	0.30	0.000291	TPS3_S148	1.12	0.04	0.000001
HSP78_S406	2.00	0.30	0.000301	YNR014W_S136	1.12	0.17	0.000357
GIP3_T264	1.98	0.18	0.000046	AIM3_T805	1.11	0.84	0.084570
PAB1_T102	1.97	0.34	0.000525	KEL1_S1003	1.10	0.42	0.010795
RTS3_S216	1.85	0.91	0.025018	SMY2_S96	1.09	0.64	0.041370
SKY1_S453	1.78	0.68	0.010763	TSL1_S129	1.09	0.02	0.000000
YPR036W-A_S32	1.64	0.41	0.002329	YLR177W_S31	1.07	0.35	0.006001
MLF3_S322	1.64	0.60	0.009229	NNK1_S426	1.06	0.32	0.004668
SBP1_T91	1.53	0.02	0.000000	HSL1_S682	1.05	0.62	0.042280
PIB2_S113	1.49	0.57	0.010500	PIK1_S384	1.05	0.63	0.045171
CDC37_S136	1.45	0.23	0.000406	MBF1_S143	1.05	0.05	0.000002
SCP160_T50	1.44	0.18	0.000156	BDF2_S264	1.04	0.46	0.017713
KEL1_S1022	1.44	0.37	0.002456	ALY2_T915	1.04	0.24	0.001717
RTG3_T150	1.44	0.26	0.000669	PTP3_S368	1.04	0.73	0.069917
SKY1_S3	1.43	0.50	0.007517	SKY1_S445	1.04	0.51	0.024290
EDE1_S848	1.42	0.16	0.000096	EAP1_S387	1.03	0.56	0.032360
SKY1_S449	1.41	0.56	0.012066	ASK10_S1095	1.03	0.68	0.057886
BAP2_S3	1.39	0.25	0.000615	UGP1_S79	1.02	0.28	0.003069
SCP160_S87	1.27	0.57	0.018450	VID27_S222	1.02	0.17	0.000529
TIF5_S268	1.26	0.38	0.004678	SEC9_S192	1.02	0.48	0.020377
RLM1_S377	1.26	0.08	0.000011	HSP42_S223	1.02	0.79	0.089809
YLR177W_T235	1.25	0.27	0.001291	POL12_T124	-1.44	0.59	0.013546
MLF3_S320	1.23	0.55	0.018059	SLA2_S308	-1.32	0.47	0.008196

P-Site	log ₂ X /25°C	St. Dev.	p-value	P-Site	log ₂ X /25°C	St. Dev.	p-value
EDE1_S853	1.22	0.10	0.000035	EIS1_S649	-1.20	0.45	0.010244
RCN2_S150	1.21	0.20	0.000433	ALR1_S176	-1.14	0.43	0.010328
ICS2_S30	1.20	0.89	0.078010	STB1_S89	-1.10	0.32	0.004018
YLR177W_S34	1.19	0.17	0.000267	KCC4_S675	-1.09	0.26	0.001849
RSF2_S303	1.18	0.43	0.008569	NBA1_S194	-1.05	0.26	0.002043
Quantified class I P-Sites after 10 min 42°C							
ZUO1_S67	4.64	0.20	0.000002	SYH1_S687	1.20	0.57	0.021364
PAB1_S119	4.12	0.83	0.001005	BBC1_T894	1.18	0.37	0.005110
PAB1_T102	4.11	0.16	0.000001	MLF3_S14	1.18	0.89	0.083065
GIP3_T264	3.89	0.48	0.000154	SSB1_S548	1.18	0.10	0.000036
EDE1_S853	3.56	0.23	0.000011	VTC2_S187	1.18	0.40	0.006953
SKY1_S453	3.24	0.63	0.000857	VID27_S222	1.16	0.24	0.001061
YDR186C_S542	3.11	1.22	0.011734	YDR348C_T23	1.16	0.24	0.001117
SEC31_S1053	3.09	0.71	0.001624	VHS2_S303	1.16	0.08	0.000012
SBP1_T91	3.04	0.25	0.000031	RGC1_S1048	1.15	0.62	0.033018
SKY1_S3	2.98	0.91	0.004703	ROM2_S193	1.14	0.08	0.000013
SKY1_S449	2.87	0.36	0.000167	PIB2_S268	1.14	0.19	0.000517
TCO89_S397	2.83	1.63	0.039808	BNA7_S9	1.14	0.36	0.005402
PIB2_S113	2.81	0.58	0.001071	ZRG8_S407	1.13	0.50	0.016713
RTG3_T150	2.77	0.24	0.000036	ERG20_S317	1.12	0.02	0.000000
CPR1_S49	2.71	0.14	0.000005	BIT61_S144	1.10	0.04	0.000001
TIF5_S268	2.54	0.52	0.001026	LSB3_T298	1.09	0.24	0.001315
RTS3_S216	2.54	0.58	0.001645	BDP1_S178	1.09	0.06	0.000005
NMD3_S427	2.50	0.96	0.010698	LTE1_S938	1.09	0.35	0.005523
BTN2_S379	2.48	0.40	0.000413	POP4_S53	1.09	0.33	0.004830
SKY1_S4	2.38	1.26	0.030998	ZRT3_S178	1.08	0.19	0.000625
SEC9_S192	2.33	0.35	0.000324	SEC9_S190	1.08	0.25	0.001682
GCS1_S260	2.32	0.44	0.000816	LTE1_S937	1.07	0.26	0.002158
CDC37_S136	2.28	0.15	0.000014	UGP1_S11	1.07	0.33	0.005210
EDE1_S848	2.23	0.12	0.000006	YLR177W_S34	1.06	0.21	0.000957
ASK10_S1095	2.22	0.19	0.000038	PIL1_S41	1.06	0.09	0.000042
YPR036W-A_S32	2.19	0.38	0.000535	NET1_S1084	1.05	0.12	0.000108
SCP160_S87	2.16	0.72	0.006493	VHS2_S172	1.05	0.26	0.002136
PDS1_S98	2.13	0.18	0.000034	REG1_S977	1.05	0.27	0.002587
RLM1_S377	2.12	0.16	0.000022	GAL83_S180	1.04	0.36	0.007315
KIN4_S450	2.09	0.89	0.014972	AIM29_S78	1.04	0.12	0.000124
PIK1_S384	2.09	0.91	0.016239	CTF4_S463	1.03	0.32	0.005292
HSP78_S406	1.98	0.25	0.000167	MLF3_S156	1.03	0.57	0.035148
SKY1_S445	1.97	0.41	0.001103	SGF73_T202	1.02	0.29	0.003879
SMY2_S96	1.96	0.36	0.000707	INP53_S1031	1.02	0.51	0.025911
YDR239C_S546	1.95	1.13	0.040394	SUR1_T351	1.02	0.15	0.000338
SKP1_T177	1.95	0.53	0.003242	SPA2_S970	1.01	0.20	0.000863
HSP104_S206	1.94	0.40	0.001076	BEM2_S1012	-1.00	0.13	0.000164
PXL1_S63	1.94	0.10	0.000004	FIN1_S74	-1.01	0.05	0.000006
RDL1_S90	1.91	0.62	0.005983	BEM1_S461	-1.02	0.34	0.006483

P-Site	log ₂ X/25°C	St. Dev.	p-value	P-Site	log ₂ X/25°C	St. Dev.	p-value
BAP2_S3	1.87	0.11	0.000009	BOI2_S519	-1.04	0.07	0.000010
BNI4_S346	1.87	0.49	0.002756	EDE1_S1087	-1.04	0.27	0.002685
AIM3_T805	1.85	0.53	0.003819	RPL24A_T83	-1.06	0.42	0.012037
LYP1_S64	1.84	0.02	0.000000	SBE2_S474	-1.07	0.29	0.003031
EFR3_S684	1.82	0.34	0.000772	DRE2_S206	-1.08	0.23	0.001220
TCO89_S290	1.81	0.05	0.000000	PBP1_S436	-1.09	0.44	0.012907
SCP160_T50	1.81	0.17	0.000049	NOG2_S60	-1.09	0.19	0.000543
NBP2_S102	1.79	0.05	0.000000	UBP6_S298	-1.13	0.11	0.000051
PXL1_S43	1.79	0.16	0.000040	TPS3_S235	-1.14	0.23	0.000977
KEL1_S1022	1.79	0.24	0.000204	PTC2_S327	-1.14	0.20	0.000623
PRK1_S402	1.78	0.27	0.000325	TCB3_S112	-1.14	0.22	0.000839
HSL1_S682	1.76	0.40	0.001565	OYE2_S353	-1.14	0.15	0.000176
SLA1_T984	1.73	0.38	0.001412	ESC1_S1326	-1.15	0.08	0.000015
YNG2_S188	1.73	1.27	0.077470	GPD2_S75	-1.16	0.14	0.000144
CAJ1_S266	1.71	0.40	0.001821	NOP53_S31	-1.19	0.13	0.000092
PEX19_S304	1.67	0.19	0.000114	NUP60_S162	-1.21	0.25	0.001193
NNK1_S426	1.66	0.08	0.000003	HSL1_S57	-1.22	0.32	0.002799
RGT1_S205	1.65	0.22	0.000197	BUD3_S1500	-1.23	0.15	0.000129
RSF2_S303	1.62	0.17	0.000072	CDC3_S498	-1.23	0.83	0.062398
TAO3_S2355	1.62	0.13	0.000025	KEL2_T455	-1.26	0.19	0.000336
MLF3_S320	1.62	0.54	0.006473	MON2_S564	-1.26	0.25	0.000971
IGO2_S63	1.60	0.29	0.000623	NAP1_S140	-1.26	0.30	0.001883
PIB2_S225	1.60	0.31	0.000837	BIR1_T694	-1.26	0.29	0.001667
YKR023W_S457	1.59	0.16	0.000059	STB1_S72	-1.27	0.31	0.002032
YMR102C_S712	1.59	1.12	0.069081	FAS2_S1872	-1.28	0.33	0.002526
MLF3_S322	1.57	0.37	0.001874	BUD3_S1501	-1.30	0.03	0.000000
NUM1_S62	1.55	0.14	0.000040	RAD9_Y135	-1.30	0.65	0.024981
GNP1_S124	1.53	0.21	0.000219	SEC16_S678	-1.30	0.24	0.000718
HAA1_S258	1.53	0.26	0.000532	BEM1_S458	-1.31	0.45	0.007395
PAM1_S659	1.51	0.32	0.001201	ZRG8_S354	-1.32	0.15	0.000111
NET1_S1082	1.50	0.31	0.001118	RCN2_S186	-1.33	1.05	0.092297
STE20_T167	1.49	0.26	0.000552	NBA1_S194	-1.35	0.47	0.007620
ZUO1_S206	1.48	0.33	0.001434	BIM1_S148	-1.36	0.44	0.005996
KEL1_S1003	1.47	0.24	0.000435	INP52_S1016	-1.41	0.32	0.001665
TAO3_S2352	1.47	0.36	0.002029	SGF29_S139	-1.42	0.39	0.003124
EDE1_S931	1.46	0.40	0.003310	DSF2_S469	-1.42	0.05	0.000001
MBF1_S143	1.45	0.09	0.000010	MYO1_S1171	-1.44	0.19	0.000192
ROD1_S725	1.43	0.49	0.007230	BOI2_S723	-1.44	0.56	0.010954
CHS3_S537	1.43	0.82	0.039734	MRH1_S289	-1.46	0.29	0.000916
TIF3_S71	1.42	0.25	0.000590	GLC8_S12	-1.47	0.28	0.000790
ALY2_T915	1.41	0.08	0.000007	SEC31_S980	-1.48	0.31	0.001143
SSB1_S591	1.41	0.35	0.002298	SEC3_S256	-1.48	0.20	0.000230
SSB2_S591	1.41	0.35	0.002298	TAO3_S1144	-1.49	0.21	0.000252
OAF1_T270	1.40	0.31	0.001386	PIK1_S10	-1.51	0.25	0.000492
YJR098C_S60	1.38	0.57	0.013591	ALR1_S176	-1.54	0.37	0.002052

P-Site	log ₂ X /25°C	St. Dev.	p-value	P-Site	log ₂ X /25°C	St. Dev.	p-value
FPK1_S300	1.36	0.38	0.003511	YEL043W_S802	-1.57	0.21	0.000205
GLN3_S273	1.36	0.09	0.000011	GIN4_S460	-1.58	0.02	0.000000
RTG3_S142	1.36	0.02	0.000000	MRH1_T295	-1.58	0.39	0.002164
EAP1_S387	1.36	0.57	0.014263	HAA1_S231	-1.59	0.62	0.011097
OLA1_S67	1.35	0.26	0.000886	SHS1_S447	-1.62	0.21	0.000189
EDE1_S1343	1.35	0.05	0.000001	NOT3_S344	-1.64	0.25	0.000320
ICS2_S30	1.34	0.86	0.054504	FBA1_T358	-1.68	0.10	0.000009
BNI4_S36	1.33	0.26	0.000841	ILV5_S174	-1.69	0.08	0.000004
NBA1_S117	1.32	0.35	0.002817	MDG1_S291	-1.70	0.15	0.000037
AIM21_S36	1.30	0.26	0.000971	NOT3_T454	-1.72	0.42	0.002064
CIN5_S41	1.29	0.53	0.013288	VTC3_S592	-1.82	1.05	0.039502
DRE2_S158	1.29	0.45	0.007747	MDG1_S288	-1.83	0.28	0.000325
YPL247C_S65	1.28	0.43	0.006553	SEC3_S254	-1.84	0.17	0.000008
SAK1_S737	1.28	0.42	0.006334	YMR111C_S42	-1.84	0.28	0.000060
VTS1_S311	1.27	0.41	0.006070	AMN1_S33	-1.85	0.79	0.003405
SIP1_S302	1.27	0.49	0.010750	STB1_S89	-1.90	0.52	0.000652
UPC2_T122	1.25	0.37	0.004288	YDR239C_S342	-1.94	0.42	0.000272
TCO89_S287	1.25	0.19	0.000313	YDR239C_S456	-1.99	0.53	0.000625
RCN2_S150	1.25	0.92	0.078398	SLA2_S308	-2.06	0.54	0.000587
ASK10_S1045	1.23	0.39	0.005268	MAD1_T502	-2.18	0.35	0.000090
YLR177W_T235	1.23	0.34	0.003133	POL12_S126	-2.57	0.34	0.000052
BLM10_S11	1.22	0.41	0.006909	KCC4_S675	-2.58	0.27	0.000023
YNG2_T185	1.22	0.17	0.000262	SRL3_S212	-2.76	0.32	0.000035
REB1_S386	1.22	0.42	0.007072	BEM3_S327	-2.76	1.55	0.013723
PBS2_S9	1.22	0.26	0.001171	ZUO1_S50	-2.81	0.21	0.000006
ENT2_T479	1.22	0.24	0.000933	NOT3_S450	-2.86	0.13	0.000001
YDR239C_S543	1.21	0.38	0.005442	POL12_S124	-3.50	0.99	0.001429
RAM1_S38	1.20	0.32	0.002960				

Table S9 Enriched and diminished proteins after 30 min of 37°C.

Two-fold higher or lower protein counts were set as threshold. Proteins are listed with their average fold change compared to unstressed control cells, standard deviation across three biological replicates and the p-value indicating significance of the fold change ($p < 0.05$).

Protein ID	log ₂ 37 /25°C	St. Dev.	p-value	Protein ID	log ₂ 37 /25°C	St. Dev.	p-value
Enriched proteins after 30 min 37°C							
ADP1	1.01	0.16	0.008283	OM45	3.26	0.18	0.001069
AGX1	1.09	0.61	0.090866	OPI10	2.82	0.19	0.001509
AHA1	1.81	0.52	0.026439	PBI2	1.10	0.25	0.016850
AIM17	3.01	0.30	0.003332	PEP4	1.01	0.19	0.011524
AIM25	1.01	0.61	0.103210	PET10	1.10	0.20	0.010473
ALD3	6.40	0.23	0.000443	PFK26	1.42	0.19	0.005729
ALD4	2.94	0.21	0.001720	PGM2	4.83	0.28	0.001116
AMS1	1.17	0.60	0.077913	PHM8	4.05	0.39	0.003039

Protein ID	log ₂ 37/25°C	St. Dev.	p-value	Protein ID	log ₂ 37/25°C	St. Dev.	p-value
APJ1	4.43	0.55	0.005027	PIG2	2.32	0.27	0.004454
ARO10	6.52	0.47	0.001711	PLB3	1.29	0.75	0.096031
ARO9	3.47	0.25	0.001706	PLB3	1.29	0.75	0.096031
ATH1	2.46	0.21	0.002526	PNC1	2.64	0.16	0.001279
BDH1	1.64	0.05	0.000304	POM33	1.14	0.43	0.043445
BDH2	6.69	0.48	0.001715	PRB1	1.08	0.49	0.061797
CAT2	4.79	3.75	0.157280	PRX1	1.05	0.09	0.002192
CIN5	3.54	0.45	0.005316	PST1	2.68	0.37	0.006440
CIT1	1.18	0.16	0.006467	PTR2	1.00	0.77	0.152835
CMK1	1.20	0.25	0.014093	RAD16	1.01	0.44	0.059190
COQ4	1.20	0.78	0.117403	RCN2	1.14	0.14	0.005189
CPR6	1.94	0.40	0.013748	RGII	6.56	0.47	0.001700
CRG1	2.94	0.58	0.012657	RIM4	3.21	0.72	0.016168
CTH1	2.59	0.47	0.010858	RNY1	1.37	0.17	0.004938
CTT1	6.93	1.22	0.010223	RRD2	1.07	0.17	0.008132
CWP1	3.66	0.74	0.013511	RTC3	6.03	0.93	0.007884
CYB2	3.42	1.52	0.059738	RTK1	1.00	1.19	0.284253
DCS1	1.45	0.09	0.001279	RTN2	7.26	0.84	0.004478
DCS2	3.60	0.23	0.001396	SDS24	2.03	0.39	0.012245
ECM21	1.65	0.19	0.004212	SIC1	2.09	0.38	0.010871
EMP46	1.12	0.56	0.075454	SIS1	1.42	0.16	0.004153
ERO1	1.06	0.56	0.080995	SOL4	5.08	0.36	0.001634
FES1	1.53	0.33	0.014920	SPE1	1.00	0.49	0.072121
FIS1	1.10	0.39	0.039857	SPT23	1.15	0.42	0.041791
FMP45	5.26	0.53	0.003409	SSA1	1.87	0.22	0.004654
GAD1	2.39	0.71	0.027886	SSA3	4.35	1.49	0.036858
GCY1	5.37	0.26	0.000799	SSA4	8.37	1.09	0.005640
GDB1	2.37	0.47	0.012879	SSE2	2.73	0.20	0.001743
GGA1	1.19	0.20	0.009030	STF2	4.55	0.07	0.000077
GLC3	1.13	0.67	0.098812	STI1	1.12	0.19	0.009508
GLG1	2.38	0.28	0.004531	TDA1	1.67	0.15	0.002596
GLG2	1.50	0.11	0.001914	TFS1	4.39	0.24	0.001008
GLK1	1.95	0.21	0.003700	TGL4	1.08	0.95	0.188004
GND2	5.84	0.35	0.001207	TMA10	17.17	3.03	0.010236
GOR1	2.70	0.05	0.000122	TMA17	1.70	0.30	0.010197
GPD1	1.49	0.11	0.001980	TPS1	2.84	0.11	0.000537
GPH1	2.41	0.36	0.007351	TPS2	2.84	0.30	0.003753
GPM2	1.68	0.44	0.022534	TSA2	4.20	1.37	0.033612
GRE1	6.30	1.75	0.024743	TSL1	4.08	0.34	0.002255
GRE3	3.03	0.05	0.000094	UBP7	1.56	0.72	0.063900
GRX1	1.02	0.23	0.015953	UGP1	1.75	0.20	0.004118
GSY2	1.59	0.32	0.013036	YBR085C-A	4.91	0.22	0.000645
GTT1	1.28	0.43	0.036405	YBR139W	1.47	0.15	0.003691
GUT2	1.33	0.28	0.014923	YBR285W	6.72	4.79	0.135507
HBT1	7.03	1.17	0.009110	YER079W	1.31	0.32	0.018948

Protein ID	log ₂ 37 /25°C	St. Dev.	p-value	Protein ID	log ₂ 37 /25°C	St. Dev.	p-value
HFD1	1.05	0.20	0.012071	YGP1	1.78	0.74	0.053373
HSC82	1.05	0.59	0.089520	YGR127W	1.82	0.27	0.007054
HSP10	1.18	0.11	0.002851	YGR250C	1.61	0.08	0.000844
HSP104	4.75	0.69	0.006935	YHR097C	1.55	0.42	0.023501
HSP12	6.10	0.51	0.002313	YHR138C	1.02	0.17	0.009503
HSP150	1.72	0.66	0.045586	YIL055C	1.60	0.35	0.015602
HSP26	7.25	0.74	0.003477	YJL016W	1.92	0.06	0.000326
HSP30	4.99	0.66	0.005712	YJR008W	1.73	0.29	0.009151
HSP31	2.33	0.40	0.009844	YJR096W	2.76	0.09	0.000345
HSP42	4.61	0.39	0.002403	YKL091C	1.87	0.44	0.017874
HSP78	4.18	0.46	0.003939	YLR149C	1.40	0.26	0.011066
HSP82	3.03	0.81	0.022849	YMR090W	1.60	0.81	0.075879
HXK1	2.73	0.32	0.004468	YMR196W	2.79	0.49	0.009942
HXT7	2.84	0.47	0.009146	YNL195C	6.69	1.25	0.011494
ICS2	2.26	0.40	0.010248	YNR034W-A	8.13	0.76	0.002894
LAP4	1.08	0.19	0.010248	YOR052C	2.92	2.56	0.186394
MCR1	1.30	0.49	0.045106	YOR289W	1.48	0.23	0.007761
MDJ1	1.83	0.18	0.003281	YPL247C	2.34	0.12	0.000858
MSC1	4.63	0.86	0.011431	YPR127W	1.55	0.22	0.006650
MSY1	1.20	0.48	0.049156	YSC84	1.44	0.33	0.016840
NGL3	4.46	5.93	0.322367	NNRD	2.72	0.13	0.000781
NQM1	6.05	0.86	0.006603	NTH1	2.59	0.06	0.000189
Protein ID	log ₂ 37 /25°C	St. Dev.	p-value	Protein ID	log ₂ 37 /25°C	St. Dev.	p-value
Diminished proteins after 30 min of 37°C							
DPH1	-1.00	0.09	0.002669	TYW3	-1.34	0.60	0.061220
HXT2	-1.00	0.65	0.116678	PRI2	-1.34	0.57	0.055757
RSN1	-1.01	0.47	0.065384	CRT10	-1.36	0.22	0.008536
TAD3	-1.02	0.08	0.002091	TOD6	-1.36	0.12	0.002733
NSR1	-1.03	0.26	0.020811	RHO2	-1.37	0.13	0.002871
INO1	-1.04	0.40	0.044932	OPY2	-1.39	0.53	0.045240
MDH2	-1.04	0.15	0.006692	BUD4	-1.40	0.25	0.010344
RAX1	-1.04	0.39	0.042834	YOL019W	-1.41	0.38	0.023920
MMS1	-1.05	0.18	0.009514	EAR1	-1.43	1.03	0.136260
MIP1	-1.06	0.63	0.101861	PNO1	-1.46	0.39	0.023262
YJL218W	-1.07	0.13	0.004746	HXT3	-1.46	0.12	0.002330
STE6	-1.08	0.17	0.008228	DOT6	-1.50	0.57	0.045175
STE6	-1.08	0.17	0.008228	CDC34	-1.52	2.06	0.328796
GAS1	-1.08	0.35	0.032705	DOT1	-1.58	1.11	0.132359
NOB1	-1.08	0.29	0.022631	MSG5	-1.61	0.15	0.002815
REE1	-1.09	0.74	0.125758	TY1B-ER1	-1.61	0.26	0.008679
PMA1	-1.09	0.20	0.010955	IRR1	-1.62	1.69	0.240437
REX3	-1.10	0.90	0.168169	RNH70	-1.71	0.09	0.000996
UTR2	-1.11	0.36	0.033395	YAL044W-A	-1.73	0.29	0.009216
TIM10	-1.12	0.41	0.041149	ZRT1	-1.74	0.12	0.001559
MSN4	-1.12	0.76	0.126342	CIN8	-1.75	0.76	0.057389

Protein ID	log ₂ 37 /25°C	St. Dev.	p-value	Protein ID	log ₂ 37 /25°C	St. Dev.	p-value
SSK2	-1.12	0.67	0.100131	ENA5	-1.86	0.36	0.012231
CHS3	-1.15	0.44	0.044764	YLR413W	-2.10	0.21	0.003286
EXG1	-1.18	0.57	0.070041	CTR1	-2.13	0.81	0.045012
NTO1	-1.19	0.79	0.121101	ADH4	-2.25	0.70	0.030536
QDR2	-1.20	0.35	0.026946	HIP1	-2.32	0.16	0.001500
ASH1	-1.20	0.27	0.016255	ZPS1	-2.39	0.20	0.002384
RAS1	-1.20	0.54	0.060474	CDC4	-2.40	0.16	0.001487
DUS4	-1.21	0.12	0.003241	PHO84	-2.41	1.75	0.139669
TYE7	-1.24	0.34	0.024550	YRF1-8	-2.45	0.30	0.004837
MKT1	-1.25	0.52	0.053869	FRE1	-2.55	0.80	0.031238
CTI6	-1.26	0.32	0.021090	NOP10	-2.77	4.03	0.355366
CPR2	-1.28	0.29	0.016468	SPT21	-3.32	1.63	0.071537
DRE2	-1.28	0.37	0.026417	FET4	-3.85	0.46	0.004631
CNN1	-1.29	1.02	0.160190				

Table S10 Enriched and diminished proteins after 30 min of 42°C.

Two-fold higher or lower protein counts were set as threshold. Proteins are listed with their average fold change compared to unstressed control cells, standard deviation across three biological replicates and the p-value indicating significance of the fold change ($p < 0.05$).

Protein ID	log ₂ 42/25°C	St. Dev.	p-value	Protein ID	log ₂ 42/25°C	St. Dev.	p-value
Enriched proteins after 30 min 42°C							
ACF2	1.2	0.47	0.047902	OPI10	2.95	0.32	0.003848
AGP1	1.42	0.21	0.007195	PGM2	1.46	0.77	0.081246
AHA1	1.16	0.33	0.026045	PHM8	1.58	0.23	0.007216
AIM17	1.20	0.51	0.054522	PIG2	1.06	0.24	0.017011
ALD3	2.65	1.06	0.049172	PIN3	3.02	0.15	0.000828
ALD4	1.12	0.9	0.163863	PNC1	1.77	0.48	0.023327
APJ1	4.87	0.32	0.001475	QCR6	1.62	0.47	0.02711
ART10	1.01	0.37	0.041604	RGH1	6.57	0.44	0.001462
BDH1	1.08	0.28	0.021069	RTC3	6.32	1.04	0.008875
BDH2	2.26	1.13	0.07485	RTG1	4.23	6.37	0.369539
BTN2	8.70	2.22	0.021099	RTN2	3.46	1.84	0.082526
CIN5	4.13	0.31	0.00187	SED5	1.82	1.12	0.106439
CPR6	2.57	0.11	0.000587	SIS1	2.19	0.08	0.000469
CTH1	6.37	1.44	0.016618	SOL4	2.50	0.37	0.007111
CTT1	2.52	1.67	0.120566	SSA1	1.52	0.17	0.004279
DCS2	1.23	0.8	0.117267	SSA3	6.80	0.88	0.005555
ECM21	1.52	0.15	0.003051	SSA4	9.52	0.19	0.000138
ERO1	1.19	0.44	0.04331	SSE2	1.68	0.56	0.035248
FES1	3.56	0.29	0.002153	STF2	3.58	0.58	0.008682
FMP45	3.20	0.6	0.011635	STH1	1.86	0.15	0.002096
GCY1	1.64	0.45	0.024588	TFS1	2.07	0.88	0.055057
GND2	2.75	0.79	0.026334	TMA10	19.33	2.19	0.004246

Protein ID	log ₂ 42/25°C	St. Dev.	p-value	Protein ID	log ₂ 42/25°C	St. Dev.	p-value
GNP1	1.02	0.29	0.025447	TPO2	1.46	0.45	0.030488
GRE1	4.00	0.49	0.004934	TPS1	1.57	0.52	0.035052
GRE3	1.63	0.45	0.024302	TPS2	1.39	0.77	0.087872
HSP10	1.35	0.17	0.005462	TSL1	2.04	0.8	0.047285
HSP104	4.51	0.13	0.000278	TUB2	1.09	0.27	0.01957
HSP12	5.04	1.21	0.018615	TUB3	1.02	0.21	0.014076
HSP150	3.01	0.83	0.024681	TYE7	1.35	0.77	0.092374
HSP26	6.02	0.38	0.001311	UBP7	1.40	0.16	0.004162
HSP31	2.41	0.31	0.005486	YBR085C-A	4.68	0.06	0.000048
HSP42	3.48	0.17	0.00083	YBR285W	5.46	1.09	0.012919
HSP78	4.66	0.05	0.000042	YDJ1	1.12	0.28	0.019731
HSP82	2.70	0.27	0.003308	YER079W	1.13	0.58	0.077825
HXK1	1.30	0.51	0.047482	YGR250C	2.78	0.27	0.003206
HXT7	1.68	0.64	0.045559	YJR096W	1.37	0.9	0.11949
KAR2	1.26	0.16	0.005417	YNL195C	3.52	1.31	0.043239
MDJ1	1.86	0.2	0.003841	YNR034W-A	6.77	0.56	0.002252
MSY1	1.28	0.16	0.004993	YOX1	2.00	0.21	0.003674
NIS1	1.02	0.54	0.082653	YPI1	1.55	0.91	0.09778
NQM1	2.25	1.54	0.127444	YPL247C	1.24	0.25	0.013793
NTH1	1.96	0.35	0.010393	YPR036W-A	3.88	0.61	0.008168
OM45	1.53	1.08	0.133366				

Protein ID	log ₂ 42/25°C	St. Dev.	p-value	Protein ID	log ₂ 42/25°C	St. Dev.	p-value
Diminished proteins after 30 min 42°C							
ACO2	-1.03	0.4	0.046746	PBP2	-1.48	0.23	0.008227
AFT1	-1.45	0.4	0.024947	PBP4	-1.39	0.33	0.018570
AGC1	-1.21	0.49	0.051712	PET127	-1.27	0.73	0.094172
AIM41	-1.48	0.35	0.018501	PEX15	-1.19	0.34	0.025427
ALT2	-1.70	0.8	0.066904	PEX5	-1.67	0.37	0.015574
APC5	-1.01	0.36	0.039555	PHO4	-1.26	1	0.160779
ASH1	-2.29	0.66	0.026468	PHR1	-1.50	0.62	0.052266
ATG4	-1.07	0.78	0.140681	PIR1	-1.42	0.77	0.085118
BCP1	-1.90	0.27	0.006615	PMU1	-4.34	0.04	0.000025
BEM1	-1.20	0.61	0.075459	PNO1	-2.84	0.32	0.004264
BER1	-1.69	0.24	0.006517	POL1	-2.44	0.08	0.000397
BFR2	-1.39	0.26	0.011079	POL12	-1.24	0.4	0.033281
BIM1	-1.92	0.22	0.004537	POL3	-1.46	0.22	0.007737
BIO4	-1.52	0.93	0.105771	PPM2	-2.28	0.85	0.043283
BMS1	-1.40	0.24	0.009464	PRI1	-1.45	0.17	0.004343
BUD20	-1.08	0.9	0.173139	PRI2	-1.71	0.32	0.011138
BUD23	-2.08	0.35	0.009320	PRP11	-1.16	0.32	0.025142
CDC34	-2.61	1.53	0.097886	PRP9	-1.86	0.16	0.002318
CDC4	-2.59	0.21	0.002143	RAD2	-2.28	0.42	0.010970
CHAC	-4.77	0.65	0.006186	RAD4	-1.23	0.41	0.035260
CHD1	-1.64	0.39	0.018084	RAD5	-2.80	1.28	0.062961

Protein ID	log ₂ 42/25°C	St. Dev.	p-value	Protein ID	log ₂ 42/25°C	St. Dev.	p-value
CIC1	-1.45	0.21	0.006809	RAD61	-1.29	1.26	0.217627
CKI1	-1.45	0.06	0.000626	REX2	-1.15	0.62	0.086123
COG7	-1.36	0.19	0.006486	REX3	-1.49	0.27	0.010858
CPR2	-1.26	0.42	0.035199	RIM4	-1.11	0.56	0.075278
CRT10	-2.73	0.54	0.012951	RIO2	-2.02	0.14	0.001694
CSM3	-1.56	0.13	0.002399	RIT1	-2.14	0.52	0.018784
CTI6	-1.79	0.19	0.003854	RLF2	-1.36	0.39	0.026758
CWC2	-1.21	0.45	0.042501	RLP24	-2.88	0.18	0.001272
DAS1	-1.06	0.22	0.014129	RLP7	-2.69	0.33	0.005081
DBP2	-2.37	0.66	0.025008	RMT2	-2.22	0.25	0.004308
DBP3	-1.56	0.17	0.003815	RNH202	-2.92	0.41	0.006434
DBP8	-1.51	0.25	0.008777	RNH70	-3.84	0.19	0.000796
DCN1	-2.09	1.77	0.177263	RPF1	-2.15	0.18	0.002347
DHR2	-1.74	0.34	0.012348	RRP1	-1.58	0.26	0.008867
DIM1	-1.20	0.29	0.018304	RRP12	-1.20	0.36	0.029125
DOT6	-1.35	0.45	0.035345	RRP3	-1.02	0.57	0.091182
DPH2	-1.02	0.25	0.019540	RRP5	-1.55	0.3	0.012665
DPH6	-1.43	0.09	0.001371	RRP6	-1.13	0.6	0.082009
DRS1	-1.14	0.44	0.046518	RRP8	-1.27	0.17	0.005626
DUN1	-1.84	0.25	0.006037	RTT101	-1.91	0.25	0.005823
DUS4	-2.85	0.11	0.000452	SAF1	-1.32	0.65	0.072755
EAR1	-1.02	0.96	0.207401	SCP1	-3.27	0.17	0.000906
EDC3	-1.04	0.33	0.031871	SDA1	-2.55	0.44	0.009900
ENP1	-2.50	0.23	0.002784	SDT1	-1.90	0.77	0.050272
ENP2	-1.31	0.44	0.035061	SFB2	-1.36	0.06	0.000756
ESF1	-1.18	0.18	0.007688	SGD1	-1.06	0.35	0.034313
ETT1	-2.87	0.65	0.016679	SIP3	-1.34	0.5	0.044381
EXG1	-1.22	0.73	0.103039	SLH1	-1.11	0.19	0.010061
FAL1	-1.18	0.25	0.014213	SLX4	-1.27	0.29	0.016962
FAP7	-3.24	0.97	0.028684	SOK1	-1.14	0.51	0.060112
FPR3	-2.39	0.15	0.001273	SPT21	-1.97	1.05	0.083422
FPR4	-2.10	0.36	0.009570	SQS1	-1.89	0.57	0.029193
FSH3	-1.06	0.13	0.004771	SRB2	-1.24	0.28	0.016179
FUN30	-1.12	0.04	0.000536	SRP40	-1.55	1.27	0.169790
FZO1	-2.14	1.29	0.103446	SSF2	-1.07	0.12	0.003971
GBP2	-2.43	0.18	0.001779	SST2	-2.64	0.67	0.020673
GPM3	-1.55	0.46	0.027784	STE23	-1.66	0.16	0.003036
GSH1	-1.56	0.2	0.005368	STE6	-1.95	1.16	0.100265
HAP1	-1.20	0.36	0.029381	TAD1	-2.13	1.68	0.159096
HAS1	-1.25	0.25	0.012703	TMA16	-2.47	0.43	0.009765
HEM4	-1.49	0.15	0.003572	TMA23	-1.01	0.38	0.044001
HIS6	-1.18	0.38	0.033193	TOD6	-1.01	0.49	0.070010
HST1	-1.04	0.52	0.072793	TRF5	-3.31	0.15	0.000671
IAH1	-1.41	0.08	0.001139	TSR2	-1.22	0.6	0.071385
IFH1	-1.62	1.02	0.111750	TSR4	-3.24	0.15	0.000750

Protein ID	log ₂ 42/25°C	St. Dev.	p-value	Protein ID	log ₂ 42/25°C	St. Dev.	p-value
IMP3	-1.10	0.09	0.002027	TY1B-ERI	-1.76	0.31	0.010174
IOC4	-1.24	0.99	0.162373	TY2B-GR2	-1.50	0.51	0.035867
IWR1	-1.28	0.52	0.051410	UBA4	-2.02	0.34	0.009132
KRE33	-1.17	0.39	0.035197	UBC6	-1.08	0.18	0.008993
KRI1	-1.19	0.05	0.000522	UBR2	-1.21	0.61	0.075071
LCP5	-1.05	0.34	0.032623	UFD4	-1.52	0.21	0.006022
LIP5	-1.43	0.39	0.024342	ULP1	-1.81	1.26	0.129646
MAE1	-1.80	0.38	0.014669	ULS1	-1.83	1.06	0.095370
MAG2	-1.16	0.42	0.040171	URB1	-1.01	0.33	0.033850
MAK16	-1.70	0.26	0.007853	UTP6	-1.10	0.34	0.030781
MAK21	-1.08	0.18	0.009048	UTP8	-1.03	0.1	0.002976
MAP1	-2.68	0.09	0.000363	WHI3	-1.33	0.45	0.036668
MEU1	-2.31	0.27	0.004673	WHI4	-1.54	0.43	0.024639
MKT1	-1.25	0.04	0.000269	YAL044W-A	-2.09	1.39	0.121457
MLP1	-1.25	0.07	0.001134	YBP2	-1.01	0.96	0.210480
MMS1	-2.31	0.31	0.006052	YCR051W	-1.03	0.28	0.023719
MMS4	-1.84	0.88	0.069498	YDL057W	-2.7	0.4	0.007192
MOD5	-1.81	0.27	0.007194	YDR026C	-3.1	0.2	0.001375
MPH1	-1.12	0.21	0.011762	YDR161W	-1.54	0.94	0.105432
MRC1	-2.41	0.23	0.002913	YDR514C	-1.04	0.42	0.050954
MRD1	-1.56	0.36	0.017631	YGL039W	-2.24	0.51	0.017135
MRN1	-2.63	0.31	0.004501	YGL101W	-1.66	0.29	0.010202
MRT4	-1.64	0.03	0.000084	YIH1	-1.7	0.25	0.007149
MSG5	-1.25	0.32	0.021528	YIL096C	-1.05	0.82	0.159030
MSN1	-1.32	0.45	0.037334	YKL033W-A	-1.79	0.08	0.000674
MSN4	-1.23	0.78	0.111431	YLR126C	-1.77	0.68	0.045979
MUB1	-1.17	0.68	0.096505	YLR460C	-1.27	0.25	0.012940
NAB6	-1.01	0.09	0.002784	YMR111C	-1.5	0.76	0.075154
NAM8	-1.15	0.25	0.015556	YMR130W	-1.09	0.61	0.091787
NAN1	-1.03	0.28	0.023099	YMR310C	-1.4	0.23	0.008893
NGL2	-2.57	0.33	0.005542	YNL022C	-1.49	0.18	0.005037
NOB1	-2.39	0.26	0.003790	YNL108C	-2.18	0.46	0.014320
NOG1	-2.74	0.19	0.001618	YOR131C	-1.39	0.15	0.003591
NOG2	-2.67	0.62	0.017350	YPK3	-1.32	0.37	0.024811
NOP10	-1.59	2.04	0.309859	YPL108W	-2.27	0.53	0.017818
NOP14	-1.05	0.32	0.030065	YRF1-8	-3.04	0.65	0.014741
NOP15	-1.50	0.42	0.024857	YVH1	-2.44	0.26	0.003640
NOP4	-3.04	0.13	0.000609	ZPS1	-1.28	0.83	0.116011
NOP53	-1.96	0.06	0.000311	CTS2	-1	0.45	0.060092
NOP7	-1.14	0.18	0.008528	DRE2	-1.01	0.28	0.023774
NRK1	-1.60	0.53	0.035228	NOP1	-1.07	0.22	0.013170
NSA2	-2.38	0.19	0.002113	NOP56	-1.05	0.17	0.008972
NUG1	-1.95	0.31	0.008591	NOP58	-1.08	0.2	0.011715
NUM1	-1.40	0.11	0.001939	SSF1	-1	0.31	0.030688
OTU1	-1.55	0.13	0.002366	TRE2	-1.15	0.66	0.094903

Protein ID	log ₂ 42/25°C	St. Dev.	p-value	Protein ID	log ₂ 42/25°C	St. Dev.	p-value
PAP2	-2.33	0.45	0.012141	YLR001C	-1.56	2.48	0.387959

Table S11 Class-1 P-sites with a differential phosphorylation state after 30 min of 37°C heat shock. P-sites with $\hat{\alpha} \geq$ two-fold increase or decrease in their phosphorylation state after heat shock compared to unstressed levels were selected. Only P-sites that showed the same direction of regulation in all three replicates were selected. Proteins with the respective P-sites are listed, the average ratio and standard deviation over three biological replicates and p-value indicating significance ($p < 0.05$).

P-site	log ₂ 37/25°C	St. Dev.	p-value	P-site	log ₂ 37/25°C	St. Dev.	p-value
Enriched P-Sites 30 min 37°C							
SPG4_S66	5.67	2.16	0.045112	SIS2_S121	1.48	0.54	0.040922
HSP42_S223	5.17	0.54	0.003556	GPH1_T31	1.47	0.21	0.006635
SPG4_S63	5.02	1.76	0.038495	YMR196W_S1019	1.47	0.32	0.015355
HBT1_S303	4.91	1.4	0.025965	YBR085C-A_S52	1.47	0.92	0.109901
HSP26_T163	4.89	0.85	0.009944	SMY2_S12	1.46	0.46	0.031772
HBT1_S41	4.85	0.78	0.008439	PIG2_S196	1.45	0.21	0.007067
TMA10_S28	4.39	0.91	0.014046	YMR196W_S1020	1.45	0.44	0.029584
HBT1_T766	4.06	1.06	0.022111	SWI6_S178	1.45	0.53	0.041205
HBT1_S1036	4.04	1.36	0.035793	INP53_T988	1.44	0.23	0.008604
HSP42_S213	3.97	0.61	0.007823	SET3_T682	1.43	0.47	0.034018
GIP2_S137	3.95	0.25	0.001364	CAB3_S116	1.42	0.67	0.066101
GIP2_S221	3.87	0.23	0.001186	ICS2_T26	1.42	0.51	0.040019
HSP12_S73	3.82	0.27	0.001616	INP53_S1031	1.42	0.32	0.016615
GIP2_S194	3.78	0.42	0.004140	TIF4632_T196	1.4	0.08	0.001224
HSP42_S215	3.67	0.75	0.013811	AIM3_S476	1.39	0.17	0.005179
HSP42_S214	3.54	0.76	0.015167	YPR172W_T103	1.39	0.22	0.007986
USV1_S177	3.46	0.57	0.009054	PEX19_S304	1.38	0.31	0.016694
HBT1_S400	3.32	0.4	0.004699	EAP1_S30	1.36	0.23	0.009631
GOR1_T31	3.3	0.34	0.003536	PWP1_S108	1.36	0.6	0.059138
IGD1_S14	3.24	0.68	0.014561	GIN4_S689	1.35	0.23	0.009165
SEC31_S1053	3.2	0.51	0.008393	YLR257W_S200	1.34	0.54	0.050383
PSK1_S1035	3.14	0.47	0.007532	ICS2_S27	1.33	0.38	0.026609
GCY1_S281	3.09	0.26	0.002369	MAM3_S522	1.31	0.09	0.001498
MSC1_S54	3.02	0.59	0.012326	MAM3_S523	1.31	0.09	0.001498
PAB1_S249	2.93	0.26	0.002545	SPA2_S970	1.3	1.74	0.324781
LSP1_T233	2.89	0.94	0.033609	HSP82_S297	1.29	0.45	0.038377
TSL1_S53	2.8	0.47	0.009303	HSC82_S293	1.29	0.45	0.038377
EDE1_S848	2.71	0.35	0.005456	RPG1_T502	1.29	0.52	0.049308
HSP104_S768	2.69	0.31	0.004386	ECM21_S140	1.28	0.32	0.020664
YMR196W_S963	2.69	0.49	0.010750	PAB1_S119	1.28	0.31	0.019466
TSL1_S161	2.67	0.35	0.005801	TPO1_S72	1.28	1.15	0.194159
RGA2_T325	2.66	0.31	0.004390	SEC16_S2130	1.27	0.73	0.094711
RGA2_S324	2.62	0.18	0.001597	YER079W_S39	1.27	0.81	0.112087

P-site	log ₂ 37/25°C	St. Dev.	p-value	P-site	log ₂ 37/25°C	St. Dev.	p-value
TSL1_T142	2.61	0.36	0.006438	ICS2_S30	1.26	0.52	0.053162
TSL1_S56	2.6	0.91	0.038386	YMR196W_S1016	1.26	0.66	0.081139
RGA2_T320	2.59	0.25	0.003180	PDR16_S346	1.25	0.14	0.004089
PGM2_S119	2.57	0.31	0.004796	SEC31_S999	1.25	0.11	0.002396
TSL1_S49	2.52	1.41	0.089671	TFG1_S198	1.25	0.75	0.102980
OM45_S69	2.49	1.09	0.058645	ICS2_S24	1.24	0.24	0.011765
TSL1_S155	2.48	0.22	0.002569	RTT107_T532	1.24	0.29	0.017695
TSL1_S157	2.46	0.22	0.002537	SSK1_S195	1.22	0.23	0.011354
GSY2_S467	2.42	0.66	0.024019	BBC1_T895	1.21	0.81	0.122832
YMR196W_S1010	2.42	0.35	0.006962	JSN1_S160	1.21	0.12	0.003021
RTS3_T48	2.42	1.07	0.059275	BCK1_S1058	1.2	0.23	0.011622
GIS1_S670	2.41	0.6	0.020036	GRX2_S91	1.2	0.73	0.103759
ARO9_S90	2.4	0.72	0.028684	PWP1_S105	1.2	0.4	0.034312
DCS2_S58	2.38	0.77	0.033312	BUD2_S854	1.19	0.44	0.042114
HXK1_S419	2.29	0.5	0.015800	CET1_S15	1.19	0.18	0.007355
IGD1_S164	2.24	0.08	0.000377	INP53_T1061	1.19	0.56	0.065901
YOR052C_S41	2.24	0.17	0.001896	NUP2_S84	1.19	0.35	0.027171
YBT1_S955	2.23	1.96	0.186910	SNT1_S318	1.19	0.22	0.011056
AIM21_S36	2.22	0.44	0.012989	CDC60_T142	1.18	0.16	0.005678
RCN2_S152	2.19	0.18	0.002126	HOS4_S507	1.18	0.64	0.084287
YOR052C_S43	2.09	0.19	0.002616	HOS4_S512	1.18	0.64	0.084287
PIL1_T233	2.08	0.06	0.000258	HSP82_S80	1.18	0.35	0.028965
SIS1_S275	2.08	0.57	0.024473	HSC82_S80	1.18	0.35	0.028965
RBL2_S94	2.06	0.12	0.001145	STF2_S28	1.18	0.21	0.009949
BBC1_T894	1.98	0.07	0.000443	YRO2_S293	1.18	0.95	0.162641
PWP1_S266	1.96	0.6	0.030174	RDS2_T231	1.17	0.41	0.039395
YMR196W_S984	1.93	0.84	0.057687	TCO89_S287	1.17	0.17	0.007330
HXK1_S293	1.92	0.85	0.059454	TCO89_S290	1.17	0.94	0.163664
GIS1_S747	1.91	0.05	0.000232	YPR172W_S99	1.17	0.23	0.012944
MDG1_S52	1.91	0.77	0.050265	KEL1_S1022	1.15	0.15	0.005545
YMR196W_S1081	1.87	0.5	0.022914	ALY1_S569	1.14	0.31	0.024327
ZUO1_S281	1.87	0.64	0.037509	DIP5_S13	1.14	0.32	0.025104
CRP1_T384	1.85	1.09	0.098732	KNS1_T562	1.13	0.59	0.080519
STE23_S439	1.85	0.7	0.045051	PDR16_S349	1.13	0.14	0.005011
NTH1_S60	1.84	0.36	0.012452	SNU114_T88	1.13	0.33	0.027498
BRX1_S285	1.82	0.9	0.072295	KNS1_T183	1.12	0.56	0.074554
P53719_S136	1.82	0.5	0.024346	HOG1_Y176	1.11	0.6	0.085312
GPH1_T308	1.81	0.26	0.006676	NOP13_T102	1.11	0.44	0.047460
ICS2_S195	1.81	0.38	0.014671	PDR16_T350	1.11	0.7	0.109384
CAF20_T102	1.8	0.5	0.024613	AMD1_S19	1.1	0.25	0.016914
TDA1_T451	1.79	1.06	0.099346	ALY2_S581	1.09	0.63	0.095161
ABP1_S383	1.75	0.35	0.013065	HSP82_S619	1.09	0.24	0.015824
RCN2_S160	1.74	0.25	0.007016	HSC_S615	1.09	0.24	0.015824
RUD3_S55	1.74	0.14	0.002195	JIP4_S510	1.09	0.25	0.016729

P-site	log ₂ 37/25°C	St. Dev.	p-value	P-site	log ₂ 37/25°C	St. Dev.	p-value
UIP4_S98	1.74	0.64	0.042209	RSC2_T243	1.09	0.72	0.119963
YNG2_S188	1.74	2.12	0.289651	ALY2_S582	1.08	0.65	0.103426
HOG1_T174	1.72	0.68	0.048136	CRN1_T520	1.07	0.26	0.018378
DDP1_S26	1.69	0.38	0.016140	TIF5_S268;251	1.07	0.11	0.003257
KCS1_S580	1.68	0.58	0.036795	YBR225W_S533	1.06	0.01	0.000045
SER33_T28	1.68	0.32	0.011811	PIN3_S52	1.06	0.03	0.000277
BTN2_S219	1.64	1.28	0.157051	UGP1_S11	1.06	0.21	0.012193
CIN5_S41	1.64	0.8	0.070212	YAT1_S392	1.06	0.22	0.014543
NBP2_S102	1.64	1.63	0.222497	PDR16_S348	1.05	0.29	0.023633
YJL016W_T25	1.63	0.25	0.007843	RSC2_T249	1.05	0.06	0.001025
YJL016W_T25	1.63	0.25	0.007843	CYS4_S109	1.04	0.1	0.003318
SYCR_S15	1.62	0.28	0.009547	KIN2_S24	1.04	0.32	0.030606
SYCR_S15	1.62	0.28	0.009547	NVJ1_S272	1.04	0.11	0.003504
RSC1_S670	1.61	0.3	0.011047	YPR172W_T101	1.04	0.47	0.061484
TFG1_T673	1.61	0.23	0.006682	YRB2_T123	1.04	0.02	0.000147
YER079W_S41	1.6	0.35	0.015580	CHA4_S6	1.02	0.19	0.010934
ARO9_S5	1.57	0.87	0.088563	PMD1_S1664	1.02	0.27	0.023129
CDC25_S596	1.56	2.11	0.328848	SIC1_S201	1.02	0.42	0.051639
MBF1_S143	1.56	0.1	0.001278	VHS3_S264	1.02	0.36	0.039788
TPO1_S76	1.56	0.77	0.073321	VPS13_S1364	1.02	0.52	0.075708
SEC16_S2143	1.55	0.72	0.064481	WHI5_S62	1.02	0.85	0.172616
ISW1_S760	1.54	0.28	0.010616	YAT1_T404	1.02	0.24	0.018168
RLM1_S164	1.53	0.56	0.042281	AHA1_S35	1.01	0.32	0.031589
INP53_S1035	1.52	0.26	0.009517	CBF1_T138	1.01	0.18	0.010385
MON2_S571	1.52	0.45	0.028449	HXT6_S288	1.01	0.89	0.190368
TFG1_T200	1.52	0.39	0.021562	HXT7_S288	1.01	0.89	0.190368
BNA7_S9	1.51	0.19	0.004985	SIS2_T84	1.01	0.41	0.049563
PSP2_S340	1.51	0.27	0.010495	TOP2_S1307	1.01	0.23	0.017490
NTH1_T58	1.49	0.1	0.001492	TOP2_T1314	1.01	0.23	0.017103
PTP2_S258	1.49	0.39	0.022115	GCS1_S157	1	0.87	0.185318
GAT1_S418	1.48	0.45	0.029149	SIS2_S54	1	0.3	0.027976
YMR196W_T1013	1.48	0.52	0.038957	SSK1_S90	1	0.38	0.044346

pSites	log ₂ 42/25°C	St. Dev.	p-value	pSites	log ₂ 42/25°C	St. Dev.	p-value
Diminished P-Sites 30 min 37°C							
SAM3_S20	-3.31	0.17	0.000852	SFL1_S599	-1.3	0.65	0.073923
SPA2_S1080	-3.23	0.44	0.006144	YDR090C_S229	-1.3	0.68	0.079934
ZRT2_T188	-3.19	0.29	0.002780	DOT6_S491	-1.29	0.38	0.028533
FCY2_S18	-3.01	1.2	0.048674	RFA2_S122	-1.29	0.29	0.016137
BEM3_S306	-2.77	0.33	0.004748	RHR2_S90	-1.28	1.26	0.221726
POL12_S101	-2.76	0.21	0.001882	YLR413W_S652	-1.28	0.63	0.072748
ALR1_S176	-2.64	0.38	0.006857	ILV5_S174	-1.27	0.85	0.121359
POL12_S126	-2.37	0.37	0.008210	KEL1_T572	-1.27	0.56	0.059346
STE2_S398	-2.37	0.6	0.020929	SPA2_S937	-1.26	0.27	0.015006

P-site	log ₂ 37/25°C	St. Dev.	p-value	P-site	log ₂ 37/25°C	St. Dev.	p-value
STE20_S492	-2.29	0.27	0.004671	DRN1_S242	-1.25	0.26	0.013945
THR4_T104	-2.24	0.46	0.014001	GNP1_S113	-1.25	0.57	0.062262
FIR1_S84	-2.21	0.63	0.026418	CDC3_S503	-1.24	0.16	0.005190
ASK1_S250	-2.14	1.3	0.103746	KCC4_S841	-1.24	0.3	0.018531
NET1_T1042	-2.12	0.79	0.043279	RPA190_T1651	-1.23	0.62	0.074834
PHO84_S321	-2.06	0.74	0.040794	ORM1_S32	-1.22	0.55	0.061795
GIN4_S460	-2.05	0.11	0.001006	SKG1_S280	-1.22	0.15	0.005277
KCC4_S675	-1.99	0.62	0.031143	BIR1_S765	-1.21	0.16	0.005982
NET1_S830	-1.99	0.25	0.005176	SKN1_S200	-1.21	0.5	0.052021
ALR1_S173	-1.96	1.42	0.139808	STE20_S502	-1.2	0.31	0.021045
HSL1_S57	-1.95	0.22	0.004186	IES1_T567	-1.19	0.2	0.009226
PTC2_S327	-1.92	0.3	0.007844	NUP60_S352	-1.19	0.57	0.068606
BUD3_S1549	-1.9	0.15	0.002052	UTP14_T582	-1.19	1.02	0.181646
HXT3_S26	-1.87	0.29	0.007747	YRA1_S8	-1.18	0.05	0.000635
GIN4_T435	-1.85	0.13	0.001534	HSL1_S682	-1.17	0.25	0.014799
BUD4_S96	-1.83	0.33	0.010852	NUP60_S81	-1.17	0.26	0.016248
KIN2_S549	-1.83	0.16	0.002588	RPL12B_S38	-1.17	0.16	0.006208
PHO84_T317	-1.83	0.36	0.012694	RPL12A_S38	-1.17	0.16	0.006208
ITR1_S46	-1.82	0.29	0.008063	BUD6_S342	-1.16	0.12	0.003467
SHS1_S447	-1.82	0.26	0.006869	MET6_T450	-1.16	0.83	0.137431
DNF1_T58	-1.77	0.34	0.012094	NUP60_S78	-1.16	0.25	0.014903
STE2_S366	-1.76	0.03	0.000107	LTE1_S689	-1.15	0.21	0.010683
BEM3_S324	-1.72	0.38	0.015837	SWI4_S806	-1.15	0.66	0.094120
BUD3_S1515	-1.68	0.12	0.001704	MCM3_S845	-1.14	0.16	0.006444
GLC8_S12	-1.68	0.44	0.022189	GSY1_S651	-1.13	0.25	0.015448
SHS1_S416	-1.66	0.13	0.002123	PIK1_S10	-1.12	0.38	0.036097
HNMI_S42	-1.65	0.28	0.009752	STB1_S72	-1.12	0.24	0.014403
LEU1_T345	-1.65	0.84	0.077452	YAP1_S17	-1.12	0.49	0.058165
PAR32_S246	-1.64	0.96	0.097015	YRB2_T31	-1.12	0.15	0.006263
BEM2_S1012	-1.61	0.39	0.019088	BCK1_S1061	-1.11	0.86	0.155371
BEM2_S1016	-1.61	0.39	0.019088	FLC1_S663	-1.11	0.14	0.005240
POL1_S215	-1.61	0.17	0.003635	NBA1_S38	-1.11	0.08	0.001642
BFR1_T336	-1.6	0.33	0.013686	STB1_S89	-1.11	0.37	0.035641
PHD1_S165	-1.6	0.19	0.004913	POL5_S814	-1.1	0.63	0.094600
PSO2_S193	-1.6	0.65	0.050362	VMA1_S347	-1.1	0.14	0.005484
LTE1_S854	-1.59	0.3	0.011760	KIN4_S460	-1.09	0.42	0.045116
YLR413W_S665	-1.59	0.47	0.027573	LCB4_S133	-1.09	0.38	0.038129
IGO2_S128	-1.55	0.45	0.026805	UBR1_S296	-1.09	0.2	0.011481
BDF2_S273	-1.53	0.2	0.005766	CYK3_S118	-1.08	0.21	0.011892
SPA2_S883	-1.52	0.07	0.000657	MUK1_S245	-1.08	0.19	0.010554
SPA2_S979	-1.52	0.19	0.005206	NUP60_S162	-1.08	0.23	0.014394
TPO3_S132	-1.49	0.33	0.016373	RGPI_S450	-1.08	0.24	0.015430
BUD3_T1566	-1.46	0.14	0.003214	TAT1_S84	-1.08	0.28	0.021454
NOT3_S344	-1.46	0.28	0.011898	RAD9_S56	-1.07	0.14	0.005640

P-site	log ₂ 37/25°C	St. Dev.	p-value	P-site	log ₂ 37/25°C	St. Dev.	p-value
SLA2_S308	-1.46	0.29	0.012962	AKL1_S801	-1.06	0.08	0.002048
TY1B-PR3_S995	-1.46	0.2	0.006496	DOT6_T489	-1.06	0.68	0.114581
DRE2_S206	-1.42	0.18	0.005254	PMA1_T912	-1.06	0.1	0.003000
ENT1_S328	-1.41	0.06	0.000706	PMA2_S940	-1.06	0.1	0.003000
TY1B-H_S1033	-1.41	0.13	0.002646	MET6_S675	-1.05	0.39	0.043698
SPA2_S274	-1.4	0.32	0.016615	PMA1_S911	-1.05	0.39	0.043708
CDH1_S239	-1.39	0.08	0.000991	PMA2_S941	-1.05	0.39	0.043708
MRH1_T295	-1.39	0.47	0.035549	RPL24A_T83	-1.05	0.33	0.031804
SKG1_S276	-1.39	0.79	0.093392	RPL24B_T83	-1.05	0.33	0.031804
SKG1_T273	-1.39	0.38	0.024000	SEC3_S256	-1.05	0.22	0.014455
GUK1_S149	-1.38	0.09	0.001427	CYK3_S122	-1.04	0.16	0.007760
INP52_S1016	-1.37	0.17	0.005095	NUP42_S137	-1.04	0.43	0.053191
NUP2_S284	-1.37	0.25	0.010500	SMY2_S602	-1.03	0.29	0.025435
PKC1_S577	-1.37	0.15	0.004194	YPR117W_S2278	-1.03	0.87	0.175840
TOD6_S329	-1.37	0.37	0.023912	EFT1_T713	-1.02	0.47	0.062767
ALR1_S172	-1.36	0.18	0.005905	YMR226C_S260	-1.02	0.9	0.189928
CDC25_S649	-1.36	0.61	0.060938	RPL24A_S86	-1.02	0.12	0.004714
PAR32_S39	-1.35	0.19	0.006681	RPL24B_S86	-1.02	0.12	0.004714
RPS21A_S65	-1.35	0.4	0.027314	RPS17B_S89	-1.02	0.36	0.039168
SRL3_S212	-1.35	0.3	0.015782	TAF4_S36	-1.02	0.12	0.004890
STE20_S547	-1.35	0.74	0.087787	ASF1_T270	-1.01	0.35	0.038241
FLC3_S687	-1.34	1.42	0.244404	JJJ1_T471	-1.01	0.29	0.025420
SEC7_S215	-1.34	0.48	0.039811	MDR1_S871	-1.01	0.23	0.016359
TY1B-PR1S1081	-1.34	0.21	0.007764	RPS13_S12	-1.01	0.35	0.038389
EIS1_S775	-1.33	0.79	0.100494	CYC8_S755	-1	0.23	0.017136
LTE1_S850	-1.33	0.25	0.011736	PET494_S385	-1	0.22	0.015368
HXT1_S3	-1.32	0.46	0.039045	PET494_S387	-1	0.22	0.015368
HXT3_S3	-1.32	0.46	0.039045	UME6_S150	-1	0.62	0.106432
MLP1_S1731	-1.32	0.66	0.074346	YFL034W_S1037	-1	0.18	0.010798
ASH1_S56	-1.31	0.19	0.007027				

Table S12 Class I P-sites after 30 min of 42°C heat shock. P-sites with an at least two-fold increase or decrease in their phosphorylation state after heat shock compared to unstressed levels were selected. Only P-sites that showed the same direction of regulation in all three replicates were selected. Proteins with the respective P-sites are listed, the average ratio and standard deviation over three biological replicates and p-value indicating significance ($p < 0.05$).

P-site	log ₂ 42/25°C	St. Dev.	p-value	P-site	log ₂ 42/25°C	St. Dev.	p-value
Enriched P-sites after 30 min 42°C							
PAB1_S249	4.95	0.22	0.000668	HSP82_S297	1.33	0.20	0.007084
ZUO1_S67	4.82	0.69	0.006812	HSC82_S297	1.33	0.20	0.007084
HSP26_T163	4.73	0.48	0.003465	SMY2_S12	1.33	0.17	0.005147
TMA10_S28	4.64	0.88	0.011780	YPR172W_S99	1.33	0.49	0.043329

P-site	log ₂ 42/25°C	St. Dev.	p-value	P-site	log ₂ 42/25°C	St. Dev.	p-value
LSP1_T233	4.45	0.71	0.008302	AIM29_S78	1.33	0.15	0.004391
BTN2_S219	4.16	0.57	0.006263	ISW1_S760	1.33	0.28	0.014532
RBL2_S94	4.10	0.17	0.000601	EAF7_S167	1.32	0.38	0.026071
HSP42_S223	4.01	0.31	0.002030	HOS4_S507	1.32	0.69	0.080744
ZUO1_S281	4.00	0.30	0.001829	HOS4_S512	1.32	0.69	0.080744
MDG1_S52	3.52	0.24	0.001486	NTH1_S66	1.31	0.17	0.005693
RTS3_T48	3.47	0.61	0.010052	ERB1_S360	1.31	0.26	0.012916
SEC31_S1053	3.44	0.60	0.010120	HSP82_T533	1.30	0.31	0.018335
SPG4_S66	3.42	1.90	0.088842	HSC_T529	1.30	0.31	0.018335
STI1_T37	3.42	1.15	0.035886	YNG2_S188	1.30	0.62	0.068091
PAN1_S621	3.34	0.32	0.002960	HXT2_T29	1.30	0.88	0.124992
PIL1_T233	3.16	0.10	0.000348	PXL1_S63	1.29	0.15	0.004179
PSK1_S1035	3.14	0.22	0.001566	HOG1_T174	1.29	0.41	0.032690
RUD3_S55	3.10	0.16	0.000856	WHI5_S62	1.29	0.67	0.079256
EDE1_S848	3.10	0.19	0.001229	PDR5_T59	1.29	0.68	0.081330
UBA2_T288	3.07	0.23	0.001926	BUD2_S854	1.28	0.28	0.015344
SRO9_S355	3.05	0.43	0.006469	SEC31_S999	1.27	0.04	0.000367
TPM1_S136	3.01	0.33	0.003928	TMA19_S9	1.27	0.32	0.019913
SPG4_S63	2.97	0.86	0.026599	TMA19_S9	1.27	0.31	0.019913
PEX19_S304	2.90	0.14	0.000827	YBT1_S955	1.26	0.94	0.145400
NTH1_S60	2.86	0.87	0.029713	GIS1_S747	1.25	0.15	0.004752
YMR196W_S963	2.85	1.02	0.039981	ESS1_S7	1.25	0.75	0.101393
TMA19_S15	2.81	0.15	0.000928	OLA1_S119	1.25	0.55	0.059201
HSP42_S213	2.80	0.82	0.027429	SWI6_S178	1.24	0.51	0.052329
SIS1_S14	2.75	0.25	0.002688	NPT1_S420	1.24	0.17	0.006371
RGA2_T325	2.74	0.35	0.005257	RAP1_T486	1.24	0.42	0.036683
RGA2_T325	2.74	0.34	0.005257	ALY1_S569	1.23	1.13	0.198795
RLM1_S164	2.71	0.51	0.011403	RCN2_S160	1.23	0.14	0.004267
HYP2_S74	2.71	0.29	0.003723	BNI4_T806	1.23	1.72	0.340977
RGA2_T320	2.69	0.29	0.003797	DCS2_S58	1.17	0.86	0.142783
RGA2_S324	2.67	0.20	0.001945	GCD11_T60	1.17	0.30	0.021256
RGA2_S324	2.67	0.21	0.001945	GIP4_S464	1.17	0.21	0.010567
PAB1_T102	2.60	0.24	0.002769	KEL1_S1022	1.17	0.17	0.007214
GPX2_S158	2.59	1.27	0.071860	NOPI3_S101	1.16	1.14	0.219554
HSP12_S73	2.55	0.64	0.020408	SPA2_S970	1.16	0.91	0.157267
SIS1_S275	2.54	0.34	0.005797	YRB2_T123	1.16	0.18	0.007634
PAB1_S119	2.51	0.45	0.010362	CIN5_S41	1.16	0.73	0.110939
STE23_S439	2.45	0.92	0.043713	PFY1_S2	1.16	0.38	0.034521
UBP6_T76	2.39	1.10	0.064337	GCY1_S281	1.15	0.96	0.172377
HSP42_S215	2.38	0.39	0.008957	ZEO1_S40	1.15	0.28	0.018970
FUN30_S567	2.37	0.39	0.008862	OM45_S69	1.15	0.81	0.131997
TIF5_S268;251	2.36	0.42	0.010423	GIP4_S462	1.15	0.37	0.032879
HSP42_S214	2.36	0.84	0.039966	NRP1_S345	1.15	0.23	0.013003
PDR16_S349	2.34	0.25	0.003920	YPR172W_T101	1.13	0.66	0.097293
YKR018C_S246	2.32	0.17	0.001770	PDR5_S58	1.13	1.11	0.218039

P-site	log ₂ 42/25°C	St. Dev.	p-value	P-site	log ₂ 42/25°C	St. Dev.	p-value
CAF20_T102	2.30	0.55	0.018546	BNI4_S476	1.13	0.36	0.031344
KCS1_S580	2.29	0.60	0.022213	CDC28_Y19	1.13	0.10	0.002548
PDR16_S348	2.27	0.48	0.014387	NOP7_T308	1.12	0.32	0.026462
TCO89_S287	2.24	0.16	0.001735	SIS2_S121	1.12	0.23	0.013843
IGD1_S14	2.24	1.24	0.088440	UBP1_S776	1.12	0.23	0.013316
TPO1_S76	2.23	1.34	0.102691	DED1_S204	1.11	0.34	0.029975
SER33_T28	2.22	0.81	0.041277	PMD1_S1660	1.11	0.53	0.069034
SER33_T28	2.22	0.80	0.041277	UBP13_S198	1.10	0.54	0.071778
GIS1_S670	2.21	0.64	0.026868	YER079W_S39	1.10	0.47	0.056673
GIN4_S689	2.17	0.43	0.012948	PXL1_S43	1.10	0.08	0.001989
MBF1_S143	2.17	0.14	0.001433	AMD1_S19	1.10	0.19	0.009904
NUM1_S648	2.14	1.40	0.118143	SNU114_T88	1.09	0.69	0.110632
PDR16_S346	2.12	0.46	0.015158	SSA1_S551	1.09	0.07	0.001308
GUK1_S125	2.10	0.32	0.007493	SSA2_S551	1.08	0.07	0.001292
PWP1_S108	2.10	0.47	0.016401	HXK1_S419	1.07	0.56	0.080835
TPO1_S72	2.08	0.54	0.021418	SSK2_S53	1.07	0.57	0.083670
PWP1_S266	2.06	0.33	0.008635	AIM21_S281	1.07	0.78	0.141365
PUF3_S563	2.06	1.63	0.160354	YPR172W_S97	1.06	0.77	0.139461
HSP104_S768	2.03	0.33	0.008618	IQG1_T264	1.06	0.30	0.025085
SSB1_S591	2.03	0.93	0.063359	PRE2_S51	1.05	0.43	0.052087
YPR172W_T103	2.03	0.12	0.001140	SYPI_T416	1.05	0.27	0.021447
SSB2_S591	2.03	0.93	0.063359	PFK1_S217	1.04	0.18	0.009914
PWP1_S105	2.01	0.90	0.061114	TSL1_S161	1.04	0.63	0.104176
AIM21_S36	2.00	0.19	0.003078	NEW1_S1181	1.04	0.08	0.002220
VHS3_S264	2.00	0.21	0.003525	MAM3_S522	1.03	0.06	0.001132
ALA1_S950	1.99	0.07	0.000367	MAM3_S523	1.03	0.06	0.001132
ALA1_S975	1.99	0.07	0.000367	YKR096W_S1146	1.03	0.41	0.047898
CPRI_S49	1.98	0.11	0.000998	PFY1_T7	1.02	0.16	0.008362
SLK19_S128	1.98	0.44	0.016272	PFY1_Y6	1.02	0.16	0.008362
OLA1_S67	1.98	0.04	0.000115	TDH3_T182	1.02	0.08	0.001954
RCN2_S152	1.96	0.24	0.004850	THS1_S195	1.01	0.21	0.013383
LEU1_T345	1.95	0.14	0.001727	OLA1_S116	1.01	0.73	0.138698
NET1_S385	1.95	0.44	0.016452	EFT1_T763	1.01	0.28	0.024638
FPR1_S15	1.94	0.10	0.000879	NCL1_T426	1.01	0.20	0.012896
YEF3_T972	1.93	0.23	0.004760	SNQ2_S80	1.00	0.47	0.066865
NOP13_T102	1.92	0.48	0.020391	TSL1_S53	1.00	0.73	0.138647
SEC16_S2143	1.89	0.58	0.030111	YER079W_S41	1.00	0.50	0.072611
GRX2_S91	1.89	0.28	0.007364	SSE1_633	1.00	0.92	0.200234
ABP1_S383	1.89	0.08	0.000657	SCP160_S85	1.00	0.35	0.038855
BBC1_T894	1.88	0.27	0.006954	SPP41_S1067	1.00	0.15	0.007217
SMT3_S33	1.88	0.06	0.000318	SSE2_S633	1.00	0.92	0.200234
MON2_S571	1.86	0.37	0.013237	CYC8_S765	1.00	0.85	0.180431
MTC4_S85	1.86	1.97	0.244256	ABP140_S93	1.00	0.40	0.049188
YMR196W_S1081	1.85	0.55	0.028088	PMD1_S1664	0.99	0.24	0.018965
TYE7_T237	1.84	0.22	0.004859	RSC1_S670	0.99	0.30	0.030066

P-site	log ₂ 42/25°C	St. Dev.	p-value	P-site	log ₂ 42/25°C	St. Dev.	p-value
YMR196W_S984	1.84	0.73	0.048604	PBP1_S106	0.99	0.36	0.040596
RPS9A_S184	1.83	0.22	0.004868	SIS2_T84	0.98	0.41	0.052642
P47072_T25	1.83	2.40	0.317718	SSA2_T416	0.98	0.29	0.027159
NOP13_T105	1.81	0.27	0.007360	SSA4_T417	0.98	0.29	0.027159
RPS9B_S184	1.77	0.04	0.000154	GIS4_S707	0.98	1.43	0.356550
BLM10_S11	1.75	0.35	0.012923	HOG1_Y176	0.98	0.38	0.046960
PDR16_T350	1.75	0.94	0.084012	SSA1_T416	0.98	0.28	0.027159
SKP1_T177	1.74	1.26	0.139530	SSA3_T417	0.98	0.28	0.027159
CUE5_T70	1.74	0.22	0.005304	DAL81_T968	0.96	0.24	0.020542
SEC16_S2141	1.72	0.65	0.043994	TSL1_S157	0.96	0.81	0.176197
BNA7_S9	1.72	0.15	0.002609	RSF2_S303	0.96	0.54	0.092818
DDP1_S26	1.72	0.10	0.001131	NOP7_T334	0.96	0.31	0.033487
SEC16_S2141	1.72	0.64	0.043994	GIP2_S137	0.95	0.70	0.143739
IGD1_S164	1.70	0.32	0.011256	RPS3_T44	0.95	0.17	0.010957
PDR5_S475	1.70	0.24	0.006448	Q08422_S43	0.94	0.32	0.036143
NUP2_S84	1.69	0.32	0.011897	MCH1_S255	0.94	0.49	0.078569
YBR085C-A_S52	1.68	0.65	0.045595	RPG1_T502	0.93	0.28	0.029025
PBI2_T74	1.67	0.57	0.036457	SEC16_S2130	0.93	0.79	0.179590
SEC14_S246	1.66	0.25	0.007435	GAT1_S418	0.92	0.22	0.017792
INP53_S1031	1.64	0.03	0.000100	NNK1_S737	0.92	0.28	0.029747
PIN3_S52	1.64	0.58	0.038843	TSL1_S56	0.91	0.97	0.245431
INP53_S1035	1.63	0.04	0.000170	CDC37_S484	0.90	0.28	0.030726
RPL6A_S12	1.60	0.24	0.007438	OXR1_S178	0.88	0.45	0.077823
SNG1_T91	1.60	0.45	0.025373	TWF1_S308	0.87	0.34	0.048515
BBC1_S69	1.59	0.61	0.044846	PAN1_S757	0.87	0.25	0.026576
CAB3_S116	1.57	0.77	0.071928	YDR239C_S477	0.86	0.21	0.018916
CDC19_S22	1.57	0.27	0.009903	BBC1_T895	0.86	1.10	0.310345
TPO1_T69	1.54	0.87	0.091618	MEH1_S146	0.85	0.22	0.020636
EAF7_S200	1.53	0.13	0.002459	STB3_S9	0.85	0.29	0.035405
HXK1_S293	1.53	0.73	0.068731	OXR1_S183	0.85	0.50	0.099010
TCO89_S290	1.52	0.13	0.002311	BRX1_S285	0.85	0.43	0.076678
GOR1_T31	1.51	0.20	0.005645	FUN12_S397	0.85	0.21	0.020037
JSN1_S160	1.50	0.28	0.011025	HSP82_S80	0.85	0.44	0.078430
YRB1_S60	1.49	0.09	0.001082	HSC82_S80	0.85	0.44	0.078430
YRB1_S60	1.49	0.08	0.001082	YEF3_S642	0.84	0.23	0.024430
NBP2_S102	1.48	0.54	0.041456	CDC25_S596	0.84	0.72	0.181010
OTU2_S96	1.47	0.93	0.111234	HSF1_S471	0.84	0.26	0.029833
DED1_S146	1.47	0.27	0.011427	HAA1_S258	0.84	0.29	0.036987
GRS1_S453	1.47	0.66	0.061051	VTC2_S187	0.84	0.32	0.045977
GRS1_S476	1.47	0.66	0.061051	GSY2_S651	0.84	0.20	0.019289
RSC2_T249	1.46	0.28	0.012222	CBF1_T138	0.83	0.21	0.019616
AIM3_S476	1.46	0.19	0.005577	PMA2_S899	0.83	0.39	0.066645
HSP104_S370	1.45	0.51	0.039162	HSP10_S31	0.83	0.37	0.059532
POP1_T524	1.44	0.03	0.000123	MDH2_T6	0.83	0.41	0.073558
CRN1_T520	1.43	0.26	0.010575	RPS0B_T96	0.83	0.24	0.026764

P-site	log ₂ 42/25°C	St. Dev.	p-value	P-site	log ₂ 42/25°C	St. Dev.	p-value
ABP1_S389	1.43	0.44	0.029816	RPS0A_T96	0.83	0.24	0.026764
TY1B-H_S177	1.43	0.44	0.029666	TSL1_T142	0.82	0.49	0.102059
TY1B-H_S177	1.43	0.43	0.029666	SCP160_S63	0.82	0.19	0.018176
PYK2_S24	1.42	0.33	0.017830	RSA1_S172	0.82	0.51	0.108960
BDF2_S264	1.40	0.27	0.011966	GLN3_S274	0.82	0.45	0.088965
ENT4_S182	1.40	0.48	0.036602	KRE6_S142	0.82	0.38	0.066338
HRR25_S330	1.40	0.05	0.000474	YMR196W_S1010	0.81	0.42	0.079676
FYV8_S280	1.40	0.20	0.006821	APL3_S736	0.81	0.67	0.170346
RGR1_T1036	1.39	0.57	0.052471	FUN12_T392	0.81	0.92	0.264852
VRP1_S519	1.39	0.59	0.054698	ABP140_S95	0.81	0.25	0.030567
EAP1_S30	1.38	0.50	0.040249	GIS4_S720	0.80	0.54	0.121757
UBP6_S470	1.37	0.15	0.003808	EIS1_S401	0.80	0.40	0.072164
HXT6_S288	1.37	0.93	0.125816	TSL1_S155	0.79	0.95	0.287502
INP53_T988	1.37	0.38	0.024472	SCP160_T50	0.78	0.42	0.085623
AIM21_S167	1.37	0.07	0.000980	SCP160_T50	0.78	0.43	0.085623
Q05506_S15	1.36	0.23	0.009647	EDE1_T1340	0.77	0.31	0.049676
VBA4_S62	1.34	0.49	0.041177	UIP4_S98	0.77	0.66	0.178692
HXT2_S32	1.34	0.28	0.014804	TUB2_S278	0.77	0.37	0.069094
HSC82_293	1.33	0.20	0.007084	PAL1_S113	0.75	0.25	0.035797
P-site	log ₂ 42/25°C	St. Dev.	p-value	P-site	log ₂ 42/25°C	St. Dev.	p-value
Diminished P-sites after 30 min 42°C							
STE20_S492	-4.07	0.722	0.010360	EIS1_S649	-1.51	0.264	0.009983
POL12_S101	-3.75	0.362	0.003089	NET1_T1042	-1.51	0.281	0.011352
POL12_S126	-3.59	0.149	0.000573	TPO3_S132	-1.5	0.127	0.002365
BEM3_S306	-3.58	0.705	0.012687	PPQ1_S208	-1.48	0.132	0.002635
SRL2_S262	-3.29	1.146	0.038128	YPK3_T82	-1.48	0.562	0.044826
PTC2_S327	-3.27	0.153	0.000726	EDE1_S1093	-1.43	0.4	0.024988
NUP60_S162	-3.16	0.038	0.000047	SKG1_S276	-1.43	1.201	0.175349
NUP60_S78	-3.1	0.177	0.001086	RNH202_S140	-1.41	0.29	0.013709
NUP60_S81	-2.98	0.89	0.028409	SHE3_S348	-1.41	1.157	0.169228
NUP60_S81	-2.98	0.89	0.027006	INP52_S1016	-1.4	0.168	0.004750
ORM1_S32	-2.92	0.162	0.001025	SFL1_S599	-1.4	0.919	0.119144
KIN2_S549	-2.76	0.521	0.011663	CUE4_S48	-1.39	0.252	0.010782
DIG2_S225	-2.72	0.147	0.000980	SQS1_S343	-1.39	0.276	0.012838
RDH54_S85	-2.6	0.449	0.009793	SWI4_S806	-1.39	0.607	0.058157
RDH54_T881	-2.45	0.447	0.010919	BCK1_S1061	-1.38	0.904	0.118389
THR4_T104	-2.45	0.421	0.009684	PAR32_S246	-1.38	0.834	0.103809
ENT1_S328	-2.44	0.139	0.001088	PAR32_S39	-1.38	0.195	0.006553
DIG1_S279	-2.42	0.309	0.005383	PIK1_S10	-1.38	0.301	0.015535
SHS1_S447	-2.4	0.148	0.001265	RPS17A_S89	-1.38	0.273	0.012696
VRP1_S709	-2.39	1.294	0.085226	RPS17B_S89	-1.38	0.273	0.012696
MRH1_T295	-2.38	1.102	0.064543	COS3_S16	-1.37	0.432	0.031472
ZUO1_S50	-2.34	0.163	0.001617	NOG2_S85	-1.37	0.368	0.023128
ALR1_S176	-2.32	0.35	0.007478	SBE22_S520	-1.37	0.175	0.005364
SAM3_S20	-2.3	0.273	0.004655	SPA2_S883	-1.37	0.159	0.004471

P-site	log ₂ 42/25°C	St. Dev.	p-value	P-site	log ₂ 42/25°C	St. Dev.	p-value
CDC3_S503	-2.29	0.169	0.001801	ALR1_S172	-1.36	0.515	0.044434
BEM3_S324	-2.28	0.187	0.002230	SHS1_S416	-1.34	0.185	0.006320
SMY2_S602	-2.25	0.237	0.003680	BNI1_S1344	-1.33	0.143	0.003826
ITR1_S46	-2.23	0.295	0.005779	PTP3_T75	-1.33	0.463	0.038114
PSO2_S193	-2.23	0.792	0.039575	TDA3_S372	-1.32	0.541	0.051276
NOT3_S344	-2.22	0.866	0.047300	PXR1_S230	-1.31	0.037	0.000269
LSB3_T396	-2.21	0.344	0.007964	TPI1_S79	-1.31	0.618	0.067327
SHB17_S65	-2.2	0.229	0.003567	TY1B-H_S1033	-1.31	0.154	0.004594
MON2_S564	-2.17	0.503	0.017455	BUL2_T22	-1.3	0.117	0.002707
SPA2_S1080	-2.12	0.325	0.007742	GLC8_S12	-1.3	0.14	0.003836
PDX3_S154	-2.05	0.3	0.007079	IPI1_T247	-1.3	0.092	0.001661
TY1B-PR1_S1081	-2.04	0.054	0.000234	CDH1_S239	-1.29	0.094	0.001775
GIN4_S460	-2.03	0.141	0.001601	NOG2_S155	-1.29	0.633	0.071430
KEL1_T572	-2.03	0.372	0.011050	RFA2_S122	-1.29	0.13	0.003346
DIG2_S84	-2.01	0.43	0.014968	ICS2_S176	-1.28	0.619	0.069623
BIR1_S765	-1.98	0.157	0.002106	SKO1_S94	-1.28	0.179	0.006495
MKT1_S8	-1.96	0.283	0.006888	ESF1_S225	-1.27	0.599	0.066564
NAP1_S140	-1.95	0.342	0.010108	PRP24_S19	-1.27	0.274	0.015241
MMS4_S61	-1.93	0.749	0.046604	SKG3_S623	-1.25	0.201	0.008478
NOG2_S60	-1.93	0.101	0.000909	TY1B-PR3_S995	-1.24	0.065	0.000927
CAF120_S505	-1.89	0.135	0.001706	CTR9_S1017	-1.23	0.081	0.001450
GUK1_S149	-1.89	0.197	0.003602	EK1_S23	-1.23	0.504	0.051970
KEL1_S503	-1.87	0.438	0.017680	YPR117W_S2278	-1.23	0.486	0.048406
DIG1_S395	-1.86	0.098	0.000918	LTE1_S854	-1.22	0.198	0.008636
SWI6_S176	-1.86	0.553	0.028132	PUF3_T89	-1.22	0.163	0.005840
YFL034W_S1037	-1.86	0.099	0.000948	ASF1_S264	-1.2	0.909	0.148938
STP1_S140	-1.85	0.244	0.005748	CYK3_S118	-1.2	0.324	0.023585
FIR1_S84	-1.83	1.112	0.104191	CYK3_S122	-1.2	0.138	0.004414
SKG1_S280	-1.83	0.107	0.001127	P47139_S138	-1.2	0.251	0.014164
NTE1_S634	-1.8	0.134	0.001845	GGA1_S357	-1.17	0.144	0.005013
ASH1_S56	-1.78	0.232	0.005641	MRH1_S299	-1.17	0.768	0.118274
BOI2_S523	-1.78	1.227	0.128055	PKC1_S577	-1.17	0.17	0.006971
DNF1_T58	-1.78	0.573	0.032643	ZAP1_S515	-1.17	0.292	0.020171
DIG1_S272	-1.75	0.115	0.001447	SPA2_T220	-1.15	0.682	0.099825
NUG1_S503	-1.74	0.42	0.018782	CDC3_S509	-1.14	0.077	0.001533
SHE3_S361	-1.74	0.158	0.002735	FCY2_S18	-1.14	0.75	0.119670
SQS1_S345	-1.74	0.528	0.029411	MLF3_S179	-1.14	0.212	0.011390
VRP1_S703	-1.74	0.317	0.010865	RPS13_S12	-1.14	0.464	0.050808
SNT2_S641	-1.73	0.757	0.058581	SEC14_S222	-1.14	0.433	0.044956
STE20_S547	-1.73	1.279	0.144263	PUF3_S86	-1.13	0.162	0.006816
EIS1_S775	-1.71	0.849	0.073468	UBP6_S298	-1.12	0.312	0.024974
BIM1_T152	-1.7	0.416	0.019466	BFR2_S44	-1.11	0.159	0.006801
LCB4_S133	-1.7	0.789	0.064786	KCC4_S892	-1.11	0.611	0.087872
STE12_S400	-1.7	0.134	0.002049	MKT1_S362	-1.1	0.147	0.005885
SBE2_S474	-1.69	0.264	0.008012	TOD6_S329	-1.1	0.335	0.029651

P-site	log ₂ 42/25°C	St. Dev.	p-value	P-site	log ₂ 42/25°C	St. Dev.	p-value
DRN1_S242	-1.68	0.209	0.005163	BEM3_S254	-1.09	0.344	0.031400
INP53_S986	-1.68	0.27	0.008516	CDC25_S649	-1.09	0.268	0.019706
NUP60_S352	-1.68	0.43	0.021134	CYK3_S117	-1.09	0.295	0.023438
GDS1_S359	-1.66	0.234	0.006578	PKH3_S696	-1.09	0.158	0.006938
GDS1_T363	-1.66	0.323	0.012429	SOK1_S193	-1.09	0.179	0.008854
NOC2_S149	-1.66	0.248	0.007382	TOF1_S1213	-1.08	0.422	0.047538
SEC3_S256	-1.66	0.101	0.001224	MIF2_S53	-1.07	0.203	0.011815
STB1_S89	-1.66	0.099	0.001176	STB1_S72	-1.07	0.03	0.000257
STH1_S329	-1.65	0.344	0.014196	BFR1_T336	-1.06	0.143	0.006061
BEM2_S1012	-1.63	0.136	0.002319	KRI1_T26	-1.06	0.044	0.000571
BEM2_S1016	-1.63	0.136	0.002319	MDR1_S874	-1.06	0.305	0.026352
SKG1_T273	-1.63	0.139	0.002398	MET6_S675	-1.06	0.232	0.015622
BRL1_S446	-1.61	0.342	0.014645	BFR2_S379	-1.05	0.267	0.020705
EDE1_S1087	-1.61	1.23	0.151338	MKT1_S358	-1.05	0.249	0.018142
BDF2_S273	-1.6	0.095	0.001167	MUK1_S245	-1.05	0.137	0.005618
MDR1_S871	-1.6	0.504	0.031640	ROM2_S235	-1.05	0.087	0.002296
GIN4_T435	-1.59	0.357	0.016413	JJJ1_T471	-1.04	0.419	0.050439
NET1_S830	-1.59	0.151	0.002979	SBE22_S517	-1.04	0.111	0.003823
ZRG8_S192	-1.59	0.474	0.028456	CYC8_S710	-1.03	0.095	0.002801
CYC8_S755	-1.58	0.814	0.078024	ENP2_S529	-1.03	0.172	0.009074
PKH2_S619	-1.58	0.186	0.004593	RGP1_S357	-1.03	0.094	0.002757
RGP1_S450	-1.54	0.345	0.016290	HSL1_S57	-1.02	0.32	0.031221
SLA2_S308	-1.54	0.252	0.008825	NUM1_S2743	-1.02	0.245	0.018716
STE12_S402	-1.54	0.476	0.030417	EDE1_S1095	-1.01	0.46	0.062605
VIP1_S1107	-1.54	0.091	0.001159	ILV5_S174	-1.01	0.806	0.161818
AIR2_S49	-1.53	0.121	0.002091	BUD3_S1515	-1	0.15	0.007381
DRE2_S206	-1.53	0.112	0.001763	NSG2_S93	-1	0.189	0.011663
GFD1_S106	-1.52	0.926	0.104160	VMA1_S347	-1	0.307	0.029817
HXT3_S26	-1.52	0.407	0.023039				

7. Abbreviations

α CD	Alpha Crystallin Domain
°C	Centigrade
μ m	Micrometer
μ M	Micromolar
3D	Three-dimensional
Amp	Ampicillin
approx.	Approximately
Arg, R	Arginine
ATP	Adenosinotriphosphate
clonNAT	Nourseothricin
cm	Centimeter
Cryo-ET	Cryo-Electron Tomography
CTD	C-Terminal Domain
d	Day(s)
DIC microscopy	Differential Interference Contrast Microscopy
DMA	Deletion mutant array
DNA	Deoxyribonucleic acid
DNA	Desoxyribonucleic acid
dNTP	Deoxynucleotide triphosphate
eGFP	enhanced Green Fluorescent Protein
etc.	et cetera
Exp.	Experiment
fc	Fold change
Fig.	Figure
FLAsH	Fluorescent Arsenic Helix binder
Fluc	Firefly luciferase
FlucSM; Fluc-DM	Fluc-Single Mutant, -Double Mutant
g	G-force
G418	Geneticin
GO	Gene Ontology
GO-ID	Gene Ontology Identification
GSR	General Stress Response
h	Hour
HCl	Hydrochloric acid
HEPES	2-(4-(2-hydroxyethyl)piperazin-1-yl)ethanesulfonic acid
HSE	Heat Shock Element
Hsf	Heat Shock Factor
Hsp	Heat shock protein
HSR	Heat Shock Response
INQ	Intranuclear Quality Control
IPOD	Intracellular Protein Deposit
JUNQ	Juxtannuclear Quality Control
Kan	Kanamycin
kDa	Kilo Dalton
KO	Knockout
\log_2 -fc	Fold-change on the \log_2 -scale
Lys, K	Lysine
M	Molar
min	Minute
mM	Millimolar
MS	Mass Spectrometry

7. Abbreviations

MSG	Monosodiumglutamate
NC	Nitro cellulose
NEF	Nucleotide Exchange Factor
nm	Nanometer
nM	Nanomolar
NTD	N-Terminal Domain
OD	Optical Density
ORF	Open reading frame
PBS (T)	Phosphate Buffered Saline (with Tween)
PCR	Polymerase Chain Reaction
<i>pica</i>	PolyQ induced cycle arrest
P-Site	Phosphorylation site
PTM	Posttranslational Modification
Q-Bodies	Cytosolic Quality Control Bodies
RNA	Ribonucleic acid
rpm	Rounds per minute
rRNA	Ribosomal RNA
RT	Room temperature
s, sec	Seconds
SBF-SEM	Serial Block Face Scanning Electron Microscopy
SDS-PAGE	SodiumDodecylSulfate-Polyacrylamide Gel Electrophoresis
SGA	Synthetic genetic array
SGD	<i>Saccharomyces cerevisiae</i> database
sHsp	Small heat shock protein
SILAC	Stable Isotope Labeling with Amino acids in Culture
STRE	Stress Response Element
TRIS	Tris(hydroxymethyl)-aminomethan
WB	Western Blot
wt	Wild-type
Δ	Delta, deletion
%	Percent
<; >	Smaller; bigger

8. References

- Adams, S.R., Campbell, R.E., Gross, L.A., Martin, B.R., Walkup, G.K., Yao, Y., Llopis, J., and Tsien, R.Y. (2002). New Biarsenical Ligands and Tetracysteine Motifs for Protein Labeling in Vitro and in Vivo: Synthesis and Biological Applications. *J. Am. Chem. Soc.* *124*, 6063–6076.
- Akerfelt, M., Morimoto, R.I., and Sistonen, L. (2010). Heat shock factors: integrators of cell stress, development and lifespan. *Nat. Rev. Mol. Cell Biol.* *11*, 545–555.
- Anckar, J., and Sistonen, L. (2011). Regulation of HSF1 function in the heat stress response: implications in aging and disease. *Annu. Rev. Biochem.* *80*, 1089–1115.
- Anfinsen, C.B., Haber, E., and White, F.H. (1961). The Kinetics of Formation of Native Ribonuclease. *47*, 1309–1314.
- Arndt, K.I.M.T., Styles, C., and Fink, G.R. (1987). Multiple Global Regulators Control HIS4 Transcription in Yeast. *Science (80-.)*. *237*.
- Arrigo, A.-P., Fakan, S., and Tissieres, A. (1980). Localization of the Heat Shock-Induced Proteins in *Drosophila melanogaster* Tissue Culture Cells. *Dev. Biol.* *78*, 86–103.
- Arthur, H., and Watson, K. (1976). Thermal Adaptation in Yeast Growth Temperatures, Membrane Lipid, and Cytochrome Composition of Psychrophilic, Mesophilic, and Thermophilic Yeasts. *Microbiology* *128*, 56–68.
- Asano, S., Engel, B.D., and Baumeister, W. (2015). In Situ Cryo-Electron Tomography A Post - Reductionist Approach to Structural Biology. *J. Mol. Biol.* 1–12.
- Ashburner, M., and Bonner, J. (1979). The induction of gene activity in *Drosophila* by heat shock. *Cell* *17*, 241–254.
- van Bakel, H., Strengman, E., Wijmenga, C., and Holstege, F.C.P. (2005). Gene expression profiling and phenotype analyses of *S. cerevisiae* in response to changing copper reveals six genes with new roles in copper and iron metabolism. *Physiol. Genomics* *22*, 356–367.
- Basha, E., Friedrich, K.L., and Vierling, E. (2006). The N-terminal Arm of Small Heat Shock Proteins Is Important for Both Chaperone Activity and Substrate Specificity. *J. Biol. Chem.* *281*, 39943–39952.
- Beck, M., Ecke, M., Förster, F., Plitzko, J., Melchior, F., Gerisch, G., Baumeister, W., and Ohad, M. (2004). Nuclear Pore Complex Structure and Dynamics Revealed by Cryoelectron Tomography. *Science (80-.)*. *306*, 1387–1390.
- Bejarano, E., and Cuervo, A.M. (2010). Chaperone-Mediated Autophagy. *Liver* *7*, 29–39.
- Belle, A., Tanay, A., Bitincka, L., Shamir, R., and O’Shea, E.K. (2006). Quantification of protein half-lives in the budding yeast proteome. *Proc. Natl. Acad. Sci. U. S. A.* *103*, 13004–13009.
- Benesch, J.L.P., Aquilina, J.A., Baldwin, A.J., Rekas, A., Stengel, F., Lindner, R. a., Basha, E., Devlin, G.L., Horwitz, J., Vierling, E., et al. (2010). The quaternary organization and dynamics of the molecular chaperone HSP26 are thermally regulated. *Chem. Biol.* *17*, 1008–1017.
- Bowers, K., and Stevens, T.H. (2005). Protein transport from the late Golgi to the vacuole in the yeast *Saccharomyces cerevisiae*. *Biochim. Biophys. Acta - Mol. Cell Res.* *1744*, 438–454.
- Braun, N., Zacharias, M., Peschek, J., Kastenmüller, A., Zou, J., Hanzlik, M., Haslbeck, M., Rappsilber, J., Buchner, J., and Weinkauf, S. (2011). Multiple molecular architectures of the eye lens chaperone α B-crystallin elucidated by a triple hybrid approach. *Proc. Natl. Acad. Sci. U. S. A.* *108*, 20491–20496.
- Brehme, M., Voisine, C., Rolland, T., Wachi, S., Soper, J.H., Zhu, Y., Orton, K., Ge, H., and Morimoto, R.I. (2014). A Chaperome Subnetwork Safeguards Proteostasis in Resource A Chaperome Subnetwork Safeguards Proteostasis in Aging and Neurodegenerative Disease. *Cell Rep.* *9*, 1135–1150.
- Buchan, J.R., and Parker, R. (2009). Eukaryotic Stress Granules The Ins and Out of Translation What are Stress Granules? *Mol. Cell Biol.* *36*.
- Buchner, J. (1996). Supervising the fold: functional principles of molecular chaperones. *FASEB J.* *10*, 10–19.
- Bukau, B., Weissman, J., and Horwich, A. (2006). Molecular chaperones and protein quality control. *Cell* *125*, 443–451.
- Caspers, G.J., Leunissen, J. a, and de Jong, W.W. (1995). The expanding small heat-shock protein family, and structure predictions of the conserved “alpha-crystallin domain”. *J. Mol. Evol.* *40*, 238–248.

- Causton, H.C., Ren, B., Koh, S.S., Harbison, C.T., Kanin, E., Jennings, E.G., Lee, T.I., True, H.L., Lander, E.S., and Young, R. a (2001). Remodeling of yeast genome expression in response to environmental changes. *Mol Biol Cell* 12, 323–337.
- Chen, J., Feige, M.J., Franzmann, T.M., Bepperling, A., and Buchner, J. (2010). Regions outside the alpha-crystallin domain of the small heat shock protein Hsp26 are required for its dimerization. *J. Mol. Biol.* 398, 122–131.
- Chiti, F., and Dobson, C.M. (2006). Protein Misfolding, Functional Amyloid, and Human Disease. *Annu. Rev. Biochem.* 75, 333–366.
- Christiano, R., Nagaraj, N., Fröhlich, F., and Walther, T.C. (2014). Global Proteome Turnover Analyses of the Yeasts *S. cerevisiae* and *S. pombe*. *Cell Rep.* 1959–1965.
- Cox, J., and Mann, M. (2008). MaxQuant enables high peptide identification rates, individualized p.p.b.-range mass accuracies and proteome-wide protein quantification. *Nat. Biotechnol.* 26, 1367–1372.
- Davidson, J.F., and Schiestl, R.H. (2001). Mitochondrial Respiratory Electron Carriers Are Involved in Oxidative Stress during Heat Stress in *Saccharomyces cerevisiae*. *Society* 21, 8483–8489.
- Dobson, C.M., and Karplus, M. (1999). The fundamentals of protein folding: bringing together theory and experiment. *Curr. Opin. Struct. Biol.* 9, 92–101.
- Dobson, C.M., Andrej, S., and Karplus, M. (1998). Protein Folding: A Persepctive from Theory and Experiment. *Angew. Chem. Int. Ed.* 37, 868–893.
- Dokladny, K., Zuhl, M.N., Mandell, M., Bhattacharya, D., Schneider, S., Deretic, V., and Moseley, P.L. (2013). Regulatory coordination between two major intracellular homeostatic systems: heat shock response and autophagy. *J. Biol. Chem.* 288, 14959–14972.
- E, Basha, E., O’Neill, H., and Vierling, E. (2012). Small heat shock proteins and α -crystallins: dynamic proteins with flexible functions. *Trends Biochem. Sci.* 37, 106–117.
- Echtenkamp, F.J., Zelin, E., Oxelmark, E., Woo, J.I., Andrews, B.J., Garabedian, M., and Freeman, B.C. (2011). Global functional map of the p23 molecular chaperone reveals an extensive cellular network. *Mol. Cell* 43, 229–241.
- Eisen, M.B., Spellman, P.T., Brown, P.O., and Botstein, D. (1998). Cluster analysis and display of genome-wide expression patterns. *Proc. Natl. Acad. Sci. U. S. A.* 95, 14863–14868.
- Ellis, R.J. (2001). Macromolecular crowding: obvious but underappreciated. *Trends Biochem. Sci.* 26, 597–604.
- Ellis, J.R., and Minton, A.P. (2006). Protein aggregation in crowded environments. *Biol Chem* 387, 485–497.
- Escusa-Toret, S., Vonk, W.I.M., and Frydman, J. (2013). Spatial sequestration of misfolded proteins by a dynamic chaperone pathway enhances cellular fitness during stress. *Nat. Cell Biol.* 15, 1231–1243.
- Estruch, F. (2000). Stress-controlled transcription factors, stress-induced genes and stress tolerance in budding yeast. *FEMS Microbiol. Rev.* 24, 469–486.
- Feder, M., and Hofmann, G. (1999). Heat-shock proteins, molecular chaperones, and the stress response: evolutionary and ecological physiology. *Annu. Rev. Physiol.* 61, 243–282.
- Finka, A., Sood, V., Quadroni, M., Rios, P.D.L., and Goloubinoff, P. (2015). Quantitative proteomics of heat-treated human cells show an across-the-board mild depletion of housekeeping proteins to massively accumulate few HSPs. *Cell Stress Chaperones* 605–620.
- Finley, D., Ulrich, H.D., Sommer, T., and Kaiser, P. (2012). The Ubiquitin – Proteasome System of *Saccharomyces cerevisiae*. *Genetics* 192, 319–360.
- Franzmann, T.M., Wühr, M., Richter, K., Walter, S., and Buchner, J. (2005). The activation mechanism of Hsp26 does not require dissociation of the oligomer. *J. Mol. Biol.* 350, 1083–1093.
- Franzmann, T.M., Menhorn, P., Walter, S., and Buchner, J. (2008). Activation of the chaperone Hsp26 is controlled by the rearrangement of its thermosensor domain. *Mol. Cell* 29, 207–216.
- Gasch, A.P. (2002). The environmental stress response a common yeast response to diverse environmental stresses. *Top. Curr. Genet.* 1, 11–70.
- Gasch, A.P., and Werner-Washburne, M. (2002). The genomics of yeast responses to environmental stress and starvation. *Funct. Integr. Genomics* 2, 181–192.
- Gasch, A.P., Spellman, P.T., Kao, C.M., Carmel-Harel, O., Eisen, M.B., Storz, G., Botstein, D., and Brown, P.O. (2000). Genomic expression programs in the response of yeast cells to environmental changes. *Mol.*

Biol. Cell 11, 4241–4257.

Gasteiger, E., Hoogland, C., Gattiker, A., Duvaud, S., Wilkins, M.R., Appel, R.D., and Bairoch, A. (2015). Protein Identification and Analysis Tools on the ExPASy Server. *Analysis* 571–608.

GeneChip 3' IVT Express Kit. Affymetrix User Guide (2014).

Giaver, G., Dow, S., Lucau-danila, A., Anderson, K., Arkin, A.P., Astromoff, A., Bakkoury, M. El, Bangham, R., Benito, R., Brachat, S., et al. (2002). Functional profiling of the *Saccharomyces cerevisiae* genome. *Nature* 1–5.

Gibney, P. a, Lu, C., Caudy, A. a, Hess, D.C., and Botstein, D. (2013). Yeast metabolic and signaling genes are required for heat-shock survival and have little overlap with the heat-induced genes. *Proc. Natl. Acad. Sci. U. S. A.* 110, E4393–E4402.

Gibney, P. a., Schieler, A., Chen, J.C., Rabinowitz, J.D., and Botstein, D. (2015). Characterizing the in vivo role of trehalose in *Saccharomyces cerevisiae* using the AGT1 transporter. *Proc. Natl. Acad. Sci. U. S. A.* 112, 6116–6121.

Gietz, R.D., and Schiestl, R.H. (2008). High-efficiency yeast transformation using the LiAc / SS carrier DNA / PEG method. *Lithium* 2, 31–35.

Goldstein, a L., and McCusker, J.H. (1999). Three new dominant drug resistance cassettes for gene disruption in *Saccharomyces cerevisiae*. *Yeast* 15, 1541–1553.

Goloubinoff, P., Mogk, a, Zvi, a P., Tomoyasu, T., and Bukau, B. (1999). Sequential mechanism of solubilization and refolding of stable protein aggregates by a bichaperone network. *Proc. Natl. Acad. Sci. U. S. A.* 96, 13732–13737.

Gong, Y., Kakihara, Y., Krogan, N., Greenblatt, J., Emili, A., Zhang, Z., and Houry, W. a (2009). An atlas of chaperone-protein interactions in *Saccharomyces cerevisiae*: implications to protein folding pathways in the cell. *Mol. Syst. Biol.* 5, 275.

Grably, M.R., Stanhill, A., Tell, O., and Engelberg, D. (2002). HSF and Msn2/4p can exclusively or cooperatively activate the yeast HSP104 gene. *Mol. Microbiol.* 44, 21–35.

Green, M.R., and Sambrook, J. (2012). *Molecular Cloning: A Laboratory Manual* (Cold Spring Harbor Laboratory Press).

Gross, C.A., and Craig, E. (1987). σ 32 synthesis can regulate the synthesis of heat shock proteins in *Escherichia coli*. *Genes Dev.* 179–184.

Gross, D., Adams, C., English, K., Collins, K., and Lee, S. (1990). Promoter function and in situ protein/DNA interactions upstream of the yeast HSP90 heat shock genes. *Antonie Van Leeuwenhoek* 58, 175–186.

Grousl, T., Ivanov, P., Frýdlová, I., Vasicová, P., Janda, F., Vojtová, J., Malínská, K., Malcová, I., Nováková, L., Janosková, D., et al. (2009). Robust heat shock induces eIF2alpha-phosphorylation-independent assembly of stress granules containing eIF3 and 40S ribosomal subunits in budding yeast, *Saccharomyces cerevisiae*. *J. Cell Sci.* 122, 2078–2088.

Gruhler, A., Olsen, J. V, Mohammed, S., Mortensen, P., Færgeman, N.J., Mann, M., and Jensen, O.N. (2005). Quantitative Phosphoproteomics Applied to the Yeast Pheromone Signaling Pathway *□. *Mol. Cell. Proteomics* 310–327.

Gu, W., Etkin, L.D., Le Gros, M. a, and Larabell, C. a (2007). X-ray tomography of *Schizosaccharomyces pombe*. *Differentiation.* 75, 529–535.

Gupta, R., Kasturi, P., Bracher, A., Loew, C., Zheng, M., Villella, A., Garza, D., Hartl, F.U., and Raychaudhuri, S. (2011). Firefly luciferase mutants as sensors of proteome stress. *Nat. Methods* 8, 879–884.

Gutin, J., Sadeh, A., Rahat, A., Aharoni, A., and Friedman, N. (2015). Condition-specific genetic interaction maps reveal crosstalk between the cAMP / PKA and the HOG MAPK pathways in the activation of the general stress response. 1–21.

Hagen, C., Guttman, P., Klupp, B., Werner, S., Rehbein, S., Mettenleiter, T.C., Schneider, G., and Grünwald, K. (2012). Correlative VIS-fluorescence and soft X-ray cryo-microscopy/tomography of adherent cells. *J. Struct. Biol.* 177, 193–201.

Haley, D. a, Bova, M.P., Huang, Q.L., Mchaourab, H.S., and Stewart, P.L. (2000). Small heat-shock protein structures reveal a continuum from symmetric to variable assemblies. *J. Mol. Biol.* 298, 261–272.

Handbook Affymetrix (2014). *GeneChip ® Expression Analysis Data Analysis Fundamentals*.

- Hartl, F.U., Bracher, A., and Hayer-Hartl, M. (2011). Molecular chaperones in protein folding and proteostasis. *Nature* 475, 324–332.
- Haslbeck, M., Walke, S., Stromer, T., Ehrnsperger, M., White, H.E., Chen, S., Saibil, H.R., and Buchner, J. (1999). Hsp26: a temperature-regulated chaperone. *EMBO J.* 18, 6744–6751.
- Haslbeck, M., Braun, N., Stromer, T., Richter, B., Model, N., Weinkauff, S., and Buchner, J. (2004). Hsp42 is the general small heat shock protein in the cytosol of *Saccharomyces cerevisiae*. *EMBO J.* 23, 638–649.
- Haslbeck, M., Miess, A., Stromer, T., Walter, S., and Buchner, J. (2005a). Disassembling Protein Aggregates in the Yeast Cytosol. *J. Biol. Chem.* 280, 23861–23868.
- Haslbeck, M., Franzmann, T., Weinfurtnner, D., and Buchner, J. (2005b). Some like it hot: the structure and function of small heat-shock proteins. *Nat. Struct. Mol. Biol.* 12, 842–846.
- Hecht, K.A., Donnell, A.F.O., and Brodsky, J.L. (2015). The proteolytic landscape of the yeast vacuole. *Cell. Logist.* 4.
- Heiland, I., and Erdmann, R. (2005). Biogenesis of peroxisomes Topogenesis of the peroxisomal membrane and matrix proteins. *FEBS J.* 272, 2362–2372.
- Hilton, G., Lioe, H., Stengel, F., Baldwin, A.J., and Benesch, J.L.P. (2013). Small Heat-Shock Proteins: Paramedics of the Cell. *Top. Curr. Chem.* 328, 69–98.
- Hoffmann, A., Bukau, B., and Kramer, G. (2010). Structure and function of the molecular chaperone Trigger Factor. *Biochim. Biophys. Acta - Mol. Cell Res.* 1803, 650–661.
- Huang, D.W., Lempicki, R. a, and Sherman, B.T. (2009). Systematic and integrative analysis of large gene lists using DAVID bioinformatics resources. *Nat. Protoc.* 4, 44–57.
- Huh, W., Falvo, J. V, Gerke, L.C., Carroll, A.S., Howson, R.W., Weissman, J.S., and Shea, E.K.O. (2003). Global analysis of protein localization in budding yeast. *Nature* 425, 686–691.
- Humphrey, S.J., James, D.E., and Mann, M. (2015). Protein Phosphorylation A Major Switch Mechanism for Metabolic Regulation. *Trends Endocrinol. Metab.* 26, 676–687.
- Jaenicke, R. (1987). Folding and association of proteins. *Prog. Biophys. Mol. Biol.* 49, 117–237.
- Janke, C., Magiera, M.M., Rathfelder, N., Taxis, C., Reber, S., Maekawa, H., Moreno-Borchart, A., Doenges, G., Schwob, E., Schiebel, E., et al. (2004). A versatile toolbox for PCR-based tagging of yeast genes: new fluorescent proteins, more markers and promoter substitution cassettes. *Yeast* 21, 947–962.
- Jelinsky, S.A., and Samson, L.D. (1999). Global response of *Saccharomyces cerevisiae* to an alkylating agent. *Proc. Nat* 96, 1486–1491.
- Johnston, G.C., and Singer, R.A. (1980). Ribosomal precursor RNA metabolism and cell division in the yeast *Saccharomyces cerevisiae*. *Mol. Gen. Genet.* 178, 357–360.
- Jones, R.C., and Hough, J.S. (1970). The Effect of Temperature on the Metabolism of Baker ' s Yeast growing on Continuous Culture. *J. G. Microbiol.* 60, 107–116.
- de Jong, W.W., Caspers, G.J., and Leunissen, J. a (1998). Genealogy of the alpha-crystallin--small heat-shock protein superfamily. *Int. J. Biol. Macromol.* 22, 151–162.
- Kaganovich, D., Kopito, R., and Frydman, J. (2008). Misfolded proteins partition between two distinct quality control compartments. *Nature* 454, 1088–1095.
- Kaiser, C.J.O., Grötzinger, S.W., Eckl, J.M., Papsdorf, K., Jordan, S., and Richter, K. (2013). A network of genes connects polyglutamine toxicity to ploidy control in yeast. *Nat. Commun.* 4, 1571.
- Kanshin, E., Kubiniok, P., Thattikota, Y., D'Amours, D., and Thibault, P. (2015). Phosphoproteome dynamics of *Saccharomyces cerevisiae* under heat shock and cold stress. *Mol. Syst. Biol.* 11, 813.
- Kim, K.K., Kim, R., and Kim, S.H. (1998). Crystal structure of a small heat-shock protein. *Nature* 394, 595–599.
- Kim, Y.E., Hipp, M.S., Bracher, A., Hayer-Hartl, M., and Ulrich Hartl, F. (2013). Molecular Chaperone Functions in Protein Folding and Proteostasis.
- Kriehuber, T., Rattei, T., Weinmaier, T., Bepperling, A., Haslbeck, M., and Buchner, J. (2010). Independent evolution of the core domain and its flanking sequences in small heat shock proteins. *FASEB J.* 24, 3633–3642.
- Kühl, N.M., and Rensing, L. (2000). Heat shock effects on cell cycle progression. *Cell. Mol. Life Sci.* 57, 450–463.

- Kumar, A., Agarwal, S., Heyman, J.A., Matson, S., Heidtman, M., Piccirillo, S., Umansky, L., Drawid, A., Jansen, R., Liu, Y., et al. (2002). Subcellular localization of the yeast proteome. *Genes Dev.* 707–719.
- Larabell, C. a., and Nugent, K. a. (2010). Imaging cellular architecture with X-rays. *Curr. Opin. Struct. Biol.* 20, 623–631.
- Larochelle, M., Drouin, S., Turcotte, B., Room, H., Hospital, R.V., and Ave, P. (2006). Oxidative Stress-Activated Zinc Cluster Protein Stb5 Has Dual Activator / Repressor Functions Required for Pentose Phosphate Pathway Regulation and NADPH Production. *Society* 26, 6690–6701.
- Levinthal, C. (1969). How to fold graciously. *Mössbauer Spectrosc. Biol. Syst. Proc.* 24, 22–24.
- Li, X., and Cai, M. (1999). Recovery of the yeast cell cycle from heat shock-induced G(1) arrest involves a positive regulation of G(1) cyclin expression by the S phase cyclin Clb5. *J. Biol. Chem.* 274, 24220–24231.
- Lieb, J.D., Liu, X., Botstein, D., and Brown, P.O. (2001). Promoter-specific binding of Rap1 revealed by genome-wide maps of protein – DNA association. *DNA Seq.* 28, 327–334.
- Lindquist, S. (1980). Varying Patterns of Protein Synthesis in *Drosophila* during Heat Shock: Implications for Regulation. *Dev. Biol.* 77, 463–479.
- Lindquist, S. (1986). The Heat-Shock Response. *Annu. Rev. Biochem.* 55, 1151–1191.
- Liochev, S.I., and Fridovich, I. (1999). Critical Review Superoxide and Iron Partners in Crime. *Amino Acids* 157–161.
- Liu, B., Han, Y., and Qian, S.-B. (2013). Cotranslational Response to Proteotoxic Stress by Elongation Pausing of Ribosomes. *Mol. Cell* 49, 453–463.
- Lodish, H., Berk, A., and Zipursky, S. (2000). *Molecular Cell Biology*.
- Longtine, M.S., Iii, A.M.K., Demarini, D.J., and Shah, N.G. (1998). Additional Modules for Versatile and Economical PCR-based Gene Deletion and Modification in *Saccharomyces cerevisiae*. *Yeast* 961, 953–961.
- Mamnun, Y.M., Pandjaitan, R., Mahé, Y., Delahodde, A., and Kuchler, K. (2002). The yeast zinc finger regulators Pdr1p and Pdr3p control pleiotropic drug resistance (PDR) as homo- and heterodimers in vivo. *Mol. Microbiol.* 46, 1429–1440.
- Marion, R.M., Regev, A., Segal, E., Barash, Y., Koller, D., Friedman, N., and O’Shea, E.K. (2004). Sfp1 is a stress- and nutrient-sensitive regulator of ribosomal protein gene expression. *Proc. Natl. Acad. Sci. U. S. A.* 101, 14315–14322.
- Martinez-Pastor, M.T., Marchler, G., Schüller, C., Marchler-Bauer, A., Ruis, H., and Estruch, F. (1996). The *Saccharomyces cerevisiae* zinc finger proteins Msn2p and Msn4p are required for transcriptional induction through the stress-response element (STRE). *EMBO J.* 15, 2227–2235.
- Meaden, P., Arneborg, N., Guldfeldt, L., Siegumfeldt, H., and Jakobsen, M. (1999). Endocytosis and vacuolar morphology in *Saccharomyces cerevisiae* are altered in response to ethanol stress or heat shock. *Yeast* 15, 1211–1222.
- Millan Zambrano, G., Rodriguez-Gil, A., Penate, X., Miguel-Jimenez, L. de, Morillo-Huesca, M., Krogan, N., and Chavez, S. (2013). The Prefoldin Complex Regulates Chromatin Dynamics during Transcription Elongation. *PLoS Genet.* 9, e1003776.
- Miller, S.B.M., Ho, C.-T., Winkler, J., Khokhrina, M., Neuner, A., Mohamed, M.Y.H., Guilbride, D.L., Richter, K., Lisby, M., Schiebel, E., et al. (2015). Compartment-specific aggregases direct distinct nuclear and cytoplasmic aggregate deposition. *EMBO J.* 34, 778–797.
- Minami, Y., and Minami, M. (1999). Hsc70 / Hsp40 chaperone system mediates the Hsp90-dependent refolding of firefly luciferase. *Genes to Cells* 1, 721–729.
- Miyazaki, N., Esaki, M., Ogura, T., and Murata, K. (2014). Serial block-face scanning electron microscopy for three-dimensional analysis of morphological changes in mitochondria regulated by Cdc48p / p97 ATPase. *J. Struct. Biol.* 187, 187–193.
- van Montfort, R.L., Basha, E., Friedrich, K.L., Slingsby, C., and Vierling, E. (2001). Crystal structure and assembly of a eukaryotic small heat shock protein. *Nat. Struct. Biol.* 8, 1025–1030.
- Morano, K.A., Grant, C.M., and Moye-Rowley, W.S. (2011). The response to Heat Shock and Oxidative Stress in *Saccharomyces cerevisiae*. *Yeast Genet.* 319–335.
- Morimoto, R.I. (1998). Regulation of the heat shock transcriptional response: cross talk between a family of heat shock factors, molecular chaperones, and negative regulators. *Genes Dev.* 12, 3788–3796.
- Morimoto, R.I. (2008). Proteotoxic stress and inducible chaperone networks in neurodegenerative disease

- and aging. *Genes Dev.* 22, 1427–1438.
- Natarajan, K., Meyer, M.R., Jackson, B.M., Slade, D., Roberts, C., Hinnebusch, A.G., and Marton, M.J. (2001). Transcriptional Profiling Shows that Gcn4p Is a Master Regulator of Gene Expression during Amino Acid Starvation in Yeast. *Molecular and Cellular Biology.* 21, 4347–4368.
- Neckers, L., and Workman, P. (2012). Hsp90 molecular chaperone inhibitors: Are we there yet? *Clin. Cancer Res.* 18, 64–76.
- Ogrodnik, M., Salmonowicz, H., Brown, R., Turkowska, J., Sredniawa, W., Pattabiraman, S., Amen, T., Abraham, A., Eichler, N., Lyakhovetsky, R., et al. (2014). Dynamic JUNQ inclusion bodies are asymmetrically inherited in mammalian cell lines through the asymmetric partitioning of vimentin. *Proc. Natl. Acad. Sci.* 111.
- Papsdorf, K., and Richter, K. (2014). Protein folding, misfolding and quality control: the role of molecular chaperones. *Essays Biochem.* 56, 53–68.
- Papsdorf, K., Kaiser, C.J.O., Drazic, A., Grötzinger, S.W., Haeßner, C., Eisenreich, W., and Richter, K. (2015). Polyglutamine toxicity in yeast induces metabolic alterations and mitochondrial defects. *BMC Genomics* 16, 662.
- Parsell, D.A., and Lindquist, S. (1993). The function of heat-shock proteins in stress tolerance: degradation and reactivation of damaged proteins. *Annu. Rev. Genet.* 27, 437–496.
- Patriarca, E.J., and Maresca, B. (1990). Acquired thermotolerance following heat shock protein synthesis prevents impairment of mitochondrial ATPase activity at elevated temperatures in *saccharomyces cerevisiae*. *Exp. Cell Res.* 190, 57–64.
- Pearson, K. (1895). Note on Regression and Inheritance in the Case of Two Parents. Society.
- Peschek, J., Braun, N., Rohrberg, J., Back, K.C., Kriehuber, T., Kastenmüller, A., Weinkauff, S., and Buchner, J. (2013). Regulated structural transitions unleash the chaperone activity of α B-crystallin. *Proc. Natl. Acad. Sci. U. S. A.* 1–10.
- Petko, L., and Lindquist, S. (1986). Hsp26 is not required for growth at high temperatures, nor for thermotolerance, spore development, or germination. *Cell* 45, 885–894.
- Phipps, B.M., Hoffmann, a, Stetter, K.O., and Baumeister, W. (1991). A novel ATPase complex selectively accumulated upon heat shock is a major cellular component of thermophilic archaeobacteria. *EMBO J.* 10, 1711–1722.
- Piper, P.W. (1995). The heat shock and ethanol stress responses of yeast exhibit extensive similarity and functional overlap. *FEMS Microbiol. Lett.* 134, 121–127.
- Prasad, R., Kawaguchi, S., and Ng, D.T.W. (2010). A Nucleus-based Quality Control Mechanism for Cytosolic Proteins. *Mol. Biol. Cell* 21, 2117–2127.
- Rep, M., Proft, M., Remize, F., Tama, M., Thevelein, J.M., and Hohmann, S. (2001). The *Saccharomyces cerevisiae* Sko1p transcription factor mediates HOG pathway-dependent osmotic regulation of a set of genes encoding enzymes implicated in protection from oxidative damage. *Mol. Microbiol.* 40, 1067–1083.
- Richter, K., Haslbeck, M., and Buchner, J. (2010). The Heat Shock Response: Life on the Verge of Death. *Mol. Cell* 40, 253–266.
- Ritossa, F. (1996). Discovery of the heat shock response. *Cell Stress Chaperones* 1, 97–98.
- Roth, D.M., and Balch, W.E. (2013). Q-bodies monitor the quinary state of the protein fold. *Nat. Cell Biol.* 15, 1137–1139.
- Rothman, J.E., and Schekman, R. (2011). Molecular mechanism of protein folding in the cell. *Cell* 146, 851–854.
- Roy, S., Lagree, S., Hou, Z., Thomson, J. a, Stewart, R., and Gasch, A.P. (2013). Integrated module and gene-specific regulatory inference implicates upstream signaling networks. *PLoS Comput. Biol.* 9, e1003252.
- Saibil, H. (2013). Chaperone machines for protein folding, unfolding and disaggregation. *Nat. Rev. Mol. Cell Biol.* 14, 630–642.
- Schneider, G., Guttman, P., Heim, S., Rehbein, S., Mueller, F., Nagashima, K., Heymann, J.B., Müller, W.G., and McNally, J.G. (2010). Three-dimensional cellular ultrastructure resolved by X-ray microscopy. *Nat. Methods* 7, 985–987.
- Shalgi, R., Hurt, J. a, Krykbaeva, I., Taipale, M., Lindquist, S., and Burge, C.B. (2013). Widespread regulation of translation by elongation pausing in heat shock. *Mol. Cell* 49, 439–452.

- Singer, M. a, and Lindquist, S. (1998a). Thermotolerance in *Saccharomyces cerevisiae*: the Yin and Yang of trehalose. *Trends Biotechnol.* *16*, 460–468.
- Singer, M.A., and Lindquist, S. (1998b). Thermotolerance in *Saccharomyces cerevisiae* the Yin and Yang of trehalose. *Science* (80-.). *16*.
- Sorger, P.K., and Pelham, H.R. (1988). Yeast heat shock factor is an essential DNA-binding protein that exhibits temperature-dependent phosphorylation. *Cell* *54*, 855–864.
- Specht, S., Miller, S.B.M., Mogk, A., and Bukau, B. (2011). Hsp42 is required for sequestration of protein aggregates into deposition sites in *Saccharomyces cerevisiae*. *J. Cell Biol.* *195*, 617–629.
- Speed, T.P., Bolstad, B.M., Irizarry, R.A., and Astrand, M. (2003). A comparison of normalization methods for high density oligonucleotide array data based on variance and bias. *19*, 185–193.
- Stansfield, I. (2007). *Yeast Gene Analysis*.
- Stengel, F., Baldwin, A.J., Painter, A.J., Jaya, N., Basha, E., Kay, L.E., Vierling, E., Robinson, C. V, and Benesch, J.L.P. (2010). Quaternary dynamics and plasticity underlie small heat shock protein chaperone function. *Proc. Natl. Acad. Sci. U. S. A.* *107*, 2007–2012.
- Stratil, C. (2010). Phenotypic Analysis of the Deletion of Small Heat Shock Genes in Baker's Yeast. Master's Thesis, TUM.
- Stromer, T., Fischer, E., Richter, K., Haslbeck, M., and Buchner, J. (2004). Analysis of the Regulation of the Molecular Chaperone Hsp26 by Temperature-induced Dissociation. *J. Biol. Chem.* *279*, 11222–11228.
- Szklarczyk, D., Franceschini, A., Wyder, S., Forslund, K., Heller, D., Huerta-cepas, J., Simonovic, M., Roth, A., Santos, A., Tsafou, K.P., et al. (2015). STRING v10 protein – protein interaction networks , integrated over the tree of life. *Database* *43*, 447–452.
- Tamait, K.T., Liu, X., Silar, P., Sosinowski, T., and Thiele, D.J. (1994). Heat Shock Transcription Factor Activates Yeast Metallothionein Gene Expression in Response to Heat and Glucose Starvation via Distinct Signalling Pathways. *14*, 8155–8165.
- Tamas, M., and Hohmann, S. (2003). The osmotic stress response of *Saccharomyces cerevisiae*. *Top. Curr. Genet.* *1*.
- Tarassov, K., Messier, V., Landry, C.R., Radinovic, S., Molina, M.M.S., Shames, I., Malitskaya, Y., Vogel, J., Bussey, H., and Michnick, S.W. (2008). An in Vivo Map of the Yeast Protein Interactome. *Science.* *320*, 1465–1470.
- Teixeira, M.C., Monteiro, P.T., Guerreiro, J.F., Mira, N.P., Costa, S., Cabrito, R., Palma, M., Costa, C., Freitas, A.T., and Sa, I. (2014). The YEASTRACT database an upgraded information system for the analysis of gene and genomic transcription regulation in *Saccharomyces cerevisiae*. *Database* *42*, 161–166.
- Thayer, N.H., Leverich, C.K., Fitzgibbon, M.P., Nelson, Z.W., Henderson, K.A., Gafken, P.R., Hsu, J.J., and Gottschling, D.E. (2014). Identification of long-lived proteins retained in cells undergoing repeated asymmetric divisions. *Proc. Natl. Acad. Sci.* *111*, 14019–14026.
- Tissières, A., Mitchell, H.K., and Tracy, U.M. (1974). Protein synthesis in salivary glands of *Drosophila melanogaster*: relation to chromosome puffs. *J. Mol. Biol.* *84*, 389–398.
- Toledano, M.B., Delaunay, A., Biteau, B., and Spector, D. (2003). Oxidative stress responses in yeast. *Yeast Stress Responses* *1*, 242–287.
- Tong, A.H., Evangelista, M., Parsons, A.B., Xu, H., Bader, G.D., Pagé, N., Robinson, M., Raghibizadeh, S., Hogue, C.W., Bussey, H., et al. (2001). Systematic genetic analysis with ordered arrays of yeast deletion mutants. *Science* *294*, 2364–2368.
- Trott, A., and Morano, K.A. (2003). The yeast response to heat shock. *Top. Curr. Genet.* *1*.
- Uchida, M., Sun, Y., Mcdermott, G., Knoechel, C., Gros, M.A. Le, Parkinson, D., Drubin, D.G., and Larabell, C.A. (2011). Quantitative analysis of yeast internal architecture using soft X-ray tomography. *Yeast* *28*, 227–236.
- Vainberg, I.E., Lewis, S. a, Rommelaere, H., Ampe, C., Vandekerckhove, J., Klein, H.L., and Cowan, N.J. (1998). Prefoldin, a Chaperone that Delivers Unfolded Proteins to Cytosolic Chaperonin. *Cell* *93*, 863–873.
- Vergheze, J., and Morano, K. a. (2012). A Lysine-Rich Region within Fungal BAG Domain-Containing Proteins Mediates a Novel Association with Ribosomes. *Eukaryot. Cell* *11*, 1003–1011.
- Vergheze, J., Abrams, J., Wang, Y., and Morano, K. a (2012). Biology of the Heat Shock Response and Protein Chaperones: Budding Yeast (*Saccharomyces cerevisiae*) as a Model System. *Microbiol. Mol. Biol.*

Rev. 76, 115–158.

Wallace, E.W.J., Kear-scott, J.L., Pilipenko, E. V, Pan, T., Budnik, B.A., Drummond, D.A., Wallace, E.W.J., Kear-scott, J.L., Pilipenko, E. V, Schwartz, M.H., et al. (2015). Reversible, Specific, Active Aggregates of Endogenous Proteins Assemble upon Heat Stress. *Cell* 162, 1286–1298.

Walsh, R.M., and Martin, P. a. (1977). Growth of *Saccharomyces Cerevisiae* and *Saccharomyces Uvarum* in a Temperature Gradient Incubator. *J. Inst. Brew.* 83, 169–172.

Walther, D.M., Kasturi, P., Zheng, M., Pinkert, S., Vecchi, G., Ciryam, P., Morimoto, R.I., Dobson, C.M., Vendruscolo, M., Mann, M., et al. (2015). Widespread Proteome Remodeling and Aggregation in Aging *C. elegans*. *Cell* 161, 919–932.

Welch, W.J., and Suhan, J.P. (1985). Morphological study of the mammalian stress response: Characterization of changes in cytoplasmic organelles, cytoskeleton, and nucleoli, and appearance of intranuclear actin filaments in rat fibroblasts after heat-shock treatment. *J. Cell Biol.* 101, 1198–1211.

Welker, S., Rudolph, B., Frenzel, E., Hagn, F., Liebisch, G., Schmitz, G., Scheuring, J., Kerth, A., Blume, A., Weinkauff, S., et al. (2010). Hsp12 Is an Intrinsically Unstructured Stress Protein that Folds upon Membrane Association and Modulates Membrane Function. *Mol. Cell* 39, 507–520.

Werner-Washburne, M., Braun, E., Johnston, G.C., and Singer, R.A. (1993). Stationary Phase in the Yeast *Saccharomyces cerevisiae*. *Microbiol. Rev.* 57, 383–401.

Weston, A.E., Armer, H.E.J., and Collinson, L.M. (2010). Towards native-state imaging in biological context in the electron microscope. *Scan. Electron Microsc.* 101–112.

White, H.E., Orlova, E. V., Chen, S., Wang, L., Ignatiou, A., Gowen, B., Stromer, T., Franzmann, T.M., Haslbeck, M., Buchner, J., et al. (2006). Multiple distinct assemblies reveal conformational flexibility in the small heat shock protein Hsp26. *Structure* 14, 1197–1204.

Whitesell, L., and Lindquist, S.L. (2005). HSP90 and the chaperoning of cancer. *Nat. Rev. Cancer* 5, 761–772.

Wu, C. (1985). An exonuclease protection assay reveals heat-shock element and TATA box DNA-binding proteins in crude nuclear extracts. *Nature* 317, 84–87.

Wu, C. (1995). Heat Shock Transcription factors: Structure and Regulation. *Annu. Rev. Cell Dev. Biol.* 11, 441–469.

Xie, Y., and Varshavsky, A. (2001). RPN4 is a ligand, substrate, and transcriptional regulator of the 26S proteasome: A negative feedback circuit. *PNAS* 98.

Yost, H.J., and Lindquist, S. (1986). RNA splicing is interrupted by heat shock and is rescued by heat shock protein synthesis. *Cell* 45, 185–193.

Young, J.C., Agashe, V.R., Siegers, K., and Hartl, F.U. (2004). Pathways of Chaperone Mediated Protein Folding in the Cytosol. *Nature* 5.

Zhao, R., Davey, M., Hsu, Y., Kaplanek, P., Tong, A., Parsons, A.B., Krogan, N., Cagney, G., Mai, D., Greenblatt, J., et al. (2005). Navigating the Chaperone Network Resource An Integrative Map of Physical and Genetic Interactions Mediated by the Hsp90 Chaperone. *Interactions* 120, 715–727.